

THE INVLUENCE OF SULFATE IN ALUMINUM COAGULATION OF WATER

By

Sekou Toure
M. Robin Collins
Department of Civil Engineering
University of New Hampshire
Durham, NH 03824

Technical Completion Report #58

USGS Grant 14-08-0001-G1239

December 1989

The research on which this report is based was financed in part by the United States Department of the Interior (USGS) as authorized by the Water Resources Research Act of 1984 (PL 98-242), the New Hampshire Water Resource Research Center, and the University of New Hampshire.

The contents of this publication do not necessarily reflect the views and policies of the Water Resource Research Center or the U.S. Department of the Interior, nor does mention of trade

ABSTRACT

THE INFLUENCE OF SULFATE IN ALUMINUM COAGULATION OF WATER

Aluminum salts are the most common coagulants used in water treatment to remove contaminants. The objectives of this research was to provide an understanding of some aspects of the influence of sulfate in aluminum coagulation chemistry of natural waters. Al(III) solutions were titrated with base to study the role of sulfate in the hydrolysis/precipitation of aluminum. Jar tests were conducted to treat water samples containing varying concentrations of aquatic humic substances (AHS), sulfate and pH. The kinetics and adsorption isotherms of sulfate and aquatic humic substances on aluminum precipitate were developed in adsorption experiments using aluminum precipitate adsorbents. The application of a sensor for Al(III) based on immobilized morin was investigated. Aluminum chloride and aluminum nitrate had similar hydrolysis/precipitation characteristics. Aluminum precipitation occurred at a lower formation function ratio $r = [\text{OH}]_b/[\text{Al}]_t$ for aluminum sulfate than for aluminum chloride or aluminum nitrate.

The aluminum sulfate precipitate was presumed to be an Al-OH-SO_4 solid. Equilibrium calculation (ALCHEMI) predicted jurbanite for similar conditions. The addition of sulfate to aluminum chloride solutions resulted in titration curves similar to that of aluminum sulfate. Acidification of the sample prior to titration did not impact the titration curves. An aluminum speciation scheme was presented showing the predominance of monomers at low r ratios, followed by polymers, and Al(OH)_4^- at high r ratios. pH had the most influence in the coagulation of the water samples treated. The impact of sulfate and AHS additions varied depending on the pH. Turbidity and AHS removal were greater at pH4 than at pH7. Maximum removals were obtained at pH5.5. The formation function fell within the range measured in the Al(III) titration experiments. Higher aluminum precipitates were measured at pH7. The adsorption data of aquatic humic substances (AHS) on aluminum chloride and aluminum sulfate precipitates fitted the Freundlich isotherm best. More AHS adsorbed to the aluminum sulfate precipitate. Little difference existed between the AHS adsorbed to either aluminum chloride or aluminum sulfate at pH5.5 and 7. AHS adsorbed to aluminum precipitates formed with AHS. Sulfate adsorption on aluminum precipitates increased with decreasing pH and fitted the Langmuir isotherm best. The competition between AHS and sulfate for the adsorption sites of the aluminum precipitates favored AHS. Inconsistent results were obtained with the sensor based on immobilized morin. Modifications to the procedure and the use of other ligands were recommended in lieu of morin.

FOREWORD

This research was funded by the New Hampshire Water Resource Research Center. Partial funding was also provided by the Graduate School in the form of CURF, and Summer Graduate Teaching Assistantship and Sigma Xi, the Scientific Society.

TABLE OF CONTENTS

ABSTRACT.....	i
ACKNOWLEDGMENTS	iii
FOREWORD	IV
TABLE OF CONTENTS	V
LIST OF FIGURES	X
LIST OF TABLES	XV
CHAPTER 1 INTRODUCTION	1
CHAPTER 2 LITERATURE REVIEW	8
2.1 Conventional Water Treatment	8
2.1.1 Aquatic Humic Substances and Particulate Removal Mechanisms	10
2.1.1.1 Characterization of Aquatic Humic Substances	10
2.1.1.2 Isolation, Fractionation, and Concentration of Aquatic Humic Substances	18
2.1.1.3 Aquatic Humic Substances and Particle Interaction	26
2.1.1.4 Aquatic Humic Substances and Particle Removal Mechanisms	29

2.2 Influence of Sulfate in Water Treatment	36
2.2.1 Importance	36
2.2.2 Role in Hydrolysis/Precipitation of Aluminum . . .	37
2.2.3 Sulfate Interaction with Aquatic Humic Substances and Aluminum	41
2.3 Inorganic Aluminum Chemistry	43
2.3.1 Aluminum and Other Coagulants	43
2.3.2 Aluminum Speciation	44
2.3.3 Aluminum Fractionation.	50
2.3.4 Importance of Aluminum in Anion Complexation	54
2.4 Sensor for Al(III) Measurement	58
2.4.1 Significance in Water Treatment	58
2.4.2 Theory	61
2.4.3 Limitations	64
CHAPTER 3 MATERIALS AND METHODS	66
3.1 Experimental Approach	66
3.2 Reagents and Quality Control/Quality Assurance Procedures	68
3.3 Analytical Procedures	71
3.4 Procedure for the Study of the Role of Sulfate in the Hydrolysis-Precipitation of Al(III).	78
3.4.1 Experimental Set-Up.	78
3.4.2 Procedure.	79
3.5 Concentration of Aquatic Humic Substances	80
3.5.1 Source	80

3.5.2	Concentration Scheme	81
3.5.3	Determination of Resin Adsorbent Capacity	81
3.5.4	XAD-8 Resin Cleaning and Column Packing	84
3.5.5	Concentration	85
3.6	Particle Sedimentation	90
3.7	Jar Test Procedure	91
3.7.1	Coagulant Used	91
3.7.2	Raw Water.	93
3.7.3	Jar Tests	95
3.7.4	Aluminum Speciation.	97
3.8	Kinetics of Aquatic Humic Substances and Sulfate Adsorption on Aluminum Precipitate	98
3.8.1	Reactor Description	98
3.8.2	Procedure	101
3.9	Sensor for Aluminum Measurement Based on Immobilized Morin.	105
3.9.1	Apparatus	105
3.9.2	Immobilization Procedure	107
3.9.3	Analyses	108
CHAPTER 4	RESULTS	112
4.1	Sulfate in the (AlIII) Hydrolysis/Precipitation	112
4.1.1	Titration of Aluminum Chloride, Aluminum Nitrate and Aluminum Sulfate Solutions	112
4.1.2	Impact of Increasing Sulfate Concentrations and Acidification on the Aluminum Titration Curves	116

4.2 Aluminum Coagulation.	119
4.2.1 Hydroxide Demand	120
4.2.2 Aluminum.	127
4.2.2.1 Aluminum Hydroxide Precipitate and Dissolved Aluminum.	128
4.2.2.2 Residual Aluminum.	135
4.2.3 Removal of Dissolved Organic Carbon and UV Absorbance	138
4.2.4 Turbidity and Particle Counts	142
4.2.5 Sulfate	150
4.3 Adsorption on Aluminum Precipitate	153
4.3.1 Characteristics of Aluminum Precipitate	153
4.3.2 Equilibration Time	157
4.3.3 Adsorbent Capacity	160
4.3.4 Aquatic Humic Substances Adsorption on Aluminum Precipitate.	164
4.3.5 Sulfate Adsorption on Aluminum Precipitate.	171
4.3.6 Competition between Aquatic Humic Substances and Sulfate	179
CHAPTER 5 DISCUSSION	184
5.1 Hydrolysis/Precipitation of Al(III)	184
5.1.1 Summary	201
5.2 Aluminum Chloride Coagulation	205
5.2.1 Summary	220
5.3 Aquatic Humic Substances and Sulfate Adsorption on Aluminum Precipitate	221
5.3.1 Summary	229

CHAPTER 6 CONCLUSION AND RECOMMENDATIONS
FOR FUTURE RESEARCH 232

6.1 Conclusions 232

6.2 Recommendations for Future Research 235

REFERENCES 240

APPENDICES 259

LIST OF FIGURES

<u>Figure</u>	<u>Title</u>	<u>page</u>
2.1	Conventional water treatment plant	9
2.2	Structure of humus molecule (Christman and Ghassemi, 1966)	15
2.3	Structure of humic acid (Flaigs, 1960)	15
2.4	Humic acid (Dragunov, 1966)	15
2.5	Hypothetical structure of humic acid (Stephenson and Khan, 1982)	16
2.6	Fulvic acid structure (Schnitzer and Khan, 1972).	16
2.7	Fulvic acid (Buffle, 1977)	16
2.8	Design and operational diagram for alum coagulation (Mills and Amirtharajah, 1982)	35
2.9	Relationship between sulfate emission and sulfate concentration in 82 clearwater lakes.	38
2.10	Solubility of freshly precipitated amorphous $\text{Al}(\text{OH})_3\text{S}$ (O'Melia and Dempsey, 1982)	49
2.11	Aluminum speciation test flow diagram (Hundt, 1985).	53
2.12	Aluminum speciation diagram (Hundt, 1985)	55
2.13	Formation of the morin- $\text{Al}(\text{III})$ complex	62
3.1	Frontal chromatography breakthrough curve.	83

3.2	Schematic of aquatic humic substances concentration apparatus.	86
3.3	Standard curve for aquatic substances humic substances stock solution	88
3.4	DOC and UV relationship of the stock humic substances solution	88
3.5	UV absorbance scan for the concentrated humic stock aquatic humic substances solution.	89
3.6	Standard curve for bentonite clay stock suspension.	92
3.7	Levels of the factorial design.	94
3.8	Jar test reactor.	96
3.9	Reactor cell for the adsorption study.	99
3.10	Diagram of pH sensor based on fluorescence and instrumentation	106
4.1	Titration curve relating the formation function r to pH for aluminum chloride, aluminum nitrate, and aluminum sulfate solutions	113
4.2	Titration curve relating the formation function r to pH for aluminum chloride solutions with SO_4 addition	117
4.3	The coagulation of AHS; the hydroxide demand at various pH and aluminum dosages	123
4.4	The coagulation of AHS; the aluminum precipitate formation at various pH and aluminum dosages	129
4.5	The coagulation of AHS; the dissolved aluminum at various pH and aluminum dosages	133

4.6	The coagulation of AHS; the residual aluminum at various pH and aluminum dosages	136
4.7	The coagulation of AHS; the residual DOC at various pH and aluminum dosages	139
4.8	The coagulation of AHS; the residual UV absorbance at various pH and aluminum dosages	140
4.9	The coagulation of AHS; the residual turbidity before filtration at various pH and aluminum dosages	143
4.10	The coagulation of AHS; the residual turbidity after filtration at various pH and aluminum dosages	144
4.11	The coagulation of AHS; the residual particle count before filtration at various pH and aluminum dosages	146
4.12	The coagulation of AHS; the residual sulfate at various pH and aluminum dosages	151
4.13	Aluminum precipitate formation with Al(III) solutions	156
4.14	Equilibration time for the adsorption of aquatic humic substances on aluminum precipitates	158
4.15	Equilibration time for the adsorption of sulfate on aluminum precipitates	159
4.16	Adsorption capacity for the adsorption of aquatic humic substances on aluminum precipitates	161
4.17	Adsorption capacity for the adsorption of sulfate on aluminum precipitates	162
4.18	Aquatic humic substances adsorption on aluminum precipitates	165

4.19 Aquatic humic substances adsorption on aluminum precipitates; Freundlich transformation	166
4.20 Adsorption of aquatic humic substances on aluminum precipitates; Langmuir transformation	167
4.21 Aquatic humic substances adsorption on aluminum sulfate precipitates at pH7	169
4.22 Aquatic humic substances adsorption on aluminum chloride precipitates	170
4.23 Sulfate adsorption on aluminum chloride adsorbent	172
4.24 Sulfate adsorption on aluminum chloride precipitate; Langmuir and Freundlich transformation	173
4.25 Sulfate adsorption on aluminum chloride precipitates at pH7; Langmuir transformation	175
4.26 Hypothetical adsorption curve for the adsorption of sulfate on aluminum sulfate precipitate	177
4.27 Hypothetical adsorption curve for the adsorption of sulfate on aluminum sulfate precipitate; Langmuir transformation	178
4.28 Exchange of carbon for sulfate on aluminum chloride precipitate at pH7	181
5.1 Schematic representation of aluminum species	186
5.2 Theoretical aqueous aluminum solid species	196
5.3 Theoretical aluminum solid species	197
5.4 Aluminum-sulfate and sulfate species	198

5.5 Alum coagulation stability diagrams (Mangravites, 1975;
Weisner, 1986) 212

LIST OF TABLES

<u>Table</u>	<u>Title</u>	<u>page</u>
2.1	Elemental composition of humic and fulvic acid from soil and water.	17
2.2	Properties and characterization of XAD resins (Aiken, 1979)	25
2.3	Possible mechanisms for the removal of humic substances by coagulation (Randtke, 1987)	33
2.4	Summary of aluminum hydrolysis constants.	47
3.1	Analytical procedures	69
3.2	Instrument calibration conditions	70
3.1	Raw water concentration for each run	94
4.1	Characteristics of aluminum titration curves.	118
4.2	Overall significance of the factorial design variables	121
4.3	Aluminum chloride coagulation; the hydroxide demand at various pH and aluminum dosages	122
4.4	Aluminum chloride coagulation; the formation function at various pH and aluminum dosages	126
4.5	Aluminum chloride coagulation; the aluminum precipitates at various pH and aluminum dosages	130
4.6	Aluminum chloride coagulation; the dissolved aluminum at various pH and aluminum dosages	134

4.7	Aluminum chloride coagulation; the residual aluminum at various pH and aluminum dosages	137
4.8	Aluminum chloride coagulation; the the residual DOC and UV absorbance at various pH and aluminum dosages . . .	141
4.9	Aluminum chloride coagulation; the turbidity measurements at various pH and aluminum dosages	145
4.10	Aluminum chloride coagulation; the particle count at various times during during coagulation	147
4.11	Aluminum chloride coagulation; the particle count before filtration at various pH and aluminum dosages	149
4.12	Aluminum chloride coagulation; the residual sulfate at various pH and aluminum dosages	152
4.13	Aluminum precipitate formation on 0.2 μm and 0.45 μm filters	155
4.14	Sulfate and aquatic humic substances adsorption on 0.2 μm and 0.45 μm filters	155
4.15	Freundlich equilibrium constants for the adsorption of aquatic humic substances on aluminum chloride and aluminum sulfate precipitates	168
4.16	Langmuir constants for the adsorption of sulfate on aluminum chloride precipitates	174
4.17	Sulfate adsorption on aluminum sulfate precipitate; mass balance	176
4.18	Competitive adsorption of aquatic humic substances and sulfate on aluminum chloride precipitates	180
5.1	Thermodynamic data for ALCHEMI calculations	195

5.2 Total charges associated with selected aluminum
species 211

CHAPTER 1

INTRODUCTION

Conventional water treatment plants are used to destabilize suspended, dissolved, and colloidal contaminants from water supplies. These plants employ a series of processes consisting of coagulation, flocculation, sedimentation, and filtration. A variety of coagulants are used, the most common of which are salts of aluminum because they are relatively cheap, easy to handle, and usually very effective in removing contaminants from water. The coagulants' function in conventional water treatment is to destabilize particles and produce large aggregates or flocs that settle readily (Edzwald, 1986). Destabilization of colloidal particles may be achieved by a combination of mechanisms including charge neutralization/ precipitation, adsorption onto sweep floc, and bridging by high molecular weight polyelectrolytes (Hundt, 1985; Randtke, 1987).

The uncertainty about the exact aluminum species formed when aluminum is added to water and the interaction between the aluminum species and the contaminants need to be understood in order to optimize the coagulation process. Monomeric, polymeric, and solid precipitate species have been reported (Dempsey 1987). It is not clear whether monomeric aluminum species are more

effective in removing contaminants than the polymeric aluminum hydrolysis products, but, in general, more is known about the formation of monomeric hydrolysis species than polymeric species. For example, Holmes (1968) has shown that the rate of conversion from one monomeric species to another is diffusion controlled. There is good agreement regarding the first hydrolysis constant for $\text{Al}(\text{H}_2\text{O})_6^{3+}$. However, substantial disagreement exists about the hydrolysis constant of the polymeric species, and $\text{Al}(\text{OH})_3(\text{S})$ (Johnson and Amirtharajah, 1982; May et al., 1979; Stumm and Morgan, 1981). Among the suggested polymeric species are Al_2 , Al_3 , Al_8 , Al_{13} (Dempsey et al., 1984).

The disagreement about the exact aluminum species comes from the lack of reliable analytical procedures to measure the concentration of the hydrolysis products (Batchelor et al., 1986). The main obstacle with the few methods available is the time requirement between sampling and species determination (Buffle et al. 1985; Parthasarathy et al., 1985). Most of the procedures require too much time for sample preparation or analysis compared to the shorter lived reaction products (Snodgrass et al., 1982).

The aluminum hydroxide precipitate exhibits a surface charge, the magnitude of which is a function of the chemical composition of the bulk solution (Driscoll and Letterman, 1988). In dilute solutions, reported isoelectric pH (pH at which the net surface charge is zero, zpc) ranges from 7.5 to 8.5 (Montgomery, 1985), and 9 (Driscoll, 1988). At pH values less than the zpc, the net surface charge is positive (Driscoll, 1988). It is possible for anions

such as aquatic humic substances (AHS), sulfate, phosphates, fluoride, nitrate, and chloride to adsorb on the aluminum hydroxide surface thereby significantly influencing the net surface charge (Driscoll, 1988; Hundt, 1985; Schendle and Letterman, 1986).

From the standpoint of treatment plant performance, high residual dissolved aluminum concentration may indicate incorrect coagulant dosing, inefficient use of the coagulant, or problems with the treatment units. High concentration of particulate aluminum may indicate problems in solid/liquid separation or post precipitation of aluminum. The consequence of poor water treatment plant performance would be the potential adverse health effect of high residual aluminum in the finished water. High aluminum intake has been linked to illnesses such as dialysis Encephalopathy and Alzheimer's disease (Perl, 1985; Norberg et al., 1985; Will and Savory, 1985).

From a research perspective, the knowledge of aluminum species can provide a better understanding of the coagulation chemistry and the mechanisms of contaminant removal (VanBenschoten, 1988). A precise theoretical approach could be taken to predict specific contaminant removal. The development of analytical procedures involving the reactions of different hydrolysis products of aluminum with a colorimetric reagent may be a solution to determining the aluminum species (Batchelor et al., 1986; Driscoll, 1988).

The presence of anions and particulate matter will also affect the chemistry of aluminum in solution. Aluminum can form

soluble complex species, with various ligands. The anion affinity for aluminum is influenced by solution pH, the nature of the aluminum precipitate, and the pH of minimum solubility of Al(III) (Hundt, 1985).

The treatment of water containing high concentrations of aluminum-complexing ligands (F^- , SO_4^{2-} , PO_4^{3-} , aquatic humic substances) may lead to high concentrations of soluble aluminum complexes which are not removed by filtration (Letterman and Driscoll, 1988). Costello (1984) noted that residual aluminum is a significant problem in systems that apply high dosages of alum to remove color causing organics.

Sulfate, one of the ligands of interest in this research, has been investigated by a few researchers (De Hek et al., 1978; Letterman and Vanderbrook, 1983). De Hek et al. (1978) showed that the hydrolysis precipitation of aluminum was not altered by the presence of chloride or nitrate. However, the hydrolysis precipitation process was affected by sulfate as well as the composition of the texture and structure of the resultant precipitate. Sulfate was thought to be adsorbed on the $Al(OH)_3(S)$ floc. Basic aluminum sulfate has also been reported at pH values below 4.5 when the sulfate concentration was 10^{-4} M Norstrom (1982). The experimental condition appears to determine whether or not aluminum sulfate compounds will form.

The removal of aquatic humic substances, the other ligand of concern, by coagulation has been investigated (Hundt, 1985; Gjessing, 1976; Konova, 1983). These researchers have all shown

that aluminum salts are effective coagulants. Reported removals vary from 0% to over 90% (Randtke, 1987). Schnitzer and Khan (1972) indicated that, at pH of 3.5 and 7.0, trivalent ions Al^{3+} and Fe^{3+} or their hydrolyzed counterparts were more effective in coagulating AHS than divalent ions such as Ca^{2+} or Mg^{2+} . In addition, freshly precipitated aluminum and ferric hydroxides adsorbed AHS, with aluminum hydroxide adsorbing more than the iron hydroxide. Greeland (1971) and Lind (1975) have shown that organic molecules allow aluminum to be present in solution at higher concentrations than expected due to organic-aluminum complexes which are formed, and that organic matter inhibits the polymerization of dissolved aluminum species.

Particle removal by coagulation has also been reported (Collins et al., 1987; Snodgrass, 1982; Weisner, 1986). There are differences between turbidity and AHS removals despite several similarities. In turbidity removal, solid particles may be coated with aluminum polymers that cause destabilization, thereby resulting in aggregate formation. The particle may be physically enmeshed in an $\text{Al}(\text{OH})_3$ solid (Hundt, 1985). Dempsey et al. (1985) found that turbidity increases coagulant demand in the presence of fulvic acid only slightly, whereas fulvic acid dramatically increased the dose of coagulant required for the removal of turbidity. Using an aluminum solubility diagram, Dempsey (1987) has described zones of turbidity removal when alum and polyaluminum chloride were the coagulants. Turbidity removal was maximized in the sweep floc zone.

The complexity of the interactions among the aluminum coagulant and AHS, sulfate, and particulate contaminants requires further studies. The research areas which may provide a better understanding of the process include the chemistry of aluminum hydrolysis, the aluminum-hydrolyzing salts-contaminants interaction, and the nature and the extent of specific contaminant removal mechanisms.

It would be valuable to know the impact of sulfate addition on the formation of aluminum hydrolysis products. For example, how does the hydrolysis of aluminum sulfate compare with aluminum chloride or aluminum nitrate? What are the rate, and the extent of aluminum speciation in coagulation? Would sulfate influence the hydrolysis of aluminum? Will sulfate promote or retard the aluminum hydroxide precipitate formation? Will sulfate be adsorbed on the aluminum precipitate or precipitated out? Would the adsorption of sulfate on aluminum hydroxide precipitate be in competition with AHS? What are the mechanisms of AHS and sulfate removal? What would the influence of sulfate be in the coagulation of AHS and turbidity?

Furthermore, there is a need to develop in situ analytical procedures to measure aluminum during coagulation and the residual aluminum in the finished water. The development of an in-situ aluminum measurement method could be an improvement over current discrete aluminum measurement techniques. The problems associated with sampling, and storage before analysis would be avoided using the new technique.

The objectives of this dissertation have focused on providing an answer to some of these questions. Emphasis has been placed on the hydrolysis of aluminum, the mechanisms of coagulation of AHS and turbidity with the competitive influence of sulfate in the process. The specific objectives were four fold:

- .Study of the role of sulfate in the hydrolysis precipitation of Al(III) .
- .Evaluation of aluminum coagulation of AHS and particulate matter under varying pH and sulfate concentration conditions.
- .Investigation of the extent of sulfate, and AHS adsorption on aluminum precipitates.
- .Investigation of a new analytical method, a polyvinyl alcohol morin based fiber optic technique to measure aluminum in solution.

CHAPTER 2

LITERATURE REVIEW

2.1 CONVENTIONAL WATER TREATMENT

The treatment of water for the removal of suspended, colloidal and dissolved contaminants in conventional water treatment plants is achieved by two unit processes shown in Figure 2.1. One unit process, coagulation, is accomplished in a rapid mix tank and flocculator. The other, solid liquid separation, is accomplished in a clarifier and a filter.

The raw water is pumped to the rapid mix after coarse screens or bar racks have retained floating, coarse materials. The coagulant is added either in line or in the rapid mix chamber. Aluminum sulfate has been the coagulant of choice because it is cheap and does not cause the health risks of other coagulants such as aluminum nitrate and aluminum chloride. Flocs that form in the rapid mix chamber are slowly brought into contact with one another during flocculation and are allowed to collide and grow to settleable size in the flocculator. After this step, gravity settling (sedimentation) occurs in a clarifier to let the flocs settle and minimize the amount of flocs that is applied to the filter. Where high quality raw water exists, sedimentation, and perhaps

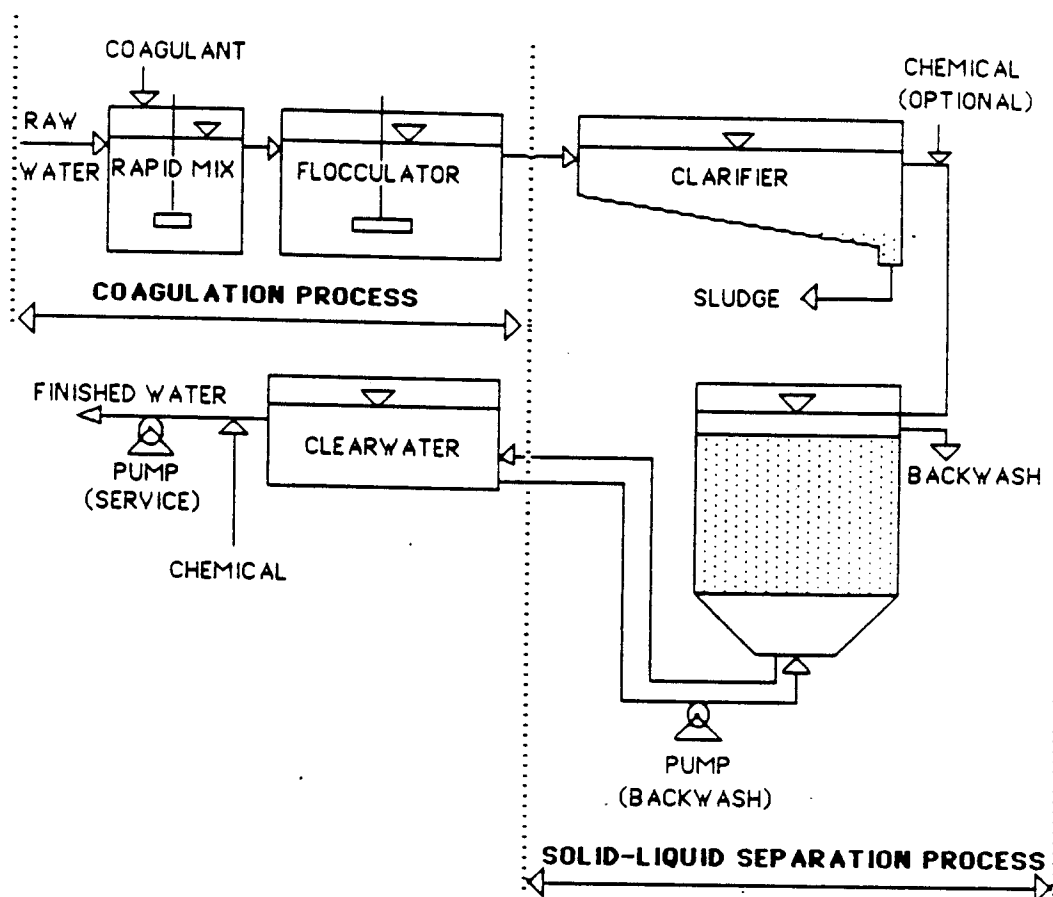


Figure 2.1: Conventional Water Treatment Plant

flocculation, can be eliminated by using direct filtration. During filtration, the water passes through sand or similar media to remove fine particles that do not settle. In the final step, water is disinfected (usually with chlorine) to reduce the number of pathogenic organisms before storage and/or distribution.

2.1.1 Aquatic Humic Substances and Particle Removal Mechanisms

2.1.1.1 Characterization of Aquatic Humic Substances

Humic substances (HS) have been studied since the eighteenth century (Schnitzer and Khan, 1972). Aiken (1985) traced the beginning of the research on aquatic humic substances (AHS) to the Swedish scientist Berzelius, who investigated colored waters of a mineral spring and later isolated colored organic compounds from swamp water by precipitation with iron. The study of HS, since Berzelius' time, has broaden to include other sources. Humic substances have been found in soils, sediment, lake water, ground water, seawater, estuarine water, and marine sediments (Schnitzer and Khan, 1972).

Extensive studies of soil humic substances have been reported in the literature from the 18th to the 20th century (Khan, 1972). In contrast, interest in aquatic humic substances was not renewed until the 1900's, when studies were initiated on the origin of color in water (Khan, 1972).

The origin of aquatic humic substances is still unknown.

Several theories have been proposed that describe aquatic humic substances formation. Five of the most accepted general overall theories include (Beck, 1974; Thurman, 1985):

- 1) the aquatic humic substances consist of soil fulvic acids that have leached or eroded from soil.
- 2) aquatic humic substances are formed by the same process as soil humic substances.
- 3) aquatic humic substances are soil fulvic acids leached from soil in the initial stages of humification and then modified, transformed, or aged by humification processes which result in humic substances unique to the aquatic environment.
- 4) aquatic humic substances are formed by a unique humification process, whereby simple reactive moieties are polymerized and condensed into humic substances unique to the aquatic environment.
- 5) humic substances are formed by continuation of the polymerization process to form larger molecular units of fulvic acid which are called humic acid.

Some workers have, however, disagreed over the premise that aquatic humic substances have their origin in soil (Aiken, 1985; Thurman and Malcom, 1981). The disagreement exists because the compounds are complex and not well characterized. Stevenson (1982) and Malcom et al. (1982) have shown that humic substances from soil and water have comparable molecular weight, elemental composition, and functional groups. They suggested that these similarities may be one reason for the link between soil and aquatic humic substances.

Aquatic humic substances are known to be a mixture of many hydrophilic compounds that have characteristics of polyelectrolytes (Saar, 1980). They have been characterized as heterodisperse, polymeric, colored organic macromolecules (Hundt, 1985). The AHS have a characteristic dark brown nearly black color when isolated from water. They are formed as a result of polymerization or condensation of various products of organic matter breakdown, plant and microbial autolysis, microbial synthesis, or a combination of the above (Hundt, 1985). Organic matter breakdown also produces biopolymers including carbohydrates, protein fragments, fats, and pigments (Reuter and Perdue, 1977).

Humic substances are believed to possess a complex aromatic core with polysaccharides, proteins, organic acids, simple phenols and chelated metals (Thurman and Malcom, 1983). Thurman (1983) suggests from separation, degradation and nuclear magnetic resonance identification that carboxyl, aromatic hydroxyl, and carboxyl groups are the primary functional groups associated with humic substances.

Humic substances are divided into several subgroups. The most common separation is based on solubility in acid and base. Humic acid is that fraction of humic substances that is not soluble in water under acid conditions (below pH1), but becomes soluble at higher pH. Fulvic acid is that fraction of humic substances that is soluble under all pH conditions. Humin is the fraction that is not soluble in water at any pH value (Aiken, 1985; Thurman and Malcom, 1983).

The structures of the AHS have yet to be defined. Aquatic humic substances are a class of compounds rather than a single compound that can be defined by molecular weight, crystal structure, and dissociation constants. They are generally characterized by average molecular weights, and ranges of dissociation constants for the class (Sarri, 1983). They range in molecular weight from a few hundred to more than ten thousand (gr/mole) (Schnitzer and Kahn, 1972). Reported values of the radius of gyration of individual subunits of colloidal soil humic acid range from 10 Å to 38 Å (Wershaw, 1967). The radius of gyration is the root mean square distance of the electrons in the particle to the center of the charge. X-ray scattering determination of the angle of gyration of aquatic humic acid range from 6.5 Å to 15.3 Å (Hundt, 1985). The angle of gyration is a useful parameter for comparing molecular or particle sizes and for evaluating if the molecules are mono or polydispersed (Malcom et al., 1982; Hundt, 1985).

Several formulas for HS have been proposed. Christman and Ghassemi (1966) have suggested the formula shown in Figure 2.2 based on the assumption that lignin plays an essential part in the humification processes. As noted by Gjessing (1976), the formula seems to be useful for theoretical purposes. A definite composition is unlikely because the number of units (N) may vary, and groups of organic and inorganic compounds may be substituted for or attached to the unit.

Other suggested structures are shown in Figures 2.3 to 2.7. Flaig's (1960) structure as well as Dragunov's (1966) contain nitrogen as a structural component. More recent proposed structures

are based on the concept that molecules of humic acid consist of micelles of a polymeric nature, the basic structure of which is an aromatic ring of the di-or trihydroxy-phenol type bridged by -O-, -CH₂-, -NH-, -N=, -S- and other groups containing both free OH groups and the double linkages of quinones (Aiken, 1985). Dragunov's (1966) structure as well as Flaig's (1960) structure contain nitrogen. Carbohydrates, and protein residues are also present in Dragunov's (1966) and Stevenson's (1982) structures. Schnitzer and Khan (1972) argue that fulvic acid consists in part of phenolic and benzene carboxylic acids held together through hydrogen bonds to form a polymeric structure. Aromatic and aliphatic components substituted with oxygen-containing functional groups are present in Buffle's model (Buffle, 1977).

On a percentage basis, humic acid has higher molecular weight, higher carbon content, and lower oxygen content than fulvic acids. A summary of elemental analyses of humic substances presented in Table 2.1 indicates the distribution of the major elements. Fulvic acids are more hydrophilic than humic acids because of their higher oxygen content, more carboxylic and hydroxyl functional groups, and lower molecular weight (800-2000). They thus comprise the largest percentage of humic substances in aquatic environment. Black and Christman (1963) indicate that fulvic acid comprised between 80 to 90% of aquatic humic substances for the waters they examined. Midwood and Felbeck (1965) measured the fulvic acid fraction of humic substances to be 90% of the total aquatic humic substances in their water samples. From the results of 50 analyses of fresh waters using an isolation procedure on XAD

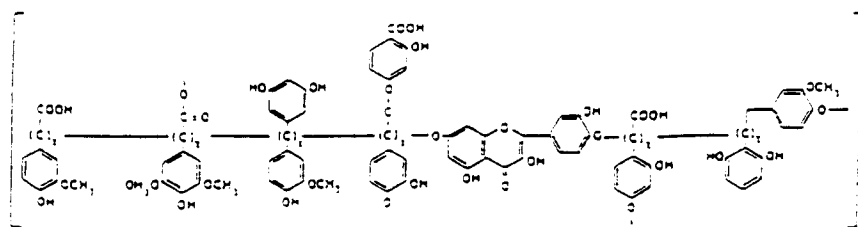


Figure 2.2: Proposed structure of the colored humus molecule according to Christman and Ghassemi (1966).

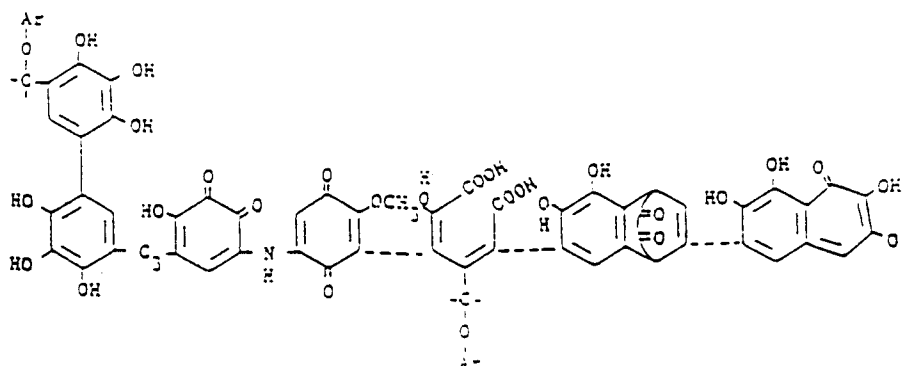


Figure 2.3: Structure of humic acid according to Flaig (1960)

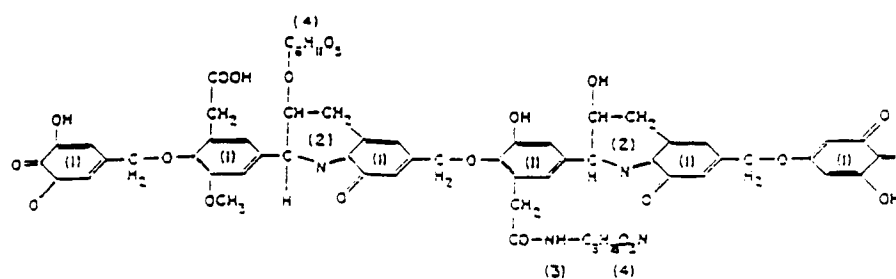


Figure 2.4: Dragunov's structure of humic acid as recorded by Konova (1966).

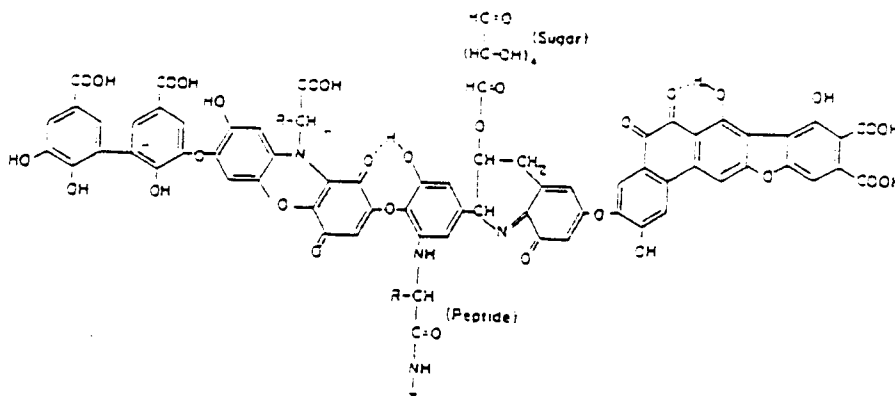


Figure 2.5: Hypothetical structure of humic acid showing free and bound phenolic OH groups, quinone structures, oxygen as bridge units and carboxyls variously placed on the aromatic ring, from Stevenson (1982).

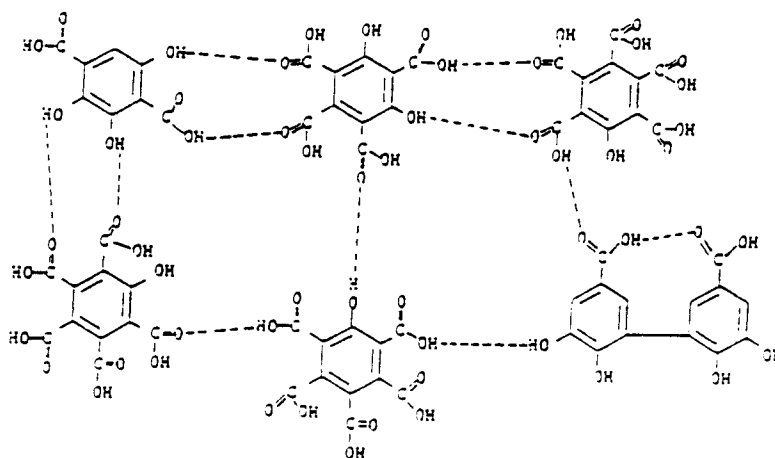


Figure 2.6: Type structure of fulvic acid as proposed by Schnitzer and Khan (1972).

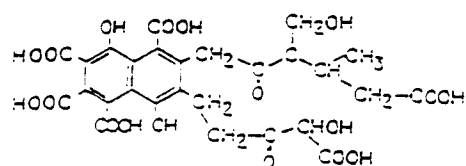


Figure 2.7: Type structure of fulvic acid as proposed by Buffle (1977).

Table 2.1: Elemental Composition of Humic and Fulvic Acid from Soil and Water

Source	C	H	N	O	S	P	%Ash	reference
Aquatic FA	46.20	5.90	2.60	45.30				1
Swanee River FA (22mgC/l)	54.65	3.71	0.47	39.20	0.50	0.20	0.95	2
Swanee River HA (8mgC/l)	57.24	3.94	1.08	39.13	0.63	0.20	0.56	2
Gota River FA	53.15	4.76	1.04	37.59	2.60			3
Gota River HA	55.29	4.53	1.26	37.08	1.78			3
Soil HA (a)	57.32	5.05	2.78	34.37	0.58			1
Soil FA (b)	47.00	4.43	1.47	46.40	0.70			1
Soil FA	51.10	3.65	1.43					4
Jewel Pond FA (a)	45.70	4.26	1.57				7.10	4
Jewel Pond FA (b)	41.60	4.17	1.00				3.80	4
Jewel Pond HA	53.50	4.86	2.14				3.50	4
Fluka Columbia HA	57.90	5.16	0.71				2.50	4
Biscayne Groundwater								
FA (6mgC/l)	55.44	4.17	1.77	35.39	1.06	0.20	0.43	2
Biscayne Groundwater								
HA (2.5mgC/l)	58.28	3.39	5.84	30.14	1.43	0.22	0.10	2
Laramie-Fox Hill								
Groundwater FA (0.05mgC/l)	62.67	6.61	0.42	29.14	0.44	0.20	1.09	2
Catania-Fox Hill								
Groundwater HA (0.03mgC/l)	62.05	4.92	3.21	23.45	0.96	0.46	5.12	2

(a) Average of 6 values

(b) Average of 3 values

(c) Fluka Columbia Co., Columbia, SC

1 Schnitzer and Khan (1972)

2 Thurman and Malcom (1981)

3 Plechanov et al. (1983)

4 Webber (1985)

resin, Thurman and Malcom (1981) concluded that humic acid accounts for 10% of the Dissolved Organic Carbon (DOC). The combination of humic acid and fulvic acid accounts for 50% of the DOC of most fresh waters that were analyzed in their study.

2.1.1.2 Isolation, Fractionation, and Concentration of Humic Substances

The study of aquatic humic substances requires their isolation from natural waters. The final product should be free from chemical impurities, which hinder the characterization of the isolated humic substances. The product should also withstand any degradation. Several isolation methodologies are available for isolating humic substances. The following discussion identifies some of the common methods employed to date.

Freeze drying, also referred to as lyophilization, is an easy and gentle method for concentrating humic substances. However, several problems are associated with this method. All solutes in the sample including inorganic solutes are concentrated except volatile organics. The method is also slow and not suitable for processing large volumes of water (Katz, 1972; Black, 1963a). The most efficient way of using freeze drying has been in conjunction with other concentration processes (Beck et al., 1974).

Another method, freeze concentration, is also slow, unsuitable for processing large volume of water. Further sample processing is required to separate humic substance from other organic solutes (Black, 1963b). However, the method is inexpensive,

and simple (Baker, 1967; Baker, 1970).

Liquid extraction has been used with some success to isolate humic substances from water (Thurman, 1985). Solvents such as ethyl acetate, butanol, isoamyl alcohol, and chloroform emulsion have all successfully been used. (Thurman, 1985). However, these methods are not quantitative, nor can carbon analysis be done to determine the amount of humic substances that are removed by the procedure (Thurman, 1981). Although inorganic salts can be effectively separated from organic matter, poor extraction efficiencies and slow extraction rates outweigh the advantages. For instance, Leenheer (1981) reported only 10% DOC extraction.

Reverse osmosis, an expensive and equipment intensive method, has similarly been used for DOC concentration from water (Deinzer, 1975; Koottatep, 1982). The major problem as reported by Koottatep is that higher molecular weight fractions of DOC are excluded at low concentrations but move across the membrane at higher concentrations.

Saari et al. (1975), Leenheer (1981), McCarty (1974) have effectively used anion exchange adsorbents to remove organic matter from water. The method is reportedly simple, and can be improved by a judicious choice of resins. Available resins include phenol-formaldehyde weak base resin, diethyl aminoethyl cellulose, and cation exchange resins. Strong-base resins that have quaternary ammonium groups, and weak-base resins that have secondary amine groups are preferred for isolating humic substances from water (Thurman, 1985). Weak anion exchange resins elude more efficiently than strong anion exchange resins, while still maintaining high

efficiencies of adsorption (Leenheer, 1981). The problem with resins is that irreversible sorption can occur especially for strong-base resins because of the high affinity of the organic compounds for quarternary ammonium sites. Large humic acid molecules can also diffuse more slowly from macroporous structures of the resins resulting in eventual fouling (Thurman, 1985). Reported recoveries from these resins range from 70 to 80% (McCarthy, 1974; Leenheer, 1981; Thurman, 1985).

Adsorption techniques using various synthetic resins and granular activated carbon are much more efficient (Leenheer, 1981). Low solute recoveries from the sorbent have, however, limited the use of these techniques (Aiken, 1985; Leenheer, 1981). In addition, irreversible sorption, molecular exclusion, and hindered elution are some of the problems associated with the techniques even though these resins are easy to handle and can be regenerated by treatment with large volumes of water (Aiken, 1985).

Various types of precipitations have been successfully used for humic substance isolation. Examples include precipitation with CaCO_3 , Mg(OH)_2 , Fe(OH)_3 , $\text{Pb(NO}_3)_2$, and FeCl_3 (Aiken, 1985; Weber and Wilson, 1975; Weber and Truitt, 1979). The disadvantages are that all are slow, give high ash contents, and concentrate only 16 to 63% of the organic material (Williams and Zirino, 1964). As with most other procedures, separation of the inorganic salts from isolated humic acid is very difficult. The procedure is also unsuitable for large volumes of water.

Ultrafiltration fractionation and gel permeation are effective methods of humic substance fractionation. Both give a

range of molecular weights thereby permitting separation of humic substances into molecular weight fractions. Molecular weight separation in gel permeation is achieved by size exclusion. A given type of gel is characterized by a unique molecular weight range over which molecules can be fractionated (Amy et al., 1985). Separation is obtained through the ability of the various humic acid molecules to diffuse into the pores of the gel. The gel acts as the stationary phase. Large molecules do not enter far into the pores of the gel, and thus are quickly eluded. Smaller molecules enter the gel pores, their movement is retarded in the stationary phase. The overall process leads to the elution of molecules in order of decreasing molecular size.

Ultrafiltration involves the selective rejection of humic acid molecules by convective flow through a membrane. Molecules of a size larger than the specified membrane "cut-off" are quantitatively retained while smaller molecules flow through the membrane. Humic acid can be concentrated by ultrafiltration by selecting one membrane size that would retained all the humic acid molecules.

Oliver (1980) fractionated aquatic humic substances into a series of eight molecular weight fractions utilizing DIAFLO Ultrafiltration Membranes (Amicon, Inc., Danvers, MA) with molecular weight cutoffs ranging from 500 to 300,000. The samples were processed in a TRIS buffer (pH 8.4, I=1.5). DIAFLO UF membrane with manufacturer-designated cutoffs of 10,000 were reported to retain 50 to 90% of aquatic humic acid in various Swedish natural waters (Wilander, 1972). Amy et al. (1985), compared UF and gel

permeation chromatography determination of molecular weight fractions of water samples from several rivers in the United States. They concluded that gel permeation was more profoundly affected by pH, suggesting that the UF method is better in cases where pH variations are of concern. They also stressed that one must exert caution in interpreting molecular weight data with these methods. Experimental conditions must be maintained the same at all times.

Gjessing (1970) also used DIAFLO UF membranes. He concluded that about 10% of the organic carbon and 1% of the color matter have MW below 1000. Moreover, more than 85% of the color is present in the >20,000 MW fraction. The method suffers from problems associated with surface and electrostatic effects. The permeability is affected by a concentration polarization effect because the macromolecules adhere to the sides of the membrane pores and create a gel layer that becomes the principal resistance to flow (Amy et al., 1985; Buffle et al., 1978). An unequal distribution of ions across the membrane creates a potential due to the Donnan effect, in which one of the solutes is excluded from the membrane. This phenomenon may render the membrane ineffective (Amy et al., 1985).

Alumina, nylon and polyamide have been used to isolate humic substances. The presence of oxide groups on the alumina surface provides basic binding sites and weak acids sorb more strongly (Aiken, 1985). Moed (1970) has isolated lake organic matter on alumina. Ninety eight percent of the solute was adsorbed, but poor recovery (66-80%) was obtained by desorption with 0.008M and 0.3M NaH_2PO_4 buffer. Davis (1981) found that organic matter

with molecular weight greater than 1000 formed strong complexes with the alumina surface, but low molecular weight compounds were weakly adsorbed. Most of the organic matter adsorbed was in the molecular weight range of $1,000 < M < 3,000$. Sea water humic material has been concentrated using nylon in the form of white crylon stockings (Sieburth et al., 1968). Efficient elution was obtained with 0.1N NaOH.

Recently, successful concentration of aquatic humic acid has been achieved with pH adjustment followed by liquid/solid adsorption chromatography on nonionic resins. The resins commonly used in the procedure are Amberlite XAD resins. These resins are nonionic, macroporous copolymers which possess large surface areas (Aiken, 1979). Several types of XAD resins exist. XAD-1 and XAD-2 resins have been shown to be effective adsorbents for removal of humic substances from sea water (Mantoura and Riley, 1975). They have also been used to isolate humic substances from river water (Hundt, 1985; Thurman, 1981; Mantoura, 1975). These resins have the advantage over other adsorbents that they are easier to elute and are free from the risk of chemical alteration of the humics (Mantoura, 1975). In addition, XAD resins have greater adsorption capacity and are easier to elute than alumina, nylon, silica gel, and polyamide powder (Aiken, 1985). Several investigators including Liao (1982), Thurman and Malcom (1981), Leenheer (1981), Aiken (1979), Aiken et al. (1978), Weber et al. (1975), and Mantoura and Riley (1975) have used XAD resins. Studying the adsorption of humic acid on XAD-2, Mantoura and Riley (1975) found that adsorption fits the Langmuir isotherm. The

standard free energy of adsorption ΔG^0 was -36.4 KJ/mole at 21°C, and the standard entropy of adsorption, ΔS , was 103 J/mole/K at the same temperature. Weber and Wilson (1975) also used XAD-2 to fractionate humic substances from soil and water samples.

A comprehensive procedure proposed by Leenheer (1981) includes a combination of pH adjustment and adsorption chromatography to separate humic substances into several fractions. Aiken (1979) studied five Amberlite XAD resins as indicated in Table 2.2. This work shows that XAD-7 and XAD-8 are much more efficient than XAD-1, XAD-2, and XAD-4 in the recovery of humic acid. The results also indicated that elution at pH 13 was approximately 100% effective due to ionization of carboxylic and phenolic hydroxyl groups on XAD-7 and XAD-8. Moreover, hydrophobic styrene-divinylbenzene resins XAD-1, XAD-2, XAD-4 were found more difficult to elute due to the hydrophobic interaction and possible π - π bonding with the aromatic resin matrix of styrene divinyl benzene resins. Additionally, sorption of fulvic acid on these resins is slow since diffusion through the resin is the rate controlling step (Aiken, 1975). XAD-7 showed excessive bleeding problems when eluted with 0.1N NaOH, even when elution was quick and efficient. Table 2.2 also shows that XAD-4 has greater than twice the surface area of XAD-2, but the capacity for fulvic acid on the XAD-2 resin is almost twice the capacity on XAD-4. XAD-7, and XAD-8 have higher adsorption capacities and are more efficient adsorbents for the concentration of fulvic acid.

The hydrophobic effect is the principal driving force for sorption on these resins. Sorption of humic acid is determined by the

Table 2.2: Properties and Characteristics of XAD Resins
(Aiken, 1979)

Resin	Composition	Average Pore Diameter (Å)	Specific Surface Area (m ² /g)	Specific Pore Volume (cm ³ /g)	Distribution Coefficient KD	Solvent Uptake (g/g dry resin)	Elution Efficiency (%)
XAD-1	Styrene						
	Divinylbenzene	200	100	0.69	475		70
XAD-2	Styrene						
	Divinylbenzene	90	330	0.69	515	0.65-0.70	75
XAD-4	Styrene						
	Divinylbenzene	50	750	0.99	332	0.99-1.10	70
XAD-7	Acrylic Ester	80	450	1.08	1480	1.89-2.13	98
XAD-8	Acrylic Ester	250	140	0.82	604	1.31-1.36	98

solutes' aqueous solubility and solution pH (Malcom et al., 1978). The sorption process is achieved by lowering the pH of the sample, resulting in the protonation of the weak acids. These weak acids then adsorb to the resin. Elution of the adsorbed humic substance is achieved at higher pH when desorption is favored as weak acids are ionized. Resins such as XAD-12 and XAD-16 have also been introduced (Cheng, 1977). Cheng (1977) found that XAD-12 with weak base functional groups was a very hydrophilic XAD resin and the best sorbent for humic acid. However, because of precipitation of humic acid at low pH, pH 5 was found best for sorption of fulvic acid. XAD-7, XAD-8, XAD-12, and XAD-16 need further comparison to determine the most efficient resin.

2.1.1.3 Aquatic Humic Substances and Particle Interaction

There is a growing body of evidence indicating that the surface charge of most suspended particles from a variety of estuaries and natural waters is negative (Loder and Liss, 1985; Hunter and Liss, 1979; Hunter, 1983; Tipping and Ohnstad, 1984; Tipping, 1981; Tipping et al., 1981; Hunter, 1982; Hunter, 1980). These researchers have shown that the surface charge, hence, the electrophoretic motility (U_E) of the particles in estuaries falls in the range of -0.7 to $-2.0 \times 10^{-8} \text{ m}^2 \text{ S}^{-1} \text{ V}^{-1}$. In fresh waters, Hunter and Liss (1979) also identified negatively charged particles with narrower U_E between -0.55 to $-2.0 \times 10^{-8} \text{ m}^2 \text{ S}^{-1} \text{ V}^{-1}$ for several rivers. Particulate matter from natural waters, contains a variety of minerals as well as organisms. Some of these minerals, e.g. iron

oxides, and hydroxides, would be expected to exhibit positive electrophoretic mobility in pure systems of similar pH (Parks and DeBruyn, 1962). It is therefore surprising that electrophoretic measurements of natural samples have not detected more positively charged particles.

The predominance and the limited range of the negative U_E that are observed, despite the wide mineralogy of the samples examined, is usually attributed to the particles being covered by a coating of organic or oxide material. Studies by Neihof and Loeb (1972), Neihof and Loeb (1974), Loder and Liss (1984), Hunter and Liss (1979), and Tipping (1986) have all shown that adsorbed humic substances are of overriding importance in determining the surface charge (electrokinetic shear potential) of the particles. Researchers have shown that goethite particles added to surface water samples from lakes of widely differing chemistry become negatively charged because of the adsorption of humic substances (Tipping and Cooke, 1982; Loder and Liss, 1984). The magnitude of the negative charge decreased with increasing concentration of the divalent cations, Ca^{2+} and Mg^{2+} . They proposed that the large molecular size of the humic substances causes the plane of electrokinetic shear to be some distance from the oxide surface. The shear potential is due to increased humic functional groups not involved in adsorptive interactions with the oxide surface.

Tipping (1981) found that humic substances are adsorbed on iron oxides (α -FeOOH, α -Fe₂O₃, amorphous Fe-Gel). The extent of adsorption decreased with increasing pH. They proposed a mechanism involving ligand exchange of humic anionic groups with H₂O and OH-

of the surface Fe-OH_2^+ and Fe-OH groups. The degree of protonation of the adsorbed humic increased as the adsorption density increased at constant pH.

Hunter and Liss (1982) found that in rivers of low dissolved cation content, especially Ca^{2+} , the electrophoretic mobility, U_E , was negative at all salinities. U_E increased as ionic strength decreased. In rivers draining calcareous terrain and having relatively high Ca^{2+} content, U_E showed a similar dependence on salinity above 5-10 ppt but no marked increase in magnitude at lower salinities. The absence of positively charged particles, and the high uniformity of the charge distribution of the samples, in spite of the mixed nature of the suspended matter, led them to conclude that there was a dominant control of surface properties by adsorbed organic matter, metallic oxides, or both. Further supporting evidence was obtained by the DOC measurements which indicated a sufficient supply of organic matter for the adsorption process.

Davis (1982) reported that organic matter is readily adsorbed by alumina and kaolinite in the pH range of natural waters, and adsorption occurred by complex formation between surface hydroxyls and the acidic functional groups of the organic matter. Oxides with relatively acidic surfaces hydroxyls (e.g. silica) do not react strongly with organic matter. Potentiometric titration and electrophoresis measurements indicated that most of the acidic functional groups of the adsorbed organic matter were neutralized by protons from solution. Davis (1982) stated that under conditions typical for natural waters, almost complete surface coverage by organic matter may be expected for alumina, hydrous iron oxides,

and the edge sites of aluminosilicates. He concluded that the extent of surface charge coverage by adsorbed organic material is dependent on pH, the relative amounts of surface area and adsorbable organic compounds in the system, the nature of solid surface, and the inorganic electrolyte composition.

Humic substances may affect the surface chemistry of particulate matter in natural aqueous systems in view of their interaction with particles. The coating of particulates with humic substances and the influence of parameters such as pH should be understood if successful coagulation of particulate matter is expected.

2.1.1.4 Aquatic Humic Substances and Particle Removal Mechanisms

Aquatic humic substances and particles can both exert a significant coagulant demand. They may compete for the hydrolysis species when aluminum or iron are used for coagulation. Although one may attempt to discuss their removal separately, as it has widely been reported in the literature, their removal is not independent from one another because they both occur in water sources where coagulation is used for drinking water supplies.

Understanding colloidal chemistry is the key to approaching the coagulation process. Destabilization of colloidal particles consists of two steps. The first involves the transport to effect contact. This is mainly due to hydraulic considerations. The second process is the destabilization to permit attachment. The size of

colloid (0.001 to 1 μ m) is such that attractive body forces between particles are considerably less than the repelling forces of the electrical charges. Under these conditions, particle growth does not occur, and Brownian motion keeps the particles in suspension (Tchobanoglous and Schroeder, 1985). The principal mechanism controlling the stability of hydrophilic and hydrophobic particles is electrostatic repulsion. In the case of hydrophobic surfaces, an excess of anions or cations may accumulate at the interface, producing an electrical potential that can repulse particulates of similar surface potential. For typical hydrophilic surfaces, electrical charges arise from dissociation of inorganic groups located on the particle surface or interface. In addition, particles can also be stable due to the presence of adsorbed water molecules that provide a liquid barrier to successful particulate collisions (Montgomery, 1985). The principal electrical charges on the particle surface arise from crystal imperfection, preferential adsorption of specific ions, and specific chemical reactions of inorganic groups on the particulate surfaces.

Colloidal coagulation is achieved by an electrostatic mechanism in which various oppositely charged species compact the electrical double layer surrounding a colloidal particle, thereby reducing its repulsive forces (Rubin and Blocksidge, 1979). According to Randtke (1987), colloidal destabilization, precipitation and coprecipitation are the three primary mechanisms whereby coagulation can remove organic contaminant. He proposed that there are four secondary mechanisms whereby colloids can be destabilized; electrical double layer (EDL) compression, adsorption

and charge neutralization, adsorption and bridging, and enmeshment in a precipitate commonly referred to as sweep floc. EDL compression is not likely to be significant under water treatment conditions, but the other three mechanisms can and do occur during water treatment, depending upon the specific conditions of the treatment and water quality. Each of the mechanisms can result in the removal of particulate organic matter.

Colloidal destabilization results only in the removal of particles and not the removal of dissolved contaminants from true solution. Precipitation and coprecipitation also can remove contaminants from solution. Kolthoff (1932) distinguished four types of coprecipitations: isomorphic inclusion, nonisomorphic inclusion, occlusion, and surface adsorption. In isomorphic inclusion the impurity substitutes into the crystal lattice for a lattice ion of similar chemical characteristics. This is not possible for humic substances removal because the size and characteristics of these molecules are such that they cannot be incorporated into the lattice structure of the metal hydroxides. Nonisomorphic inclusion results in the impurities appearing dissolved in the precipitate. Occlusion occurs when the impurity, differing in size or chemical characteristics from the lattice ions, is adsorbed at the lattice sites as the crystals are growing, producing crystal imperfections. In surface adsorption, the impurity is not incorporated into the internal structure but is adsorbed only on the outer surface of the precipitate.

There is a phenomenon, generally overlooked in particulate natural organic matter removal, which involves the adsorption of

organic substances onto inorganic particles and some organic particles such as plant debris (Randtke, 1987). The portion associated with the particles can be removed through colloid destabilization. Identification of the mechanisms of contaminant removal requires that a determination be made whether the material being removed is colloidal or truly dissolved. This is difficult in the case of humic substances since there is debate as to their physical state. In practice, dissolved versus colloid separation is accomplished with 0.45 μm filtration. But one should keep in mind that this is an operational means of separation and does not reflect whether the material is truly dissolved or not.

A strong case can be made for the colloidal behavior of humic substances although they pass through a 0.45 μm filter. A summary of mechanisms of humic acid removal is presented in Table 2.3. The table shows the removal conditions as colloid destabilization (Edwards and Amirtharajah, 1985), or precipitation and coprecipitation (Hall and Packham, 1965). The removal of fulvic acid may be similar to that of humic acid by coagulation, but there is one very important difference between humic and fulvic acid. Fulvic acid is soluble at pH1.0. This is highly significant because it suggests that fulvic acid cannot be coagulated by simple charge neutralization. Colloids can generally be coagulated at their zero point of charge, which should be at approximately pH2 for fulvic acid (Randtke, 1985). The solubility at pH value below the zero point of charge is a strong evidence that fulvic acid is in true solution and not colloidal.

The pathways and mechanisms of aluminum reacting with

Table 2.3: Possible Mechanisms for the Removal of Humic Substances by Coagulation (Randtke, 1987)

<u>Conditions</u>	<u>Removal Mechanism(s) assuming Humic acid is Colloidal</u>	<u>Removal Mechanism(s) assuming Humic acid is in True Solution</u>	<u>Comments</u>
Acid addition to pH 1.0	Charge neutralization by H ⁺ perhaps accompanied by EDL compression	Precipitation of the insoluble acid of a soluble salt	Humic acid is insoluble at pH 1.0 by definition
Metal salts at low pH (5-6)	Charge neutralization by positively charged hydrolysis products	Precipitation of Aluminum or Iron humate	Relatively low dosage required; hydroxides may not ppt.; dosage proportional to humic acid conc.
Metal salts at high pH (7-8)	Enmeshment in a precipitate: adsorption and bridging; or perhaps charge neutralization, with higher dosages required due to competition with hydroxide or to less positively charged hydrolysis species	Precipitation of Aluminum or Iron humate impeded by precipitation of hydroxides; or coprecipitation, involving adsorption of humic acid onto metal hydroxide particles	A higher dosage of coagulant is required than at low pH; dosage increases as humic acid and pH increase; metal hydroxides are precipitated
Polymers	Charge neutralization or adsorption and bridging	Precipitation of insoluble polymer-humate complexes	Dosage proportional to humic acid concentration
Lime softening pH 9.5-10.5	Enmeshment in precipitating calcite, perhaps with heterogeneous nucleation on humic particles	Precipitation of calcium humate; adsorption of humic acid onto calcite nuclei and crystals	Removal may be poor unless another coagulant is added
Lime softening pH above 11	As above, aided by charge neutralization by positively charged magnesium hydroxide complexes and nuclei	As above, but with adsorption onto positively charged Magnesium hydroxide particles the primary mechanism	Magnesium hydroxide also precipitated; excellent removal possible

turbidity (particles) are better understood than those involving its reactions with organics. Turbidity removal can be achieved by two mechanisms: Charge neutralization and $\text{Al}(\text{OH})_3(\text{S})$ precipitation resulting in sweep floc (Stumm and O'Meila, 1968; Snodgrass et al., 1984). Charge neutralization involves the adsorption of positively charged monomers and hydroxo polymers of aluminum onto negatively charged particles. This neutralizes the charge on the particles and permits aggregation to occur during flocculation processes. The precipitation mechanism involves the formation of aluminum hydroxide solid which can collide and aggregate with particles responsible for turbidity.

Extensive review of turbidity and humic substance removal can be found in the literature. Amirtharajah and Mills (1982), for example, have established domains of humic acid and turbidity removal as a function of pH and $\log \text{Al}_t$ concentration as shown in Figure 2.8. The removal mechanisms for each zone are described. Hubel et al. (1987) found that high molecular weight polymers used as coagulant aids with alum produced turbidity removal but not trihalomethane formation potential (THM) precursor removal. High charge density cationic polymers, as coagulant aid with alum, provided good precursor removals at low alum dosages. Sinsabaugh III et al. (1986) reported that larger molecular weight organics were more readily precipitated than smaller ones. Ionic compounds were more effectively removed than neutral compounds. Hydrophilic and hydrophobic organics were preferentially removed over compounds of intermediate solubility. Fulvic acid was readily precipitated. Low molecular weight neutral compounds were the dominant precursor

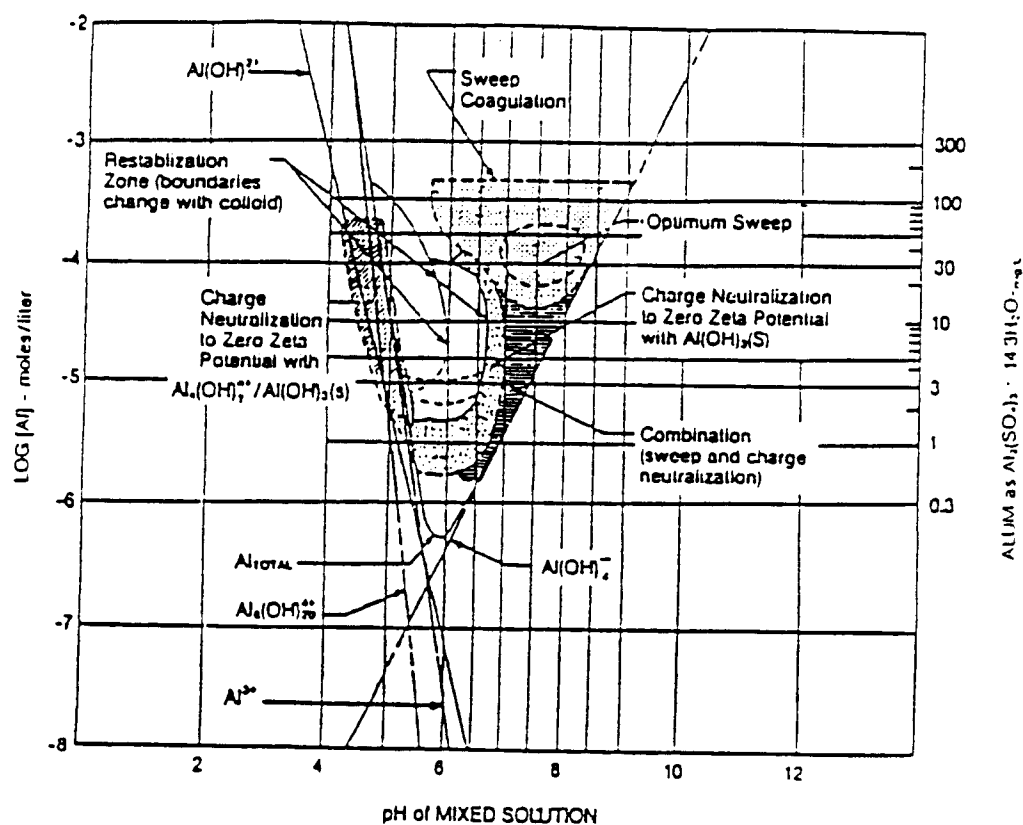


Figure 2.8: Design and operation diagram for alum coagulation (Mills and Amirtharajah, 1982)

group remaining in treated water.

Humic substances removal can be obtained by other processes in water treatment. For example, softening processes improve fulvic acid removal (Marcia et al., 1983; Randtke, 1987). Marcia et al. (1983) found that fulvic acid adsorbs to calcium carbonate crystal during the early stage of the softening reactions. Randtke (1987) suggested that the softening process can be modified to improve the removal of fulvic acid without compromising the removal of hardness. Research by Dempsey et al. (1981), Wiesner and Veronique (1986), Rubin and Blocksidge (1979), Snodgrass et al. (1982), Edzwald (1986), Gordon (1979), Edzwald et al. (1974), Letterman et al. (1986) have all shown the extent of humic substance and particle removal.

2.2 INFLUENCE OF SULFATE IN WATER TREATMENT

2.2.1 Importance

Sulfate is generally introduced in water supplies from several sources including watershed drainage from rainfall and snowmelt. The other source of sulfate comes from the use of aluminum sulfate during coagulation of water. The proportion of sulfate added in coagulation can always be calculated.

The increase in atmospheric deposition is being strongly cited for the increase in sulfate concentration in natural waters (Nichols et al., 1986; Chung, 1978; Tang et al., 1986; Dillons et al., 1986). Nichols et al. showed the relationship between wet

deposition and sulfate concentration in 82 clearwater lakes from North Central Minnesota to Central Lower Michigan as indicated in Figure 2.9. deGrosbois et al. (1986) measured sulfate concentrations ranging from 100 $\mu\text{eq/l}$ to 250 $\mu\text{eq/l}$ in streams in a small catchment basin in central Ontario. Kerekes et al. observed that as emission of SO_2 in Sudbury, Ontario declined, so did the sulfate concentration in four lakes studied in the area. Measured concentrations in the lakes varied from about 350 $\mu\text{eq/l}$ to 1200 $\mu\text{eq/l}$.

Most water treatment plants in the USA use alum as a coagulant. As a result of the alum addition, sulfate is usually added in the treatment process. Sulfate addition and sulfate from watershed drainage make this ion ubiquitous in natural waters along with other major anions, such as chloride, nitrate, and carbonate species. The exact role played by sulfate ion is of significance because of its possible impact on coagulation.

2.2.2 Role in Hydrolysis precipitation of Aluminum

Sulfate, a tetrahedral polyvalent anion, is reported to have various effects in coagulation. Schraroenchaikit and Letterman (1987) found that at pH6 and low sulfate concentration ($<3 \times 10^{-4}\text{M}$), the kinetics of coagulation of 10 μm diameter polystyrene particles treated with aluminum salt can be described using a first order rate equation. However, at higher sulfate ion concentration ($\geq 3 \times 10^{-4}\text{M}$) the kinetics of aggregation were no longer first order. The extent of the deviation from the predicted first order rate equation was

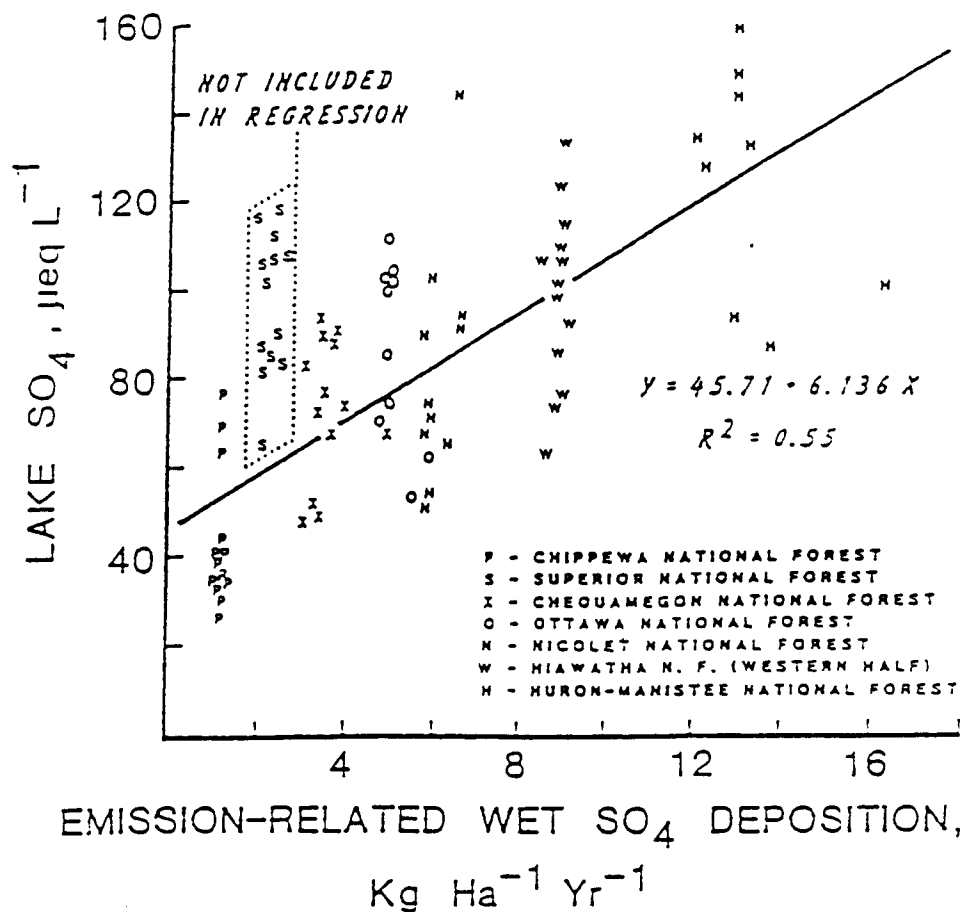


Figure 2.9: Increase sulfate concentration in 82 clearwater lakes relation to emission-related wet sulfate deposition
(Nichols and McRoberts, 1986)

thought to be dependent on the concentration of sulfate ion, aluminum salt, and the mixing intensity. At the high sulfate concentration, the kinetics of polystyrene particle aggregation were described by a modified Saffman and Turner model (1956). The modification was based on the author's assumption that upon sulfate addition, initially unadsorbed aluminum hydrolysis products in a polynuclear, possibly microcrystalline form, are transported to the surface of the aluminum hydrolysis product-coated particles by a combination of turbulent fluid transport and Brownian diffusion. When double layer repulsion between interacting coated polystyrene particles was negligible, the model suggested that the uptake of unadsorbed aluminum hydrolysis products causes the total volume concentration of the polystyrene particle suspension to increase, and the collision efficiency for colliding particles to decrease. However, when double layer repulsion is significant, the expanded model predicted that the uptake of unadsorbed aluminum hydrolysis products is negligible because of the high positive charge of the microcrystals and coated polystyrene particles.

Snodgrass et al. (1984) found that sulfate accelerates the rate of particle formation and changes the particle size distribution over time (1-40 μm size range). The rate of detectable particle formation was increased by sulfate at high pH. A decrease in aluminum to sulfate ratio ($\text{Al}:\text{SO}_4$), from 1:1.5 to 1:0.5, resulted in an increase in the time for the detection of the smallest particle size by up to 12 minutes. Particle sizes of $1\mu\text{m}$ were detected in aluminum solution ($\text{Al}:\text{SO}_4$ of 1:1.5) within 15 minutes, while no particles were detected in aluminum chloride solution (Aluminum =

$1.8 \times 10^{-4} \text{M}$).

In aluminum fulvate solutions, sulfate may catalyze the formation of aluminum hydroxide, and aluminum polymers which react with negatively charged fulvic acid. This reaction can result in particles growing to form large aggregates (De Hek, 1978). Sulfate has been reported to form complexes with aluminum ions during formation of aluminum hydrolysis species (DeBruin et al., 1975). Complex formation, due to screening of positive charges on polynuclear species by sulfate, allows nucleation and particle growth. Randtke (1987) hypothesized that sulfate can widen the optimum pH range for removal of particulate organics by complexing with positively charge particles, while at the same time competing with organics in solution for hydrolyzed metal species, and for adsorption sites.

De Hek et al. (1978) developed titration curves of aluminum (III) solutions (OH/Al vs pH) showing differences when sulfate, or nitrate is present. Precipitation occurred at a much earlier stage when sulfate was present ($\text{OH}/\text{Al} = 0.4$, pH3), and a plateau develop in all aluminum titrations where little change in pH occurred with the hydroxide addition. A characteristic second second plateau seen in aluminum chloride and aluminum nitrate titration disappeared except at low sulfate cocentration for aluminum sulfate titrations. They found that most, if not all of the sulfate ions removed from solution during precipitation were adsorbed. No evidence for the existence of basic sulfate in the precipitate was found. The role of sulfate was seen as that of a catalyst. Sulfate lowers the free energy barrier to the orientation and ordering of plate-like, highly

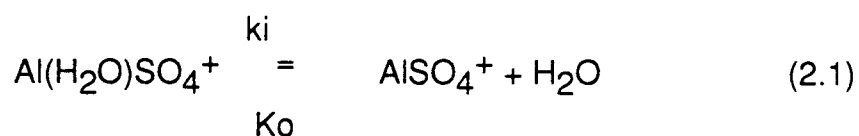
charged, polynuclear complexes into growing solid phases. A comparison of the precipitation behavior in sulfate solution to that in nitrate solutions indicated floc formation at a later stage when chloride was present. Observation led them to conclude that aluminum supersaturation develops in the chloride solution which eventually results in the nucleation and initial growth of the solid phase on the second plateau. The conclusion reached for the nitrate solution was similar to that of chloride solution. The occurrence of two characteristic plateaus was also observed by Vermeulen et al. (1975).

Hsu (1977) suggested that sulfate tends to link OH-Al polymer together, in a distorted arrangement due to steric effects. This may explain why most basic salts containing sulfate are amorphous. Norstrom (1982) indicated that at a sulfate concentration of 10^{-4}M and pH below 4.5, aluminum sulfate may precipitate. Hsu and Bates (1964) also noted the formation of amorphous basic aluminum sulfate and chloride precipitates.

2.2.3 Sulfate Interaction with Aquatic Humic Substances and Aluminum

From the work of De Hek et al. (1978), Vermeulen et al. (1975), Stol et al. (1976), Hayden and Rubin (1976), adsorption and precipitation appear to be the two modes of sulfate removal from solution. Under acid conditions where complications due to hydrolysis of the metallic cation Al^{3+} may be minimized, formation of AlSO_4^+ is likely to occur. This complex has been reported by

Stryker et al. (1969). However, because of the unavoidable interference of the action of hydrolysis of aluminum, there is a wide spread in the measured values for the stability constants for aluminum sulfate complexes (De Hek, 1978). A distinction is made between inner and outer sphere complexes as illustrated by:



where k_i is the rate constant for the formation of the inner sphere complex and K_o is that for the outer sphere complex $\text{Al(H}_2\text{OSO}_4^+)$. Behrb and Went (1962) believed that the outer sphere complex $\text{AlH}_2\text{OSO}_4^+$ makes the major contribution to the observed complexation reaction. These complexation studies provide evidence for ion pair formation between Al^{3+} and SO_4^{2-} .

De Hek et al. (1978) suggested that the sulfate ion strongly adsorbed on the growing positive solid particles. They concluded that it is possible to view the interfacial region separating the solid phase from the bulk solution phase chemically as a basic sulfate surface complex. This surface complex has a varying composition depending on the pH and cannot be treated as a bulk phase. Hayden and Rubin (1976) postulated that soluble and insoluble polynuclear sulfatohydroxo-aluminum (III) species occur based on their precipitation studies. Hsu and Bates (1964) reported that the amorphous precipitates they observed were basic aluminum sulfate or chloride.

2.3 INORGANIC ALUMINUM CHEMISTRY

2.3.1 Aluminum and Other Coagulants

The two primary functions of a chemical coagulant are particle destabilization and strengthening of flocs to reduce floc breakup (Montgomery, 1985). Chemicals serving one or both of these purposes must also satisfy several practical constraints, including low cost, ease of handling and availability, and chemical stability during storage. In addition, the coagulant must form either highly insoluble compounds or adsorb strongly on particulate surfaces. The objective is to minimize the concentration of soluble residuals that pass through the treatment plant.

The most common inorganic coagulants used in water treatment are salts of aluminum, $\text{AlCl}_3 \cdot \text{XH}_2\text{O}$, $\text{Al}(\text{NO}_3)_3 \cdot \text{XH}_2\text{O}$, alum ($\text{Al}_2(\text{SO}_4)_3 \cdot \text{XH}_2\text{O}$), and iron salts. Alum has been extensively used in the United States. Alum can be purchased in either dry or liquid form. However, dry alum cost 50% more than an equivalent amount of liquid alum. Usually only users of small amounts purchase dry alum (Davis and Cornwell, 1985).

Organic polymers, also called polyelectrolytes, were introduced in the United States by the early 1950s and have been widely used in water coagulation. Polymers are long chain molecules consisting of repeating chemical units with a structure designed to provide distinctive physico-chemical properties (Montgomery, 1985). In water treatment, they are designed to be soluble, and to adsorb completely or react rapidly with particulates. In contrast to

aluminum or ferric ions, polymers do not produce voluminous flocs. This makes them advantageous in applications where low floc volumes are desirable, as is the case with direct filtration. Their cost constitutes their major disadvantage.

Both natural (i.e. sodium alginate, chitosan) and synthetic organic polymers are available. Among the synthetic organic polymers are nonionic, anionic, and cationic polymers. Cationic polymers destabilize particles such as clay suspension through charge neutralization. Anionic polymer destabilize particles through polymer-bridging mechanisms.

A recently introduced coagulant in the United States, polyaluminum chloride (PACl), has been used in Japan and to some extent in Europe for some time (Hundt, 1985). The commercial preparation of this coagulant involves the partial neutralization of an AlCl_3 solution at elevated temperature and pressure. Alum is then added to produce an Al_2O_3 equivalent concentration of about 10% by weight and a ratio of 0.16 moles of sulfate per mole of aluminum. The neutralization ratio of the coagulant ($\text{OH}:\text{Al}$) is reported by the manufacturer to lie between 1.35 and 1.8 (Wiesner et al., 1986). PACl has been reported to successfully remove humic substances and particulate from water (Weisner, 1986; O'Meila and Dempsey, 1984; Hundt, 1985).

2.3.2 Aluminum Speciation

The hydrolysis of aluminum is one of the most researched areas in water chemistry. Despite these efforts, however, there is

no consensus on the exact species of aluminum present because the aqueous chemistry of aluminum is complex. A number of workers (Hsu et al., 1964; Serna et al., 1977) favor the concept that OH-Al polymers are fragments of solid aluminum hydroxide, their size varying with their basicity. Other researchers believe that species of aluminum can be separated into several categories (Bersillon, 1980). The only agreement is that dissolution of aluminum salts in water in the absence of complexing anions results first in the hydration of the free metal ion Al^{3+} to form several species.

A good account of the conflicting views is described in a series of publications by Akitt et al. (Akitt et al., 1972; Akitt et al., 1981 part 1; Akitt et al., 1981 part 2; Akitt et al., 1981 part 3). The majority of the reported studies have been made by potentiometric techniques. The studies can be categorized into two groups.

The first group noted that as alkali is added to a dilute aluminum salt solution, there is only a slow change in pH until 2.5 moles of alkali have been added per mole of aluminum. Equilibrium is attained slowly in these solutions and aging must be allowed to take place before meaningful pH values can be obtained (Brosett, 1952). This behavior has been interpreted as indicating the formation of the ion $Al_n(OH)_{2.5n+0.5n}$, where n can have numerous (mostly even) values from 2 to 13, high values being preferred. X-ray crystallographic analysis has supported this view (Akitt et al., 1981).

The second group of experiments (Grunwald and Wing, 1969; Sullivan, and Singley, 1980), in which the effect of adding acid or progressive dilution of the pure salt solution is measured, resulted

in the conclusion that the monomer hydrolysate $[\text{Al}(\text{OH})(\text{H}_2\text{O})_5^{2+}]$ or the dimers are the only species formed. Akitt et al. (1981) indicated that both views are correct and speciation depends on the degree of hydrolysis of aluminum. The monomer $\text{Al}(\text{H}_2\text{O})_6^{3+}$ and its hydrolysate are still present at high degrees of hydrolysis.

Various monomeric and polymeric species have been proposed. Baes and Mesmer (1976) proposed monomeric species Al^{3+} , AlOH^{2+} , $\text{Al}(\text{OH})_2^+$, $\text{Al}(\text{OH})_3$, and $\text{Al}(\text{OH})_4^-$, and polymers $\text{Al}_2(\text{OH})_2^{4+}$, $\text{Al}_3(\text{OH})_4^{5+}$, $\text{AlO}_4(\text{Al}(\text{OH})_2)_{12}^{7+}$ (or Al_{13}), and a solid precipitate $\text{Al}(\text{OH})_3\text{S}$. Benschoten et al. (1988) indicated that above pH4, monomeric forms $\text{Al}(\text{OH})_n^{3-n}$ ($n=1-4$), and polynuclear hydrolysis species $\text{Al}_m(\text{OH})_n^{3m-n}$ are formed. Bersillon et al. (1978) concluded that at pH7, Al^{3+} , $\text{Al}(\text{OH})_2^+$, and $\text{Al}(\text{OH})_3$ are the predominant monomers. $\text{Al}(\text{OH})_2^+$ is present in the pH range of 4.5 to 5.0. In alkaline solution (pH7.7 to 9.5), the $\text{Al}(\text{OH})_4^-$ species is reported by Hem and Roberson (1967) to be the predominant monomer.

Several hydrolysis constants taken from Hundt (1985) and Rezanian (1985) are shown in Table 2.4. These values are based on a statistical analysis of titration experiments and on chemical identification of the polymers.

Polymeric species have been suggested. Such species include $\text{Al}_2(\text{OH})_2^{4+}$, $\text{Al}_3(\text{OH})_2^{5+}$, $\text{Al}_8(\text{OH})_{20}^{4+}$, and $\text{Al}_{13}\text{O}(\text{OH})_{20}^{7+}$ (Hayden and Rubin, 1974; Hayden and Rubin, 1976; Rezanian, 1985; Hundt, 1985). In general, the polymeric species are considered as metastable structural intermediates between aluminum monomers and $\text{Al}(\text{OH})_3(\text{S})$ (Hundt, 1985). Rezanian (1985) suggested that although the existence of $\text{Al}_8(\text{OH})_{20}^{4+}$ has been reported by Hayden

Table 2.4: Summary of Aluminum Hydrolysis constants

Hydrolysis	logK	reference
Monomers		
$\text{Al}^{3+} + \text{H}_2\text{O} = \text{AlOH}^{2+} + \text{H}^+$	-4.97	(1)
	-5.0	(4)
	-5.03	(2)
Mixed Constant	-5.55	(3)
$\text{Al}^{3+} + 2\text{H}_2\text{O} = \text{Al}(\text{OH})_2^+ + 2\text{H}^+$	-9.3	(1)
$\text{Al}^{3+} + 3\text{H}_2\text{O} = \text{Al}(\text{OH})_3 + 3\text{H}^+$	-15.0	
$\text{Al}^{3+} + 4\text{H}_2\text{O} = \text{Al}(\text{OH})_4^- + 4\text{H}^+$	-23.0	(1)
	-22.75	(3)
	-21.84	(1)
Polymers		
$2\text{Al}^{3+} + 2\text{H}_2\text{O} = \text{Al}_2(\text{OH})_2^{4+} + 2\text{H}^+$	-7.7	
	-6.27	(2)
$3\text{Al}^{3+} + 4\text{H}_2\text{O} = \text{Al}_3(\text{OH})_5^{25+} + 4\text{H}^+$	-13.94	
$8\text{Al}^{3+} + 2\text{OH}_2\text{O} = \text{Al}_8(\text{OH})_{20}^{4+} + 20\text{H}^+$	-68.7	(3)
$13\text{Al}^{3+} + 28\text{H}_2\text{O} = \text{Al}_{13}\text{O}_4(\text{OH})_{20}^{7+} + 32\text{H}^+$	-98.73	
or		
$13\text{Al}^{3+} + 34\text{H}_2\text{O} = \text{Al}_{13}(\text{OH})_{34}^{5+} + 34\text{H}^+$	-97.4	(4)
	-96.7	(2)

1 Baes and Mesmer (1976)

2 Black and Chen (1967)

3 Hayden and Rubin (1974)

4 Stum and O'Meila (1968)

and Rubin (1974), such species are probably important only in the initial stages of coagulation, and at low pH values (less than 5).

The solid precipitate $\text{Al}(\text{OH})_3(\text{S})$ as, mentioned, earlier has been observed. Its nature, however, is uncertain (Dempsey, 1987). Reported values for pK_{so} at 25°C and $I=0$ range from 8.1 (Gibbsite) (May, 1979) to 10.8 (amorphous solid) (Stumm and Morgan, 1981). Hem (1967) Found that the microcrystalline gibbsite that formed at slightly acid conditions has a pK_{so} of 9.35. Johnson and Amirtharajah (1982), and Amirtharajah and Mills (1982) assumed a value of 10.37 for the construction of stability and removal diagrams. The calculated values for the pK s depend on the selection of hydrolysis constants for the monomeric species of aluminum. Dempsey (1987) reported that $\text{Al}(\text{OH})_3(\text{S})$ forms over a broad pH range when alum is used to remove fulvic acid. Hem et al (1967) found that $\text{Al}(\text{OH})_3(\text{S})$ forms between pH 7.5 and 9.5 and is initially composed of a boehmite material which changes to bayerite after aging for 10 days. The uncertainties in the solubility product of $\text{Al}(\text{OH})_3(\text{S})$ have been discussed by Hsu and Bates (1984), O'Meila and Dempsey (1982), and Stumm and Morgan (1981). The concentration of soluble aluminum in equilibrium with $\text{Al}(\text{OH})_3(\text{S})$ may be much higher than in equilibrium with Gibbsite, because of the range of solubility constants reported.

The solubility diagram shown in Figure 2.10 is also often used to establish the zone of aluminum species formation with respect to pH (from O'Meila and Dempsey 1982). The data for Figure 2.10 was taken from Baes and Mesmer. The solubility of Gibbsite was used in this diagram. The dashed lines represent uncertainties

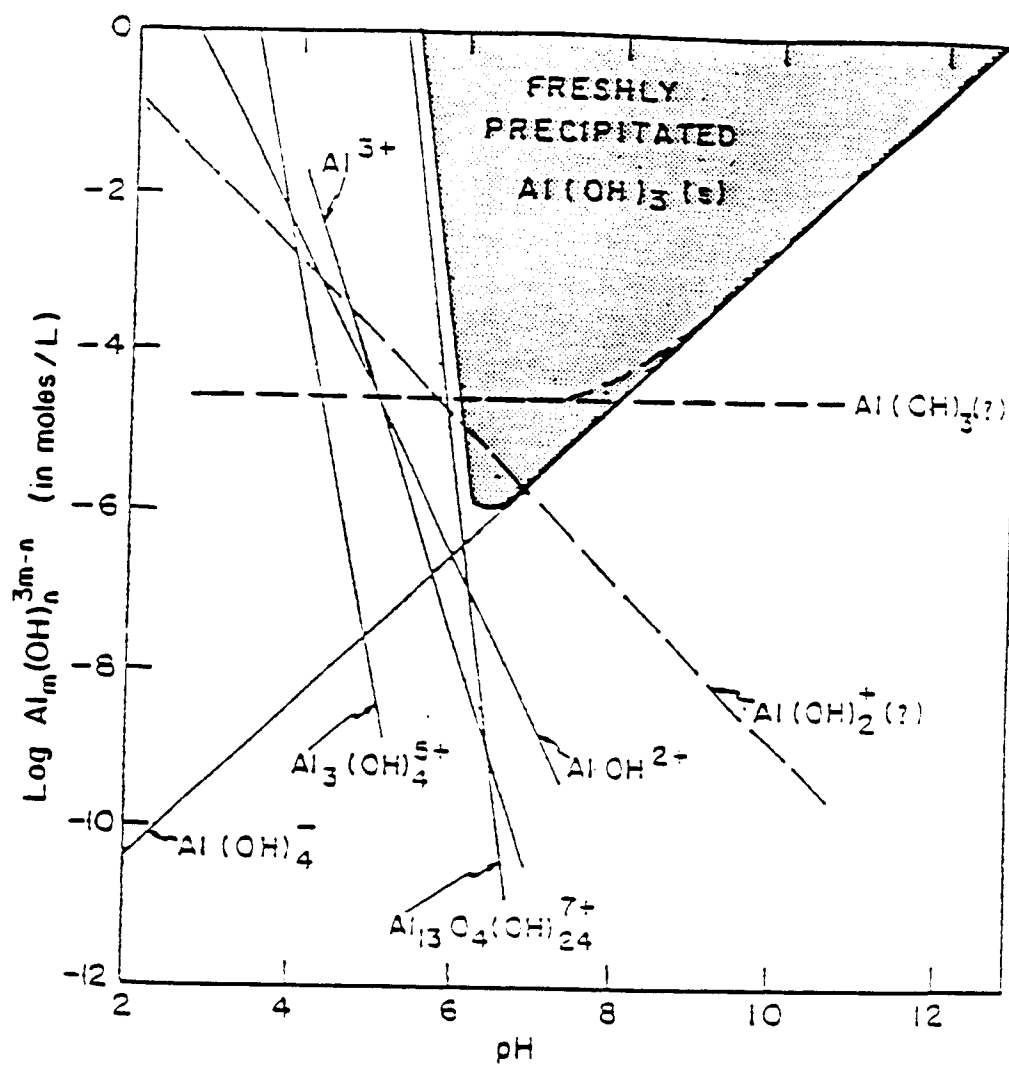
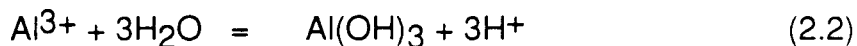


Figure 2.10: Solubility of precipitated amorphous $\text{Al}(\text{OH})_3(\text{s})$
O'Melia and Dempsey (1982)

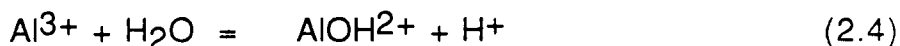
of the data for Al(OH)_2^+ and $\text{Al(OH)}_3 \text{ aq.}$

Species determination can also be done graphically (Rezania, 1985). In the presence of $\text{Al(OH)}_3 \text{S}$, the following relation is obtained:



$$\text{with } K = \{\text{H}^+\}^3 / \{\text{Al}^{3+}\} \quad (2.3)$$

All other hydrolysis species in equilibrium with $\text{Al(OH)}_3 \text{S}$ (Table 2.4) would be just a simple function of $\{\text{H}^+\}$. For example given:



$$K_{1,1} = \{\text{AlOH}^{2+}\} \{\text{H}^+\} / \{\text{Al}^{3+}\} \quad (2.5)$$

therefore,

$$\{\text{AlOH}^{2+}\} = K_{1,1} \{\text{Al}^{3+}\} / \{\text{H}^+\} \quad (2.6)$$

$$\{\text{AlOH}^{2+}\} = K_{1,1} \{\text{H}^+\}^2 \quad (2.7)$$

If AlOH^{2+} is the predominant dissolved species, a plot of \log (dissolved aluminum ion concentration) versus pH gives a slope of -2; if the major species is Al(OH)_2^+ , the slope is -1; a slope of 0, and +1 is given for $\text{Al(OH)}_3 \text{S}$, and Al(OH)_4^- respectively.

2.3.3 Aluminum Fractionation

The existence of aluminum species and their importance has led to numerous attempts to analytically fractionate these species in water. Turner (1969) developed a timed colorimetric procedure with Oxine (8-hydroxyquinoline) to distinguish between fast reacting, presumably monomeric aluminum species (reaction time $t=10-30$ sec) and slow reacting polynuclear forms (reaction time $t=30$ min). Barnes (1975) described a modification of the Oxine method in

which filtered samples ($0.1\mu\text{m}$) were reacted with 8-Hydroxyquinoline, adjusted to pH8.3, and extracted in 30 sec or less with methyl isobutyl ketone. The extract was analyzed by flame atomic absorption spectrophotometry. Batchelor et al. (1986) have also characterized species of aluminum using a timed colorimetric analysis procedure. Their procedure was based on the rate and extent of reaction of the hydrolysis products with ferron. Four types of aluminum species were identified; instantaneously, rapidly, moderately, and slowly dissolving aluminum.

Bersillon et al. (1980) have also grouped the soluble aluminum species into at least four categories based on a modified aluminum-ferron method where sulfate precipitation and resin treatment were added to the original procedure. The first category, high OH-aluminum polymers, with residual positive charge of 0.33 or less per aluminum atom, are rapidly precipitated by Na_2SO_4 giving rise to the formation of non crystalline basic aluminum sulfate. Medium OH-aluminum polymers, the second group, form crystalline basic aluminum sulfate of composition $\text{Al}(\text{OH})_{2.56}(\text{SO}_4)_{0.22} \cdot \text{XH}_2\text{O}$, and enter the resin slowly. The third category, low OH-aluminum polymers, is not precipitable with Na_2SO_4 , and enter the resin rapidly. The final group, monomeric ions, enter the resin and react with ferron rapidly.

Modifications to these methods have been used by several researchers to determine the species of aluminum in water (Barnes, 1975; Driscoll et al., 1980; Driscoll, 1984). The method of Driscoll, for example, divides aluminum into reactive aluminum species, monomeric aluminum, as with Barnes' method, non-labile monomeric

aluminum, and labile monomeric aluminum. The reactive aluminum fraction was determined by acidifying the sample to pH1 and analyzing aluminum species using the method of Barnes. Non-labile monomeric aluminum, and labile monomeric aluminum were obtained using a cation exchange resin (Amberlite 120).

Campbell (1986) separated aluminum species into monomeric hydroxo-fluoro aluminum complexes, and aluminum fulvic and humic acid complexes by filtration and Chelex 100 ion exchange resin. Van Benschoten et al. (1988) presented another fractionation technique by a combination of acidification, filtration, complexation with 8-hydroxyquinoline, and cation exchange resin. Species reported included total reactive and dissolved aluminum, dissolved monomeric aluminum, dissolved organically bound aluminum, and dissolved organic monomeric aluminum. A modified cation exchange resin procedure originally developed by Driscoll was proposed by Tipping et al. (1988).

Hundt (1985) devised a protocol for determining species of aluminum shown in Figure 2.11. Five groups were identified; $\text{Al}(\text{OH})_3(\text{S})$, monomers, small polymers, medium polymers, and large polymers. $\text{Al}(\text{OH})_3(\text{S})$ is the precipitant obtained after filtration through a 0.45 μm membrane filter and then dissolved in 6N HCl. Monomeric species are determined from the filtrate. Stirring over a 10 minute period and adsorption on a Fisher Rexyn 101H (Fisher Scientific) provide for the conversion of some monomeric to polymeric forms. The filtrate contains the polymers and the remaining monomers. Precipitation with Na_2SO_4 and filtration through a 0.45 μm membrane filter speciates the large polymers.

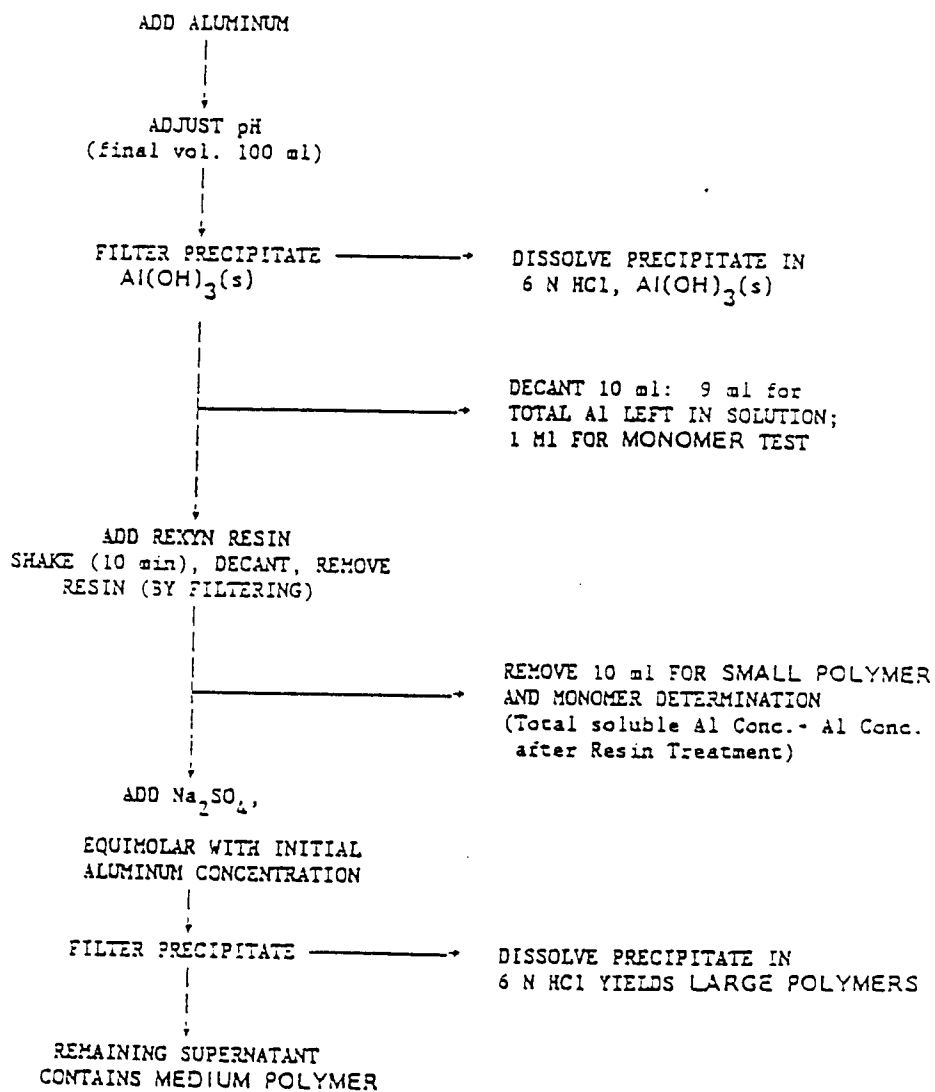


Figure 2.11: Aluminum speciation flow diagram
(Hundt, 1985)

The remaining supernatant supposedly contains medium polymers. The concentration of monomers and small polymers is calculated by taking the difference between the total soluble aluminum concentration minus the aluminum concentration after resin treatment. From this value, subtraction of the monomer concentration gives the concentration of the small polymers.

The results of aluminum speciation are dependent on the analytical procedure used. The distribution of four species of AlCl_3 at a concentration of $10^{-3.75}\text{M}$ is presented in Figure 2.12.

2.3.4 Importance of Aluminum in Anion Complexation

The chemical speciation of aluminum is further complicated in natural water because the hydrolysis species come in contact with contaminants, including anions. For example in acidic water, Al^{3+} forms complexes with OH^- , F^- , SO_4^{2-} , and organic compounds such as humic substances (Hem, 1968; Tipping et al., 1988). The treatment of water containing high concentrations of these alumino complexing ligands may lead to high concentrations of soluble Al complexes. These complexes may not be removed by filtration because the soluble complexes may not be incorporated in the filterable precipitates. In a precipitation study, Costello (1984) noted that residual aluminum is a significant problem in systems that apply high dosages of alum to remove color-causing organics. Driscoll and Letterman (1988) reported aluminum species formation in a study on the Metropolitan Water Board of Onondaga County Plant in Oswego, NY. The use of alum increased the total aluminum

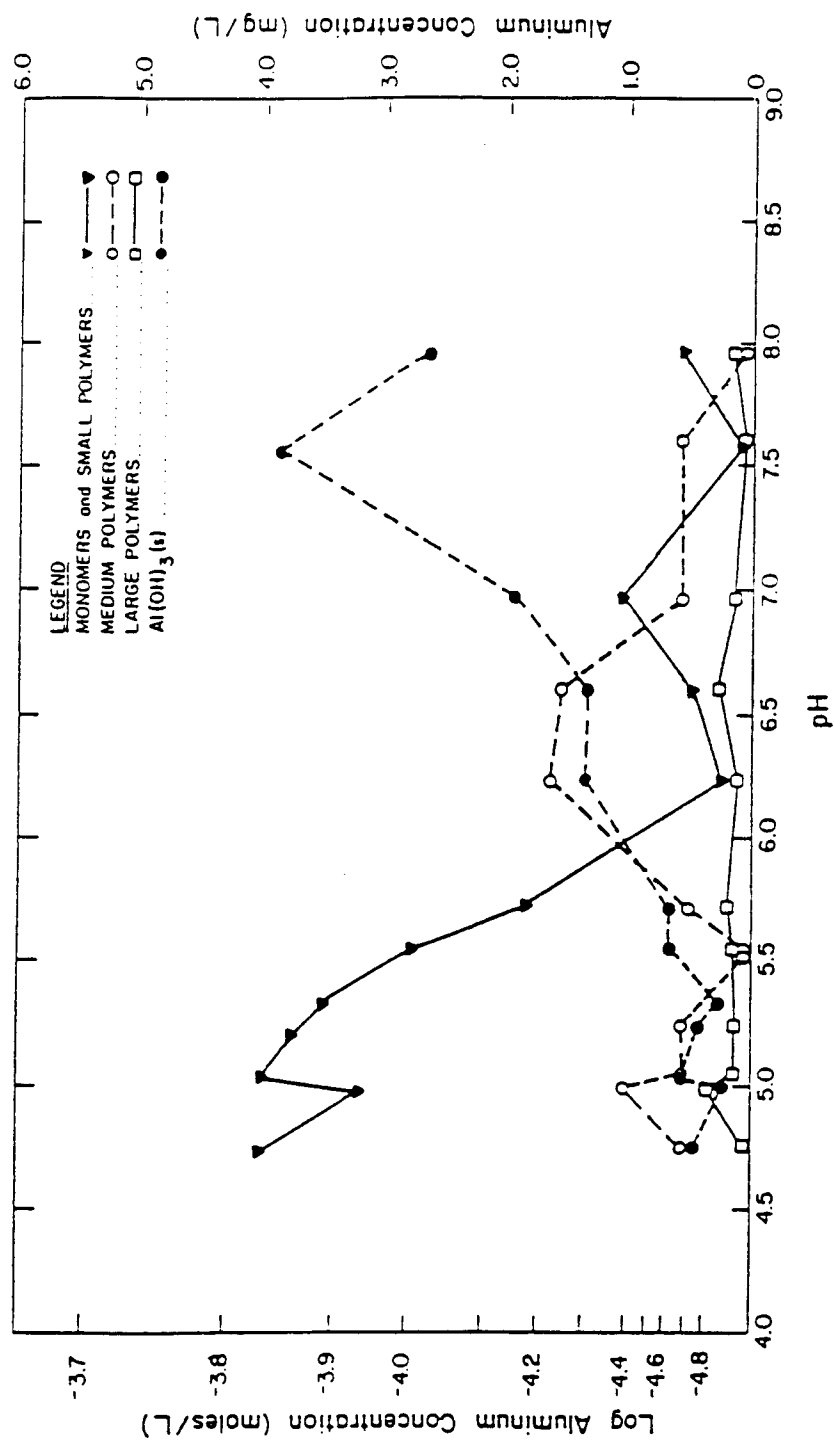


Figure 2.12: Aluminum speciation diagram, AlCl_3 ($10^{-3.75}\text{M}$)
(Hundt, 1985)

concentration from $0.37 \pm 0.33 \mu\text{mole/l}$ in the raw water to $1.8 \pm 0.33 \mu\text{mole/l}$ in the filtered water. The treated water contained only a small amount ($0.26 \pm 0.26 \mu\text{mole/l}$) of particulate aluminum. Of the remaining aluminum ($1.5 \pm 0.33 \mu\text{mole/l}$), 29% was associated with organic matter ($0.44 \pm 0.30 \mu\text{mole/l}$), 52% was present as monomeric alumino-hydroxide complexes ($0.81 \pm 0.37 \mu\text{mole/l}$), and 19% was complexed with Fluoride ($0.30 \pm 0.15 \mu\text{mole/l}$).

The presence of anions in solution such as sulfate, nitrate, oxalate, and phosphate has long been reported to influence the coagulation chemistry (Miller, 1925). The pH of coagulation was found to be dependent on the anions present. Miller postulated that the effects were due to the formation of a solid aluminum hydroxide. Chloride ion at high concentrations was found to shift the pH of optimum coagulation slightly to the acid side. Sulfate in concentrations from 25 to 250 mg/l, widened the range of rapid coagulation toward the acid side. The widening effect became greater with increasing sulfate concentration. However with phosphate, even at very low concentrations, a marked shift in the pH of optimum coagulation to lower values resulted with little or no broadening of the pH range.

Marion and Thomas (1946) developed a theory to explain the effect of anions on the pH of maximum precipitation of aluminum hydroxide. They suggested the formation of complexes. Aluminum species stability and solubility were considered to have a strong dependence on the anions present. A mechanism proposed for the behavior of the anion was based on the basicity of the anion, the affinity of the anion for aluminum, and its resistance to

displacement by hydroxide ion. The rules advanced were as follows:

- 1) If the anion is a strong coordinator with aluminum and not replaced by hydroxide ion, the pH of optimum precipitation will drop sharply with increase in anion concentration.
- 2) If the anion is a strong coordinator with aluminum but can be displaced by hydroxide ion, the pH of optimum precipitation increases with a very basic anion, and decreases with a weakly basic anion.
- 3) If the anion is only a very weak coordinator with aluminum, it exerts only a slight effect on optimum precipitation generally in the direction of lower pH values.

Stumm and Morgan (1962) reported results of alkalinity titrations confirming that coordinating anions have a marked effect on the pH of optimum precipitation. They concluded that in the case of strongly coordinating anions the chemical equilibria involving complex formation were more important in coagulation than the double layer compaction by counterions. The reverse was true in the case of weakly coordinating anions.

Evidence was presented by Dempsey (1987) that complexation occurs between aluminum and fulvic acid. The average stability function ($\log K$) reported was 3.39 within pH range from 4.30 to 8.08. This value is higher than would be expected in complexation of carboxylic functional groups but considerably lower than complexation of Al(III) by hydroxide.

Several computer models have been developed to perform chemical equilibrium calculations to determine the concentration

and distribution of inorganic and organic species (Cosby et al., 1985). The models rely on thermodynamic calculations for prediction. Aluminum speciation models are based on equilibria with the solid phase $\text{Al}(\text{OH})_3(\text{S})$ (O'Melia and Dempsey, 1982). However departure from $\text{Al}(\text{OH})_3$ solubility have been reported (Schecher et al., 1987).

A computer program (ALCHEMI) developed by Schecher and Driscoll (1987), Schecher and Driscoll (1988) attempts to predict pH-aluminum species distributions with F, SO_4 , and inorganic C in water. ALCHEMI considers aqueous complexes with OH^- , F, and SO_4 ligands. The program is flexible enough to permit calculation at equilibria with hydroxide, hydroxysilicate, or hydroxysulfate mineral phase or without solid phase considerations. Solution pH is the master variable. Electroneutrality relations are also incorporated. The concentration of the water chemistry parameters (concentrations, initial pH, temperature, etc...) are set before running the program. Titration is performed by the program and the equilibrium aluminum species are plotted at incremental pH values.

2.4 SENSOR FOR $\text{Al}(\text{III})$ MEASUREMENT

2.4.1 Significance in Water Treatment

Despite extensive use of aluminum coagulants in water treatment, treatment plant operators, typically, do not monitor effluent aluminum because of the difficulties and time constraint in measuring aluminum. Turbidity and color are monitored instead.

Additionally, there is no incentive to monitor the residual aluminum in finished water because the USEPA has not set a maximum contaminant level. USEPA has only proposed a guidance level of 0.05 mg/l; a maximum contaminant level may be recommended at a later date. Nevertheless, there are serious implications concerning the lack of aluminum monitoring. Barnett et al. (1969) reported that the use of aluminum sulfate as a coagulant in the treatment of drinking water increased the aluminum concentration in the finished water. Robert et al. (1984) indicated that there was a 40 to 50% chance that aluminum coagulation increases the aluminum concentration of the finished water above its original concentration in the raw water. A similar observation was reported for the Onondaga County, N.Y., water treatment plant (Driscoll et al., 1988). Aluminum concentration increased from $0.37 \pm 0.33 \mu\text{mole/l}$ in raw water to $1.8 \pm 0.33 \mu\text{mole/l}$ in the filter water. About 11% of the aluminum input was released to the distribution system in the treated water.

There is an urgent need to improve and expand analytical capabilities at the water treatment plant level that will provide the operator with real time in situ evaluation of aluminum concentration. Fiber optic sensing presents a great opportunity to provide for this need. Currently, interest in the use of fiber optics for remote in-situ chemical measurement is increasing in areas of biomedical as well as environmental applications (Angel, 1987; Hirschfeld, 1986; Seitz, 1984). In most applications, though, spectroscopy determination cannot be done directly. Usually, solid phase indicators attached to the end of a single optical fiber or a fiber bundle is used. The analyte interacts with the indicator to

produce an optical detectable charge which is probed through the optical fiber.

Among the analytical possibilities, continuous Al(III) is particularly amenable to optical sensing (Sarr, 1983; Saari, 1983) because Al(III) forms fluorescence complexes with several otherwise nonfluorescent ligands. The method is selective because Al(III) measurements are made in the 3 to 6 pH range where relatively few other metal ions complex with the ligands that respond to Al(III). In the context of water treatment, Fe(III) is probably the only interference of concern. In high concentrations, Fe(III) will interfere negatively by forming a non fluorescent complex (Saar, 1980). Recently, Saari (1983), and Seitz et al. (1989) have successfully identified and used indicators in fiber optic chemical sensing. Their optical fiber instrument was used to evaluate the feasibility of Al(III) measurement in the present study. A morin-based polyvinyl alcohol (PVOH) sensor was developed and experimented with.

The indicator used, Morin (3, 5, 7, 2', 4', - pentahydroxy flavone), belongs to the large class of flavonoid compounds which are aromatic phenols of the general structure C6-C3-C6. Flavones are compounds of plant origin, which have been studied in relation to subjects such as the fermentation of tea, tanning of leather, manufacture of cocoa, and the flavor of food (Saari, 1983). Morin, one of the most reactive and sensitive among the flavones, can be synthesized from the wood of Artocarpus integrifolia and Toxylon pomiferum (Katyal, 1968). Morin has also been widely used for the fluorometric analyses of Al(III) (Katyal, 1977).

Morin is only weakly fluorescent by itself, but forms highly fluorescent complexes with Al^{3+} as shown in Figure 2.13. Complexation ties up nonbonding electrons which reduces their energy state. Therefore it is fairly common to have molecules that have $n-\pi^*$ lowest energy singlets when uncomplexed, and $\pi-\pi^*$ lowest excited singlets when complexed with metal ions (Saar, 1983). Complexation can cause a non fluorescent ligand to become fluorescent by changing the nature of the lowest excited singlet. The fluorescence and color of the metal complexes formed depends upon the number and position of the hydroxyl groups in the flavone molecule. The hydroxyl groups at the 3, 5, and 2' positions show the greatest effect on the fluorescence of the complex. Therefore Morin (3, 5, 7, 2', 4' - tetrahydroxyflavone) is one of the most reactive and sensitive among the flavone. Morin has also been used as a reagent for fluorometric analyses of aluminum and other metals as well as for spectrophotometric analyses of metals that do not form fluorescent complexes (Seitz, 1983; Katyal, 1977).

2.4.2 Theory

A brief discussion of the theory is presented. A detailed development is shown in Saari (1983). It is assumed that the total number of mobilized morin molecules, C , is much less than the number of aluminum ions in solution. Under these circumstances, the insertion of the sensor will not significantly affect the aluminum ion concentration in solution. Assuming a 1:1 complex, the equilibrium for aluminum binding to immobilized Morin can be

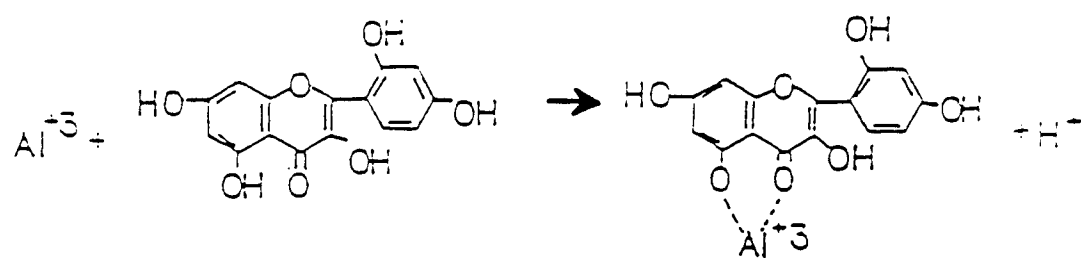


Figure 2.13: Formation of the morin-Al(III) complex.

represented as:

$$K = M_{Al} / (M a_{Al}) \quad (2.8)$$

where

M = number of immobilized Morin ligands not associated with aluminum

M_{Al} = number of immobilized Morin ligands associated with aluminum ion

a_{Al} = the aluminum metal ion activity in solution

K = equilibrium constant

Because the total number of immobilized Morin molecules C is fixed,

$$C = M + M_{Al} \quad (2.9)$$

Since Morin is essentially non fluorescent by itself and the Morin-aluminum complex is fluorescent, the fluorescence signal will depend on the amount of aluminum bound to the Morin:

$$I = k M_{Al} \quad (2.10)$$

where

I = fluorescence intensity

k = proportionality constant

In relating fluorescence intensity to the amount of aluminum bound to Morin, it is assumed that the conditions are such that intensity is proportional to the number of sites (i.e. no inner filter effects).

M_{Al} is calculated by substituting equation (2.9) into equation (2.8) as follows:

$$M = C - M_{Al} \quad (2.11)$$

$$k = M_{Al} / \{(C - M_{Al}) a_{Al}\} \quad (2.12)$$

$$k a_{Al} = M_{Al} / (C - M_{Al}) \quad (2.13)$$

$$(1 / K a_{Al}) = (C / M_{Al}) - 1 \quad (2.14)$$

$$M_{Al} = (C k a_{Al}) / (1 + a_{Al} k) \quad (2.15)$$

By substitution of equation (2.15) into equation (2.10), an expression for fluorescence intensity as a function of aluminum ion activity is obtained

$$I = (k C K a_{Al}) / (1 + a_{Al} k) \quad (2.16)$$

Using a linear form of equation (2.16),

$$a_{Al} / I = a_{Al} / k C + 1 / k C \quad (2.17)$$

K can be obtained from the slope and intercept of a plot of a_{Al} / I vs. a_{Al} .

2.4.3 Limitations

There are several potential problems with the fiber optics Al(III) sensing. These include the need to immobilize Morin on PVOH, the amount and shelf life of the immobilized morin, pH, and interfering compounds in solution. The pH is an important parameter in this technique because the equilibrium constant is pH dependent. In previous studies, Seitz et al. (1988) have determined that pH4.8 is the optimum at which 100% fluorescence intensity is obtained. The procedure can only be useful in water treatment if its utilization can be feasible in a wider pH range. It is possible to develop calibration curves at varying pH values and establish the change in fluorescence intensity.

The immobilization technique may also be too elaborate since it requires a trained operator, and additional reagent preparation time. This is a relatively minor concern, compared to the

advantages of the method. Interference from other compounds in solution may present the most difficult task to address. The claim of in-situ usage of the probe implies that it should be interference free. If not, the interfering compounds should be removed or inhibited. The most likely interferent would be iron because it can form non fluorescent complexes with Morin. These problems can only be addressed by investigating potential interferents. The study should focus on evaluating the performance of the immobilized morin, a matrix to encapsulate the immobilized morin.

CHAPTER 3

MATERIALS AND METHODS

3.1 EXPERIMENTAL APPROACH

The experiments were designed to address the four general objectives set forth for this work. The aim was to provide an understanding of some aspects of the influence of sulfate in aluminum coagulation chemistry of water. The objectives included a study of the role of sulfate in the hydrolysis precipitation of aluminum, the evaluation of aluminum coagulation of aquatic humic substances and particulates under varying pH and sulfate concentration conditions, the kinetics and adsorption isotherm of sulfate and aquatic humic substance on aluminum precipitates, and an investigation of a new analytical procedure to measure aluminum.

The first experiments consisted of a set of titrations to investigate the role of sulfate in the hydrolysis/precipitation of Al(III). Potentiometric titrations of $5 \times 10^{-2} \text{M}$ (as aluminum) aluminum chloride, aluminum nitrate, and aluminum sulfate solutions were done with 2N NaOH solutions. The resulting titration curves were evaluated and compared.

Several jar test experiments were performed next to evaluate the removal of AHS, and particulate under varying pH and

CHAPTER 3

MATERIALS AND METHODS

3.1 EXPERIMENTAL APPROACH

The experiments were designed to address the four general objectives set forth for this work. The aim was to provide an understanding of some aspects of the influence of sulfate in aluminum coagulation chemistry of water. The objectives included a study of the role of sulfate in the hydrolysis precipitation of aluminum, the evaluation of aluminum coagulation of aquatic humic substances and particulates under varying pH and sulfate concentration conditions, the kinetics and adsorption isotherm of sulfate and aquatic humic substance on aluminum precipitates, and an investigation of a new analytical procedure to measure aluminum.

The first experiments consisted of a set of titrations to investigate the role of sulfate in the hydrolysis/precipitation of Al(III). Potentiometric titrations of $5 \times 10^{-2} \text{M}$ (as aluminum) aluminum chloride, aluminum nitrate, and aluminum sulfate solutions were done with 2N NaOH solutions. The resulting titration curves were evaluated and compared.

Several jar test experiments were performed next to evaluate the removal of AHS, and particulate under varying pH and

sulfate concentrations conditions. Water samples containing aquatic humic substances, sulfate and bentonite clay were treated with varying concentrations of aluminum chloride. The variables of the experimental design were sulfate, aquatic humic substances, and pH. The aquatic humic substances (AHS) used were concentrated from a surface water sample. A sedimentation experiment was also undertaken to obtain a uniform size bentonite clay suspension which was used to provide constant turbidity to the water sample treated with aluminum. A titrimer (Fisher Scientific, Pittsburgh, PA) was used to maintain constant pH during each jar test.

The third set of experiments involved the adsorption of AHS and sulfate onto aluminum precipitate. Aluminum chloride and aluminum sulfate precipitate adsorbents were tested, along with the effect of pH variations on the adsorption process. Adsorption of sulfate and AHS on an aluminum chloride precipitate formed with AHS was studied in the second phase to simulate water treatment conditions where the aluminum precipitate forms in the presence of the contaminants. The last phase of these experiments examined the competitive adsorption between sulfate and AHS on the aluminum precipitate.

Finally, a sensor for Al(III) based on immobilized morin was introduced and its application in water treatment was investigated. This alternative continuous aluminum measurement technique was developed and tested. Several experiments were conducted with the morin immobilized on cellulose. The procedure was altered by entrapping immobilized morin on cellulose in a polyvinyl alcohol

matrix. The modification was introduced to improve the measurement techniques using the cellulose.

3.2 REAGENTS AND QUALITY CONTROL/QUALITY ASSURANCE PROCEDURES

All procedures were designed to ensure that the data obtained in this research were collected using standards and sound analytical procedures and instrumentation. The analytical methods are presented in Table 3.1. Most procedures were provided in Standard Methods (1980). Additions and exceptions are discussed where applicable. Table 3.2 describes the calibration procedures for each analytical/instrumental method.

Double distilled and deionized water (Milli Q, Millipore, Inc. Bedford, MA) was used to dilute all prepared reagents and standards unless otherwise stated. The system uses cartridges in four successive purification stages. The distilled water flows through a Super C cartridge, two ion exchange cartridges, and a MU-15 ultrafiltration cartridge. Dissolved species including carbon are removed to give a final effluent resistivity of 18 megohms/cm.

Type A glassware was used through the study. All chemicals were analytical reagent grade or higher unless otherwise stated. Reagent preparations are described with each procedure.

There were generally three glassware cleaning procedures. All glassware was initially washed with phosphate free soap and

Table 3.1: Analytical Procedures

Parameter Measured	Procedure	References
pH	Potentiometric	Standard Methods (1985)
Temperature	NBS calibrated Thermometer	Standard Methods (1985)
Turbidity	Nephelometric Turbidity	Standard Methods (1985)
UV Absorbance	Absorbance at pH7	Collins (1985)
Aluminum	AAS	Standard Methods (1985)
	Erichrome Cyanine R	Standard Methods (1985)
	Fiber Optic Sensing	Seitz (1985)
Sulfate	Ion Chromatograph	Standard Methods (1985)
	Modified Methyl Thymol Blue	Mc Swain et al. (1974)
DOC	UV-Promoted Persulfate Oxidation	Standard Methods (1985)
Particle Count	Electrical Conductivity	Coulter Electronics (1980)
Aquatic Humic Substances Concentration	Adsorption Chromatography	Aiken (1985)
Bentonite Clay	Sedimentation	Black (1965)

Table 3.2: Instrument Calibration Conditions

Instrumentation	Calibration and Routine procedures
AAS (Perkin Elmer, Norwalk, CT)	Daily Calibration
DC-80 TOC Analyzer (Dohrmann, Santa Clara, CA)	Daily Calibration Updates (Daily Read Backs)
Spectronic 2000 (Bausch and Lomb, Rochester, N.Y.)	Daily Zeroing
HF Turbidimeter (Hatch, Co., Ames Iowa)	Daily Calibration (Monthly Calibration check)
pH meter (Fisher Scientific, Bedford, MA)	Daily Standardization
Coulter Counter (Coulter Electronics, Inc, Hialeah, FL)	Calibrated as needed
Ion Chromatograph Dionex Co, Sunnyvale, CA)	Calibrated when needed (Daily read back)
Thermometer	
8200 Ultrafiltration Cell (Amicon, Co, Danvers, MA)	Daily Pressure Check

water and rinsed twice with Milli Q water. Most of the glassware was subsequently soaked in 50% HNO_3 for 24 hours, rinsed consecutively three times with distilled water, three times with Milli Q water and air dried before re-use. The 50% HNO_3 was replaced with fresh solution when the solution turned yellowish. All other glassware used in the analyses involving AHS were treated similarly except they were soaked in a chromic acid cleaning solution (CA). The CA solution was prepared by dissolving 120 g $\text{Na}_2\text{Cr}_2\text{O}_7$ in 1000 mL Milli Q water. While stirring the solution, 872 mL of concentrated sulfuric acid was slowly added. The solution was allowed to cool at room temperature and stored in a glass bottle. The CA solution was replaced when the solution started to turn turned green, indicating that the cleaning solutions had been reduced, and thus was no longer suitable for cleaning.

Gases used during this research included: 0 grade nitrogen in the adsorption study and 4.5 grade nitrogen for DOC analyses, AAS grade acetylene (2.6 grade), and AAS grade nitrous oxide (99.0% pure) for the AAS analysis, and helium (99% pure) and nitrogen 4.5 grade for the ion chromatographic analyses.

3.3 ANALYTICAL PROCEDURES.

Sulfate Analyses

Sulfate was analyzed according to either an improved Methyl Thymol Blue procedure for automated sulfate determination

(MTB) developed by Mc Swain et al. (1974) or using a Dionex Ion Chromatograph (Dionex Co., Sunnyvale, CA). The methyl thymol blue procedure was used for sulfate measurements in the coagulation study, and the Ion Chromatograph (IC) was used for all other sulfate measurements. A 1000 mg/L stock sulfate solution was prepared from reagent grade Na_2SO_4 . The stock solution was replaced monthly.

The MTB procedure depends on the relative reactivity of methyl thymol blue and sulfate with barium. When no sulfate is present, all the barium is complexed with methyl thymol blue producing a deep blue color. Barium sulfate is produced in the presence of sulfate ion and only the excess barium is complexed with methyl thymol blue producing a decrease in the blue color. When methyl thymol blue is uncomplexed, its color is gray. The barium-sulfate reaction must take place at pH 2.5-3.0, and the barium-methyl thymol blue reaction at pH 12.5-13.0.

The modification to the Technicon (Technicon Instrument Co., Tarry Town, NY) automated method consisted of the installation of a 16-0492 bubbler, instead of a 116-0489 bubbler recommended by the standard procedure, followed by a 157-B095 fitting. A debubbler was added on the methanol and color reagent lines. The sample to wash ratio was changed to 1:1. These modifications improved the bubbling pattern which is critical in the procedure. Daily standards (0.5, 1, 2, 4, 6, and 8 mg/L) were used to obtain calibration curves from which the sample concentrations were determined. Reproducibility was good in the 0 to 10 mg/L range. The

detection limit was estimated to be 0.08 mg/L. The detection limits were calculated as twice the instrumental response for system blank according to Miller and Miller (1984).

The Dionex IC was calibrated using 4 standards (1, 2, 4, 8 mg/L). The instrument was only calibrated every two weeks or when the reagents were replaced because little or no variation occurred within the two week period. Daily calibration checks consisted of replicate analyses of the four standards for quality control purpose. The diluents, regenerant, and all reagents required to run the IC were replaced every two weeks with fresh solutions. The Dionex Integrator Model 4270 (Dionex Co., Sunnyvale, Ca) program was updated with each calibration. Reagent blank checks consistently indicated no detectable level of sulfate in the diluents. An OnGuard-P (P/N 039597, Dionex Co., Sunnyvale, CA) pretreatment cartridge was used to remove organics from samples containing AHS. The cartridge contained a polyvinylpyrrolidone (PVP) polymer with a very high selectivity for phenolic, azo-containing compounds, aromatic carboxylic acids, and aromatic aldehydes. The cartridge removed the phenolic fraction of humic substances, which can foul anion exchange resins. The cartridge was regenerated after each use by siphoning 15 mL of Milli Q water, followed by 15 mL of 2 N NH_4OH , and 15 mL of Milli Q each at a flow rate of 4 mL/min. A 1000 mg/L of reagent grade Na_2SO_4 stock solution was used to make daily standards for both the MTB procedure and the IC. The Na_2SO_4 stock solution was replaced monthly with fresh solution.

Ultraviolet Absorbance Measurement

A Bausch and Lomb Spectronic 2000 (Bausch and Lomb Co., Rochester , N.Y.) with a 1 cm Spectrosil spectrophotometer cell (VWR Scientific, San Francisco, CA) was used for UV absorbance measurements. The sample and reference cells were matched 1 cm quartz cuvettes (Fischer Scientific, San Francisco, CA). The reagent blank and samples were adjusted to pH7 with a 0.001M phosphate buffer. The cells were cleaned by rinsing several times with Milli Q water. They were air dried before use.

DOC measurement

Dissolved organic carbon analyses (DOC) were performed on a Dohrmann DC-80 Automated Laboratory Total Organic Carbon Analyzer (Dohrmann Division; Xertex Corporation, Santa Clara, CA).

Sample and standards were acidified with two drops of 50% H_3PO_4 per 10 mL of sample and purged with 4.5 grade N_2 for 5 minutes to remove inorganic carbon. The sparging time was established in preliminary experiments. Several samples containing up to 10 mg/L AHS as DOC, 40 mg/L CaCO_3 alkalinity, and 0.001M C NaCl (see jar test experiment) were sparged for varying periods of time. No change in sample concentration was noted after sparging for 5 minutes. A similar conclusion was reached with the standard used for instrument calibration.

A single calibration was done with a 10 mgC/l KHP

standard. Readbacks standards of 1, 5, 10, 15, and 20 mgC/l standard showed that the calibration was linear over this range. The single point calibration was updated with daily injections of the 10 mgC/l standard. Daily readback standardization using 1, 5, 8, and 10 mgC/l standards were also performed after the calibration was updated. The calibration was always linear within this range. The DC-80 was recalibrated each time the instrument was not used for over a month or when the N₂ was replaced. The detection limit of the DC-80 was estimated to be 0.2 mg C/l (Miller and Miller, 1984).

Turbidity and Particle Count Measurements

The turbidity was measured with a HF turbidimeter model 2100A (Hach Chemical Co., Ames, Iowa). The meter was calibrated daily with sealed AEPA turbidity standards (Advanced Polymer Systems Inc., Redwood City, CA) after warming up for 30 min. The sealed standards were checked against primary turbidity standards from the same company every three months. These standards contained styrene divinyl benzene spheres with uniform particle size.

Particle count measurements were done using a Coulter Counter, model ZBI (Coulter Electronics, Inc., Hialeah, FL) fitted with a 30µm orifice and connected to a 100 window channelyzer. The settings were: Manometer, 70µl; matching switch, 40K; aperture current⁻¹, 0.25; and aperture, 0354. The samples were diluted with an Isoton (Coulter Electronics, Inc., Hialeah, FL) solution. The

solution provided the ionic strength adjustment necessary for the counting mechanism to work. The isoton diluent was also used for cleaning the particle counter.

The Coulter Counter was calibrated with 2.02 μm latex particles (Coulter Electronics, Inc., Hialeah, FL). Several dilutions of the latex particles were run through the counter to establish the optimum setting. This setting was used for sample analysis.

Aluminum Measurements

Aluminum was measured using three methods: Atomic absorption spectrophotometry (AAS), the eriochrome cyanine R colorimetry method as described in Standard Methods (1985), and a newly developed fiber optic sensor for Al(III) based on immobilized morin. A Perkin Elmer Model 2380 Atomic Absorption Spectrophotometry (AAS), equipped with a graphite furnace, model HGA 400 (Perkin Elmer Co., Norwalk, Connecticut) was used for low level aluminum measurements. The modified HGA program and a sample calibration curve are shown in the appendix. Flame analyses were also performed for sample containing 10 mg/L aluminum or higher. Gases used included acetylene, argon, and nitrous oxide.

Colorimetric measurements for the eriochrome cyanine R method were performed on a Bausch and Lomb Spectronic 2000 (Bausch and Lomb Co., Rochester, N.Y.) with a 5 cm Spectrosil spectrophotometer cell (VWR Scientific, San Francisco CA). The cells were treated as described in the procedure for UV

measurements. The detection limit was estimated to be 3 ppb (Miller and Miller, 1984).

Aluminum standards were prepared from either Fisher Scientific (Fisher Scientific, Pittsburgh, PA) or Baker Analyzer Certified Reagent Grade (J.T. Baker Analyzed, Phillipsburg, NJ) metal stock solutions (1000 mg/L). Aluminum solutions for flame AAS analyses contained 1% KCl and 1% HNO₃ in the flame mode. 0.05 mg Mg(NO₃) was added as a matrix modifier when the graphite furnace was used.

Aluminum standards were made in acetate buffer solutions for the morin-based fluorescence measurements. Acetate buffers were prepared according to the procedure described in Walpole (1914). Predetermined volumes of 0.2M acetic acid and 0.2M sodium acetate solutions were mixed to yield pH4.8 (optimum condition for the analysis) solution except for the experiments in which the effect of pH variations was studied. Dilution water was prepared by adding 20 mL of 0.2M acetic acid to 30 mL of 0.2M sodium acetate. This was diluted to a final volume of 100 mL with a final pH of 4.8. Serial dilutions consisting of two steps were made to prepare the daily aluminum standards. First, 2 mL of the 1000 mg/L stock aluminum solution were pipetted into a 200 mL volumetric flask. The solution was made up to volume with the buffer solution to give a 10 mg/L aluminum standard. The other standards were prepared from this 10 mg/L aluminum standard in the second step using the acetate buffer as diluent.

pH Measurements

A Fisher Scientific Computer Aided Titrimeter (CAT) system (Fisher Scientific, Pittsburgh, PA) equipped with a gel-filled Orion pH Combination Electrode (Orion Co., Boston, MA) model 91-55 and a Fisher Titration Controller equipped with a Fischer Scientific Platinum combination electrode model 13-639-281 were used to measure and control the pH. The precision of the systems were ± 0.001 pH or ± 0.1 mv respectively. The pH meters were calibrated before use with standards (VWR Scientific, Boston, MA) of pH4, 7, or 10 depending on the pH range of the samples.

3.4 PROCEDURE FOR THE HYDROLYSIS/PRECIPITATION OF Al(III)

3.4.1 Experimental Set-up

The behavior of Al(III) upon addition to water is of primary interest in coagulation. As discussed in Chapter 2, aluminum forms various species as a result of its reaction with hydroxide. The aluminum species formed react with the contaminants present in water as a function of parameters such as pH and aluminum dosage. This study was designed to evaluate titration curves of aluminum chloride, aluminum nitrate, and aluminum sulfate coagulants. The study focused particularly on the influence of SO_4^{2-} and other competing ions in the hydrolysis/ precipitation of Al(III). A 3 L

reactor, similar in design to the jar test reactor in the coagulation experiments (Figure 3.8), was used in conjunction with the Fisher Automatic Titrimeter.

3.4.2 Procedure

Two procedures were established in this determination. First, aluminum solutions were prepared by dissolving reagent grade aluminum chloride, aluminum sulfate, or aluminum nitrate in Milli Q water. The pH of the solutions was adjusted to 3 with 0.1 N HCl or 0.1N NaOH. The entire solution was filtered through a 0.45 μm membrane filter to remove particulates and hydrolysis products. 2 L of the filtrate were transferred to a 3 L Plexiglass reactor. The solutions were then titrated with 0.1N NaOH while stirring with a magnetic bar on a Nova II Stirrer (Thermoclyne Co., Dubuque, Iowa). N_2 (4.5 grade) was bubbled through the reactor (10psig) during the experiment.

A fixed end point pH titration program was set on the Fisher Titrimeter to titrate the solution to predetermined pH values and to record incremental additions of 2N NaOH. Care was taken during the titration to record the volume of 2N NaOH and pH at which visible floc was formed. The 2N NaOH was standardized with standard KHP as described in Day (1985). Titration curves relating OH/Al to pH were obtained by recording the initial pH, and determining the number of moles of OH^- added by incremental titration. The number of moles of aluminum was constant and was calculated from the

amount of titrated standard aluminum solution. The number of moles of OH^- added with the first incremental NaOH addition was added to the number of moles of OH^- calculated from the initial pH measurement. The pH corresponding to the first incremental NaOH addition was recorded after the pH reading had stabilized. Subsequent OH values were obtained by adding the number of moles of OH^- in each incremental volume of NaOH added to the number of moles of OH^- already present. The pH of each stage was recorded.

3.5 CONCENTRATION OF AQUATIC HUMIC SUBSTANCES

3.5.1 Source

Stock aquatic Humic substances were concentrated from local swamp samples near the mouth of the Oyster River in Durham, NH. A detailed description of this location is given in Weber (1973), and Weber and Truitt (1979). As has been pointed out by Davis (1980) and others, terminology regarding organic matter in natural waters is confusing. It is therefore appropriate to note that throughout the remainder of this dissertation, the total material obtained in the concentration scheme described will be referred to as Aquatic Humic Substance (AHS). The usual pH separation of the fulvic, and humic fractions was not performed since the research focused on the total fraction of the humic material that is dissolved in natural water.

3.5.2 Concentration scheme

The procedure, adopted from Malcom and Thurman (1979), is a combination of liquid-solid adsorption chromatography on non-anionic resins and pH adjustment. The AHS was concentrated on XAD-8 resin because this resin has a higher retention capacity and several advantages over the XAD resin used by other investigators (Hundt, 1985; Dempsey, 1981; Driscoll, 1980; Malcom, 1979; and Mantoura and Riley, 1975). In the procedure, the hydrophobic AHS is adsorbed on the XAD-8 resin at pH 2. The quantity of resin and the adsorption and desorption conditions were based on the hydrophobic-hydrophilic separation of Leenheer (1981). An illustration of the procedure is presented, followed by a description of the amount of resin used in this study for the AHS concentration.

3.5.3 Determination of Resin Adsorbent Capacity

Adsorption of organic solutes on XAD-8 resin, followed by elution, fractionates dissolved organic carbon (DOC) by hydrophobicity (Leenheer, 1981). The polarity of the solute and the ratio of the quantity of resin to the volume of water passed through the resin bed control the arbitrary hydrophobic-hydrophilic designation. The hydrophobic-hydrophilic break, however is not clear-cut, but is operationally-defined as the separation in which the crossover of hydrophilic solutes into the hydrophobic fraction can be mathematically defined. Hydrophobic solutes are defined in

DOC fractionation as those solutes that are greater than 50% retained on XAD-8 at a given ratio of resin to water passed through the column, and hydrophilic solutes are defined as those that are greater than 50% eluted at the same ratio of resin to water (Malcom, Thurman, 1979; Leenheer, 1981). This hydrophobic-hydrophilic designation in fractionation adsorption chromatography is illustrated in Figure 3.1. The diagram shows the breakthrough curve of a hypothetical organic solute from an XAD-8 column effluent. The breakthrough curve of Figure 3.1 shows that the integrated area of solute adsorption equals the integrated area of solute elution at:

$$V = 2 V_E \quad (3.1)$$

where V is the total elution volume and V_E is the elution or breakthrough volume.

It is useful to refer to the column distribution coefficient $K'_{0.5}$ which is the coefficient of a hypothetical solute 50% retained and 50% eluted at the hydrophobic-hydrophilic break. $K'_{0.5r}$, also called the hydrophobic-hydrophilic break, is determined by the following calculations.

The breakthrough (or elution) volume V_E of a solute from an XAD-8 resin column can be described as:

$$V_E = V_0 (1 + k') \quad (3.2)$$

Where

V_0 is the void volume and K' the mass of solute sorbed on XAD-8/mass of solute dissolved in water.

However, since the breakthrough volume V_E , where the effluent concentration is 50% of the influent concentration, does not

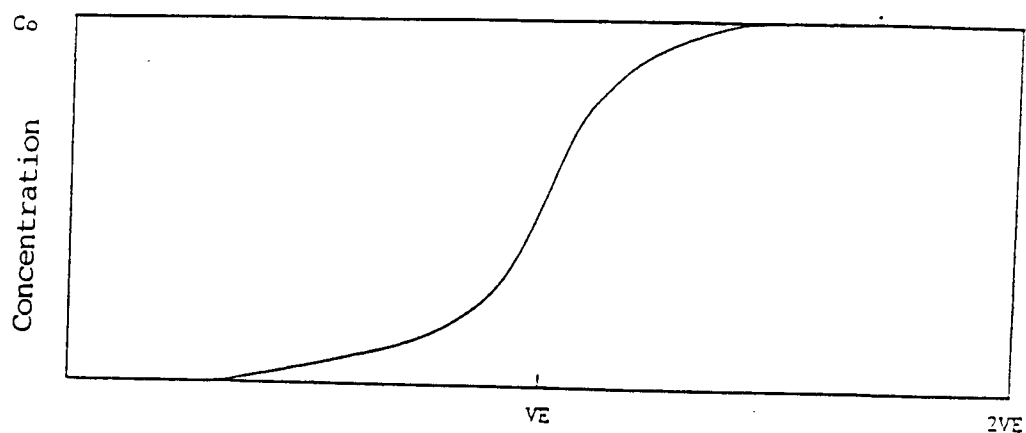


Figure 3.1: Frontal chromatography breakthrough curve
 C_0 Influent concentration
 VE Breakthrough volume (volume at $C = 0.5C_0$)
 $2VE$ Effluent volume of 50% retention, 50% elution

correspond to the effluent volume of 50% retention, a new term $V_{0.5r}$ is defined as:

$$V_{0.5r} = 2 V_E \quad (3.3)$$

To define the hydrophobic-hydrophilic break $K'_{0.5r}$ for $V_{0.5r}$, equation 3.3 is substituted into equation 3.2:

$$0.5 V_{0.5r} = V_0 (1 + K'_{0.5r}) \quad (3.4)$$

or

$$V_{0.5r} = 2 V_0 (1 + K'_{0.5r}) \quad (3.5)$$

For example, for a liter water sample processed through a DOC fractionation whose hydrophobic break is at $K'_{0.5r} = 50$, the following calculation can be made to determine the quantity of XAD-8 resin required:

$$V_{0.5r} = 1000 \text{ mL}$$

$$K'_{0.5r} = 50$$

$$1000 \text{ mL} = 2 V_0 (1 + 50)$$

$$\text{therefore } V_0 = 9.8 \text{ mL}$$

However, if the void volume of XAD-8 resin is 60% of its bulk volume as measured in this work, a $9.8/0.65$, or 15 mL column of XAD-8 resin would be required.

3.5.4 XAD-8 Resin Cleaning and Column Packing

The resin used, XAD-8, was obtained from Rohm and Haas (Rohm and Haas Co., Philadelphia, PA) and prepared by washing the beads with equal volumes (500 mL/ 200 g of resin) of 0.1N NaOH for five successive days to remove monomers and soluble, uncrosslinked

polymers. The resin was subsequently Soxhlet extracted sequentially for 24 hours with methanol, diethyl ether, acetonitrile, and methanol until ready for use. Before column packing, the resin-methanol solution was rinsed into a large beaker with Milli Q water by a slurry technique. The resin was packed as a methanol-water slurry and then rinsed with Milli Q water until free of methanol. Approximately 50 bed volumes of water were passed through the column until the DOC of the effluent to the column remained equal to that of the influent. The packed column was further rinsed 3 times, alternating from 0.1N NaOH to 0.1N HCl each time. The rinsing removed impurities which might otherwise be incorporated into the sample. The final rinse was with 0.1N HCl followed by Milli Q water. The pH was monitored to insure that the resin was acidic (pH 2). The column was immediately used following the cleaning. The resin beads were never drained throughout the process. The beaker containing the resin-cleaning agent slurry, and the column were covered with aluminum foil to prevent light from promoting any bacterial growth. The column was leveled and two siphon systems were set up to pump the water and the desorbing flow through the column. As indicated in Figure 3.2, the flow was controlled by the water level above the effluent port.

3.5.5 Concentration

The collected swamp water was filtered through a prewashed (Milli Q water), 80 μm fine mesh screen to remove

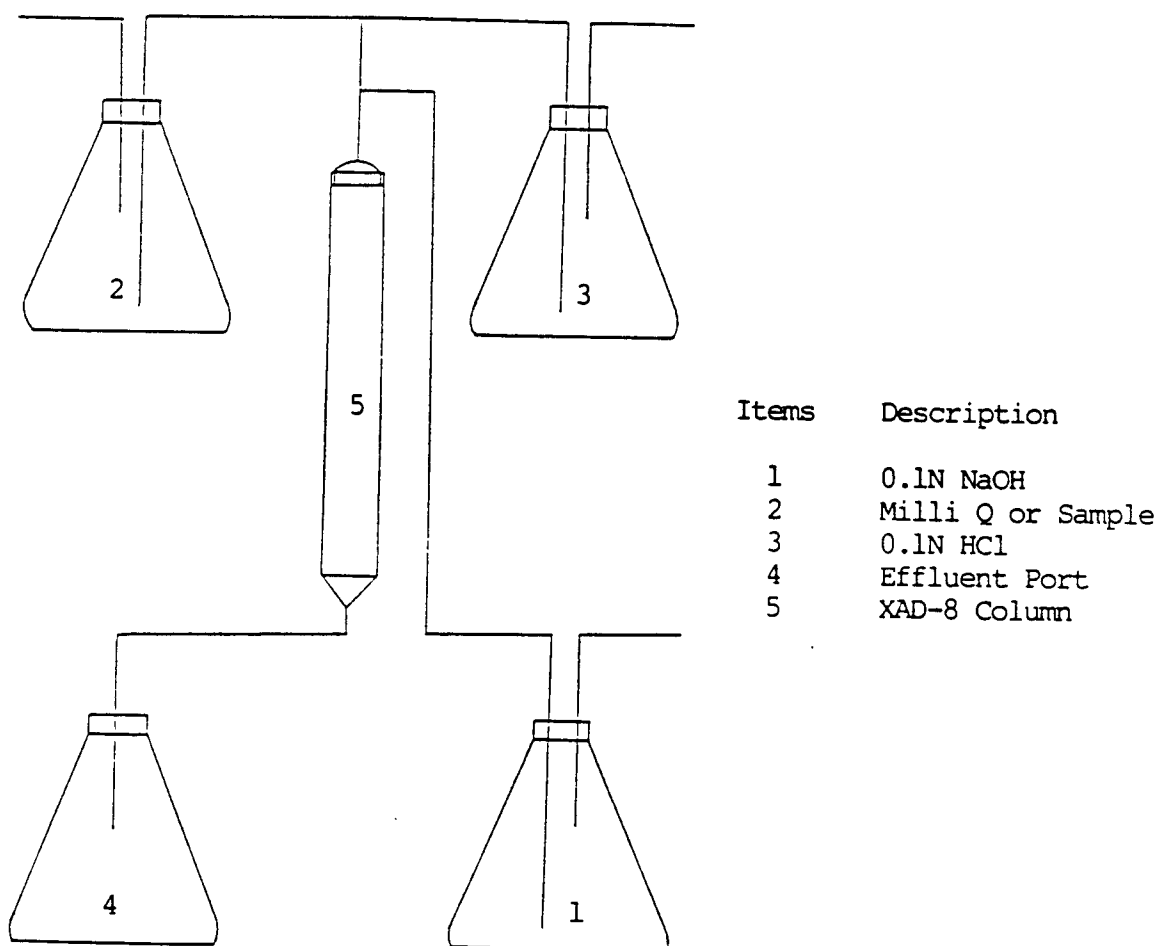


Figure 3.2: Schematic of aquatic humic substances concentration

sediments and debris. The water was then filtered through a cleaned 0.45 μm silver membrane filter (Millipore Co., Bedford, MA) to remove suspended matter. The cleaning of the filters for this, and all other uses consisted of washing with successive volumes of Milli Q water until the DOC of the filtrate remained equal to that of the Milli Q water. After filtration, the water sample was acidified to pH 2 with 0.1N HCl and siphoned through the cleaned XAD-8 resin column at a flow rate of 15 bed volumes per hour. The determination of the adsorption and desorption conditions is presented in Section 3.4.3. The hydrophobic AHS adsorbed on the XAD-8 resin was desorbed with 0.1N NaOH at a flow rate of 5 bed volumes per hour. To enhance recoveries, the sample which eluted ahead of the 0.1N NaOH eluate was saved and recycled through the XAD-8 column. The eluate was pumped through a 50 mL Fisher AGMP-50 cation exchange resin (Fisher Scientific Co., Pittsburgh, PA) for salt removal. The pH of the concentrated AHS was then adjusted to 7 to prevent denaturation of the AHS at a high pH. This eluate was used as a stock AHS solution. A standard curve shown in Figure 3.3 served to prepare the desired solutions of known DOC. A linear relationship was observed between UV absorbance and DOC as shown in Figure 3.4. Care was taken to store the solution in a dark glass sampling container at 4^o Celsius. The UV spectroscopy (Figure 3.5) indicates that the concentrated humic substances had a featureless spectra. This is consistent with other research on AHS (Schnitzer, 1972; Edzwald et al., 1985; Hundt, 1985) that have also shown that UV absorbance decreases with increasing wavelength.

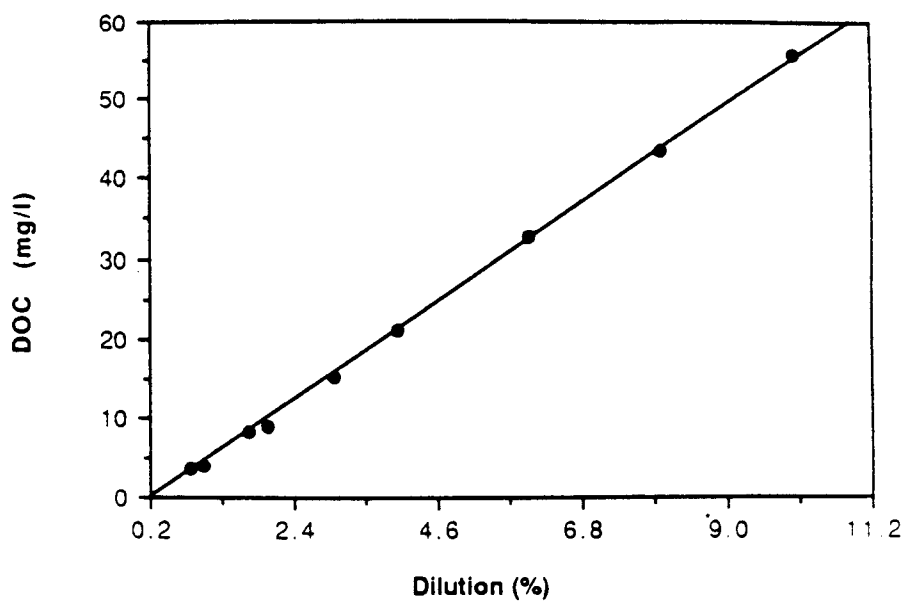


Figure 3.3: Standard curve for the aquatic humic substances stock solution

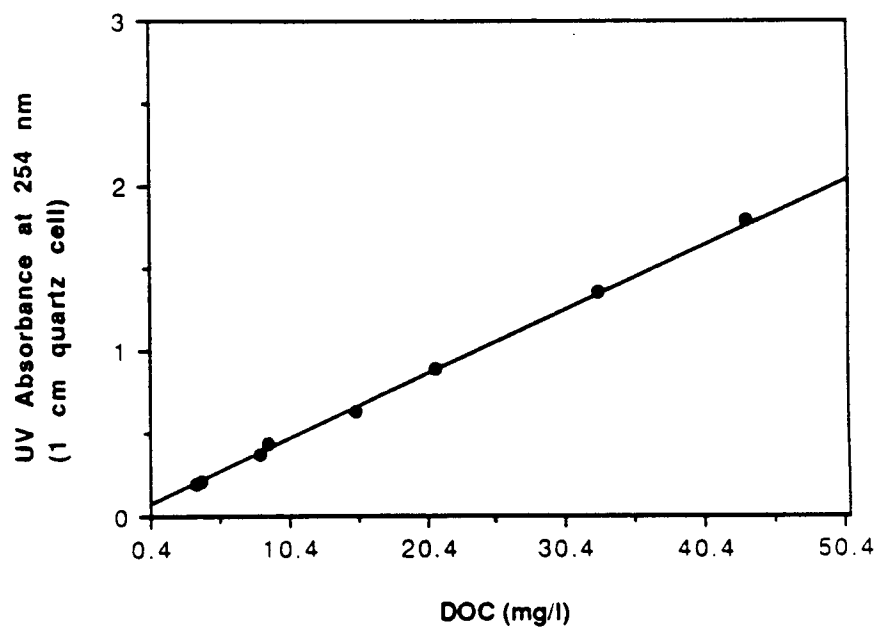


Figure 3.4: DOC VS UV absorbance of the stock humic substances stock solution

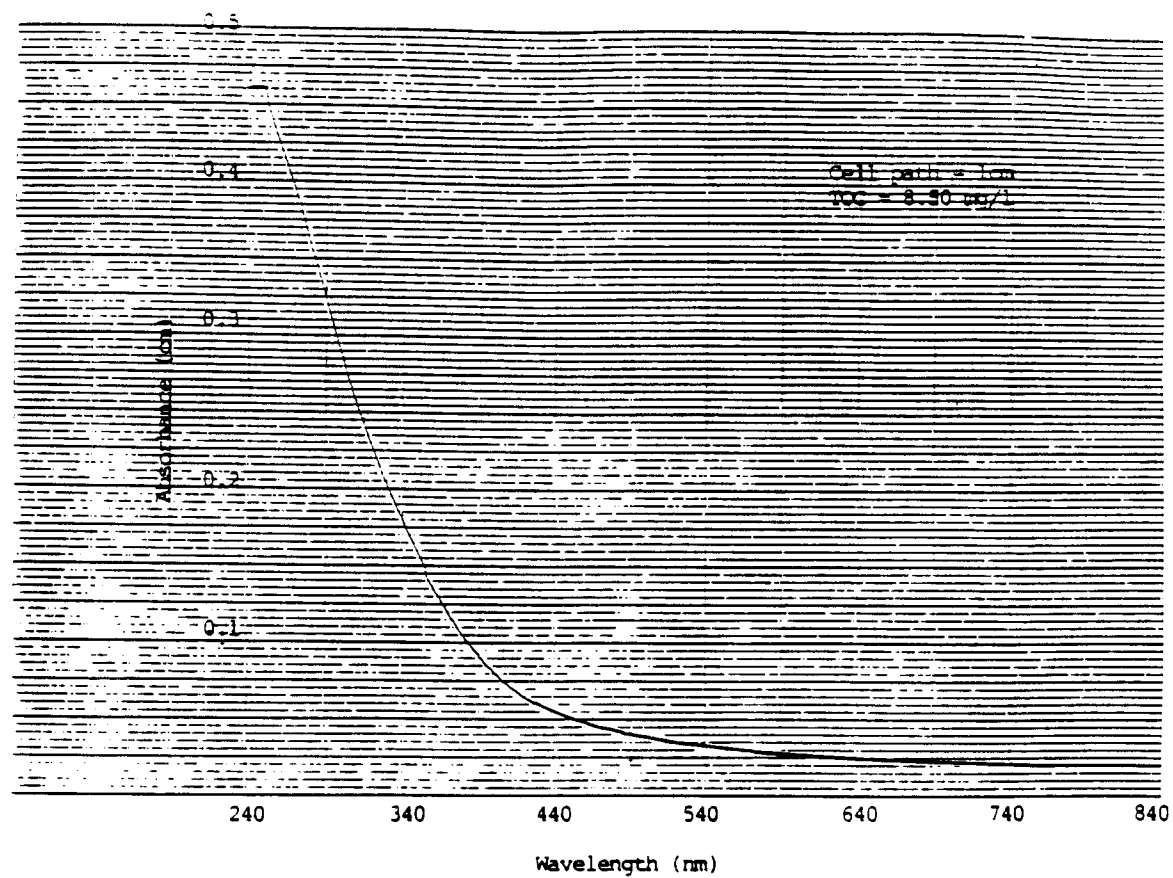


Figure 3.5: UV absorbance scan for the stock concentrated humic substances

3.6 PARTICLE SEDIMENTATION

Wyoming bentonite clay (Georgia Kaolin Co., Elizabeth, N.J.) was selected to represent the standard particle. 5000 mg/L of bentonite was kept in a 0.001 N NaCl suspension. The sedimentation procedure, based on Stokes' Law, was adapted from Black (1965).

The bentonite suspension was vigorously stirred using a Hamilton Beach#33 Mixer (Hamilton Beach Co., Racine, WI) and poured into a 1000 mL sedimentation column. The time required for 2 μ m particle to settle a distance of L was determined by the Stokes' Law equation:

$$t = 18nL/g(p_s - p_1)X^2 \quad (3.6)$$

where:

n = 0.0087 poise at 19°C

X = particle diameter (m)

g = 9.81 m/sec²

p_1 = density of water (g/l)

p_s = density of particle (g/l)

L = length of column cm

t = time required for the particle to fall distance L (sec)

The description and conceptual basis for the procedure is presented in the Appendix. The procedure was repeated five times with a settling time of 8 hr as indicated in Table A1 for every liter of suspension. The final supernatants from the sedimentation column were combined and used as a stock bentonite suspension with known

turbidity. standard curve based on dilution of the stock bentonite suspension vs turbidity. The volume of stock required to make a suspension of known turbidity was determined from the standard curve shown in Figure 3.6.

3.7 JAR TEST PROCEDURE

Jar test experiments were designed to evaluate the treatability of raw water sources containing varying concentrations of AHS and SO_4^{2-} . As indicated in Chapter 2, aluminum salts are among several salts successfully used to remove AHS and other contaminants from solution. Parameters such as pH, coagulant dosage, coagulant type, and the presence of other ions in solution are of primary significance in the process. The purpose of this study was to develop an experimental protocol that would enable one to investigate the impact of varying parameters such as pH, AHS, and SO_4^{2-} concentration on the treatment process. The set up was based on the factorial design shown in Figure 3.7. The low and high levels of AHS, SO_4^{2-} , and pH were 0 and 8 mg/L as DOC, 0 and 50 mg/L, and 4 and 7, respectively. The ranges were chosen to bracket ranges commonly found in surface water.

3.7.1 Coagulant used

Aluminum chloride was used in the jar test instead of aluminum sulfate, the coagulant of choice in conventional water

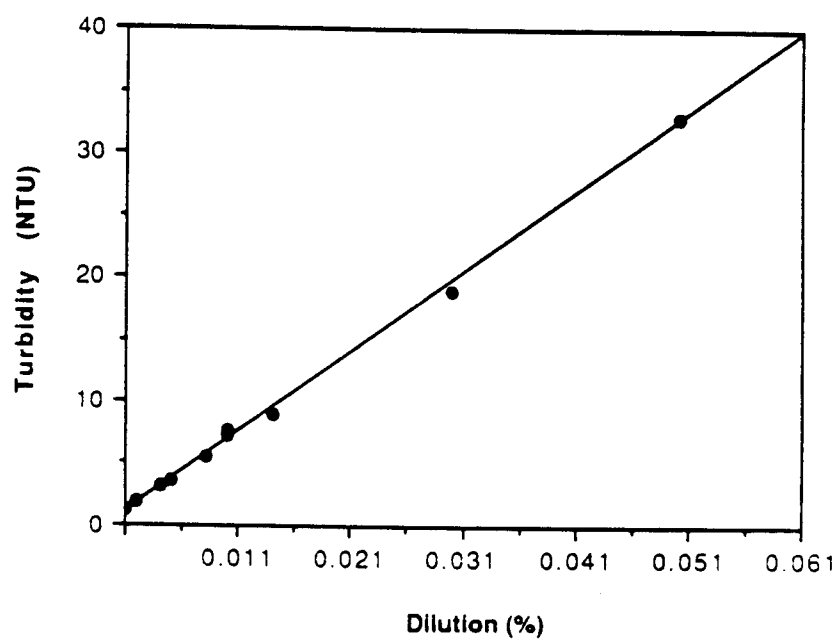


Figure 3.6: Standard curve for the bentonite clay stock solution

treatment to avoid confounding the experiment because sulfate was one of the variables being studied.

Since protons are liberated in the hydrolysis of aluminum creating acidic conditions, a pH Stat (Fisher Scientific Co., Pittsburgh, PA) was used to maintain a constant pH for each aluminum chloride coagulation experiment. Furthermore, hydroxide consumption, associated with the hydrolysis precipitation of aluminum was quantified by recording the amount of 0.1N NaOH used.

3.7.2 Raw Water

The raw water was prepared according to the variables at each level of the factorial design shown in Figure 3.7. The AHS and turbidity were added from the stock AHS solution and the stock bentonite suspension. In addition, the raw water contained 0.001M NaCl, 40 mg/L CaCO_3 alkalinity (NaHCO_3), and 5 NTU turbidity.

5 L of raw water were prepared for each run as indicated in Table 3.3. Predetermined volumes of stock AHS solution, the bentonite suspension, 1000 mg/L stock NaCl, 1000 mg/L stock NaHCO_3 , and 1000 mg/L stock sulfate solutions were transferred into 7.6 liter glass bottles to make the appropriate concentrations needed (Table 3.3). Milli Q water was added up to about 4.5 liters. The pH of this solution was adjusted and the solution was made up to final volume with pH adjusted Milli Q water. The pH of the final solution was again readjusted if needed to the desired value. The water was stirred overnight at room temperature, and the pH was

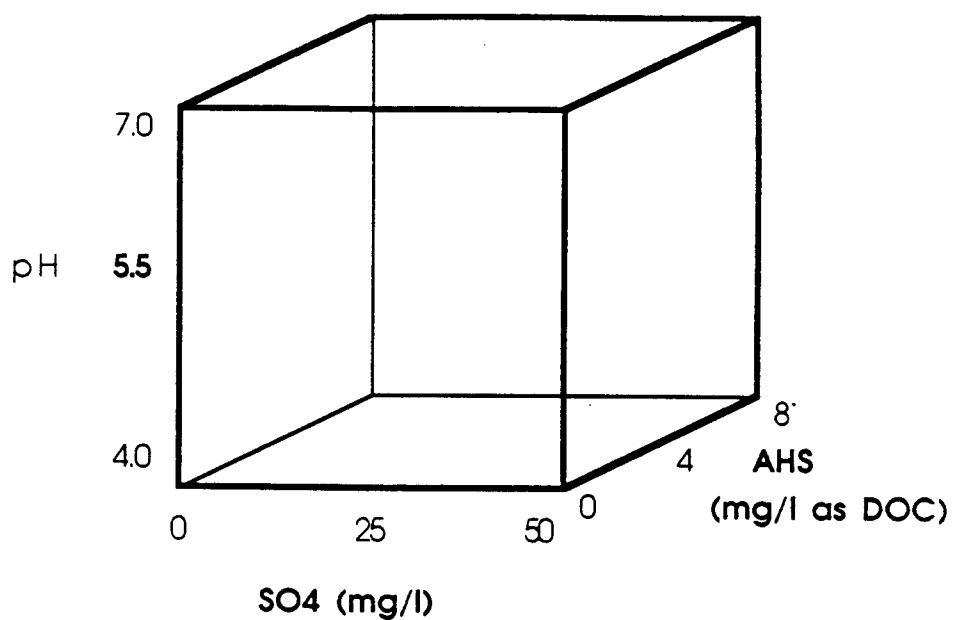


Figure 3.7: Levels of the factorial design

Table 3.3: Raw Water Concentration for Each Run

Run#	1	2	3	4	5	6	7	8	9
pH	7	5.5	7	7	4	4	4	4	7
Sulfate (mg/l)	0	25	50	0	0	50	50	0	50
AHS (mg/l)	0	4	8	8	8	0	8	0	0

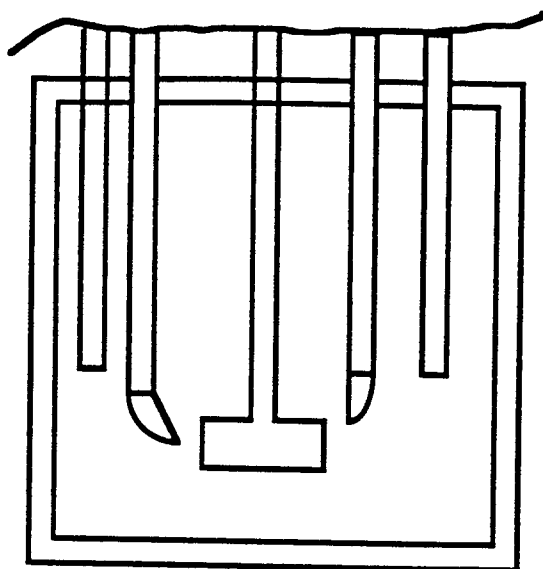
readjusted as necessary. 1 L was collected to characterize the original sample. The remaining 4 L were used for the coagulation at each of four aluminum dosages: 1, 2, 3, and 4 mg/L as aluminum. Aluminum standards were prepared daily from reagent grade $\text{AlCl}_3 \cdot 6\text{H}_2\text{O}$ to avoid the aging process that may alter the homogeneity of the coagulant.

3.7.3 Jar Tests

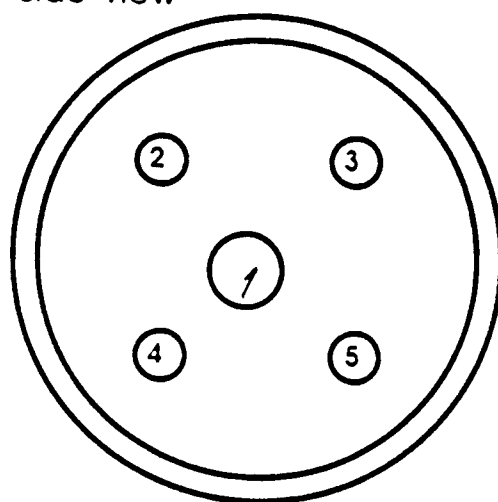
Batch jar tests were performed in a 1500 mL Plexiglass reactor (Figure 3.8) using a volume of 1000 mL. Sample collection, coagulant and 0.1N NaOH addition, and pH probe insertion were done through connection ports on the cover of the reactor. Aluminum chloride and the 0.1N NaOH solution were simultaneously added to the reactor 6.4 cm below the surface. During coagulant and hydroxide addition, the solution was stirred at 350 rpm with a GKH Heavy Duty Laboratory Stirrer (GK Heller Co., N.Y.) equipped with a 2.54 X 7.62 cm propeller. The G value was about 572 (see Appendix).

The NaOH solution was added by the pH stat until the pH stabilized. The aluminum chloride solution was added through a burette with a syringe at the tip. This injection technique was used to insure a uniform dispersion of the coagulant, preventing localized precipitate formation.

The 350 rpm mixing intensity was maintained for 15 seconds after which it was reduced to 65 rpm ($G = 46$, see Appendix) for 20 minutes. 5 mL samples were collected every 5 min from the



Side view



Top view

Items	Description
-------	-------------

- | | |
|---|-------------------------|
| 1 | Stirrer |
| 2 | 0.1N NaOH addition port |
| 3 | pH probe & thermometer |
| 4 | Coagulant addition port |
| 5 | Sampling port |

Figure 3.8: Jar test reactor

beginning until the end of the slow mixing for particle count determination. The volume of 0.1N NaOH was also recorded at 5 min intervals. The OH⁻ demand was generally satisfied within the first 5 min of the run.

At the end of the 20 min slow mixing period, 100 mL of sample was collected for aluminum speciation analysis as described in Section 3.6.4. Care was taken to collect the sample before stopping the stirrer to ensure that no settling took place prior to sample collection. After 1 hr of settling, 500 mL of supernatant was collected. 500 mL were collected for turbidity and particle count analysis. The remaining sample was filtered through a washed Whatman 40 (8 µm) filter and analyzed for dissolved organic carbon (DOC), residual aluminum, turbidity, particle count, SO₄²⁻, and UV absorbance at 254 nm.

3.7.4 Aluminum Speciation

The procedure for determining the species of aluminum in solution was adapted from Hundt (1985). The original procedure (Figure 2.11) groups aluminum into 5 categories: precipitated aluminum hydroxide, large OH-Al polymers, medium OH-Al polymers, small OH-Al polymers, and monomeric Al species.

Two categories were differentiated: aluminum precipitate, and dissolved aluminum. Aluminum precipitate referred to the fraction of aluminum that remained on a 0.45 µm membrane filter after vacuum filtration. The four other species that passed through

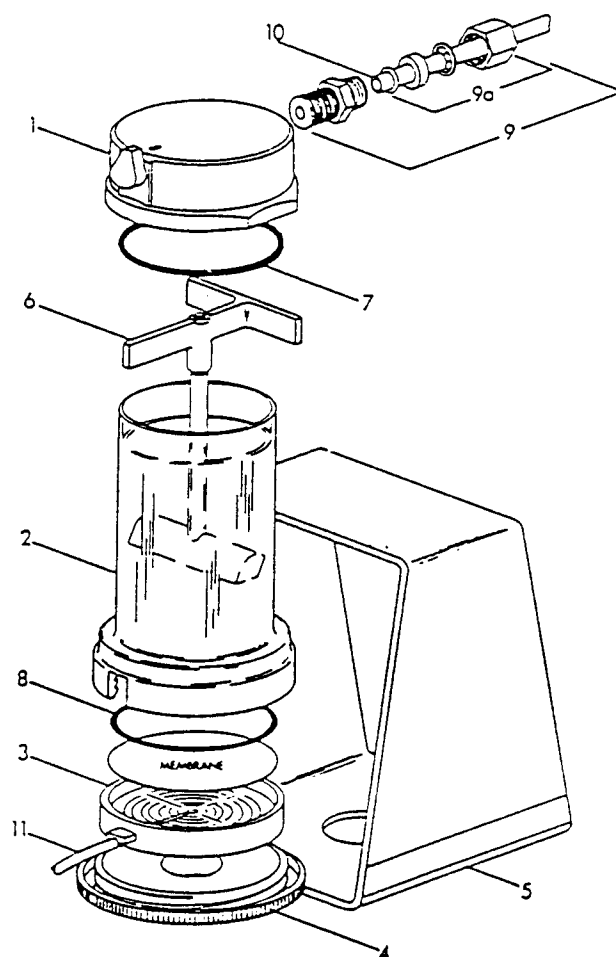
the membrane filter were grouped into one category and referred to as dissolved aluminum. Residual aluminum was generated during the jar test. It was the aluminum fraction measured in the sample after coagulation, settling, and filtration.

Aluminum precipitate was also generated in the adsorption isotherm studies in Section 3.8. Aluminum solutions were prepared from reagent grade $\text{AlCl}_3 \cdot 6\text{H}_2\text{O}$ or Alum. The sample was vacuum filtered through a $0.22 \mu\text{m}$ membrane filters. The aluminum precipitate which remained on the filter was dissolved in 100 mL 6N HCl. Preliminary studies indicated that 6N HCl was appropriate to dissolve the precipitate. The aluminum concentrations were measured by atomic absorption spectrophotometry (AAS).

3.8 KINETICS AND ADSORPTION STUDIES OF SULFATE AND AQUATIC HUMIC SUBSTANCES ON ALUMINUM PRECIPITATE

3.8.1 Reactor Description

Sulfate and AHS adsorption on pre-formed aluminum precipitates were investigated. A 200 mL capacity Amicon Stirrer Ultrafiltration Cell Model 8200 (Amicon Co., Danvers, MA) (Figure 3.9) was adapted to study the adsorption isotherm. The following sequential steps were taken to assemble the cell. The $0.22 \mu\text{m}$ membrane filter was placed in the membrane holder assembly (3), and the O ring (8) put on top of the filter and gently pushed down to



Item Number	Description
1	Cap Assembly
7	O-Ring
2	Body
3	Membrane Holder Assembly
4	Base
5	Retaining Stand
6	Stirrer Assembly
8	O-Ring
9	Fitting
9a	Tube Fitting Assembly
10	Tubing, Plastic 1x4'
11	Tubing, Elastomeric 1x4"

Figure 3.9: Reactor cell for the adsorption study
(Amicon Co., Danvers, MA)

make sure it contacted and seated the filter evenly in the bottom holder (3). The holder was fit into the cell body (2), aligning the tabs on the sides of the holder with the slots in the base of the cell body. The cell body, with the filter holder, was inverted and the base was screwed firmly into the bottom of the cell body. The stirrer assembly (6) was placed into the cell body. When properly inserted, the arms of the stirrer assembly sat on a small ridge inside the top of the cell body.

The sample was then transferred into the cell and the pH adjusted with the Fisher Titrimeter while N_2 was bubbled through the cell. The cell cap was put into place after the solution pH was adjusted. Using a twisting motion, the cap assembly (1) was pushed on as far as it would go. The nitrogen inlet port (10) was aligned directly opposite the filter holder. The pressure relief valve was turned to the horizontal position (open). The cell was slid into the retaining stand (5). The ring on the cell base was placed in the hole in the stand base making sure to obtain flattened edges on the bottom flange of the cap. This ensured that the cell was inserted properly, and any rotation of the cell in the stand was prevented.

The pressure relief valve was closed (turned to the vertical position). The nitrogen inlet line (10) was attached to the cap by screwing it onto the cap. The cell was placed on a Nova II (Thermoclyne Co., Dubuque, Iowa) magnetic stirrer, held in place and pressurized (10 psig) with nitrogen. The stirring rate was adjusted so that the vortex was not more than one fifth of the liquid volume. Filtration was done under nitrogen pressure by releasing the pinch

clamp on the filtration tubing (11).

After filtration, the nitrogen was turned off first, the cell was depressurized by turning the pressure valve to the off position. The cell was removed from the retaining stand and disassembled by removing the cap with a twisting motion, removing the stirrer by pulling it out of the cell body, and unscrewing the base from the cell body. The filter was transferred into a sampling bottle and the O ring was placed into a 250 mL beaker. The O ring was rinsed with 50 mL of Milli Q water and the rinse water was poured into the sampling bottle containing the filter. Concentrated HCl was added to the sampling bottle to make a 6N HCl solution.

3.8.2 Procedure

The results of the hydrolysis/precipitation of Al(III) (Chapter 4) indicated that the titration curves of aluminum chloride and aluminum nitrate were similar suggesting a similar aluminum hydroxide precipitate formation. As a result, the experiments were only conducted with aluminum chloride and aluminum sulfate.

Two separate experiments were conducted at this stage. In the first experiment, predetermined volumes (V_i) of aluminum standard solutions were prepared daily from reagent grade aluminum chloride or aluminum sulfate. The aluminum solutions were transferred into the ultrafiltration cell containing a 0.22 μm membrane filter. The solution's pH was adjusted to 5.5 or 7.0 with 2N NaOH using a fixed end point titration program on the Fisher

titrimeter. Nitrogen was bubbled through the solution with a gas diffusion stone while the pH was adjusted. Nitrogen bubbling prevented atmospheric CO_2 from affecting the pH of the solution. The initial aluminum solution pH values usually dropped to 3.2.

The reactor was then covered and blanketed with 10 psig of N_2 . The solution was slowly stirred for 30 min with a Nova II magnetic stirrer (Thermoclyne Co., Dubuque, Iowa), followed by 1 hr of settling. The clamp closing the sampling port was opened allowing the solution to pass through the membrane filter. The pre-formed aluminum precipitate remained on the filter. A rinse volume of pH adjusted Milli Q water equal to the pH of the initial aluminum solution was added to the reactor. The pH of the rinse water was adjusted to that of the aluminum solution used to make the precipitate (5.5 or 7) prior to its addition to the cell. The reactor cover was put into place and blanketed again with N_2 (10 psig). This solution was slowly mixed for 10 minutes and filtered under N_2 pressure.

The rinse volume, established during preliminary experiments, consisted of rinsing the $\text{Al}(\text{OH})_3$ s with pH adjusted incremental volumes of Milli Q water until no additional aluminum was detected in the filtrate (based on AAS). At pH 7, no aluminum was detected in the filtrate compared to less than 1% at pH 5.5. The rinse volume also provided for rinsing the wall of the reactor to make sure that all the precipitate was available for adsorption.

The pH of the adsorbate (sulfate, AHS, or AHS and sulfate) standard was adjusted to either 5.5 or 7 to correspond to the pH at

which the precipitate was formed. The rinse water pH was brought to 5.5 or 7. The adsorbate solution was transferred into the reactor cell containing the precipitate and the adsorption carried out. Three procedures were followed with the solution in the reactor under N_2 (10 psig).

The first procedure consisted of slowly stirring the solution and collecting filtered samples over time to determine equilibration time. The equilibration time was defined as the time after which no significant adsorption was observed. The filtrate sample was always collected after wasting 2 mL which was equivalent to twice the volume of liquid in the sampling tube. This was done to avoid cross contamination of the samples. The results from the equilibration experiments indicated that for AHS adsorption on both aluminum sulfate and aluminum chloride precipitates, no significant additional adsorption took place after a 1 hr equilibration time.

The SO_4^{2-} equilibration time was even shorter on the aluminum chloride precipitate. Virtually all of the adsorption took place within a 30 min equilibration time compared to 1 hr for AHS. No additional SO_4^{2-} adsorption took place on aluminum sulfate (see Chapter 4).

The second experimental procedure consisted of transferring pH adjusted SO_4^{2-} or AHS standard into the reactor cell containing the $Al(OH)_3$ s. The solution was equilibrated for 1 hr as established in the previous procedure. The entire solution was filtered. A new solution was again transferred into the reactor,

equilibrated for 1 hr, and filtered. This was repeated at least four times. This procedure was performed to determine the maximum amount of adsorbate that could be adsorbed.

The third procedure, representing the final adsorption isotherm, consisted of equilibrating the reactor solution for 1 hr, and then filtering the entire solution. The filtrate and standard adsorbate concentrations were then measured.

In the second experiment, 55 mL of aluminum solution was transferred to a 100 mL volumetric flask. 10 mL of an 88 mgDOC/L stock AHS solution was added and the volume was made up to 110 mL, giving a solution containing about 400 mg/L aluminum and 8 mgDOC/L AHS. 50 mL of this solution were transferred into the cell and the pH adjusted to 5.5 or 7.0 with the Fisher titrimeter while bubbling N_2 through with a gas diffusion stone. The cell cap was put into place and the solution was stirred under N_2 (10 psig) for 30 min and settled under quiescent conditions for 1 hr. The solution was then filtered and rinsed.

The pH adjusted AHS or SO_4^{2-} solution was transferred into the cell and stirred under an N_2 blanket for 1 hr. The solution was filtered, and the filtrate characterized. Similar experiments were also conducted where the DOC was increase about 65 mg/L.

The aluminum precipitate remaining on the filter in both experiments was dissolved in 50 or 100 mL of 6N HCl and its aluminum concentration was measured using the AAS. Preliminary experiments indicated that the aluminum precipitate dissolved in 6N HCl and the amounts of AHS and sulfate adsorbed on the filter were

undetectable with the analytical procedure used. A mass balance indicated that 93 to 100% of the aluminum was recovered with this procedure. Unlike other glassware, the reactor was not acid washed because of fear of deterioration due to prolong contact with acid. It was rinsed five times, and immersed in Milli Q water overnight or between runs.

3.9 SENSOR FOR ALUMINUM MEASUREMENT BASED ON IMMOBILIZED MORIN

3.9.1 Apparatus

The diagram of the fluorescence sensor and its associated instrumentation (Figure 3.10) was taken from Saar (1980). The sensor consisted of a photomultiplier tube housing with a variable slit width and the capacity to hold filters, a digital photometer power supply, two dielectric interference filters, a bifurcated fiber optic threaded to fit the other components, and a tungsten halogen lamp. Additional information can be obtained in Seitz et al. (1980), and Seitz et al. (1988).

The excitation filter had a peak transmittance at 420 nm and a band width of 10 nm at half the maximum transmittance. The emission filter had a peak transmittance at 488 nm and a bandwidth of 7 nm. The excitation spectra of the immobilized morin and its aluminum complex on the optic surface were measured with an SLM 8000 spectrofluorometer equipped with an MC 300 manual

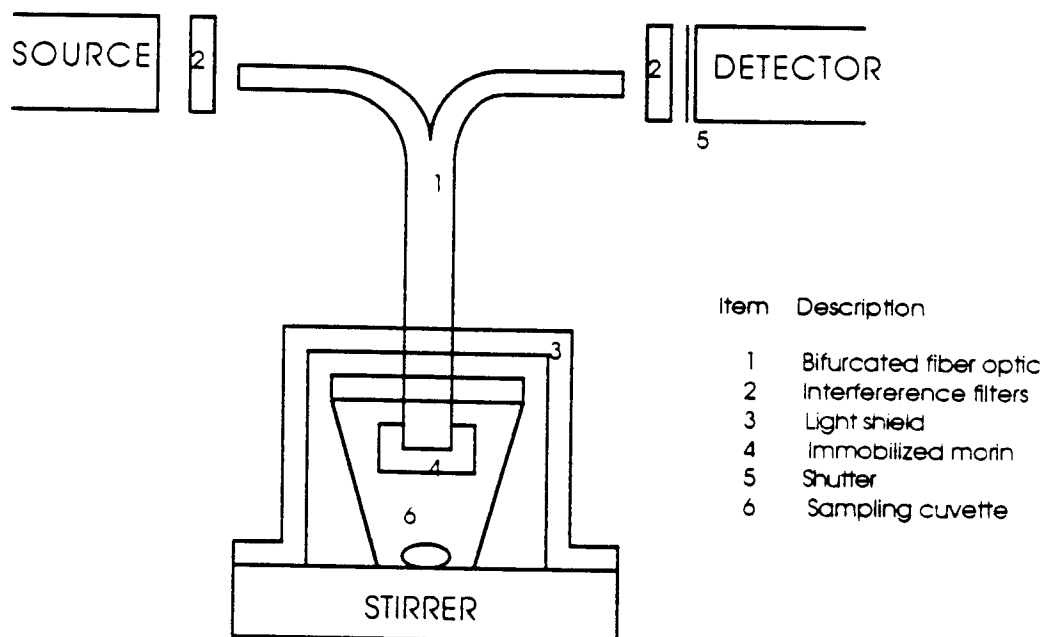


Figure 3.10: Diagram of pH sensor based on fluorescence and associated instrumentation (Seitz, 1982)

monochromator. Measurements were made by attaching the excitation and emission arms of the bifurcated fiber optic to the source, and the detector lens housing in the sample chamber, by means of light-tight aluminum fittings.

3.9.2 Immobilization Procedure

Morin was immobilized on cellulose according to the procedure described in Russell (1989). The following procedure presents the preparation and entrapment of the cellulose matrix in polyvinyl alcohol matrix.

1 gr of molecular weight 14000 polyvinyl alcohol (PVOH) (Aldrich) was weighed out into a clean dry beaker. 20 mL of spectra-analyzed reagent grade acetone (Fisher) and 13.17 mg of cyanuric chloride were added to the beaker. The solution was stirred at 0° C for 40 min. After this reaction was completed, the solution was transferred to a weighing bottle and allowed to dry at room temperature. The sample was then transferred to a Buchner funnel and suction filtered. The filtrate was washed with copious amounts of acetone and transferred to a weighing bottle and allowed to dry at room temperature.

After drying, the sample was transferred to a clean, dry 50 mL beaker to which was added 21.7 mg of morin (Fisher Scientific) and 20 mL of acetone. The mixture was stirred at 40° C for 30 min. After completion of this reaction, the product was transferred to a Buchner funnel and suction filtered. The filtrate was washed in

acetone and allowed to dry at room temperature.

The amount of morin immobilized was determined spectroscopically. The resulting cyanure chloride/morin/PVOH conjugate was then cross linked with glutaraldehyde under acidic conditions. The sensor was prepared by transferring 3 μ l of the PVOH indicator solution to the end of the bifurcated fiber optic bundle immediately after glutaraldehyde and HCl had been added to initiate cross linking.

3.9.3 Analyses

The initial goal of checking the performance of the probe following a modified USEPA designed Quality Assurance and Quality Control Procedures for Instrumental Analysis (1980) was abandoned because several problems were encountered. A trouble shooting procedure was instead implemented. The analyses relied on previous studies by Seitz et al. (1983). Aluminum measurements were taken with morin immobilized with both cellulose matrix described by Seitz et al. (1983), and the PVOH matrix described herein. The optimum pH for the procedure was found to be 4.8. A similar conclusion was reached in preliminary experiments in this study.

Aluminum standards were prepared by dissolving the appropriate amounts of aluminum stock solution with acetate buffer. The minimum fluorescence intensity detectable was with an aluminum concentration of 10^{-6} M. Longer diffusion time was

observed at concentrations higher than 10^{-3} M. The performance of the instrument was checked within this range.

A series of tests were performed to determine the performance of the instrument while varying the solution pH from 4.0 to 7.0. A series of samples were prepared at varying pH values and the fluorescence intensity was recorded.

CHAPTER 4

RESULTS

Results from laboratory experiments used to investigate the influence of sulfate in aluminum coagulation of water are grouped into four sections. The titration curves used to evaluate the hydrolysis precipitation of Al(III) are presented first. Aluminum chloride, aluminum nitrate, and aluminum sulfate titration curves are compared along with the effects of acidification of the aluminum solutions and increasing sulfate concentration in an aluminum chloride solution.

The data for the study on the implication of aluminum speciation and interaction with the contaminants are presented in the aluminum coagulation work. The results include the hydroxide demand (OH^- demand), aluminum species, DOC, UV, turbidity, particle counts, and sulfate. Analysis of variance (ANOVA) was performed to compare the efficiencies of aluminum dosages for each treatment condition. The Duncan multiple range test was chosen because it accounts for the differences in removal mechanisms of coagulation at the levels of the factorial design. All comparisons were made at the 95% confidence level. The experiments and

analyses were designed such that the estimate of the error associated with the center point of the factorial design was the overall estimate of error.

The third section focuses on adsorption, one of the two main removal mechanisms reported in the coagulation study. The results of experiments examining sulfate and aquatic humic substances (AHS) adsorption on aluminum precipitate are presented. The first phase of the adsorption study consisted of investigating the adsorption of sulfate and AHS on aluminum precipitate formed with aluminum chloride and aluminum sulfate at pH 5.5 and 7. The aluminum precipitates were formed by dissolving aluminum chloride or aluminum sulfate in water. The pH was then adjusted and the adsorption experiment was carried out. The procedure in the second phase was altered to simulate more closely water treatment conditions. In this phase, concentrated AHS was added to the aluminum solution and the pH adjusted to form the aluminum precipitate. The data were fitted to Langmuir and Freundlich isotherms.

The results of the morin based Al(III) fluorescent sensing analytical method are presented and discussed in the appendix because we were not successful in developing and implementing the objectives sought. The evaluation of the procedure consisted of trouble shooting and developing a frame work for future research.

4.1 SULFATE IN AL(III) HYDROLYSIS/PRECIPITATION

Several aluminum solutions were titrated with NaOH to pH above 12. The results were analyzed by developing the titration curves for each Al(III) solution. The titration curves were compared and the specific characteristics of each curve interpreted. In addition, a series of experiments were conducted in which aluminum chloride solutions were prepared with increasing sulfate concentrations by addition of Na₂SO₄. The aluminum solutions were titrated with NaOH to study the potential impact of varying sulfate concentrations.

4.1.1 Titration of Aluminum Chloride, Aluminum Nitrate and Aluminum Sulfate Solutions

Titration curves relating bound hydroxide per total aluminum, r , as a function of pH of three different aluminum solutions are shown in Figure 4.1. Bound hydroxide per total aluminum, also referred to as the formation function r , reported by Sullivan et al. (1968) is defined as:

$$r = [\text{OH}^-]_b / [\text{Al}]_t \quad (4.1)$$

where $[\text{OH}^-]_b$ is the molar concentration of hydroxide bound by the aluminum, and $[\text{Al}]_t$ is the total aluminum concentration in solution. The concentration of hydroxide bound is equal to the hydroxide originally present in solution, plus the amount that has been added,

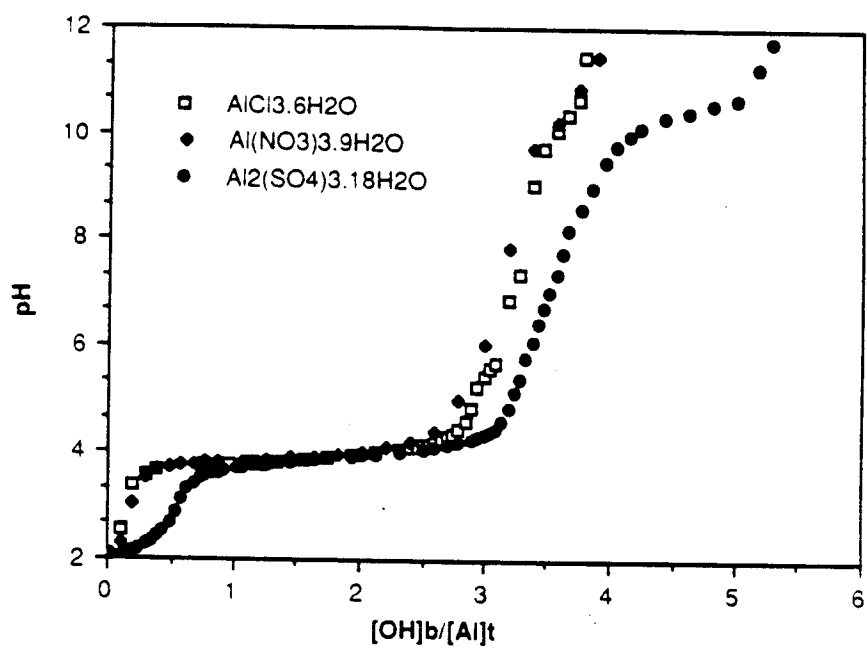


Figure 4.1: Titration curves relating the formation function r ($[\text{OH}]_b/[\text{Al}]_t$) to pH (Solutions titrated: 2 L of 1400 mg/L $\text{Al}(\text{III})$)

less the amount that is present in the final solution. The formation function gives the average number of moles of hydroxide bound per mole of aluminum. The r value is a good indicator of the reaction of OH^- with aluminum.

Figure 4.1 shows that the titration curve of aluminum chloride is similar to that of aluminum nitrate. Both curves present three characteristics:

- (i) an exponential increase in pH occurred at $[\text{OH}^-]_b/[\text{Al}]_t$ ratios of up to 0.3 followed by the development of a plateau in the $[\text{OH}^-]_b/[\text{Al}]_t$ ratio range of 0.3 to 3. The pH increased from 2 to 4 before stabilizing within the first 0.3 $[\text{OH}^-]_b/[\text{Al}]_t$ ratio change.
- (ii) a sharp jump in pH was observed at $[\text{OH}^-]_b/[\text{Al}]_t$ of 3. The change in pH per change in $[\text{OH}^-]_b/[\text{Al}]_t$ was identical to the $0 < [\text{OH}^-]_b/[\text{Al}]_t < 0.3$ region. The pH increased from 4 to 12. A very small second plateau was noted for the aluminum chloride titration curve at $[\text{OH}^-]_b/[\text{Al}]_t$ ratio of 3. The shape of the plateau was much narrower than the first plateau. Replicate titration curves did not show the second plateau consistently.
- (iii) a visible floc formed for both curves at about $[\text{OH}^-]_b/[\text{Al}]_t$ ratios of 2.69 (Aluminum nitrate), and 2.79 (aluminum chloride). The floc was a dense, gel like material which settled quickly upon standing.

There were four major differences between the aluminum

nitrate and aluminum chloride titration curves compared to the aluminum sulfate titration curve:

- (i) the aluminum sulfate titration curve ran below the former two for the entire $[\text{OH}^-]_b/[\text{Al}]_t$ range.
- (ii) a smaller slope of the sulfate curve occurred in the region of $[\text{OH}^-]_b/[\text{Al}]_t$ ratios of less than 0.5.
- (iii) a dense precipitate appeared at a lower $[\text{OH}^-]_b/[\text{Al}]_t$ ratio of 0.6.
- (iv) the final difference was the appearance of a third plateau (not to be confused with the second plateau reported by De Hek et al., 1978, with aluminum nitrate) with midpoint at $[\text{OH}^-]_b/[\text{Al}]_t$ of 4.7 (pH10.5). The third plateau was not observed by any of the previous investigators because they discontinued their titration at pH of about 10. The third plateau appeared only at pH above 10.

Resuspension of the aluminum precipitates began for all the titrated solutions at the earlier stage of the third plateau. The resuspension was noted at $[\text{OH}^-]_b/[\text{Al}]_t$ ratios of 3.75 (pH10.88), 3.75 (pH10.69), and 4.81 (pH10.55) for aluminum nitrate, aluminum chloride and aluminum sulfate solutions respectively. The turbidity of the solution changed gradually. The solution varied from a dense gelatin white precipitate (amorphous precipitate) to colorless. Little 2N NaOH addition was generally required above pH 10 to observe the change.

4.1.2 Impact of Increasing Sulfate Concentrations and Acidification on the Aluminum Titration Curves

Figure 4.2 shows the results of the titrations where several varying sulfate concentrations were added to the aluminum chloride solutions to give Al:SO₄ molar ratios of 1:1.5 and 1:3. The resulting curves are strikingly similar to the titration curve of aluminum sulfate solutions. The same major components of the titration curve of aluminum sulfate solutions were observed.

At low $[\text{OH}^-]_b/[\text{Al}]_t$ ratios, the small slope identical to the slope observed on the aluminum sulfate titration curve was noticed. The precipitate formation was first noted in the low $[\text{OH}^-]_b/[\text{Al}]_t$ of about 0.7. The first plateau occurred within the same $[\text{OH}^-]_b/[\text{Al}]_t$ range. The sharp jump in pH at $[\text{OH}^-]_b/[\text{Al}]_t$ around 3.2 followed by the development of the third plateau and the subsequent dissolution of the precipitate in the pH range above 10 were also noted.

The increase of the Al:SO₄ molar ratio to 1:3 (open squares in Figure 4.2) did not significantly affect the characteristics of the titration curves. The curve followed the same general trend. No further increase in Al:SO₄ molar ratio was investigated.

The characteristics of the titration curves of acidified aluminum solutions are shown in Table 4.1. The aluminum solutions were acidified to pH2 before titration. Acidification of the aluminum solutions prior to titration did not affect the characteristics of the curves.

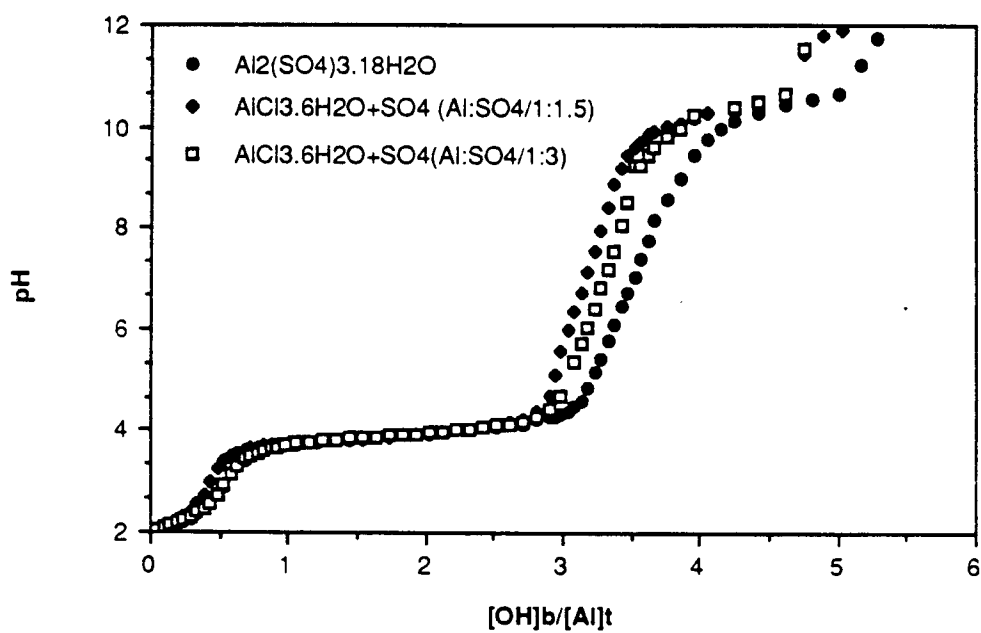


Figure 4.2: Titration curves relating the formation function r ($[\text{OH}]_b/[\text{Al}]_t$) to pH (Solutions titrated: 2 L of 1400 mg/L Al(III))

Table 4.1: Characteristics of Aluminum Titration Curves

Aluminum Type	Visible		Midpoint		Midpoint		Resuspension	
	Floc		(first plateau)		(third plateau)			
	[OH]b/[Al]t	pH	[OH]b/[Al]t	pH	[OH]b/[Al]t	pH	[OH]b/[Al]t	pH
Alum Acidified with 1 N HCl	0.43	3.3	2	3.85	4.3	10.4	4.62	10.63
AlCl ₃ ·6H ₂ O Acidified with 1N HCl	0.62	3.47	1.8	3.95	4	10.5	4.18	10.64
AlCl ₃ ·6H ₂ O Acidified with 1N H ₂ SO ₄	0.57	3.71	1.8	4.1	4	10.6	4.27	10.75
AlCl ₃ ·6H ₂ O + Na ₂ SO ₄ (Al/SO ₄ :1/3)	0.77	3.58	1.7	3.9	4.5	10.5	4.42	10.48
Alum	0.58	3.13	2	3.95	4.7	10.5	4.81	10.55
Al(NO ₃) ₃ ·9H ₂ O	2.69	4.5	1.6	3.93	none		3.75	10.88
AlCl ₃ ·6H ₂ O	2.79	4.48	1.6	3.8	none		3.75	10.69
AlCl ₃ ·6H ₂ O + Na ₂ SO ₄ (Al/SO ₄ : 1/1.5)	0.72	3.64	1.7	3.87	4.5	10.5	4.61	10.61

The aluminum hydrolysis species interactions with contaminants was the subject of the results of the coagulation study presented next. The results were obtained from aluminum chloride coagulation of water containing sulfate, AHS, and particulate at varying pH values.

4.2 ALUMINUM COAGULATION RESULTS

A jar test study was performed to evaluate the removal of HA and particulate matter from water. The raw water was prepared by adding bentonite clay, NaHCO_3 , NaCl , AHS, and Na_2SO_4 to Milli Q water. The concentrations of the contaminants and the pH were adjusted to the level of the factorial design described in section 3.6. The water samples corresponding to each level of the factorial design were treated with aluminum chloride coagulant dosages of 1, 2, 3, and 4 mg/L as aluminum. The pH was maintained constant at each level with a pH stat. The control of pH required the addition of 0.1N NaOH.

The results of the removal efficiencies will be reported as remaining measured parameter (C/C_0) versus aluminum dosages (1, 2, 3, and 4 mg/L). The Duncan multiple range results are presented for all 9 experimental conditions within a given aluminum dosage block. The results of the center point are replicates of four separate experiments. The estimate of error for the center point is reported. The overall statistical comparison among the variables of the

factorial design (pH, aquatic humic substance, and sulfate) is shown in Table 4.2.

4.2.1 Hydroxide Demand

The addition of aluminum to water can result in acid formation and a drop in pH because of the hydrolysis of aluminum. The OH^- demand measured for each jar test was generally satisfied within 1 to 2 minutes after the aluminum chloride addition. The results are shown in Figure 4.3 and the statistical comparison in Table 4.3.

The OH^- demand was significantly greater at pH7 compared to pH4 for all the treatment conditions. The difference in the OH^- demand was due to the higher acid formation when the initial pH was greater. The pH dropped after the aluminum coagulant addition in both cases. However the depression was much higher when the initial pH was 7. A greater amount of OH^- was then required to bring the pH back to 7. This was also true at pH5.5. The OH^- demand increased with increasing initial pH values.

The presence of sulfate did not significantly affect the OH^- demand at pH4 when AHS concentration was 0 mgC/L. The same observation was seen when the AHS concentration was increased to 8 mgC/L. The variation of the aluminum dosage from 1 to 4 mg/L produced a steady increase in the OH demand for all the treatment conditions.

Table 4.2: Overall Significance of the Factorial Design Variables (ANOVA)

Variables	Hydroxide Demand	Aluminum Precipitate	Dissolved Aluminum	Residual Aluminum+	DOC+ UV+	Turbidity Before Filtration	Turbidity After Filtration	Particle Count Before Filtration	Sulfate+
AHS	*	*	***	*	*	***	***	*	*
SO ₄	*	*	*	*	*	*	*	*	*
pH	***	***	***	***	***	***	***	*	*
AHS*SO ₄	*	*	*	*	*	*	*	*	*
AHS*pH	*	*	*	*	*	***	***	*	*
SO ₄ *pH	*	*	*	*	*	*	*	*	*
AHS*SO ₄ *pH	*	*	*	*	*	*	*	*	*

Comparisons were made with aluminum dosages range of 1 to 4 mgAl/L

*** Significant ($p < 0.01$)

** Significant ($p < 0.05$)

* Not significant ($p < 0.05$)

+ Analyses on filtered water

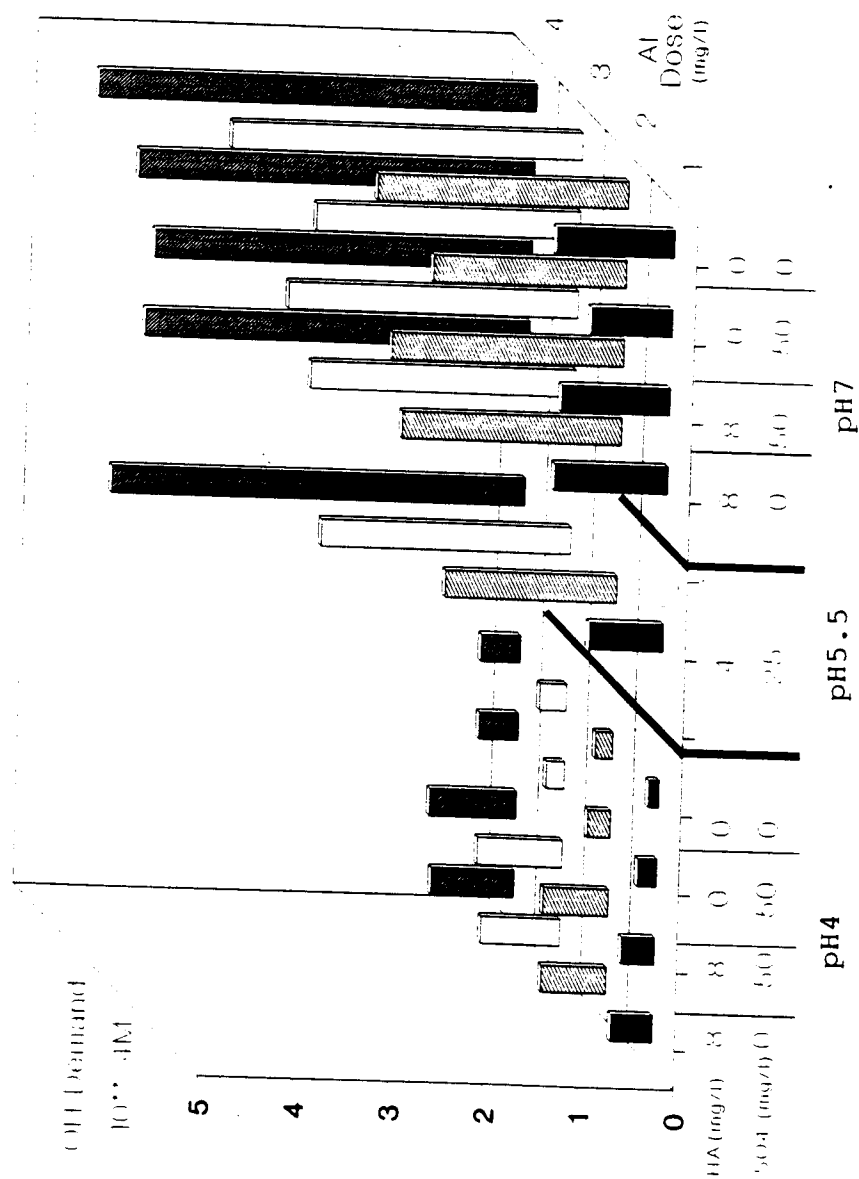


Figure 4.3: The coagulation of AHS using AlCl_3 ; the hydroxide demand at various pH and aluminum dosages

Table 4.3 : Aluminum Chloride Coagulation Results.
Hydroxide Demand (10⁻³-4M)

Raw water parameters			Aluminum Dosage (mg/l)											
			1			2			3			4		
pH	SO ₄ (mg/l)	HA (mg/l as TOC)	C	SD	A	C	SD	A	C	SD	A	C	SD	A
7	0	0	1.24		A	2.64		A	3.69		A	4.6		A
5.5	25	4	0.79	0.04	B	1.82	0.067	D	2.63	0.078	C	4.35	0.05	B
7	50	8	1.14		A	2.44		A	3.05		B	3.97		C
7	0	8	1.19		A	2.31		B	2.79		B	4.05		C
4	0	8	0.44		C	0.68		E	0.83		D	0.87		D
4	50	0	0.2		D	0.24		F	0.19		E	0.41		E
4	50	8	0.35		C	0.68		E	0.89		D	0.91		D
4	0	0	0.11		E	0.18		F	0.28		E	0.41		E
7	50	0	0.85		B	2.03		C	2.78		B	4.16		B

Measurements with the same letter are not significantly different (95% confidence level)

The addition of 8 mgC/L AHS to the water samples at pH4, with sulfate concentrations of 0 and 50 mg/L, resulted in a significant increase in OH⁻ demand in both cases. The increased OH⁻ demand due to 8 mg/L AHS addition was 0.33×10^{-4} M (0 mg/L sulfate), and 0.15×10^{-4} M (50 mg/L sulfate) at the aluminum dosage of 1 mg/L. The effect of AHS addition was more pronounced at higher aluminum dosages. The hydroxide demand reached 0.66×10^{-4} M (0 mg/L sulfate) and 0.40×10^{-4} M at aluminum dosage of 4 mg/L.

At pH7, an almost 1 to 1 relationship existed between the number of moles of hydroxide added to maintain the pH constant and the aluminum dosages (mg/L). With no AHS in solution, the addition of 50 mg/L sulfate resulted in a decrease in OH⁻ demand with all four aluminum dosages. The decrease varied from 0.39×10^{-4} M at the aluminum dosage of 1 mg/L to 0.44×10^{-4} M at the aluminum dosage of 4 mg/L. The difference no longer existed when the AHS concentration was 8 mg/L.

In contrast to the results of the OH⁻ demand at pH4, the addition of 8 mgC/L AHS did not systematically increase the demand in the water samples with sulfate concentration of 0 and 50 mg/L. When sulfate concentration was 0 mg/L, the demand decreased significantly only when the aluminum dosage was greater than 1 mg/L. The decrease dropped from 0.33×10^{-4} M at the aluminum dosage of 2 mg/L to 0.55×10^{-4} M at the aluminum dosage of 4 mg/L. No consistent change occurred when sulfate concentration was 50 mg/L. A significant decrease was noted at the aluminum dosages of

1 and 2 mg/L, but no difference was noted when the aluminum dosage was 3 and 4 mg/L.

The OH^- demand range at pH5.5 was much closer to the results of pH7. The 1 to 1 relationship was also observed. The demand ranged from 0.79×10^{-4} M at the aluminum dosage of 1 mg/L to 4.35×10^{-4} M at the aluminum dosage of 4 mg/L.

The data was transformed to obtain the formation function r ratios ($[\text{OH}]_b/[\text{Al}]_t$) for each experimental condition. The r results are presented in Table 4.4. The $[\text{OH}]_b$ was equal to the $[\text{OH}^-]$ added in this experiment because the pH was maintained at a constant level. The initial and final $[\text{OH}^-]$ values were equal. It should be noted that AHS (high and low levels of the factorial design) and particulate bentonite were added to the water samples.

The r ratios vary from 0.17 (pH4, 50 mg/L sulfate, 0 mgC/L, and aluminum dosage of 3 mg/L) to 3.57 (pH7, 0 mg/L sulfate, 0 mgC/L, and aluminum dosage of 2 mg/L). Significantly lower r values were obtained at pH4.

At pH4, and AHS concentration of 0 mgC/L, the addition of 50 mg/L sulfate resulted in a significant increase in r values at the aluminum dosages of 1 mg/L only. The formation function r increase was 0.24×10^{-4} M. No difference existed at the aluminum dosages of 2 through 4 mg/L.

The addition of 8 mgC/L AHS consistently increased the r ratios regardless of the variation in sulfate concentrations. The formation function change as a function of sulfate concentration

Table 4.4: Aluminum Chloride Coagulation Results.
Formation Function (r)

Raw water parameters			Aluminum Dosage (mg/l)											
			1				2				3			
pH	SO ₄ (mg/l)	HA (mg/l as TOC)	C	SD	.	A	C	SD	.	A	C	SD	.	A
7	0	0	3.35		A		3.57		A	3.32		3.11		A
5.5	25	4	2.14	0.1	B		2.44	0.089	D	2.37	0.068	2.94	0.03	B
7	50	8	3.08		A		3.29		A B	2.74		2.68		D
7	0	8	3.22		A		3.12		B C	2.51		2.74		C D
4	0	8	1.19		C		0.92		E	0.75		0.59		E
4	50	0	0.54		D E		0.32		F	0.17		0.28		F
4	50	8	0.95		C D		0.92		E	0.8		0.61		E
4	0	0	0.3		E		0.24		F	0.25		0.28		F
7	50	0	2.3		B		2.74		C D	2.5		2.81		B C

Measurements with the same letter are not significantly different (95% confidence level)

varied from $0.31 \times 10^{-4} \text{M}$ to $0.89 \times 10^{-4} \text{M}$ (0 mg/L sulfate), and from $0.33 \times 10^{-4} \text{M}$ to $0.41 \times 10^{-4} \text{M}$ (50 mg/L sulfate).

Higher r values were observed at pH7 because of the higher OH^- demand. A decrease in r with the addition of 50 mg/L sulfate occurred when AHS concentration was 0 mgC/L. A significant increase in the aluminum precipitate was seen for the same condition (Figure 4.2) at all the aluminum dosages. The shift to the lower r ratio by the addition of sulfate seemed to have resulted from the increased amount of aluminum precipitate.

The shift in r ratio was also observed with the aluminum hydrolysis experiments. Aluminum precipitation occurred at a lower r ratios (0.5) because of sulfate addition. The low r values, however, were in the pH region of 3 to 4. The difference could be due to pH recording procedures. In the jar tests, the pH was maintained constant while the pH values in the hydrolysis experiments were not.

The r ratios did not vary consistently with 0 or 50 mg/L sulfate mg/L addition for AHS concentration of 8 mgC/L at pH7. The ratio decreased at the aluminum dosage of 1 and 4 mg/L, and increased at the aluminum dosage of 2 and 3 mg/L.

4.2.2 Aluminum

Two sets of aluminum results are reported. The first set includes the results of the aluminum speciation experiments. One hundred mL of solution collected after the 20 min slow mixing

period during the jar tests were split through the aluminum speciation procedure as described in Chapter 3. The aluminum in the precipitate retained on the 0.45 μm membrane filter and the fraction in the filtrate are referred to as aluminum precipitate and dissolved aluminum respectively. It should be emphasized that no further distinction was made between species, i.e., organically bound aluminum or rapidly reactive aluminum. The other set, the residual aluminum, is the aluminum measured in the finished water (after rapid mix, slow mix, sedimentation and filtration).

4.2.2.1 Aluminum Precipitate and Dissolved Aluminum

The aluminum precipitate formation at varying aluminum chloride dosages is shown in Figure 4.4. The aluminum dosage ranged from 1 mg/L to 4 mg/L. The analysis of variance (ANOVA) results are presented in Table 4.5.

Significantly more aluminum precipitate was formed at pH7 compared to pH4 for all four aluminum dosages. The aluminum precipitate increased consistently with increasing initial aluminum dosages at pH7. The increase however, was not as consistent at pH4 because little precipitate existed.

The effect of the addition of 50 mg/L sulfate to the water sample with 0 mgC/L varied with the aluminum dosage at pH4. No difference occurred at the aluminum dosage of 1 mg/L. A decrease was noted at the aluminum dosage of 2 mg/L (300 $\mu\text{g/l}$ 198 $\mu\text{g/l}$),

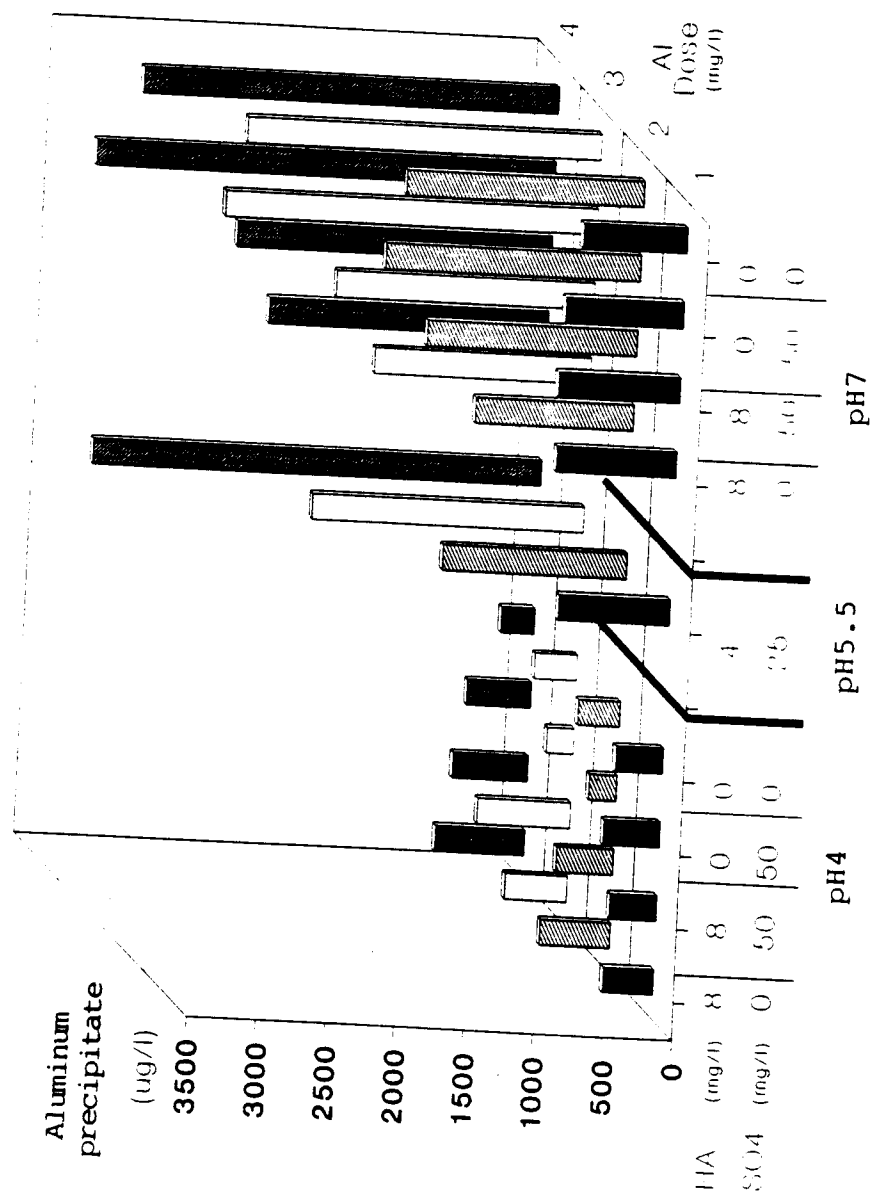


Figure 4.4: The coagulation of AHS using $AlCl_3$; the aluminum precipitate formation at various pH and aluminum dosages

Table 4.5: Aluminum Chloride Coagulation Results.
Aluminum Precipitate (µg/l)

Raw water parameters			Aluminum Dosage (mg/l)															
			1				2				3				4			
pH	SO4 (mg/l)	HA (mg/l as TOC)	C	SD	.	C	SD	.	C	SD	.	C	SD	.	C	SD	.	
7	0	0	746		C	1708		B	2550		B	2990		B	3233		17.4 A	
5.5	25	4	799	16	B C	1327	14 D		1962	24 C		2268		C	2016		646 E	
7	50	8	876		A	1512	C		1860		C	462 H		E	542 F		240 H	
7	0	8	864		A B	1140	E		1560		D	306 G		D	3304 A		2846 A	
4	0	8	360		D	504	F		450		F			F				
4	50	0	404		D	198	I		192		H			H				
4	50	8	336		D	410	G		670		E			E				
4	0	0	340		D	300	H		306		G			G				
7	50	0	850		A B	1837	A		2846		A			A				

Measurements with the same letter are not significantly different (95% confidence level)

and 3 mg/L (306 $\mu\text{g/l}$ to 192 $\mu\text{g/l}$), followed by an increase (240 $\mu\text{g/l}$ to 462 $\mu\text{g/l}$) at the dosage of 4 mg/L.

The addition of 50 mg/L of sulfate, with 8 mg/L AHS present did not consistently affect the aluminum hydroxide formation at pH4. The aluminum precipitate was not significantly different at the aluminum dosage of 1 mg/L. The precipitate increased at the aluminum dosage of 3 mg/L (450 $\mu\text{g/l}$ to 670 $\mu\text{g/l}$), and decreased significantly at the aluminum dosages of 2 mg/L (504 $\mu\text{g/l}$ to 410 $\mu\text{g/l}$), and 4 mg/L (646 $\mu\text{g/l}$ to 542 $\mu\text{g/l}$).

The addition of AHS resulted in a significant aluminum precipitate formation at the aluminum dosages greater than 1 mg/L (pH4). The aluminum precipitate concentration was significant regardless of the sulfate concentration. The increase varied from 198 μg to 410 $\mu\text{g/l}$ at the dosage of 2 mg/L, and 462 $\mu\text{g/l}$ to 542 $\mu\text{g/l}$ at the dosage of 4 mg/L, when sulfate concentration was 50 mg/L. When no sulfate was added, the increase varied from 300 $\mu\text{g/l}$ to 504 $\mu\text{g/l}$, and 240 $\mu\text{g/l}$ to 646 $\mu\text{g/l}$, at the aluminum dosage of 2 and 4 mg/L respectively.

At pH7, the aluminum precipitate increased significantly with the addition of 50 mg/L of sulfate. The only exception was at the aluminum dosage of 1 mg/L with AHS concentration of 8 mg/L where no difference existed.

The sulfate addition caused a 24.6%, 16.1%, and 11.1% increase for aluminum dosages of 2, 3, and 4 mg/L respectively when AHS concentration was 8 mgC/L. The increase was 12 %, 7%,

10.4%, and 9.5% at the aluminum dosages of 1, 2, 3, and 4 mg/L respectively for AHS concentration of 0 mg/L.

The addition of 8 mgC/L AHS to the water containing 0 mg/L sulfate (pH7) resulted in a consistent decrease in the aluminum precipitate at aluminum dosages greater than 1 mg/L. The decrease varied from 1708 $\mu\text{g/l}$ to 1140 $\mu\text{g/l}$ at the dosage of 2 mg/L, 2550 $\mu\text{g/l}$ to 1560 $\mu\text{g/l}$ at the dosage of 3 mg/L, and 2990 $\mu\text{g/l}$ to 2016 $\mu\text{g/l}$ at the dosage of 4 mg/L. The decrease was as consistent when 8 mgC/L AHS was added to the water containing 50 mg/L sulfate. The impact of AHS addition at pH7 was opposite the effect of AHS addition at pH4.

The amount of aluminum precipitate formed at the center point was as high as the amount formed at pH7. The amount increased with increasing aluminum concentration.

The dissolved aluminum results (Figure 4.5, and Table 4.6) correlated well with the aluminum precipitate formation. More dissolved aluminum were found at pH4 than at pH7. The more aluminum precipitate formed, the less the dissolved aluminum.

A few exceptions were observed at pH4, with AHS concentration of 8 mgC/L. The dissolved aluminum concentration decreased by 23 $\mu\text{g/l}$, 130 $\mu\text{g/l}$, 300 $\mu\text{g/l}$ at the aluminum dosages of 1, 2, and 3 respectively, and increased by 295 $\mu\text{g/l}$ at the aluminum dosage of 4 mg/L, with the addition of 50 mg/L sulfate. The aluminum precipitate did not vary at the aluminum dosage of 1 mg/L, decreased by 94 $\mu\text{g/l}$, at aluminum dosage of 2

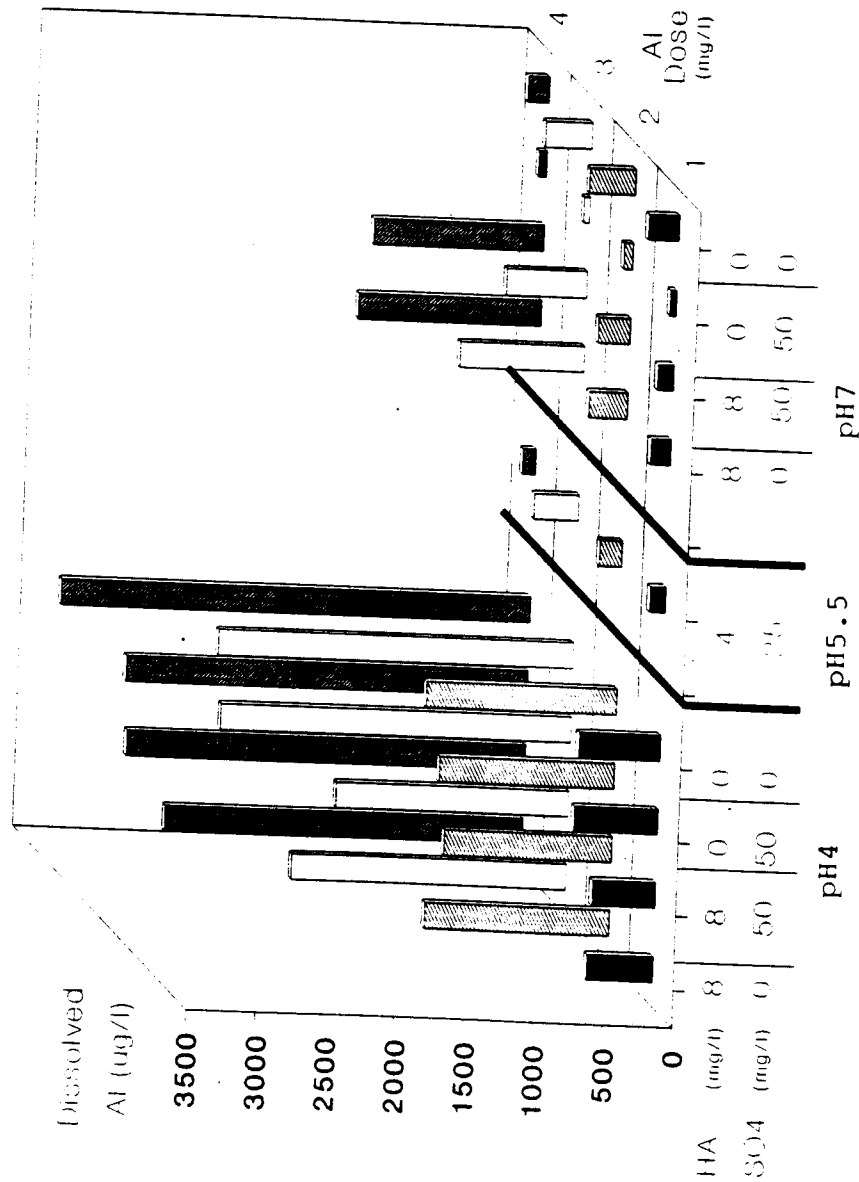


Figure 4.5: The coagulation of AHS with $AlCl_3$; the dissolved aluminum concentration at various pH and aluminum dosages

Table 4.6 : Aluminum Chloride Coagulation Results.
Dissolved Aluminum (µg/l)

Raw water parameters			Aluminum Dosage (mg/l)											
			1				2				3			
pH	SO ₄ (mg/l)	HA (mg/l as TOC)	C	SD	.	C	SD	.	C	SD	.	C	SD	.
7	0	0	220		C	330		E	336		F	153		G
5.5	25	4	112.3	10.1	D	162	7.3	H	323.3	13.4	F	93.5	5.5	H
7	50	8	115		D	230		G	578		E	1229		F
7	0	8	146		D	276		F	897		D	1319		E
4	0	8	475		B	1332		B	1979		B	2578		D
4	50	0	601		A	1260		C	2526		A	2897		B
4	50	8	452		B	1202		D	1676		C	2873		C
4	0	0	587		A	1372		A	2560		A	3380		A
7	50	0	45		E	66		I	41		G	56		I

Measurements with the same letter are not significantly different (95% confidence level)

mg/L, and 104 μ g/l at aluminum dosage of 4 mg/L. The precipitate increased at the aluminum dosage of 3 mg/L. The discrepancy could be due to the experimental technique and the relatively low aluminum precipitation at pH4.

4.2.2.2 Residual Aluminum

The residual aluminum concentrations after filtration of the treated water through Whatman#40 (8 μ m) are presented in Figures 4.6 and Table 4.7. The use of the large size filter makes the interpretation of the data harder because the filter was not small enough to retain all the small aluminum precipitate. This is reflected by the high residual aluminum measurements in the finished water samples.

Less residual aluminum was measured at pH4. The residual aluminum concentration ranged from 103 μ g/l (50 mg/L sulfate, 0 mgC/L, and aluminum dosage of 2 mg/L) to 378 μ g/l (50 mg/L sulfate, 0 mgC/L, and aluminum dosage of 1 mg/L). Sulfate did not have a significant impact at pH4.

At pH7, the residual aluminum concentration ranged from 110 μ g/l (0 mgC/L, 50 mg/L sulfate, aluminum dosage of 3 mg/L) to 520 μ g/l (8 mgC/L AHS, 0 mg/L sulfate, and aluminum dosage of 3 mg/L). The addition of 50 mg/L of sulfate improved the residual aluminum concentration when AHS concentrations were 0 mg/L and 8 mgC/L. The decrease in the residual aluminum concentration was higher

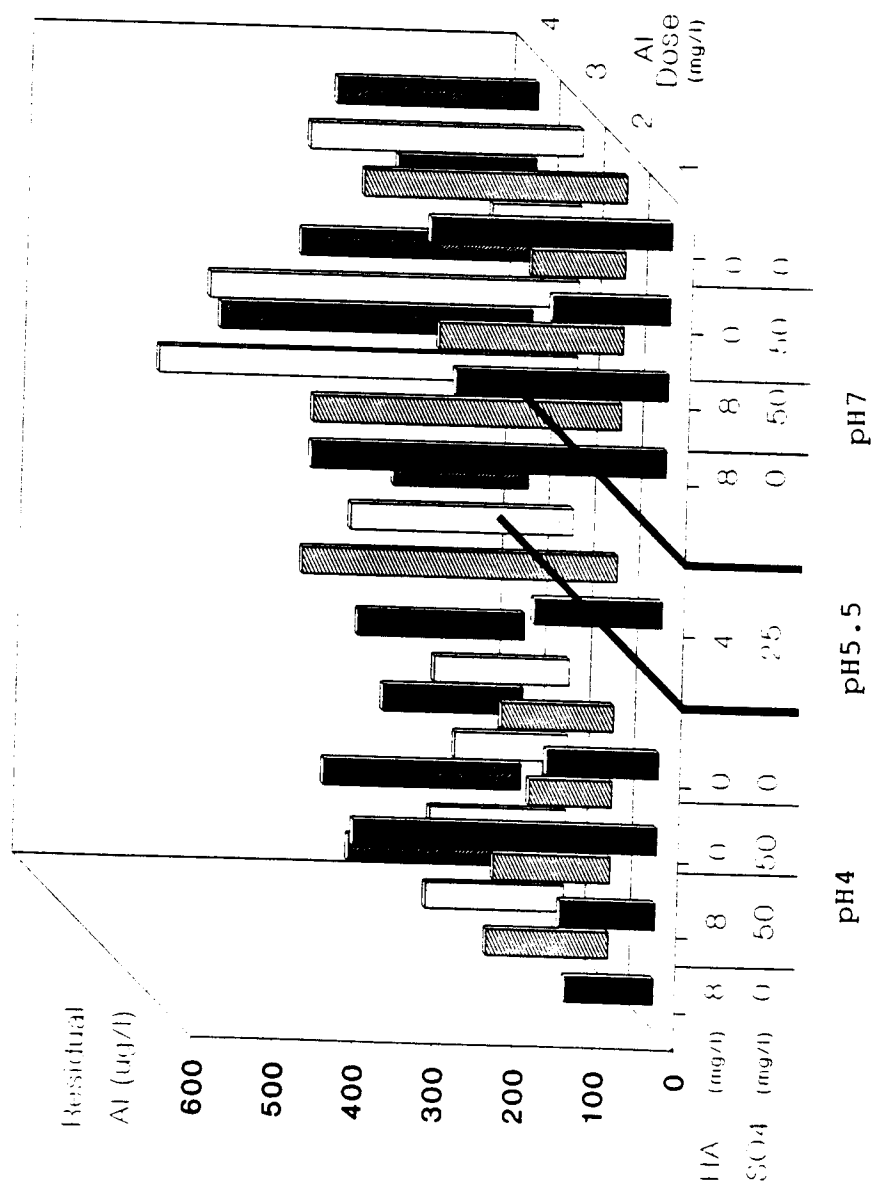


Figure 4.6: The coagulation of AHS with $AlCl_3$; the residual aluminum concentration at various pH and aluminum dosages

Table 4.7 : Aluminum Chloride Coagulation Results.
Residual Aluminum (µg/l)

Raw water parameters			Aluminum Dosage (mg/l)															
			1				2				3				4			
pH	SO4 (mg/l)	HA (mg/l as TOC)	C	SD	.	C	SD	.	SD	.	C	SD	.	C	SD	.	SD	
7	0	0	300		C		327		B		339		C	250		C		
5.5	25	4	159	9.1	D		393	12.3	A		277		7.6 D	166		9 F		
7	50	8	264		C		229		C		459		B	290		B		
7	0	8	442		A		384		A		520		A	388		A		
4	0	8	110		E		152		D		172		E	213		C D		
4	50	0	378		B		103		D		140		E F	174		E F		
4	50	8	118		E		145		D		169		E	246		C D		
4	0	0	139		D E		139		D		168		E	208		D E		
7	50	0	146		D E		116		D		110		F	172		E F		

Measurements with the same letter are not significantly different (95% confidence level)

when no AHS was present.

4.2.3 Removal of Dissolved Organic Carbon and Ultraviolet Absorbance

The results of Dissolved Organic Carbon (DOC) and UV measurements after filtration are presented in Figure 4.7 and Figure 4.8, respectively. The results of the statistical analysis are shown in Table 4.8. No AHS was added to the raw water for the jar tests corresponding to the low level of the factorial design. The DOC measurements of the low level were below the detection limit of the TOC analyzer (0.2mg/l).

The residual DOC at pH7 ranged from 0.7 (50 mg/L sulfate, aluminum dosage of 2 mg/L) to 0.9 (0 mg/L sulfate, and aluminum dosage of 4 mg/L). The addition of 50 mg/L sulfate significantly improved the DOC removal by 16% at the aluminum dosage of 4 mg/L. The lower residual DOC was confirmed at the aluminum dosage of 3 mg/L with the UV data. No significant differences were noted at lower aluminum dosages.

Maximum DOC removal was achieved at the center point (4 mgC/L AHS, 25 mg/L sulfate, pH5.5). The AHS residual dropped from 0.98 to 0.23 at the aluminum dosages of 1 and 4 mg/L respectively. The highest removal was obtained with the aluminum dosage of 4 mg/L.

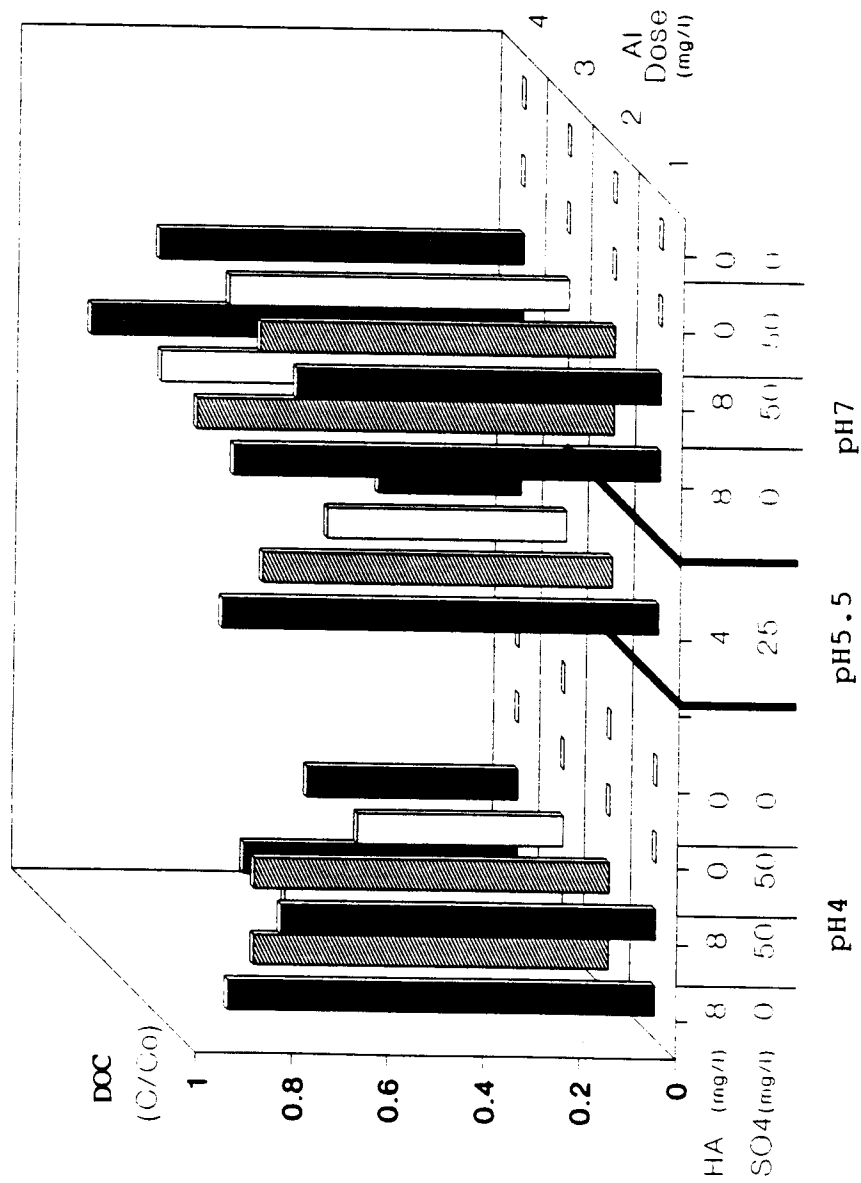


Figure 4.7: The coagulation of AHS with AlCl₃; the residual DOC at various pH and aluminum dosages

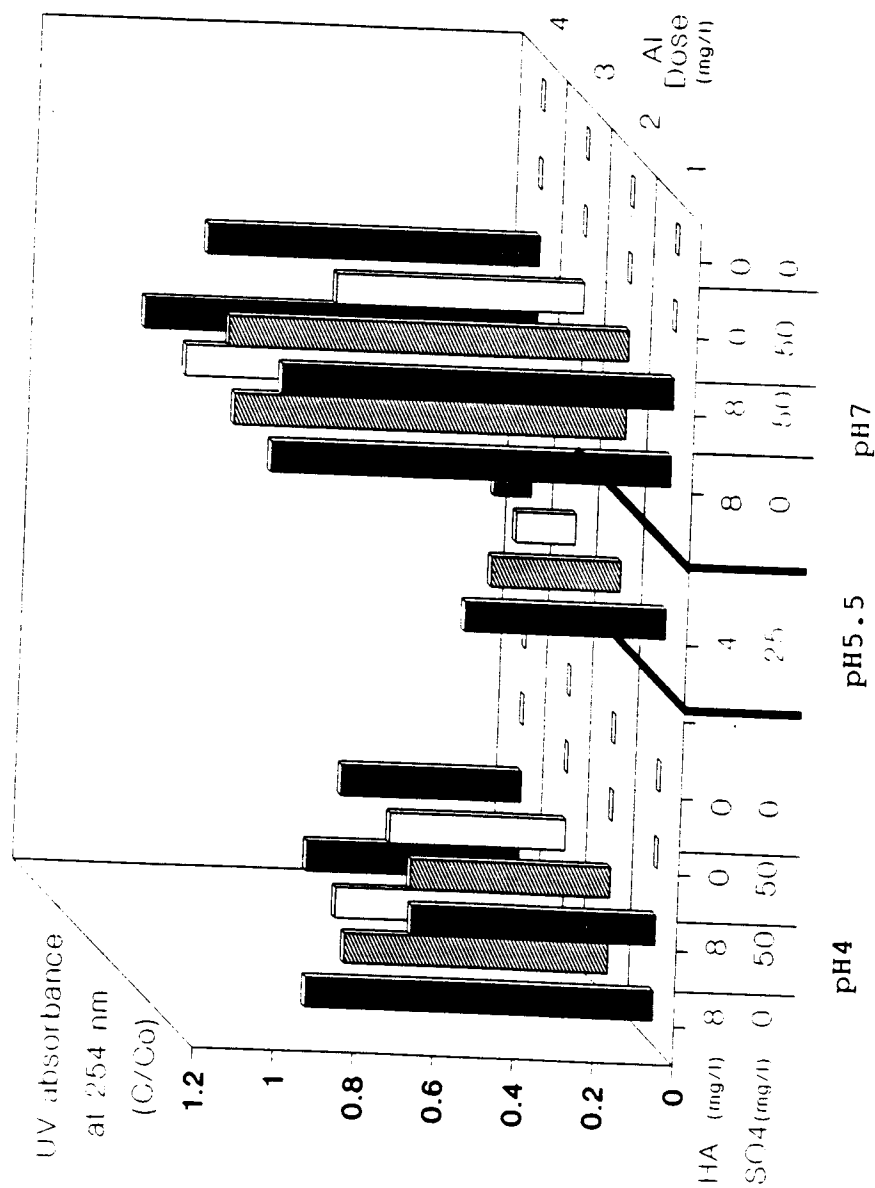


Figure 4.8: The coagulation of AHS with AlCl_3 ; the residual UV absorbance at various pH and aluminum dosages

Table 4.8 Aluminum Chloride Coagulation Results
DOC and UV measurements

a) DOC

Raw water parameters		Aluminum Dosages (mg/l)							
		1		2		3		4	
pH	SO ₄ (mg/l)	HA (mg/l as TOC)	C/Co	SD	C/Co	SD	C/Co	SD	C/Co
7	0	0	0.98	0.04	A	0.48	0.058	B	0.3
5.5	25	4	0.76	0.04	A	0.7	0.71	A	0.23
7	50	8	0.89	0.04	A	0.87	0.85	A	0.76
7	0	8	0.89	0.04	A	0.7	0.58	A	0.9
4	0	8	0.89	0.04	A	0.7	0.58	B	0.57
4	50	0							
4	50	8	0.78	0.04	A	0.74	0.43	C	0.44
4	0	0							
7	50	0							

b) UV Absorbance at 254 nm (1cm cell)

Raw Water Parameters		Aluminum Dosage (mg/l)							
		1		2		3		4	
pH	SO ₄ (mg/l)	HA (mg/l as TOC)	C/Co	SD	C/Co	SD	C/Co	SD	C/Co
7	0	0	0.5	0.03	B	0.32	0.043	C	0.15
5.5	25	4	0.98	0.03	A	1	0.6	B	0.09
7	50	8	1	0.03	A	0.98	0.99	A	0.8
7	0	8	0.87	0.03	A	0.66	0.57	B	0.98
4	0	8	0.61	0.03	B	0.5	0.44	C	0.53
4	50	0							
4	50	8	0.61	0.03	B	0.5	0.44	C	0.45
4	0	0							
7	50	0							

Measurements with the same letter are not significantly different (95% confidence level)

The residual AHS concentration was lower at pH4. With 50 mg/L sulfate added, the DOC residual varied from 0.89 at the aluminum dosage of 1 mg/L to 0.57 at the aluminum dosage of 4 mg/L. The variation was 0.78 at the aluminum dosage of 1 mg/L to 0.43 at the aluminum dosage of 3 mg/L. The addition of 50 mg/L of sulfate decreased the DOC removal by 23% at the aluminum dosage of 4 mg/L, as opposed to the 16% improvement seen at pH7. The shift in the UV measurement occurred at the aluminum dosage of 2 mg/L compared to 3 mg/L at pH7.

4.2.4 Turbidity and Particle Count

Turbidity removal before filtration at pH4 ranged from 29% (50 mg/L sulfate, 8 mgC/L AHS, and 1 mg/L aluminum dosage) to 92% (0 mg/L sulfate, 0 mgC/L AHS, and 4 mg/L aluminum dosage) as seen in Figure 4.9 and Table 4.9 a).

The addition of sulfate to the water containing no AHS did not have a significant impact on the residual turbidity. However, sulfate increased the residual turbidity before filtration when 8 mgC/L AHS was added to the water at all but the aluminum dosage of 2 mg/L. The residual turbidity increased ranged from 9% (aluminum dosage of 3 mg/L) to 61% (aluminum dosage of 1 mg/L) before filtration. The turbidity increased after filtration (Figure 4.10 and Table 4.9 b) was not as consistent. The difference was only significant at the aluminum dosages of 1 and 4 mg/L.

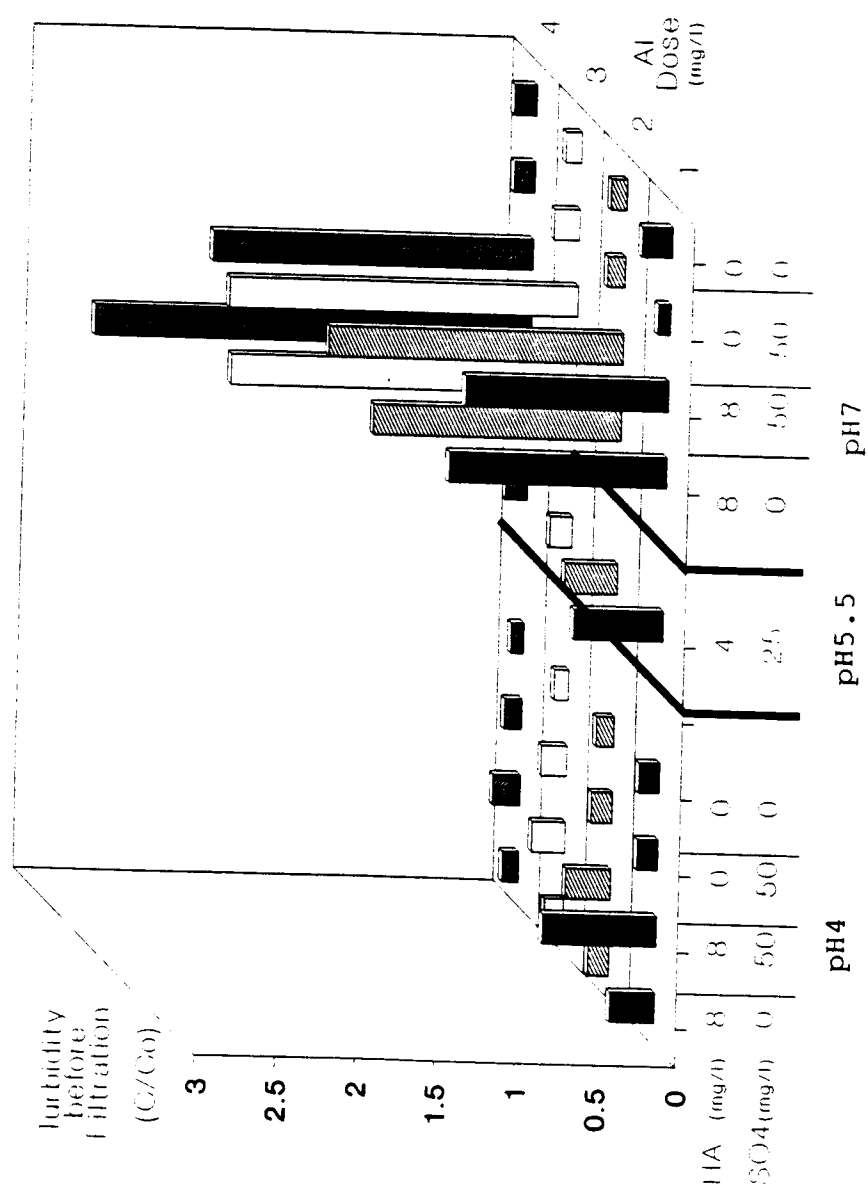


Figure 4.9: The coagulation of AHS with AlCl_3 ; the residual turbidity before filtration at various pH and aluminum dosages

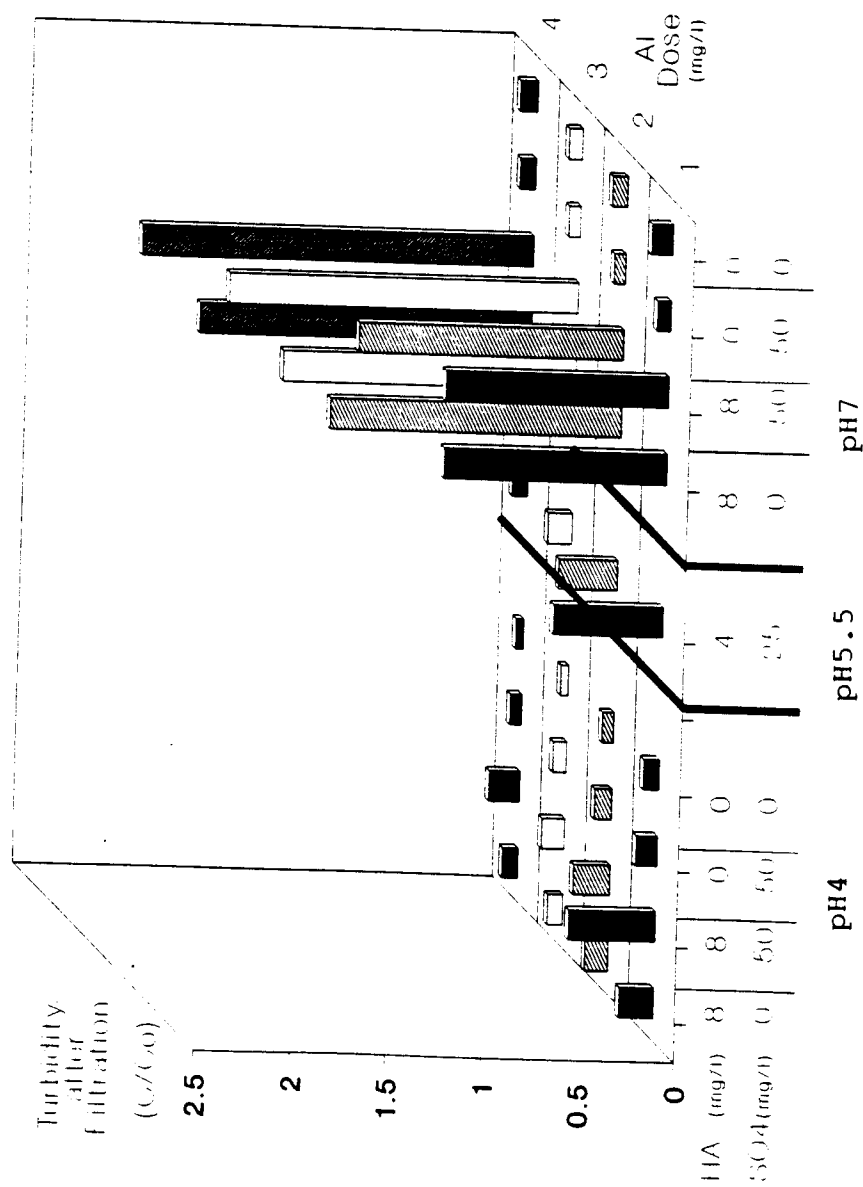


Figure 4.10: The coagulation of AHS with ALC13; the residual turbidity after filtration at various pH and aluminum dosages

Table 4.9 Aluminum Chloride Coagulation Results
Turbidity Measurements

a) Before Filtration (NTU)

Raw water parameters		Aluminum Dosage (mg/l)							
		1		2		3		4	
pH	SO ₄ (mg/l)	HA (mg/l as TOC)	C/Co	SD	C/Co	SD	C/Co	SD	
7	0	0	0.19	0.04	0.19	0.04	0.19	0.04	C D
5.5	25	4	0.6	0.04	0.6	0.04	0.6	0.04	C D E
7	50	8	1.27	0.04	1.27	0.04	1.27	0.04	B
7	0	8	1.36	0.04	1.36	0.04	1.36	0.04	A
4	0	8	0.28	0.04	0.28	0.04	0.28	0.04	D E
4	50	0	0.13	0.04	0.13	0.04	0.13	0.04	D E
4	50	8	0.71	0.04	0.71	0.04	0.71	0.04	C
4	0	0	0.13	0.04	0.13	0.04	0.13	0.04	E
7	50	0	0.08	0.04	0.08	0.04	0.08	0.04	C D E

b) After Filtration (NTU)

Raw water parameters		Aluminum Dosage (mg/l)							
		1		2		3		4	
pH	SO ₄ (mg/l)	HA (mg/l as TOC)	C/Co	SD	C/Co	SD	C/Co	SD	
7	0	0	0.11	0.05	0.11	0.05	0.11	0.05	D
5.5	25	4	0.57	0.05	0.57	0.05	0.57	0.05	D E
7	50	8	1.16	0.05	1.16	0.05	1.16	0.05	A
7	0	8	1.16	0.05	1.16	0.05	1.16	0.05	B
4	0	8	0.18	0.05	0.18	0.05	0.18	0.05	D E
4	50	0	0.11	0.05	0.11	0.05	0.11	0.05	D E
4	50	8	0.45	0.05	0.45	0.05	0.45	0.05	C
4	0	0	0.08	0.05	0.08	0.05	0.08	0.05	E
7	50	0	0.07	0.05	0.07	0.05	0.07	0.05	D E

Measurements with the same letter are not significantly different (95% confidence level)

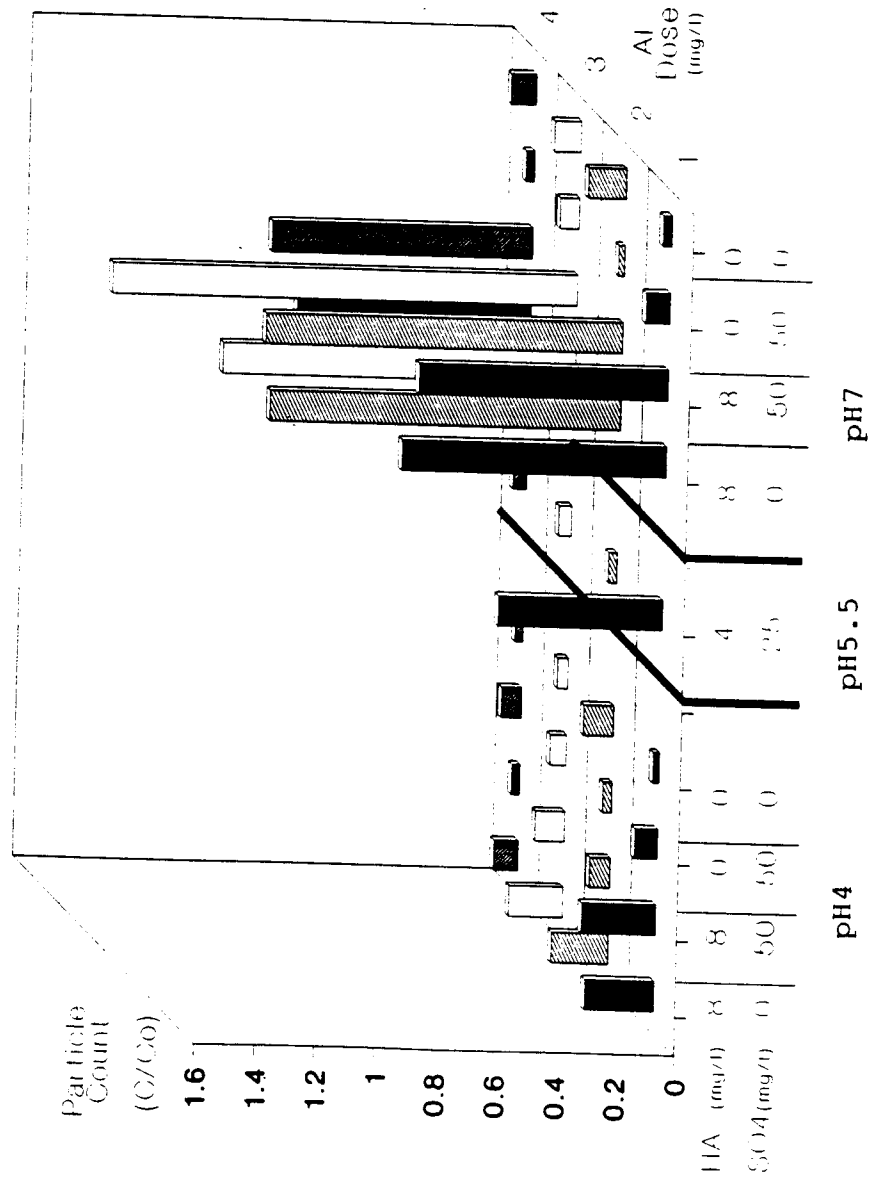


Figure 4.11: The coagulation of AHS with AlCl₃; the residual particle count before filtration at various pH and aluminum dosages

Table 4.10: Particle Count at Various Times
During Coagulation.

AHS [*] Sulfate ^{**} pH	Aluminum Dosage (mg/l)	Sampling Time (min)	Water Sample									
			0	4	8	8	8	8	8	0	0	50
			0	25	50	0	0	0	0	50	0	0
			7	5.5	7	7	4	4	4	4	4	7
1		0	31000	26360	27041	27456	24785	28453	25768	23023	220546	
		5	64188	16092	38004	80800	28765	32456	29878	27546	245678	
		10	111344	140054	38946	78025	20567	60987	47865	26798	298769	
		15	59469	146246	38296	103392	76589	65785	30786	28760	564329	
		20	68431	134425	37567	97233	56789	56732	45365	22908	342980	
2		5	90329	105275	34167	93738	64324	45778	45674	79432	42340	
		10	71941	104588	34971	53904	76895	60056	39876	78976	45675	
		15	96550	10400	32425	62229	54675	78965	68745	65231	47342	
		20	73860	104746	27933	81296	45789	47869	30987	56742	36587	
3		5	76781	17179	36688	77629	67547	89564	67548	78654	67856	
		10	74550	10929	28113	44917	96786	83677	54678	98453	76032	
		15	71806	6175	33688	47808	89765	45769	66543	87985	77402	
		20	65547	45633	35117	74629	84322	65476	62310	83908	63423	
4		5	26388	8581	36417	38300	104325	87610	73108	188754	74532	
		10	23663	8581	30946	37046	78743	98504	67432	178342	78620	
		15	20781	3585	38001	39221	67843	83419	78645	105643	67535	
		20	21059	3658	34258	42317	87654	79641	77489	119865	66789	

* mgC/l

** mg/l

The particle count results (Figure 4.11 and Table 4.11) were opposite the turbidity data with 8 mgC/L AHS. Sulfate decreased the residual particle count at the aluminum dosages greater than 1 mg/L. The results suggested that a greater number of smaller particles, not detectable by the particle counter were formed when sulfate was in solution.

An increase in residual turbidity occurred with the addition of 8 mgC/L AHS to the water sample with 50 mg/L sulfate. No significant increase was observed when the sulfate concentration was 0 mg/L.

Particle formation and growth to nonfilterable size occurred at pH7 when AHS concentration was 8 mg/L. The final turbidity values (before and after filtration) were consistently greater than the initial turbidity at all the aluminum dosages. The residual turbidity before filtration ranged from 1.27 (50 mg/L sulfate, and aluminum dosage of 1 mg/L) to 2.73 (0 mg/L sulfate, and aluminum dosage of 4 mg/L). The range was 1.16 (0 and 50 mg/L sulfate, and aluminum dosage of 1 mg/L) and 2.04 (50 mg/L sulfate, and aluminum dosage of 4 mg/L) after filtration.

The turbidity residual before filtration ranged from 0.07 (50 mg/L sulfate, and aluminum dosage of 1 mg/L) to 0.11 (0 mg/L sulfate, and aluminum dosage of 1 mg/L) with no AHS present. Little improvement was noted after filtration.

The data summarized in Table 4.10 showed that particle formation and growth occurred for all the treatment conditions with

Table 4.11: Aluminum Chloride Coagulation Results.
Particle Count Before Filtration

Raw water parameters			Aluminum Dosage (mg/l)											
			1				2				3			
pH	SO ₄ (mg/l)	HA (mg/l as TOC)	C/Co	SD	*	C/Co	SD	*	C/Co	SD	*	C/Co	SD	*
7	0	0	0.030		C	0.126		C	0.092		E D	0.083		C
5.5	25	4	0.548		B	0.029		E	0.043		F G	0.045		E
7	50	8	0.830		A	1.191		A	1.55		A	0.870		A
7	0	8	0.880		A	1.173		A	1.177		B	0.780		B
4	0	8	0.230		C	0.190		B	0.18		C	0.081		C D
4	50	0	0.076		C	0.033		E	0.055		F G	0.066		D
4	50	8	0.246		C	0.068		D	0.098		D	0.027		F
4	0	0	0.020		C	0.099		C D	0.036		G	0.027		F
7	50	0	0.082		C	0.020		E	0.064		E F	0.029		F

Measurements with the same letter are not significantly different (95% confidence level)

the addition of aluminum. The particle number increased above the initial particle number before the initial five minutes of sampling during coagulation. The data did not show a consistent difference among the experimental conditions.

4.2.5 Sulfate

Sulfate removal occurred at all pH values as shown in Figure 4.12 and Table 4.12. However, no consistent difference was noted. The variation of sulfate or AHS concentration impacted little the residual sulfate measurements.

The overall statistical comparison of the variable shown in Table 4.2 shows that pH was the most important variable in term of the measured parameters. The only exception was with the sulfate data where the effects among pH, sulfate, and AHS on the parameter measured did not differ. The variation of AHS had more impact on the measured parameters than sulfate variations.

The aluminum hydrolysis experiments and the jar tests results have demonstrated the formation of aluminum precipitate at varying r values. AHS and sulfate were removed by either adsorption on the precipitate and/or precipitation by the aluminum hydrolysis species. The pH or r values can be used to delineate the zone for the mechanisms of AHS and sulfate removal. The following adsorption experiments were conducted to study the adsorption of AHS and sulfate on the aluminum precipitates. The goal was to develop the

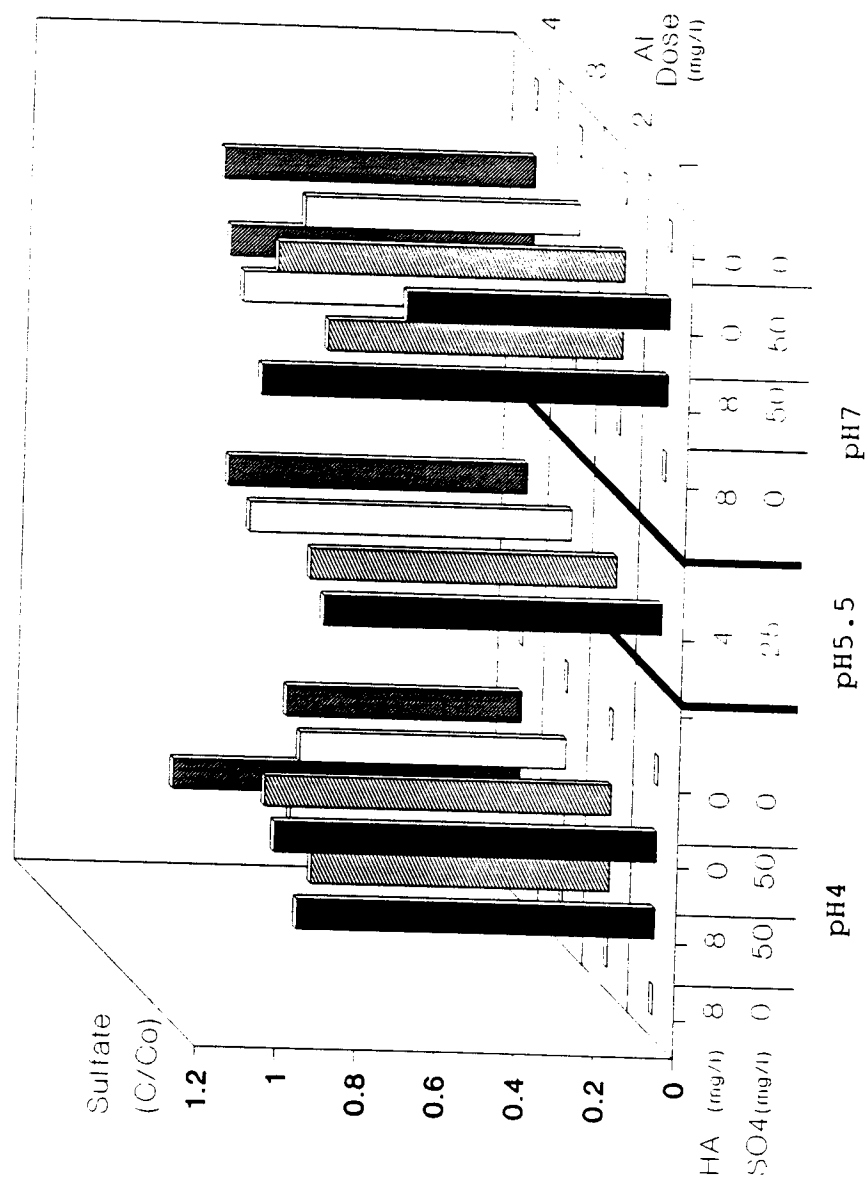


Figure 4.12: The coagulation of AHS with AlCl_3 ; the residual sulfate concentration at various pH and aluminum dosages

Table 4.12: Aluminum Chloride Coagulation Results.
Sulfate (mg/l)

Raw water parameters		Aluminum Dosage (mg/l)											
		1				2				3			
pH	SO ₄ (mg/l)	HA (mg/l as TOC)	C/Co	SD		C/Co	SD			C/Co	SD		
7	0	0											
5.5	25	4	0.85	0.06	A B	0.77	0.09	A	0.81	0.11	A	0.75	0.07
7	50	8	1.02		A	0.74		A	0.84		A	0.76	
7	0	8											
4	0	8											
4	50	0	0.96		A	0.87		A	0.67		A	0.59	
4	50	8	0.9		A	0.75		A	0.69		A	0.87	
4	0	0											
7	50	0	0.66		B	0.87		A	0.69		A	0.78	

Measurements with the same letter are not significantly different (95% confidence level)

adsorption isotherms of AHS and sulfate at pH 5.5 and 7.

4.3 ADSORPTION ON ALUMINUM PRECIPITATE

The adsorption procedures consisted of forming the precipitates with either aluminum chloride or aluminum sulfate and then adsorbing different AHS and sulfate concentrations. Aluminum nitrate was not used because it was shown in Section 4.1 that its hydrolysis precipitation was similar to that of aluminum chloride. The similarity suggested that the nature of the precipitates formed with these coagulants were identical.

4.3.1 Characteristics of Aluminum Precipitate

The aluminum precipitate in the adsorption study was formed on 0.2 μm membrane filters. The 0.2 μm membrane filters were custom made to fit the reactor cell used for the isotherm. The membrane filters used for the aluminum precipitate formation in the coagulation study were 0.45 μm in size. A series of aluminum precipitates were formed to determine whether there was a difference between the two filters. The comparison in Tables 4.13 shows that there was no difference between the aluminum precipitate formed with the 0.2 μm filter and the 0.45 μm membrane filters.

A quality check was performed to quantify the amount of

AHS and sulfate adsorbed on the 0.2 μm membrane filter. The data in Table 4.14 shows that little AHS and sulfate was adsorbed to the 0.2 μm membrane filter. The concern over aluminum loss during the aluminum precipitate formation was also addressed. The data of Figure 4.13 was used to calculate the aluminum loss through the precipitation process. A mass balance on the aluminum in the aluminum standard, the filtrates, and the rinse water gave 93 to 104% recoveries.

The results of the aluminum precipitate formation are shown in Figure 4.13. No difference existed between the precipitate formed with either aluminum chloride or aluminum sulfate (which could also be referred to as hydroxyl-aluminum-sulfate because of sulfate incorporation, see Section 4.1) precipitate. The pH variation from 5.5 to 7 did not affect the amount of aluminum precipitate formation.

The results were consistent with the theoretical aluminum species formation described by the aluminum stability diagram of Figure 2.10. $\text{Al}(\text{OH})_3$ solid is the predominant aluminum species for the aluminum concentration ranges of 10 to 150 mg at both pH 5.5 and 7. The 1 to 1 slope observed in Figure 4.4 confirmed that most of the aluminum was in the precipitate form.

Two forms of aluminum precipitate were prepared for the adsorption study. The first consisted of forming the aluminum precipitate with either aluminum chloride or aluminum sulfate. The aluminum was dissolved in Milli Q water and the pH adjusted to 5.5 or 7. The second form consisted of precipitate formed with $\text{Al}(\text{III})$

Table 4.13: Aluminum precipitate Formation on 0.2 μm and 0.4 μm Membrane Filters
(based on 50 ml volume)

Aluminum	Aluminum in standard (mg)	Al(OH) ₃ on 0.2 μm membrane filter (mg)	Al(OH) ₃ on 0.45 μm membrane filter (mg)
Aluminum Chloride	20	19.78	19.92
	18.5	17.2	16.87
	22.1	21.9	21.5
	19.1	18.5	18.7
Aluminum Sulfate	21.6	20.46	20.78
	17.9	17.3	17.4
	18.3	17.8	17.7
	25.1	24.5	24.4
	30.2	29.5	29.7
	20.8	18.8	18.7

Table 4.14: Sulfate and AHS Adsorption on 0.2 μm Membrane Filter

Filtration sequence	SO ₄ before filtration (mg/l)	SO ₄ after filtration (mg/l)	TOC HA before filtration (mg/l)	TOC HA after filtration (mg/l)
1	14.39	14.25	9.98	10.03
2	14.22	14.2	10.02	9.86
3	14.51	14.39	10.06	9.95
4	14.5	14.45	10.16	9.98
5	14.22	14.21	9.85	10.01
6	14.3	14.24	9.79	9.91

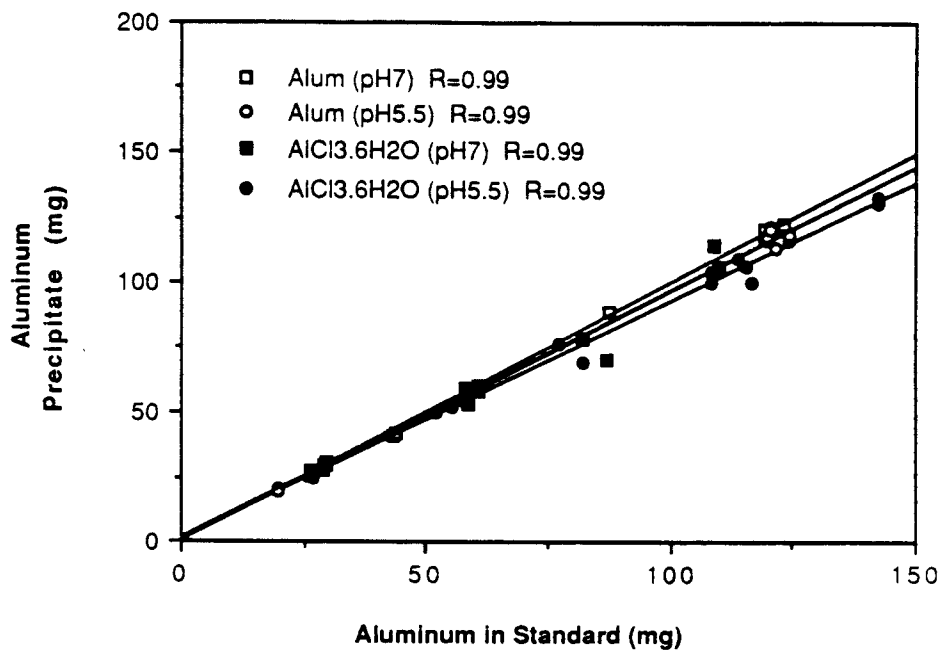


Figure 4.13: Aluminum precipitate formation with Al(III) solutions

and AHS solutions. AHS was added to the aluminum solution before pH adjustment. The later precipitate form is closer to water treatment conditions because it contains AHS.

4.3.2 Equilibration Time

The equilibration times for the adsorption of AHS on the aluminum chloride and aluminum sulfate precipitates are shown in Figure 4.14. AHS adsorption took place quickly. No significant additional adsorption was observed after 1 hr equilibration time. This was true at either pH for both types of aluminum precipitates.

AHS had a higher affinity for both aluminum precipitates at pH7. The surface concentration (amount of AHS adsorbed per amount of aluminum precipitate, X/M) was 0.117 for aluminum sulfate, and 0.103 for aluminum chloride after 1 hr equilibration time. The X/M ratios dropped to 0.08 for both adsorbants at pH5.5.

The X/M ratio for AHS adsorbed on the aluminum sulfate precipitate at pH7 (0.117) was greater than the X/M for AHS adsorbed on aluminum chloride precipitate (0.103). Little difference existed between the aluminum precipitates at pH5.5.

Sulfate adsorption on the aluminum chloride precipitate was quicker (Figure 4.15). Virtually no noticeable adsorption was observed after 30 min equilibration time compared to 1 hr for AHS. The 30 min was sufficient for both pH5.5 and 7. The affinity of sulfate for the aluminum chloride precipitate was opposite that of

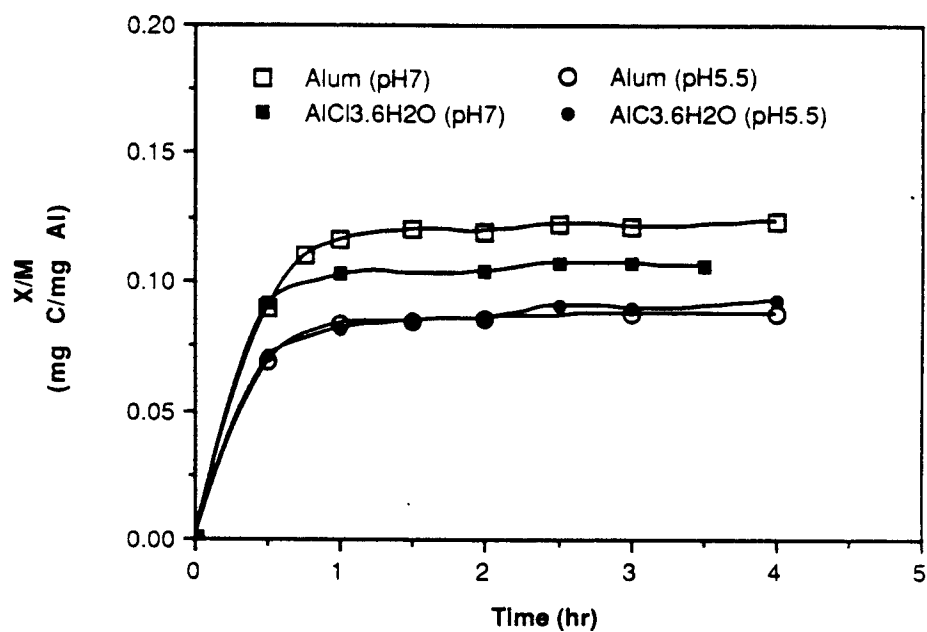


Figure 4.14: Equilibration time for the adsorption of aquatic humic substances on aluminum precipitates

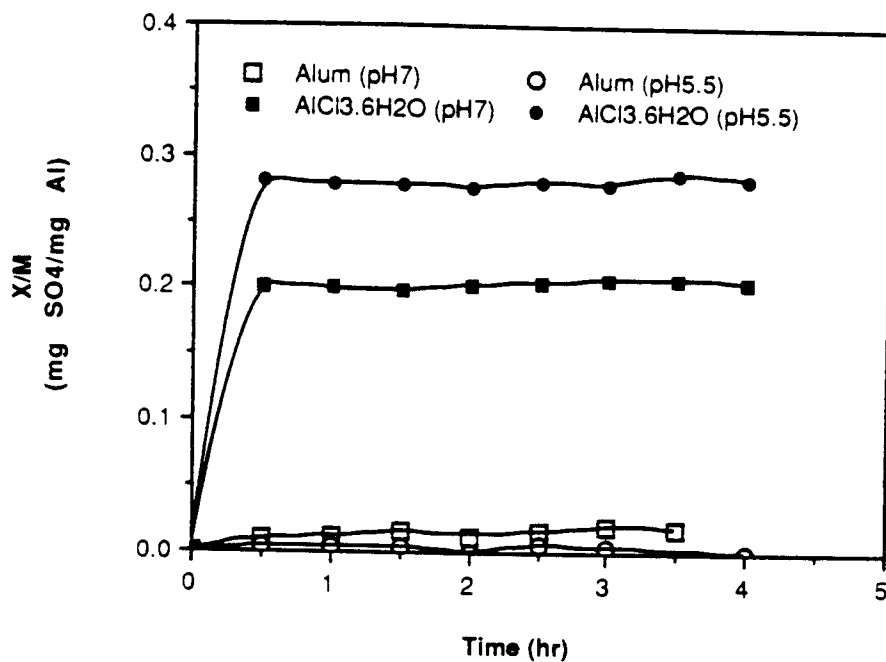


Figure 4.15: Equilibration time for the adsorption of sulfate on aluminum precipitates

AHS. The X/M at pH5.5 was 0.28 compared to 0.2 at pH5.5. Little sulfate was adsorbed on the aluminum sulfate precipitate regardless of the pH.

4.3.3 Adsorbent Capacity

The results of experiments designed to evaluate the adsorption capacity of Al(III) precipitate adsorbent are shown in Figure 4.16 and Figure 4.17. Twenty mg of the aluminum precipitate were formed at either pH5.5 or 7. Fifty mL of the AHS adsorbate was sequentially equilibrated, four times, for 1 hr at each sequence. The same procedure was repeated for the sulfate adsorbate. The amount of aluminum precipitate and the volume of adsorbate were increased to about 140 mg (100 mL of 14 00mg/l Al) and 100 mL respectively.

Figure 4.16 indicated that the total AHS adsorbed was a function of the concentration of the adsorbate solution. Successive replenishment of the adsorbate AHS solution caused an additional adsorption of AHS. The adsorption capacity of the adsorbent was not totally exceeded even after the 3rd and 4 th sequences.

The adsorption capacity of the aluminum sulfate precipitate did not vary with pH until the third sequence. The adsorption capacity was increased at the third and fourth sequences at pH5.5. The identical AHS adsorption for the first sequence at pH5.5 and 7 contrasted with the results of the equilibration experiments. The equilibrium surface concentration in the equilibration experiments

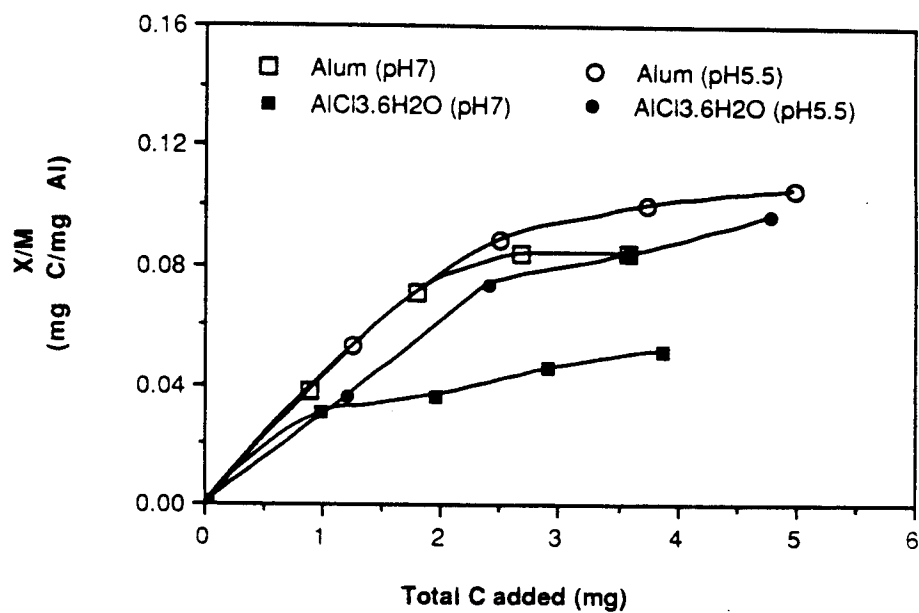


Figure 4.16: Adsorbent capacity for the adsorption of aquatic humic substances on aluminum precipitates

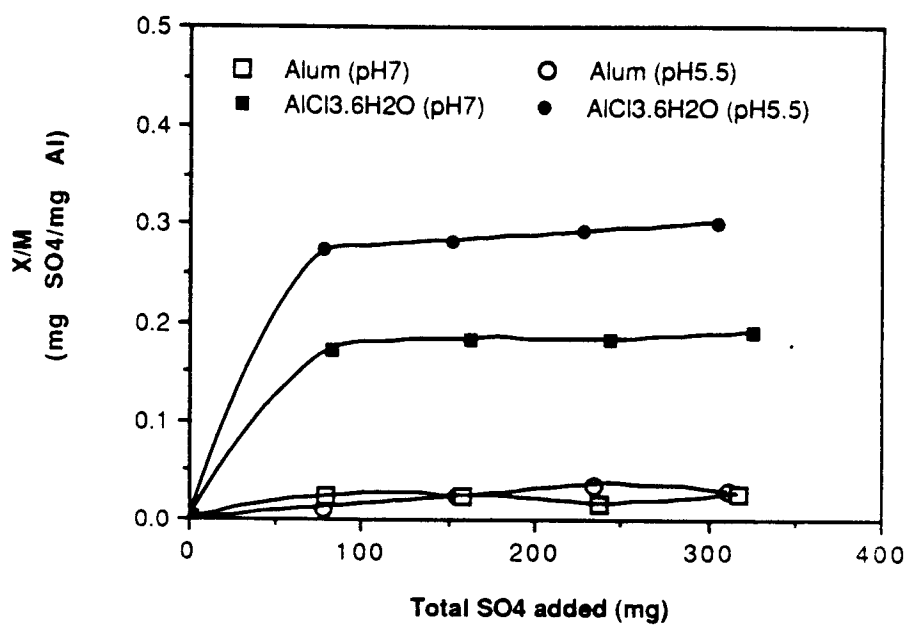


Figure 4.17: Adsorbent capacity for the adsorption of sulfate on aluminum precipitates

was higher at pH7.

No difference existed at the first sequence between the adsorption capacity of the aluminum chloride precipitate at pH5.5 and 7. The adsorption capacity at pH5.5 was almost twice the capacity at pH7 for the later sequences. The affinity of AHS for the aluminum sulfate precipitate was higher than that of aluminum chloride at both pH values.

The data indicated that the equilibration condition reached after 1 hour reflected an equilibrium between the adsorbent and the adsorbate solution. The equilibrium condition was not the condition for maximum adsorption. The results suggest that the AHS adsorption on the two aluminum precipitate followed a multi-layer type of adsorption.

The aluminum chloride adsorbent capacity was exhausted after only the first sequence of adsorption of sulfate (Figure 4.16). No additional adsorption occurred with the remaining 3 sequences at both pH5.5 and 7. The adsorption capacity was greater at the lower pH5.5.

Little adsorption occurred for the adsorption of sulfate on the aluminum sulfate precipitate. The results agreed with the data of Figure 4.17). Sulfate had a greater affinity for the aluminum chloride precipitate at pH5.5.

4.3.4 Aquatic Humic Substances Adsorption on Aluminum Precipitate

Adsorption isotherms of AHS and their Langmuir and Freundlich transformation are shown in Figures 4.18, 4.19, and 4.20. Figure 4.18 confirmed the greater affinity of AHS for the aluminum sulfate adsorbent. The surface concentration for a 10 mgC/L residual AHS concentration was about 0.05 mg/mg for the aluminum chloride adsorbent. The ratio almost doubled to about 0.1 mg/mg for the aluminum sulfate adsorbent.

Figure 4.19 shows that the data fit Freundlich best. The Freundlich fit was consistent with the initial observation where successive adsorptions on the aluminum chloride and aluminum sulfate precipitates did not result in a saturation of the adsorption sites. AHS adsorption continued until the 4th sequence of adsorption. The surface concentration of AHS did not approach a saturation value as the concentration increased. The Freundlich constants for the isotherms are shown in Table 4.15.

Other experiments were conducted to determine whether the addition of AHS to the aluminum solution would impact the adsorption phenomenon. The aluminum precipitate was formed by mixing the aluminum chloride or aluminum sulfate and AHS solutions and adjusting the pH to 7. The results are summarized in Figures 4.21 and 4.22.

The aluminum to carbon ratio (mass ratio) was 45 to 1 in

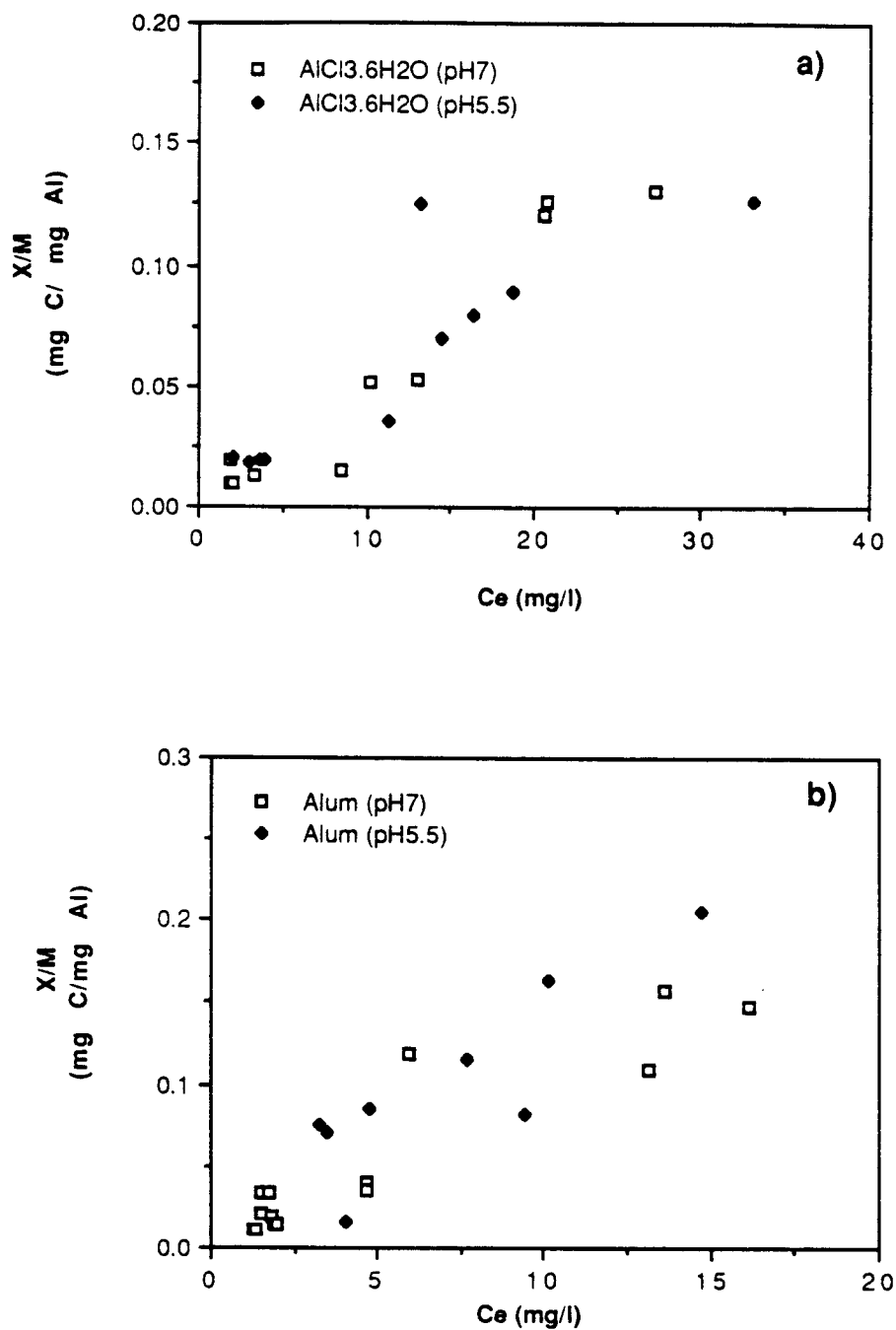


Figure 4.18: Aquatic humic substances adsorption on aluminum precipitates
a) Aluminum chloride adsorbant
b) Aluminum sulfate adsorbant

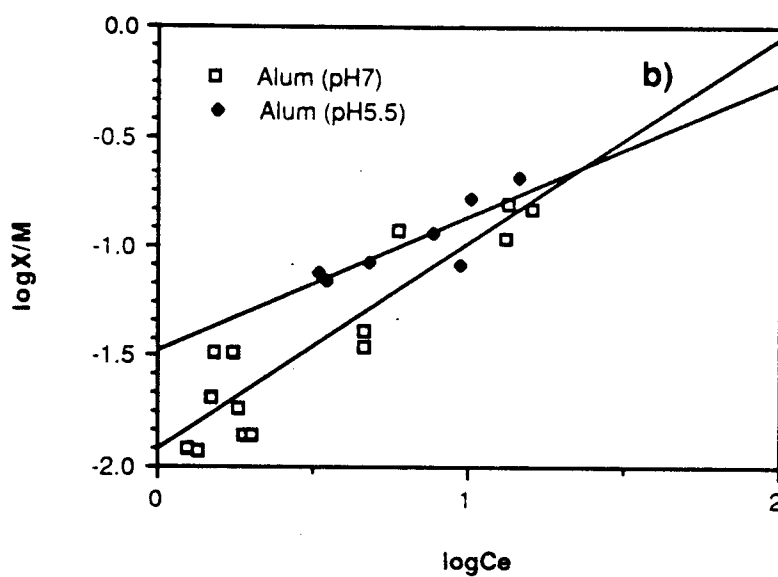
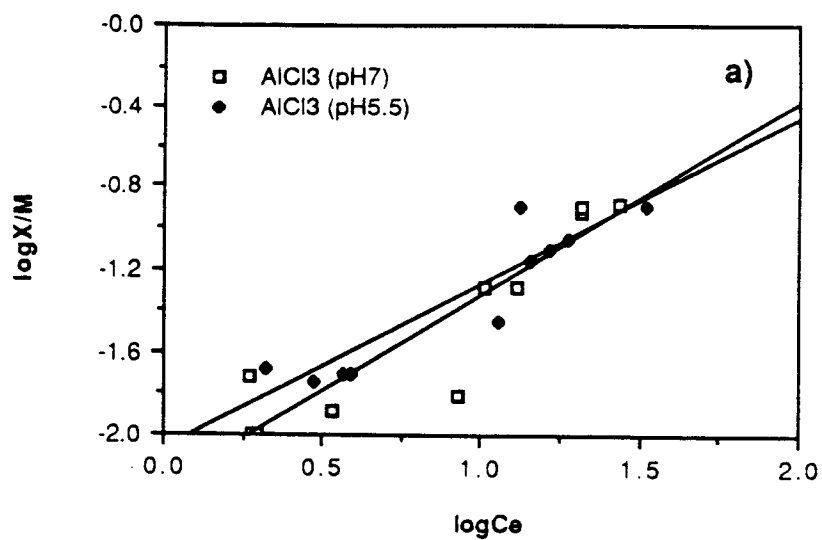


Figure 4.19: Aquatic humic substances adsorption on aluminum precipitate: Freundlich transformation
a) Aluminum Chloride
b) Aluminum Sulfate

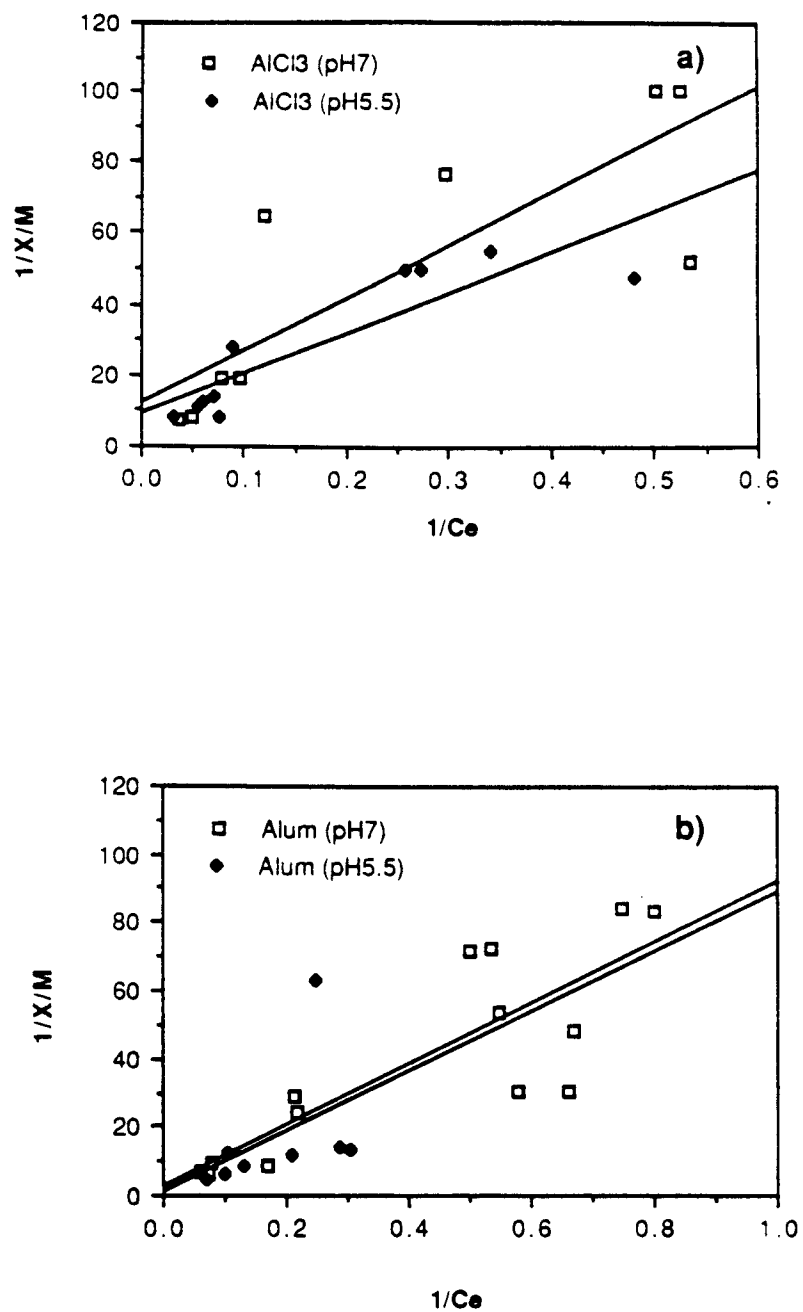


Figure 4.20: Adsorption of aquatic humic substances on aluminum precipitates: Langmuir transformation
a) Aluminum Chloride
b) Aluminum Sulfate

Table 4.15: Freundlich Equilibrium Constants for the Adsorption of AHS on Aluminum Chloride and Aluminum Sulfate Precipitates.

pH	7		5.5	
Constants	n	a (mg/mg)	n	a (mg/mg)
AlCl ₃ ·6H ₂ O Precipitate	1.09	5.6 10 ⁻³	1.25	8.3 10 ⁻³
Alum Precipitate	1.06	11.7 10 ⁻³	1.64	33.1 10 ⁻³

n = constant

a = mass AHS adsorbed/mass aluminum precipitate

the first set of experiments (black circle in Figure 4.21 and 4.22). The data fit Freundlich best. The slope of the curves indicated that adsorption of AHS occurred during the precipitate formation for both the aluminum chloride and the aluminum sulfate precipitates.

The ratio of aluminum:C was varied to 5.6 to 1 in the second set of experiments (open triangle) with the aluminum chloride adsorbent to determine the impact of the increased AHS

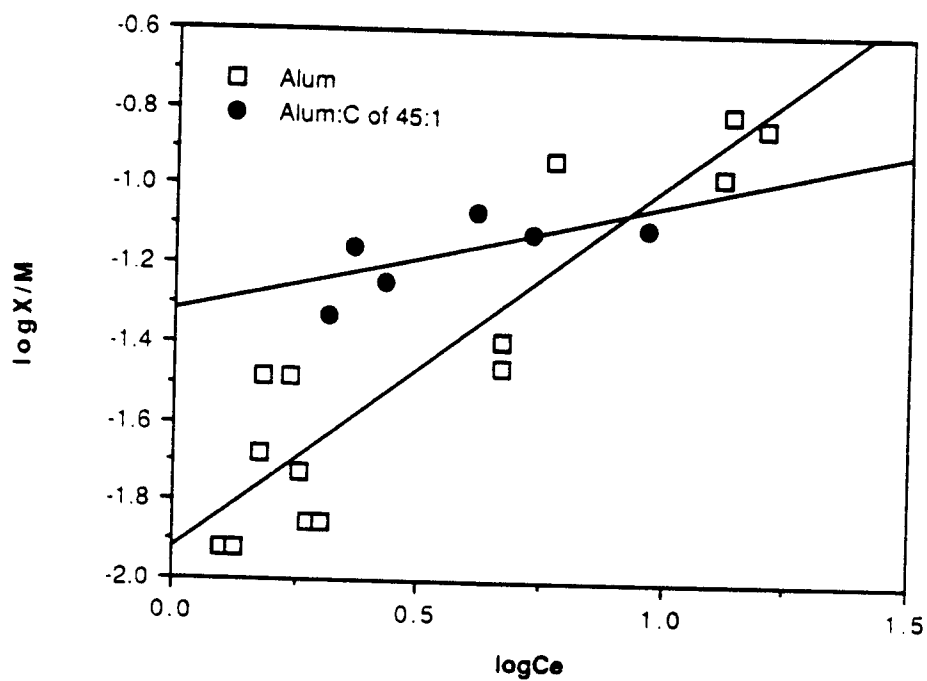


Figure 4.21: Aquatic humic substances adsorption on aluminum sulfate precipitates at pH7

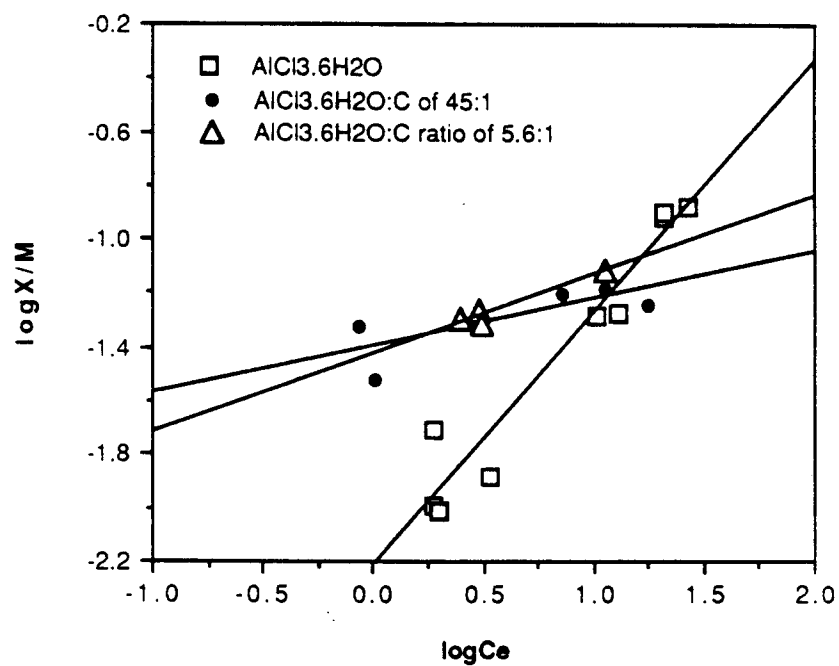


Figure 4.22: Aquatic humic substances adsorption on aluminum chloride precipitates at pH7.

concentration on the isotherm. The isotherm was not impacted by the increase.

4.3.5 Sulfate Adsorption on Aluminum Precipitate

Sulfate adsorption results fitted Langmuir best as shown in Figures 4.23 and 4.24. The surface concentration (X/M) was higher at pH7 the saturation surface concentration was about 2.5 mg/mg at pH5.5 compared to 0.3 mg/mg at pH7. The increased X/M at pH5.5 was also noted for the determination of adsorption capacity. The Langmuir constants are given in Table 4.16.

The addition of AHS in the aluminum chloride precipitate to give an aluminum:C ratio of 45:1 at pH7 resulted in the disruption of the Langmuir model as shown in Figure 4.25.

The data in Table 4.17 confirms the conclusion that no sulfate adsorption took place on the aluminum sulfate precipitate. The data was collected by carrying out the adsorption experiment with sulfate and aluminum sulfate as the adsorbate and adsorbent respectively. The sulfate concentration in the filtrate after adsorption was equal to that of the adsorbate sulfate solution concentration.

The results showed, however, that sulfate was removed because the total sulfate added to the reactor cell was greater than the total sulfate filtered. Similar to the adsorption results, a greater amount of sulfate was removed at pH5.5.

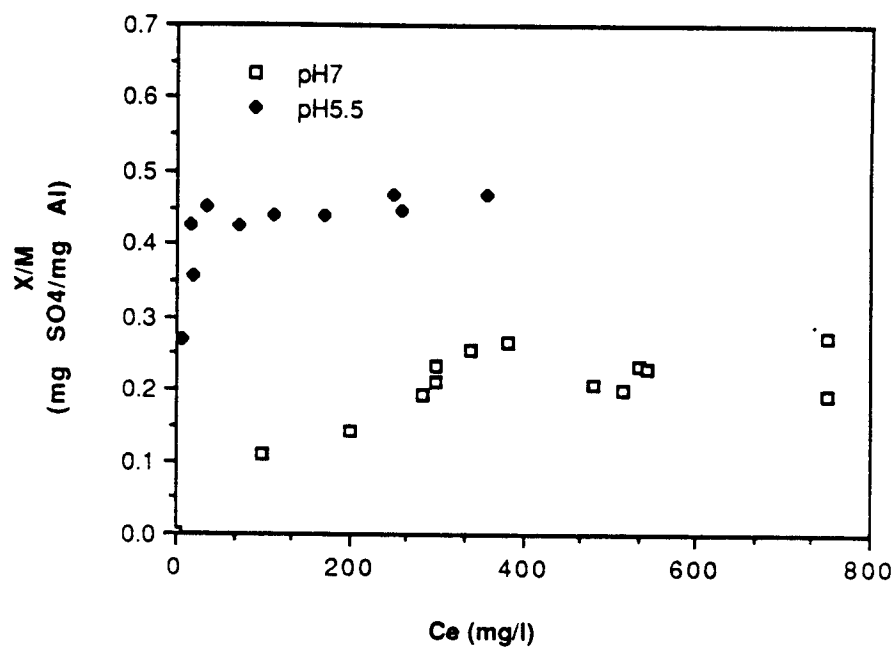


Figure 4.23: Sulfate adsorption on aluminum chloride adsorbent

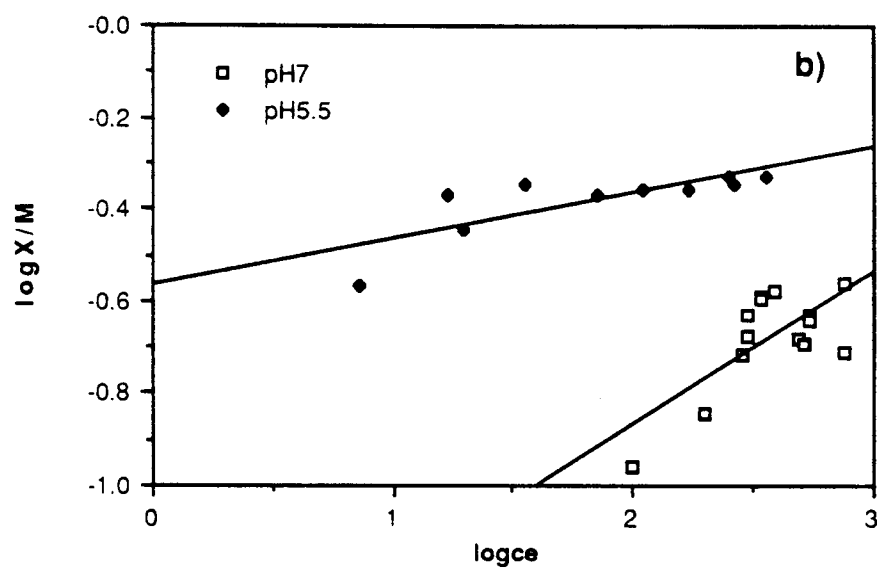
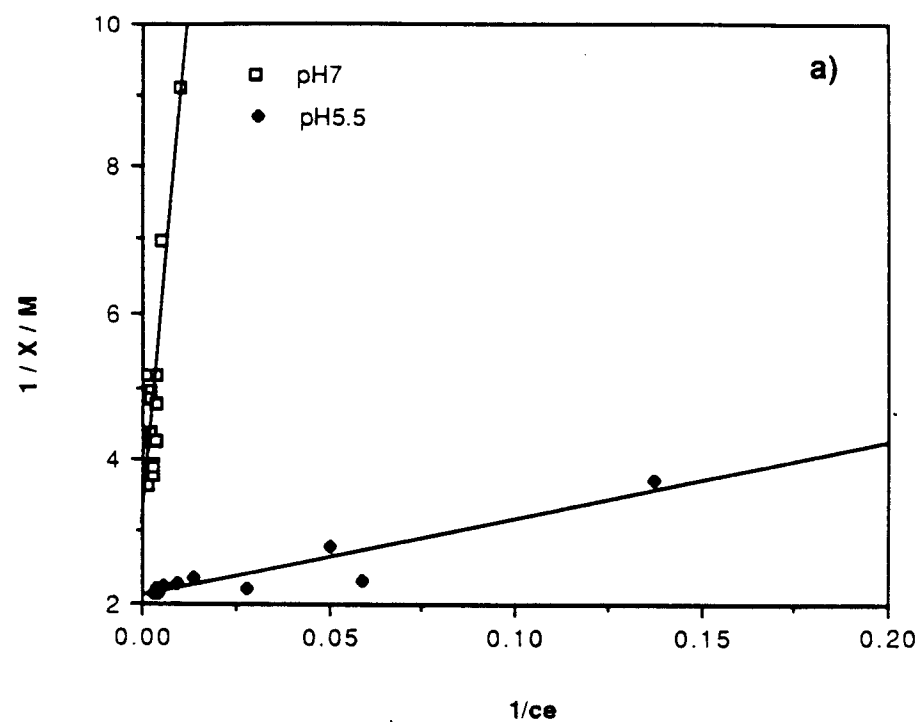


Figure 4.24: Sulfate adsorption on aluminum chloride adsorbent:

- a) Langmuir Transformation
- b) Freundlich Transformation

Table 4.16: Langmuir Equilibrium Constants for the Adsorption of Sulfate on Aluminum Chloride Precipitates.

Constants	b (l/mg)	Q (mg/mg)	Line of best fit
pH7	5.3 10 ⁻³	0.32	(581/Ce + 3.1)
pH5.5	0.199	0.47	(10.61/Ce + 2.11)

b = empirical constant

Q = Maximum mass of adsorbate/mass of adsorbent

The isotherm fits to Freundlich and Langmuir are shown in Figure 4.26 and 4.27. The plot of Ce against the surface concentration X/M in Figure 4.26, however, did not indicate a maximum surface concentration. The results do not give a conclusive sulfate removal mechanism when sulfate is removed from solution during the aluminum precipitate formation.

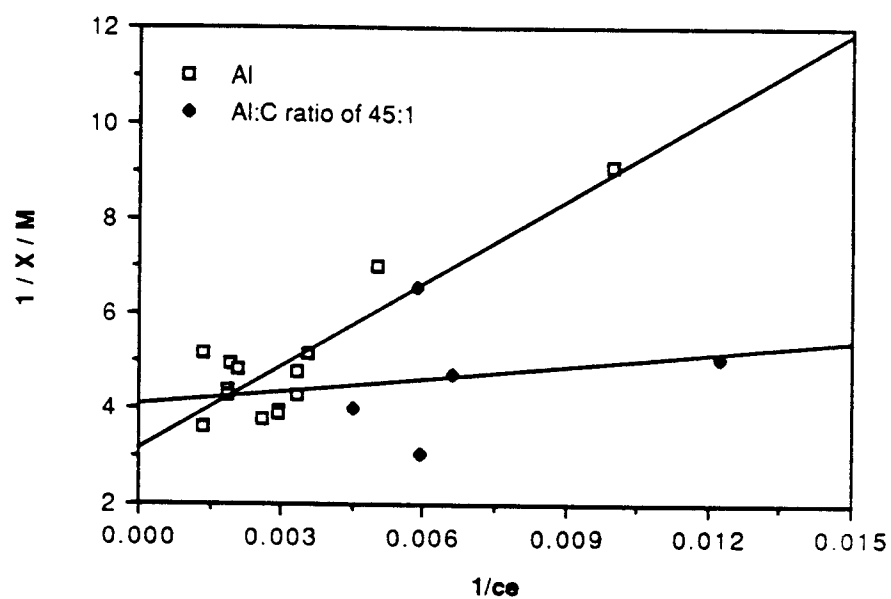


**Figure 4.25: Sulfate adsorption on aluminum chloride precipitates at pH7:
Langmuir transformation**

Table 4.17: Sulfate Adsorption on Aluminum Sulfate precipitate; Mass Balance
(Sulfate in mg based on 100 ml adsorbate)

run#	Ci	Ce (mg/l)	Ce	Aluminum Sulfate	Rinse Solution	Filter Solution	Rinse +filter Solutions	Total output	Total input	X (mg)
	1	2	3	4	5	6	5+6	3+5+6	1+4	
pH7	57.63	570.4	57.04	639.66	13.24	584.8	562.04	619.08	697.3	78.21
	57.63		55.73	639.66					697.3	
	77.43	755.18	75.52	637.28	15.02	553.56	568.58	644.1	714.7	70.61
	77.43		76.89	637.28					714.7	
	37.95	379.65	37.97	627.2	15.89	553.98	569.87	607.84	665.2	57.31
	37.95		37.71	627.2					665.2	
pH5.5	18.7	269.77	26.98	629.72	17.44	534.8	552.24	579.22	648.4	69.2
	18.47		19.37	629.72					648.2	
	18.64	183.81	18.38	635.46	12	482.16	494.16	512.54	654.1	141.56
	18.64	184.65	18.47	635.46					654.1	
	38.14	386.92	38.69	628.46	18.96	489.3	508.26	546.95	666.6	119.65
	38.14	378.4	37.84	628.46					666.60	
	58.17	569.74	56.97	630.56	16.13	450.02	519.15	576.12	688.7	112.61
	58.17	557.88	55.79	630.56					689.5	
	77.57	768.46	76.85	624.76	17	493.64	510.64	587.49	712.3	124.84
	77.57	804.06	80.41	624.76					712.3	

Ci= sulfate in adsorbate

Ce= sulfate in filtrate

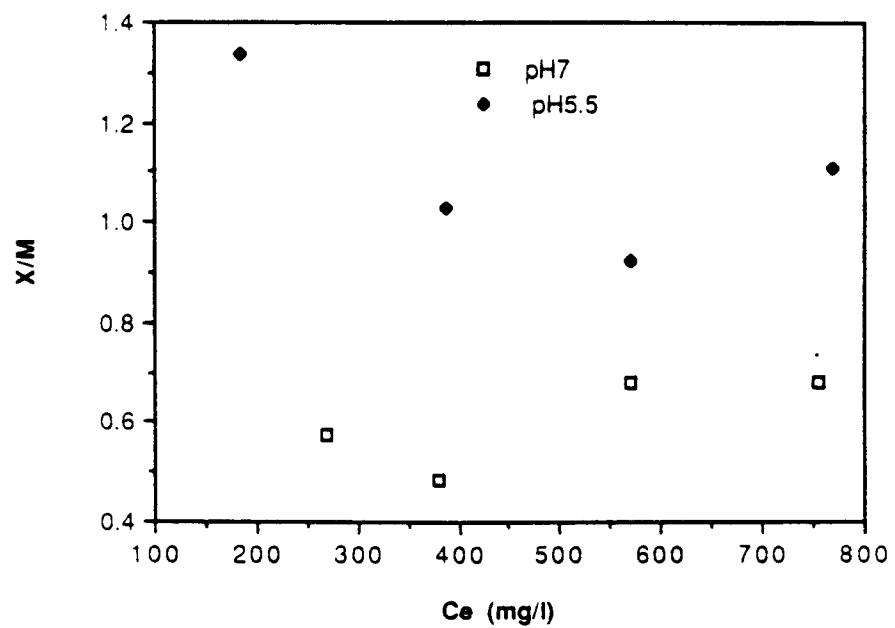


Figure 4.26: Hypothetical adsorption curve for the adsorption of sulfate on aluminum sulfate precipitate

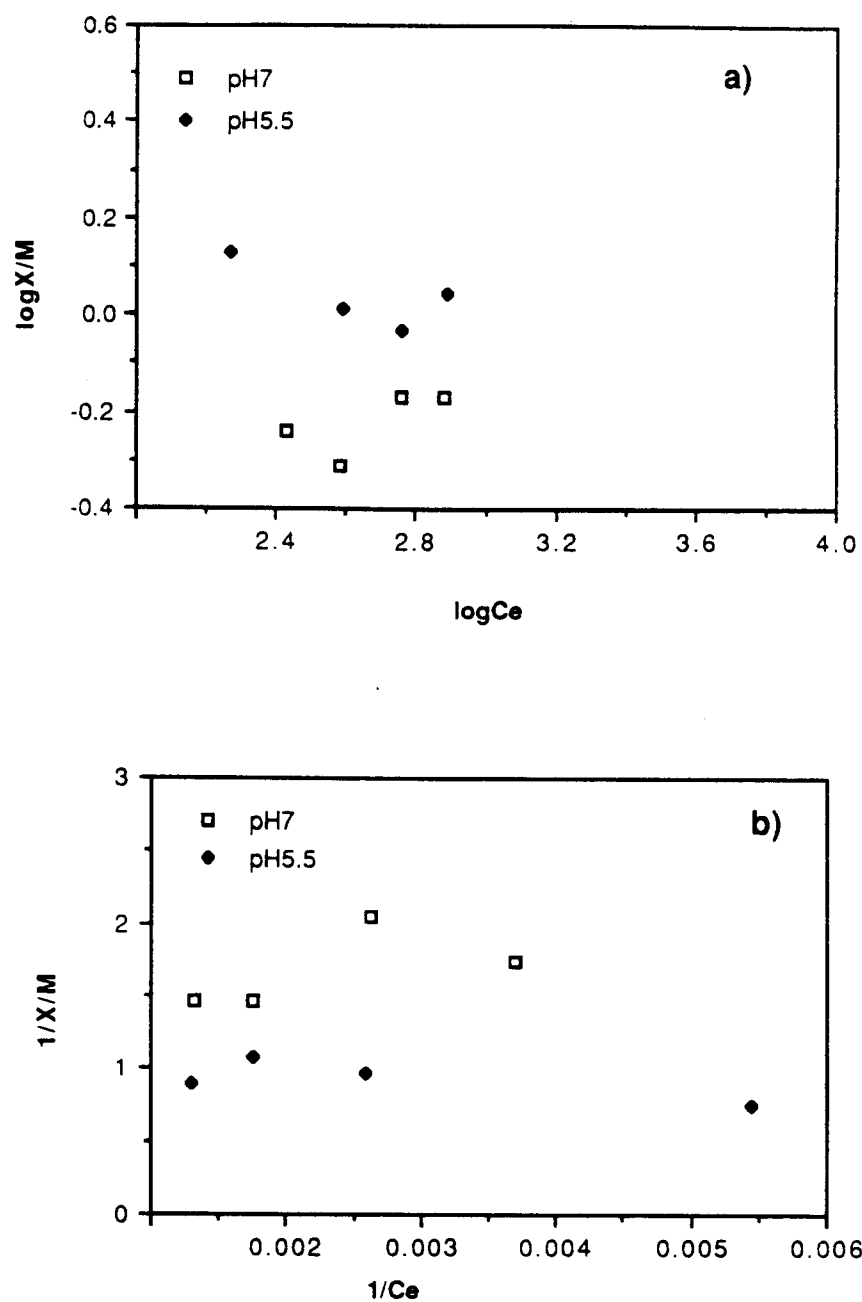


Figure 4.27: Hypothetical adsorption curve for the adsorption of sulfate on aluminum sulfate precipitate:
a) Freundlich transformation
b) Langmuir transformation

4.3.6 Competition Between Aquatic Humic Acid and Sulfate

The results of the competitive adsorption studies of sulfate and AHS on aluminum chloride precipitates are summarized in Table 4.18 and Figure 4.28. The data in Table 4.18 was obtained from a set of experiments in which a mixture of sulfate and AHS solutions were adsorbed on the aluminum chloride precipitates. The experiments for Figure 4.28 consisted of adsorbing sulfate to an AHS-aluminum chloride precipitate. The precipitate was prepared by dissolving aluminum chloride and AHS in Milli Q water to give the ratio of Al:C of 45:1 and 5.6:1. The pH of the solution was then adjusted to 7. The AHS released was the amount of AHS measured in the sulfate solution after adsorption.

The variation in pH values did not impact the competitive adsorption behavior of AHS when aluminum chloride was the adsorbent. The surface concentration (X/M) ratio was about 0.1 mg/mg at pH5.5 and 7. The surface concentration, however, was decreased, from 0.09 mg/mg at pH7 to 0.07 mg/mg at pH5.5 with the formation of the aluminum chloride with AHS. The observed decrease in AHS adsorption was also noted with the results of AHS adsorption on aluminum precipitate in Section 4.3.2. AHS adsorption took place during the aluminum chloride precipitate formation when AHS was added to the aluminum solution prior to forming the precipitate.

The presence of sulfate in the adsorbate AHS solution increased to more than 3 times the surface concentration for the

Table 4.18: Competitive Adsorption of AHS and Sulfate
on Aluminum Chloride Precipitates

Aluminum chloride Adsorbent				AlCl3.6H2) and AHS Precipitate Adsorbent				
				Al:C of 45:1				
Parameter	Adsorbates							
	AHS				Sulfate			
					AHS			
	pH7		pH5.5		pH7		pH5.5	
Ce (mg/l)	8.57	5.81	3.84	4.91	141.5	149.1	105.7	104
Cl (mg/l)	31.4	31.4	30	30	184.7	184.7	183.4	183
X (mg)	1.6	1.79	1.83	1.75	3.02	2.496	5.438	5.55
M (mg)	17	17.3	16	15.7	16.96	17.25	16.02	15.7
X/M	0.09	0.1	0.11	0.11	0.178	0.144	0.339	0.35
					0.08	0.1	0.06	0.072
					0	0	0.21	0.202

C_i initial adsorbate concentration

C_f final adsorbate concentration

X mass adsorbed

M aluminum in the precipitate

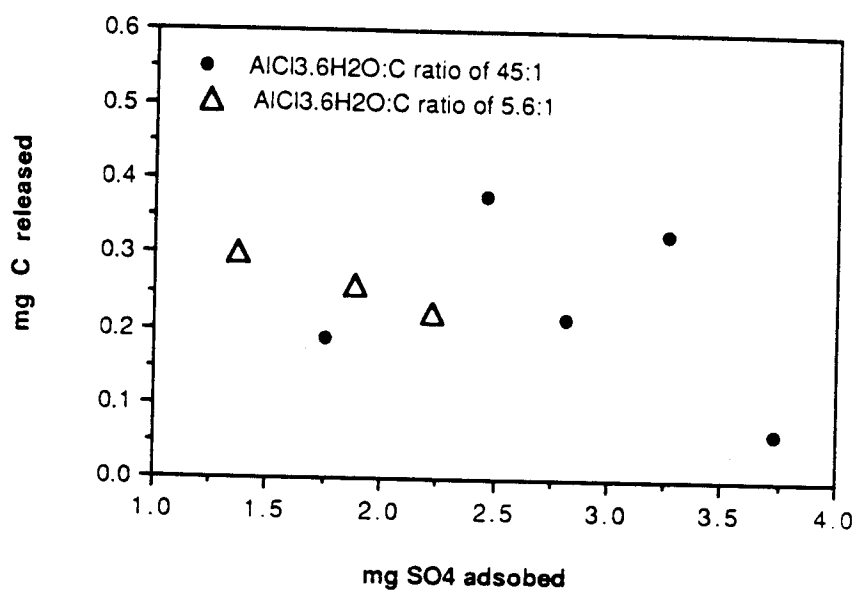


Figure 4.28: Exchange of carbon for sulfate on aluminum chloride precipitate at pH7

adsorption of AHS on aluminum chloride. The X/M corresponding to 8.6 mg/L AHS concentration after adsorption (C_e) in Figure 4.18 corresponded to about 0.03 mg/mg while the X/M for the same C_e was 0.09 mg/mg when the AHS adsorbate contained sulfate.

The surface concentration (X/M) for sulfate adsorption on the aluminum chloride precipitate decreased with increasing pH. The ratio dropped from 0.34 mg/mg at pH5.5 to 0.16 mg/mg at pH7. A similar pH variation was observed for the adsorption results of sulfate on the aluminum chloride precipitate (Figure 4.18).

In contrast to the AHS adsorption, little variation of the X/M ratio occurred when AHS was added to the sulfate adsorbate. The X/M ratio for a C_e concentration of 150 mg/L sulfate was about 0.15 mg/mg for the adsorption of sulfate on the aluminum chloride precipitate (Figure 4.18). The X/M ratio for the same C_e was 0.14 mg/mg when AHS was added to the sulfate adsorbate at pH7.

The X/M ratio corresponding to a sulfate concentration C_e of 104 mg/L was about 0.4 mg/mg at pH5.5 for the adsorption of sulfate on aluminum chloride adsorbent (Figure 4.18). The ratio decreased to 0.35 mg/mg when AHS was added to the sulfate adsorbate.

Sulfate was adsorbed to the aluminum chloride-AHS adsorbent at pH5.5. No sulfate adsorption occurred at pH7. The X/M ratio was less than the ratio for the adsorption of sulfate on the aluminum chloride precipitate.

The adsorption results of Figure 4.28 showed that

preadsorption of AHS to the aluminum chloride precipitate did not suppress sulfate adsorption at pH7. AHS was exchanged for sulfate on the aluminum chloride precipitate. The amount of AHS ranging from 0.08 mg to about 0.40 mg exchanged for about 1.4 to 3.8 mg sulfate. The amount of AHS exchanged for sulfate did not vary with the increases in the Al:C ratio in the aluminum chloride precipitate.

CHAPTER 5

DISCUSSION

The interpretations and implications of the results presented in Chapter 4 are discussed. The reasons for the similarities and differences among the hydrolysis/precipitation of the Al(III) solutions investigated are explored along with the impact of varying pH, sulfate, and aquatic humic substances on aluminum chloride coagulation process. The adsorption of AHS and sulfate on the aluminum sulfate and aluminum chloride precipitate are compared and the importance of their competitive adsorption examined. The discussion of the sensor for Al(III) based on immobilized morin is presented in the appendix. The sensor experimental procedure was modified and the discussion will be limited to steps taken to trouble shoot the procedure.

5.1 HYDROLYSIS PRECIPITATION OF Al(III)

The titration results presented in Figure 4.1 and 4.2 suggested sequential aluminum species formation with increasing $[\text{OH}^-]_b/[\text{Al}]_t$ ratios. The monomers predominate at low r values. The monomers hydrolyze further into polymers to make up the major aluminum species in the first plateau region. Aluminum hydroxide formed at the end of the plateau followed by the predominance of

aluminate ion at the higher r values.

The predominance of monomeric species has generally been agreed on in the region of $0 < [\text{OH}^-]_b / [\text{Al}]_t < 0.5$ (Stol et al., 1976; Nazarenko et al., 1969). Nazarenko et al. (1969) found that only the monomeric species $\text{Al}(\text{OH})^{2+}$, $\text{Al}(\text{OH})_2^+$, and $\text{Al}(\text{OH})_3$ were present. The monomeric species were also found to be prevalent in solutions with $C_{\text{Al}^{3+}}$ less than 5×10^{-5} M (Stol et al., 1976). The dimer $\text{Al}_2(\text{OH})_2^{4+}$ dominated, however, when the $\text{Al}(\text{III})$ concentration was increased to 5×10^{-2} M.

Theoretical aluminum equilibrium curves have been developed based on the monomers (Sullivan and Singley, 1968). The composition of the first plateau stretching over the range of $0.5 < [\text{OH}^-]_b / [\text{Al}]_t < 2.5$ as shown in Figures 4.1 and 4.2 can no longer be explained only in terms of monomeric species. The plateau indicates strong binding between OH^- and aluminum as evidenced by the flatness of the curves. Polymerization should be called upon to explain the plateau because the formation of simple monomers does not require such a high OH^- addition.

The general scheme of aluminum species formation could be viewed as a series of steps. The small aluminum ion is highly charged. As a result of this charge, it has a tight octahedral shell of water molecules ($\text{Al}(\text{H}_2\text{O})_6^{3+}$) at low pH values (Figure 5.1 a). Positively charged H^+ , associated with the polar water ligand, is oriented away from the aluminum atom, while the negatively charged oxygen is oriented toward the aluminum atom (Schecher and

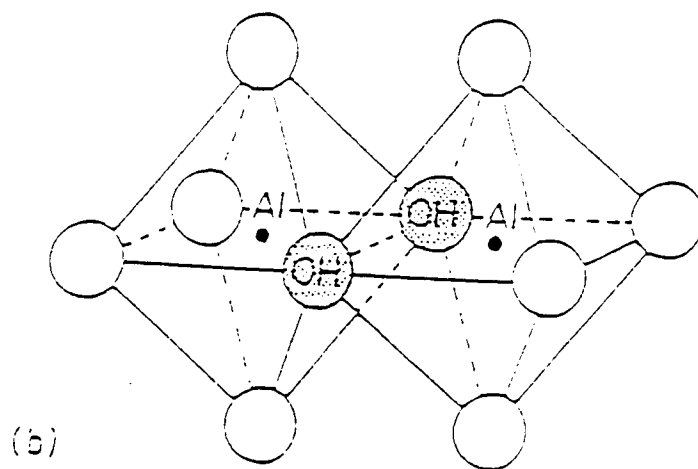
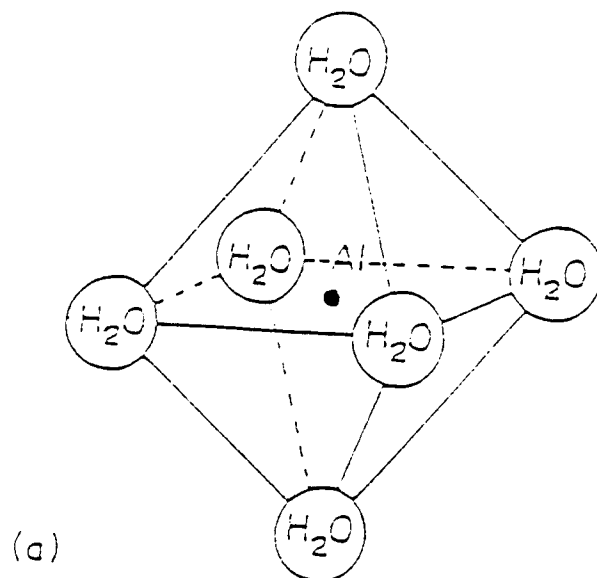
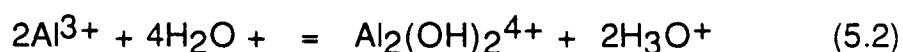
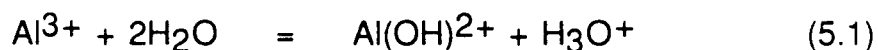


Figure 5.1: Schematic representation of aluminum species
(a) aquo aluminum
(b) aluminum dimer

Driscoll, 1988).

Under low pH conditions (low r), the aquo complex ($\text{Al}(\text{H}_2\text{O})_6^{3+}$) remains intact because the H^+ activity in the bulk solution is high. As solution pH increases the positive charge of aluminum forces hydrolysis of a water ligand producing monomers such as $\text{Al}(\text{OH})(\text{H}_2\text{O})_5^{2+}$. Deprotonation enables the OH^- ligand to come slightly closer to the aluminum ion than the neighboring water ligands. The degree of hydrolysis increases as pH increases and a series of Al-OH complexes are formed. The first species are therefore the monomers and dimers at low pH and $[\text{OH}^-]_b/[\text{Al}]_t$ values. The formation of the monomeric and dimeric species of aluminum have widely been reported (Driscoll and Letterman, 1988; Hundt, 1985; Letterman, 1987; and Van Benschoten and Edzwald, 1988). The monomers and dimers can be represented by (H_2O not included):



When the titration is continued, the charge density of the aluminum molecule decreases, due to hydrolysis, and aluminum begins to polymerize. Two monohydrated monomeric aluminum ions may coalesce to form a dimer (Figure 5.1 b). The linkage of two aluminum ions, separated by a dihydroxide bridge, is the basis of the aluminum-hydroxide crystal structure (Driscoll and Schecher, 1988). The dimers are not stable, and hydrolyze further to other polymeric species. The hydrolysis results in a mixture of species, monomers

and polymers, with the degree of polymerization gradually increasing as the first plateau develops. Little mentioned is made of the polymers in aluminum speciation methods because it is difficult to measure them. The aluminum species that are instead reported include the amount bound with ligands (Driscoll, 1984; Driscoll and Letterman, 1988; Hundt, 1985; Letterman, 1987; Lindsay, 1979).

Eventually, when polymers do not predominate, a jump in pH is observed as the OH^- added is no longer bound to aluminum. $\text{Al}(\text{OH})_3(\text{S})$ precipitation then occurs (r of about 2.7). At pH values above the minimum $\text{Al}(\text{OH})_3(\text{S})$ solubility, the aqueous aluminum concentration increases due to the formation of $\text{Al}(\text{OH})_4^-$. The precipitate starts dissolving but the pH does not drop because of the increase in $\text{Al}(\text{OH})_4^-$. The aluminate ion takes up the additional OH^- . $\text{Al}(\text{OH})_4^-$ has been reported (Dempsey, 1987; De Hek, 1978; Hundt, 1985; Lindsay, 1979; Sigel, 1988).

The dissolution of the aluminum precipitate formed in the aluminum solution containing sulfate results in the exchange of OH^- for SO_4^{2-} at the higher r ratios where $\text{Al}(\text{OH})_4^-$ species predominates. As a consequence, the pH stabilized and the third plateau developed. The third plateau, hence, the substitution of OH^- for sulfate in the third plateau region confirms that an aluminum-OH- SO_4 precipitate was formed during the aluminum sulfate titration.

Two OH^- sources accounted for the steady pH increase for the aluminum chloride and aluminum nitrate solutions. One source

was the OH^- from the dissolution of the aluminum chloride and aluminum nitrate precipitate. The excess OH^- added during titration was the other source.

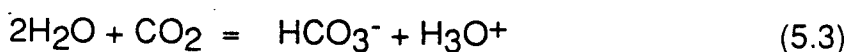
The X ray diffraction analysis of aluminum precipitates by other workers provides some relevant information to our results (Vermeulen et al., 1975; De Hek et al., 1978). At pH values below 10, the solids formed with aluminum nitrate were found to be either amorphous or microcrystalline. At temperatures below 60°C , the solid material is either amorphous or a poorly crystallized bayerite ($\text{Al}_2\text{O}_3 \cdot 3\text{H}_2\text{O}$). These precipitates consist of very small particles that are difficult to separate from the liquid phase by filtration. Well crystallized bayerite was present at room temperatures at pH10. If the precipitate formed at 60°C is aged at pH10, then gibbsite is formed.

De Hek et al. (1978) found microbayerite in the precipitate with 5×10^{-2} M Al and 7.5×10^{-2} M SO_4^{2-} at $[\text{OH}^-]_b/[\text{Al}]_t$ ratios varying from 1.2 to 2.8. Below pH3, all precipitates were essentially amorphous. Samples taken at $[\text{OH}^-]_b/[\text{Al}]_t$ ratio of 3 showed diffuse diffraction bands characteristic of poorly crystallized boehmite.

The work of Vermeulen et al. (1975), Stol et al. (1976) De Hek et al. (1978) has shown comparable aluminum speciation. Vermeulen et al. (1975) and De Hek et al. (1978) noticed, however, the development of a small second plateau with aluminum nitrate (5×10^{-2} M Al; 1.5×10^{-1} M NO_3^-) at an $[\text{OH}^-]_b/[\text{Al}]_t$ ratio of 2.5. The absence of the second plateau in most of the aluminum chloride and

aluminum nitrate titration curves in this study could be due to the rate of OH^- addition. The occurrence of the second plateau reported by these researchers was dependent on the method and rate of OH^- addition. The plateau was only noticed at a slow rate of 1 mL/min base addition. A 10 mL/min dropwise base addition reportedly seemed to have eliminated the plateau. The uncertainty on the exact rate at which the plateau developed was evidenced as the plateau diminished in extent with relatively higher base addition rate. Evidence of the dependence of the rate of base addition on floc formation has also been reported by Hayden and Rubin (1974) and Smith and Hem (1972). The plateau was not consistently seen in this research.

One may argue that the existence of the second plateau observed by the previous investigators may be related to the formation of bicarbonate according to equation 5.3.

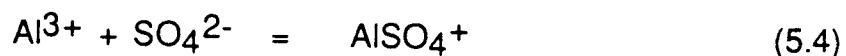


However, Vermeulen et al. (1975) showed that the titration experiments conducted with carbonate-free alkali hydroxide solutions yield similar pH curves. Furthermore, at room temperature, the inflection point due to the above reaction should occur at a pH value of 6.33, which is higher than the pH value Vermeulen et al. observed. They found that the first appearance of a colloidal solution coincided almost exactly with the plateau. Light scattering analysis obtained on samples of different ages (1 week to 2 months) all yield an identical precipitate. It could therefore be concluded that the

second plateau is associated with the formation of a solid phase.

The difference between the titration curves recorded in this study provides the indication that the sequential aluminum speciation can be altered by the anions present in solution. Sulfate ion appears to have a greater role in affecting speciation than do the chloride and nitrate ions probably because of its charge and size difference. The NO_3^- and Cl^- ions have only one negative charge and a planar structure. The planar shape will make these ions less likely to change the nature of the aluminum precipitate. The sulfate ion has two charges and a tetrahedral shape. The tetrahedral shape of the sulfate ion will increase the various reactions with aluminum. The incorporation of the sulfate ion in the solid precipitate would be more likely, and the reshaping of the structure of the precipitate may result. More interaction will also occur because of the oxygen in the tetrahedral structure.

Several interactions between sulfate and aluminum are possible. In acidic condition (low $[\text{OH}^-]_b/[\text{Al}]_t$), aluminum is mainly in the hydrated form as shown in Figure 5.1 a. The complex formation reaction with sulfate, as shown in equation 5.4,



is likely to occur as reported by other investigators (Akitt et al., 1969, Stryker et al., 1969; Hundt, 1985; Driscoll and Schecher, 1988). Kinetic measurements show that there is a distinction between inner sphere (AlSO_4^+) and outer sphere $\text{Al}(\text{H}_2\text{O})_6\text{SO}_4^+$ complexes. The predominance of either complex is not clear. Wendt

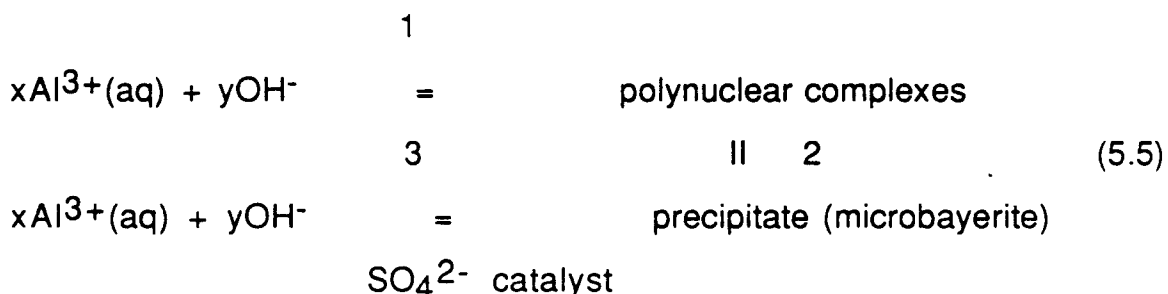
(1969), in a Raman spectroscopic investigation, concluded that the outer sphere complex makes the major contribution to the reaction of complex formation. Nuclear magnetic resonance (NMR) studies by Akitt (1969) suggested an exchange between water and HSO_4^- in the first coordination sphere of Al(III) .

The smaller slope in the acid region ($\text{pH} < 3$) for the aluminum sulfate titration curves may be explained by the formation of sulfate-aluminum complexes such as AlSO_4^+ and AlHSO_4^{2+} as hypothesized by De Hek et al. (1978). The second dissociation of hydrogen sulfate ($\text{HSO}_4^- = \text{SO}_4^{2-} + \text{H}^+$) may also support the hypothesis of complex formation. The pK_a of HSO_4^- dissociation is 2. The slope was noted at pH of 2.5 to 3.

The sequential steps of polymerization and the reported observation of $\text{Al(OH)}_3(\text{S})$ formation at the beginning of the second plateau may give a convincing case for the argument made by de Heck et al. (1978). These workers suggested that sulfate acts as a catalyst which accelerates the formation of $\text{Al(OH)}_3(\text{S})$ by lowering the kinetic barriers (energetic and/or entropic).

The planar polymeric species of aluminum have OH^- bridges connecting the Al(III) cations. The planar units therefore are basal planes of the bayerite or gibbsite lattices. These primary units, considered the building blocs of $\text{Al(OH)}_3(\text{S})$, are linked together into a three dimensional structure by hydrogen bonding of additional OH^- ions and van der Waals interactions. Nucleation and initial growth begin at this stage. Equation 4.6 is a hypothetical reaction scheme

proposed by De Hek et al. (1978) to describe the precipitate formation.



The catalytic action of sulfate makes it impossible to separate processes 1 and 2 in sulfate titration systems. The free energy change accompanying polynuclear complex formation (process 1) and the catalytic effect of sulfate (process 3) may not differ much because the titration curves in the first plateau region run parallel. A relatively small and negative change in free energy must thus attend process 2. Sulfate would lower the free energy of activation for reaction 2.

There are two main objections to these proposed mechanisms. The first is the free energy change accompanying process 1 and 3. De Hek et al. (1978) did not give any evidence of precipitation on the first plateau for the aluminum nitrate titration. The small difference in free energy between process 1 and 3 would suggest that precipitation in nitrate or chloride solutions should be observed. It may be possible that proper experimental conditions would result in confirming this point of view.

The second argument was supported by our experimental results. Titration to a higher pH value of 12 revealed a difference in the resulting titration curves. In aluminum chloride and aluminum nitrate solutions, no other inflection point was observed whereas in all aluminum solutions containing sulfate, a third plateau occurred as shown in Figures 4.1 and 4.2. The plateau should not have been observed if sulfate were just acting as a catalyst in the formation of $\text{Al}(\text{OH})_3(\text{S})$ because the catalytic effect does not explain the pH stabilization over the pH range noted on the third plateau.

Our results suggested that sulfate was incorporated in the precipitate. This conclusion was supported by the equilibrium calculations (ALCHEMI) which follows and the aluminum precipitate formation in the coagulation work.

The equilibrium calculation results using ALCHEMI are shown in Figures 5.2, 5.3, and 5.4. The calculations were made over the pH range 2-12. The equilibrium constants of Table 5.1 were used for the modeling. The concentrations of the water chemistry parameters not of concern in our work, i.e. Ca^{2+} , Mg^{2+} , etc..., were set to the minimum allowable by the model (10^{-10}M). Consequently, the predicted species involving the parameters were negligible. Sulfate concentration in the aluminum nitrate and aluminum chloride equilibrium calculation was set at 10^{-10}M , so were the concentrations of nitrate and chloride in the aluminum sulfate calculation. Detailed information on ALCHEMI can be obtained from Schecher and Driscoll (1988).

Table 5.1: Thermodynamic Data for ALCHEMI Calculations

a) Aqueous data

b) Solid data

a)

Reaction	log K		H _f , cal/mol
	Value	Reference	Value
$\text{Al}^{3+} + \text{H}_2\text{O} = \text{AlOH}^{2+} + \text{H}^+$	-4.99	<i>Bail et al. [1980]</i>	11,900
$\text{Al}^{3+} + 2\text{H}_2\text{O} = \text{Al(OH)}_2^+ + 2\text{H}^+$	-10.00	<i>Bail et al. [1980]</i>	22,000
$\text{Al}^{3+} + 4\text{H}_2\text{O} = \text{Al(OH)}_4^- + 4\text{H}^+$	-23.0	<i>Bail et al. [1980]</i>	44,060
$\text{Al}^{3+} + \text{F}^- = \text{AlF}^{2+}$	7.02	<i>Hem et al. [1973]</i>	1,100
$\text{Al}^{3+} + 2\text{F}^- = \text{AlF}_2^+$	12.76	<i>Hem et al. [1973]</i>	2,000
$\text{Al}^{3+} + 3\text{F}^- = \text{AlF}_3$	17.03	<i>Hem et al. [1973]</i>	2,500
$\text{Al}^{3+} + 4\text{F}^- = \text{AlF}_4^-$	19.73	<i>Hem et al. [1973]</i>	2,200
$\text{Al}^{3+} + 5\text{F}^- = \text{AlF}_5^{2-}$	20.92	<i>Hem et al. [1973]</i>	1,800
$\text{Al}^{3+} + \text{SO}_4^{2-} = \text{AlSO}_4^+$	3.01	<i>Bail et al. [1980]</i>	2,150
$\text{Al}^{3+} + 2\text{SO}_4^{2-} = \text{Al(SO}_4)_2^-$	4.90	<i>Bail et al. [1980]</i>	2,340
$\text{H}_2\text{CO}_3 = \text{H}^+ + \text{HCO}_3^-$	-6.35	<i>Bail et al. [1980]</i>	2,247
$\text{HCO}_3^- = \text{H}^+ + \text{CO}_3^{2-}$	-10.33	<i>Bail et al. [1980]</i>	-3,617
$\text{CO}_2(\text{g}) = \text{CO}_2(\text{aq})$	-1.452	<i>Bail et al. [1980]</i>	5,000
$\text{H}^+ + \text{F}^- = \text{HF}$	3.17	<i>Bail et al. [1980]</i>	3,460

b)

Reaction	log K		H _f , cal/mol	
	Value	Reference	Value	Reference
$\text{Al(OH)}_3 + 3\text{H}^+ = \text{Al}^{3+} + 3\text{H}_2\text{O}$				
Synthetic gibbsite	8.11	<i>May et al. [1979]</i>		
Natural gibbsite	8.77	<i>May et al. [1979]</i>		
Monocrystalline gibbsite	9.35	<i>Hem et al. [1973]</i>		
Amorphous aluminum trihydroxide	10.80	<i>Stumm and Morgan [1981]</i>	-22,800	<i>Bail et al. [1980]</i>
$\frac{1}{3}\text{Al}_2\text{Si}_2\text{O}_7(\text{OH})_4 + 3\text{H}^+$				
$= \text{Al}^{3+} + \text{H}_4\text{SiO}_4 + \frac{1}{3}\text{H}_2\text{O}$				
Kaolinite	3.30	<i>Stumm and Morgan [1981]</i>		
Halloysite	5.64	<i>Stumm and Morgan [1981]</i>		
$\text{AlOHISO}_4 + \text{H}^+ = \text{Al}^{3+} + \text{SO}_4^{2-} + \text{H}_2\text{O}$	-3.80	<i>Nordstrom [1982]</i>		

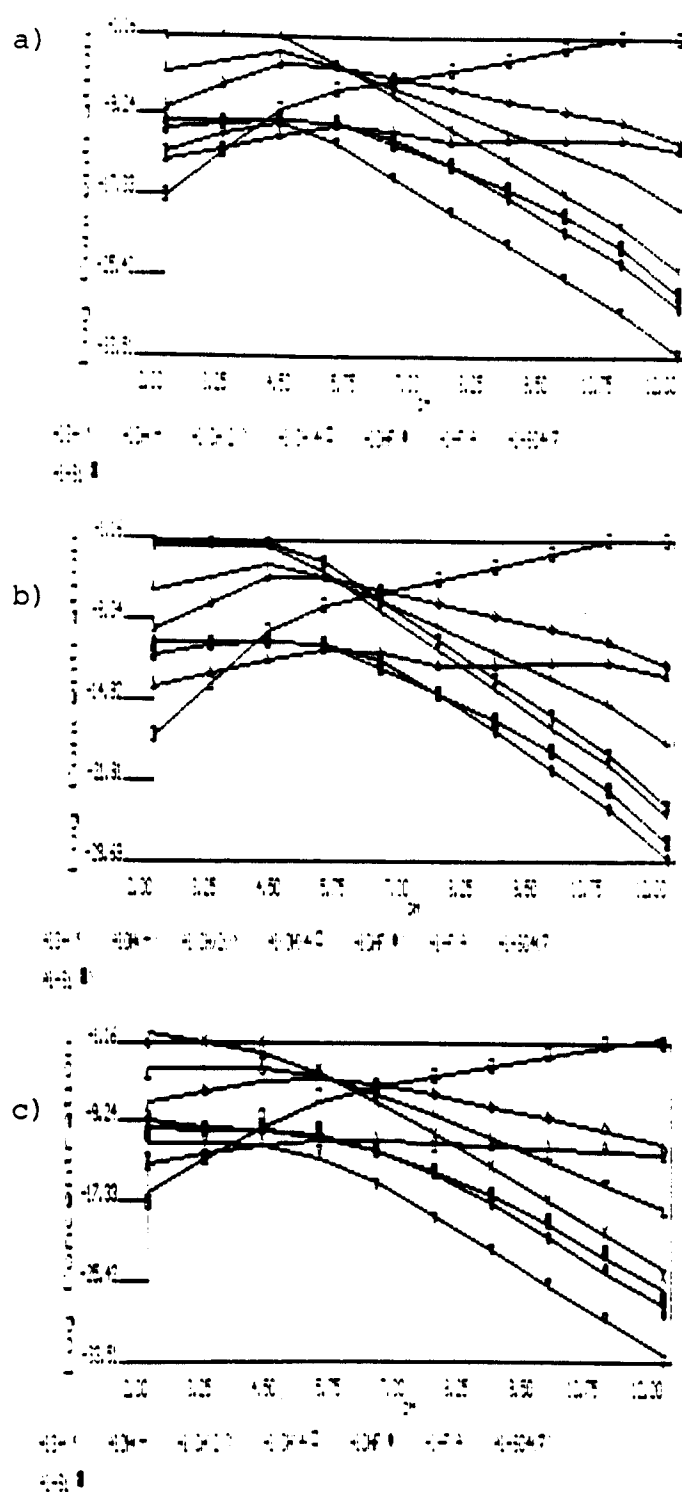


Figure 5.2: Theoretical aqueous aluminum species

a) AlCl_3

b) Alum

c) AlNO_3

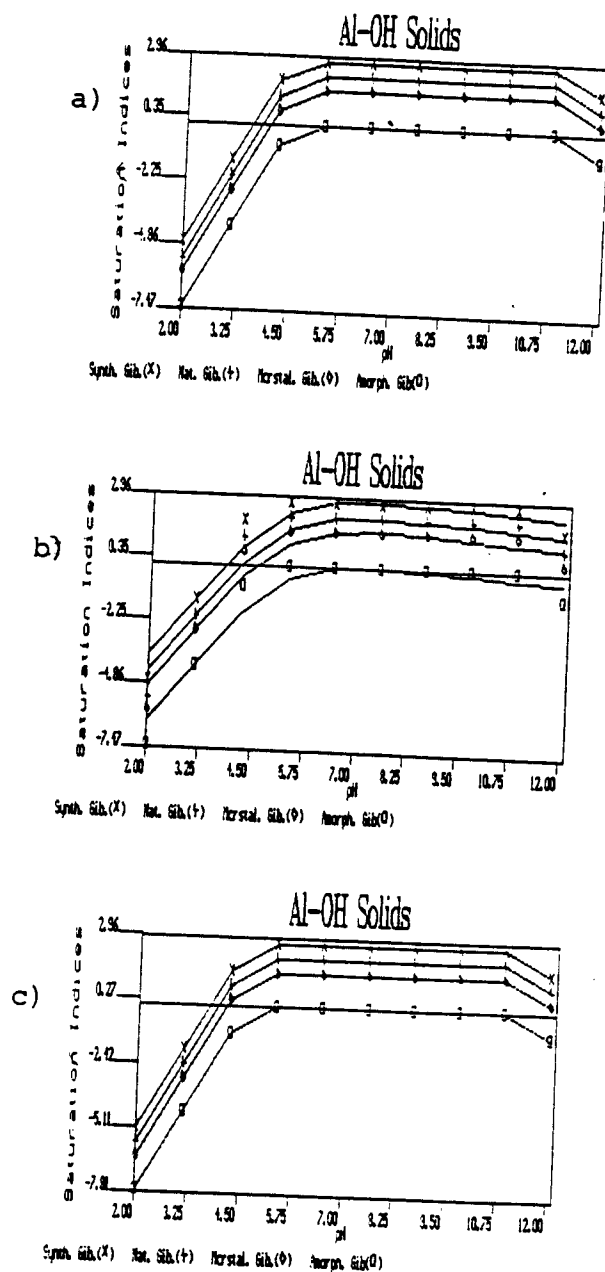


Figure 5.3: Theoretical aluminum solid species.
 a) AlCl_3
 b) AlNO_3
 c) Alum

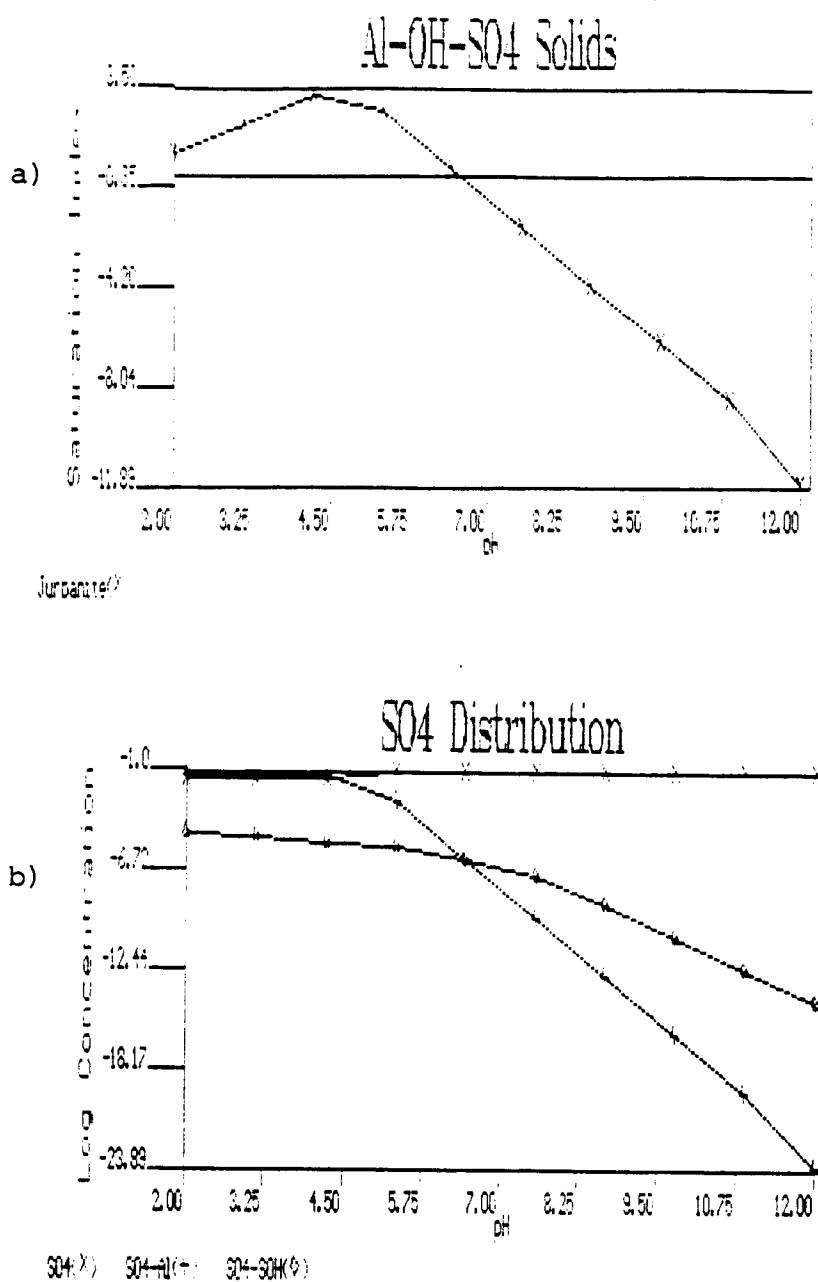


Figure 5.4: Aluminum-sulfate and sulfate species (Aluminum Sulfate)

- a) Jurbanite
b) Sulfate species

Aquo Al^{3+} was the predominant species between pH 2 to 6 (Figure 5.3 a and Figure 5.3 b) for aluminum nitrate and aluminum chloride. Aquo Al^{3+} and Al-SO_4 complexes were in equal amounts in aluminum sulfate (Figure 5.3 c and 5.3 b). The concentration of Al^{3+} and Al-SO_4 decreased at $\text{pH} > 4.4$ in all cases. Low concentrations of AlOH^{2+} , and Al(OH)_2^+ increased up to pH 5.0 and subsequently decreased consistently to pH 12. Al(OH)_4^- concentration increased consistently to become the predominant species at pH values above 7.

The saturation indices shown in Figure 5.4, describe the solid distributions. The model predicted synthetic, natural, microcrystalline and amorphous gibbsite as Al-OH solid. No Al-OH solid was formed below pH 4.0. Jurbanite (Al-OH-SO_4 solid) was predicted at pH values 2 to 7 for aluminum sulfate Figure 5.5 a. The theoretical calculations suggest that the solid formed in the aluminum sulfate titration experiments was jurbanite.

The process leading to jurbanite formation at low r , and pH values is not clear. Hundt (1985) suggested that the steric effect can contribute to the formation of aluminum precipitate. The effect may induce the rearrangement of aluminum and OH^- in such a way to favor Al-OH-SO_4 formation at a lower $[\text{OH}^-]_b/[\text{Al}]_t$ ratio.

The species formation suggested are in agreement with Hundt (1985). Hundt show that at low pH ($\text{pH} < 5.5$) and low r values, monomeric and small polymeric species of aluminum were present. The same species were thought to be prevalent at the low r ratio in

this study. As pH increased, medium polymers were formed in the approximate pH range of 6 to 6.5. Concurrently, an increase in $\text{Al}(\text{OH})_3(\text{S})$ developed. As the medium polymers and $\text{Al}(\text{OH})_3(\text{S})$ were formed, a concomitant decrease in small polymers and monomers took place. In the pH region of 7 and above, the predominant aluminum species was $\text{Al}(\text{OH})_3(\text{S})$. The r values, the OH^- demand, and the aluminum species results of this study compared well with the work of others (Mesmer, 1976; De Hek et al., 1978; Hundt, 1985; and VanBenschoten et al., 1988). These researchers have shown the predominance of $\text{Al}(\text{OH})_3(\text{S})$ at high pH, and the variation of the hydrolysis species of aluminum with pH.

The problem with this model is its limited scope. It was designed for calculations of a specific physicochemical system; acidic low ionic strength waters. The equilibrium equations are only those of monomeric species. No polymeric species of aluminum were considered. The calculations may, therefore, not reflect the exact species formation. The anions interaction with aluminum takes only into account complexation. The steric effect was not considered. Nevertheless, the prediction was close to our experimental data despite the shortfalls of the model.

The equilibrium results of the titration experiments should be interpreted with care because the technique may give kinetic results and not necessary equilibrium data if the rate of reaction with OH^- is slower than the rate of addition of the titrant to the aluminum solution. Stol et al. (1976), for example, investigated

whether equilibrium was reached during the continuous titration by performing a go-and-stop experiments in which the base addition was interrupted at various stages ($[\text{OH}^-]_b/[\text{Al}]_t$) of the titration for long periods of time as opposed to the short periods in this study. They found that in the $[\text{OH}^-]_b/[\text{Al}]_t$ range between $0 < [\text{OH}^-]_b/[\text{Al}]_t < 2.5$ the observed drift in pH (after stopping base addition) was negligibly small but on the second plateau a noticeable larger drift of pH with time was observed. This shift towards lower pH persisted over a long period although the total change in $[\text{H}^+]$ was not large. The pH drift was not observed in our experiments. The addition of OH^- was only interrupted for less than 1 minute after the pH had been recorded.

No change occurred as the result of acidification of the aluminum solutions prior to titration because at the lower r values, little change can be expected. The aluminum will be predominantly in the monomeric form. De Hek et al. (1978) noted also in their experiments that acidification to pH as low as pH2 did not result in a departure from the unacidified aluminum nitrate and aluminum sulfate titration curves.

5.1.1 Summary

The titration curves giving the formation function r ($[\text{OH}^-]_b/[\text{Al}]_t$) ratios versus pH showed that aluminum chloride and aluminum nitrate have a similar hydrolysis/precipitation. A rapid

increase in pH was observed for both aluminum solutions at low $[\text{OH}^-]_b/[\text{Al}]_t$ ratio of 0.3. Monomeric and possibly dimeric species were thought to predominate at the low $[\text{OH}^-]_b/[\text{Al}]_t$ ratios.

A plateau developed at $[\text{OH}^-]_b/[\text{Al}]_t$ ratios between 0.3 and 3. Polymerization of aluminum was suggested to have resulted in the development of this first plateau where the increase in aluminum polymers formation was responsible for binding of OH^- . As a result, no noticeable pH change occurred.

The pH increased sharply following the first plateau, when aluminum polymerization was completed. An aluminum hydroxide precipitate was formed at the end of the jump in pH at $[\text{OH}^-]_b/[\text{Al}]_t$ of about 2.7 (pH 4.3). The OH^- added after this stage was taken up in the formation of $\text{Al}(\text{OH})_4^-$. The aluminum precipitate started dissolving at a pH value of 10.7 ($[\text{OH}^-]_b/[\text{Al}]_t$ of 3.75).

Aluminum sulfate titration curve on the other hand exhibited several differences. The curve ran parallel and below the aluminum chloride and aluminum nitrate curves and developed a plateau at $[\text{OH}^-]_b/[\text{Al}]_t$ ratio of 0.5. A smaller slope due, possibly, to the second dissociation of sulfuric acid and the formation of sulfate-aluminum complexes was noted in the acid region ($0 < [\text{OH}^-]_b/[\text{Al}]_t < 0.7$). Aluminum equilibrium model (ALCHEMI) predicted Al-OH-SO_4 solid (jurbanite) at the pH where a visible floc was formed (lower $[\text{OH}^-]_b/[\text{Al}]_t$ ratio of 0.58). A distinctive third plateau (different from a second plateau on the aluminum chloride titration curve noted by De Hek, 1978) appeared at $[\text{OH}^-]_b/[\text{Al}]_t$ of

4.5 at pH10.5.

Titration curves similar to that of aluminum sulfate curves developed as a result of sulfate addition to aluminum chloride solutions. The titration curves were not altered by varying the Al:SO₄ ratio from 1:1.5 to 1:3.

The characteristics of the titration curve remained unchanged by acidifying the aluminum solutions prior to titration. Sulfuric acid, nitric acid, and hydrochloric acid were used for the acidification of aluminum sulfate, aluminum nitrate, and aluminum chloride solution respectively.

Our experimental data have added two main contributions to the work of others. First, the addition of sulfate to an aluminum chloride solution results in the development of a titration curve similar to that of aluminum sulfate titration curve. Increasing the sulfate concentration to give an aluminum to sulfate molar ratio of 1:3 does not alter the titration curve. The results suggest that little difference exists in the hydrolysis/precipitation of Al(III) when sulfate is present. Secondly, experimental evidence of an aluminum sulfate precipitate was provided.

The data has also supported the aluminum species distribution described by other researchers (Smith and Hem, 1972; Hayden and Rubin, 1974; Vermeulen et al., 1975; De Hek et al., 1978; Hundt, 1985). The aluminum species distribution was shown to vary with r ratios. Monomeric and dimeric species are predominant at low r ratios. These species polymerize as OH⁻ concentration

increase leading to the formation of a solid precipitate. Further OH⁻ addition results in the predominance of Al(OH)₄⁻ at pH values greater than 7.

The implication of the titration results to water treatment can be viewed from the following perspectives: 1) the choice of aluminum coagulants, 2) the potential increase in sulfate concentration in drinking water supplies treated with aluminum coagulants, and 3) the relationship between the species formation and the contaminants present in various water treatment conditions.

Aluminum sulfate would be the preferred coagulant because most water treatment plants operate in the sweep floc zone. The precipitate formation at low $[\text{OH}^-]_b/[\text{Al}]_t$ will necessitate less hydroxide addition for the same aluminum concentration. But for water supplies with sufficient amount of sulfate, there will be no advantage of alum over aluminum chloride or aluminum nitrate in terms of the hydrolysis/precipitation process because the precipitate formation occurs at the same $[\text{OH}^-]_b/[\text{Al}]_t$ ratio. However, The health concern of Cl⁻ and NO₃⁻, and cost considerations will be the determining factor in selecting the coagulant.

The data of the coagulation study, discussed below, was obtained to further research the interaction of aluminum species with sulfate and AHS in water treatment. The formation function, r , and the aluminum species measurement of the experimental conditions are compared. The Aluminum-hydroxide interactions, the

effect of this interaction on the removal of AHS, particulate, and the possible influence of sulfate, are analyzed.

5.2 ALUMINUM CHLORIDE COAGULATION

The OH^- demand, formation function r , aluminum species, DOC, turbidity and particle count, and sulfate data presented in Figure 4.3 to 4.12. Table 4.12 indicated that pH had the most influence in the coagulation of the AHS and bentonite. The hydroxide demand or the formation function were within the $0.17 < r < 3.57$ range. The values covered the range on the first plateau of the Al(III) titration curves only. The difference between these r values and those of the Al(III) titration curves were probably due to the different experimental conditions.

The results of Hundt (1985) are of particular interest regarding the influence of the formation function r . In a study of the aluminum chloride speciation ($\text{Al}_t = 10^{-3.75}$ or 4.8 mg/L), Hundt reported r values ranging from 0.5 to 3.5. The aluminum precipitation was done by dissolving the aluminum into distilled water. The r value in our work ranged from 0.17 to 3.57 despite the variation in experimental conditions.

The AHS and bentonite removals are related to the formation function. At higher r values (higher pH), the predominant AHS and particulate removal will be achieved via adsorption and enmeshment on solid aluminum hydroxide. The adsorption and

enmeshment removal mechanism prevail partially because of the increase OH^- demand, therefore the greater amount of aluminum precipitate.

Charge neutralization/precipitation (CNP) will be prevalent at the lower r values (low pH) because of the predominance of dissolved aluminum. Little or no aluminum is involved in the $\text{Al}(\text{OH})_3(\text{S})$ formation at lower r values. Less base is needed to maintain the pH as a portion of the aluminum is complexed with the HA and/or reacted in the CNP removal mechanism.

The aluminum precipitate formation relationship to pH was consistent with the results of the solubility diagrams for $\text{Al}(\text{OH})_3(\text{S})$ (Figure 2.10). The solubility diagram describes the distribution of aluminum species with varying pH values. The diagram shows that little or no $\text{Al}(\text{OH})_3(\text{S})$ is formed at pH4 with the aluminum dosage range of 1 to 4 mg/L (our study). $\text{Al}(\text{OH})_3(\text{S})$ is the predominant species at pH 7.

The high aluminum precipitate formation with increasing pH values compared well with the results of other workers (Hundt 1985; VanBenschoten et al., 1988). Hundt (1985) noted that an increase in aluminum precipitate did not occur until pH values greater than 6. The difference in aluminum speciation formation between our work and Hundt's may be the reason for the discrepancy. Hundt formed the $\text{Al}(\text{OH})_3(\text{S})$ by dissolving aluminum chloride or aluminum sulfate in distilled water. In this study, the precipitate was formed with NaHCO_3 , NaCl , AHS, SO_4 , and particulate (5 NTU

turbidity) in solution. The contaminants may well have affected the amount of aluminum precipitate at various pH values.

The decrease in aluminum precipitate due to the addition of AHS at pH7 (Figure 4.4) could be due to Al-Organic complexation. A portion of the aluminum added can be involved in the complexation with AHS. The complex formed may not be necessarily included in the precipitate. As a result, less aluminum precipitate would be measured when AHS are added to the water. The complexes not accounted for would be included in the dissolved aluminum fraction.

The opposite conclusion at pH4, could be explained by the difference in the removal mechanisms of AHS and particulates. At such low pH, little aluminum precipitate existed. HA and particulate contaminants are mainly removed by charge neutralization /precipitation (CNP). The Al-organic interaction did not result in the reduction of aluminum precipitate.

The high residual aluminum measured with the addition of AHS (Figure 4.6) may be due to the increase in particulate aluminum concentration. The particulate were not large enough to be removed by filtration. The aluminum species and the residual aluminum data suggested that aluminum was mainly in the precipitate form. Filtration did not retain most of the precipitate because of the large size pores of the filter.

The results show that AHS removal was a function of pH, aluminum dosage, and the initial AHS concentration. The relation between these variables has been well documented (Akitt et al.,

1972; Amirtharajah and Mills, 1982; Dempsey, 1987; Hundt, 1985). The pH change results in various aluminum species formation. As a result, a wide variation of AHS removal occurs because different aluminum species react with the contaminants.

The DOC removal at pH7 corresponds to the region where $\text{Al}(\text{OH})_3(\text{S})$ is the theoretical predominant aluminum species as shown in Figures 2.10. The data obtained in the aluminum precipitate formation in Section 4 (Figure 4.4) indicated the prevalence of aluminum precipitate at pH7. The predominance of aluminum precipitate at this pH value has been reported by Mangravite (1975), and Hundt (1985). AHS removal at pH7 may be mainly attributed to adsorption on the precipitate.

The work of Hundt (1985) demonstrated that the removal of fulvic acid by adsorption occurs at an aluminum dosage of $10^{-3.75}$ M and pH5. Adsorption was the predominant mechanism for fulvic acid removal. The conclusion was based on the high $\text{Al}(\text{OH})_3(\text{S})$ formation at pH values above 5. Adsorption at higher pH has also been suggested by Matijevic (1973). Dempsey et al. (1984) reported that adsorption of fulvic acid (FA) or aluminum-fulvic acid complexes on $\text{Al}(\text{OH})_3(\text{S})$ was an important mechanism in zone I defined on pH-logAl diagram. Zone I occurred entirely within pH-logAl region where precipitation of $\text{Al}(\text{OH})_3(\text{S})$ would occur in the absence of FA.

The dissolved aluminum measured in this research should have a minimal impact on the AHS removal because of the predominance of the aluminum precipitate. The measured dissolved

aluminum may also not reflect the true dissolved aluminum concentration. The separation using 0.45 μ m filter is merely an operationally-defined cut off between dissolved and precipitate forms. The present dissolved aluminum portion may have contained precipitate not retained on the 0.45 μ m membrane filter.

At pH4 where a better DOC removal was obtained, aluminum is mainly in the dissolved form. The DOC removal is therefore achieved, not through adsorption, but charge neutralization/precipitation (CNP). CNP is the chemical reaction between soluble cationic polymers and soluble anionic HA. Hydrolyzed Al-HA interaction is usually followed by the precipitation of an aluminum humate. At this pH, it is likely that monomeric and polymeric aluminum species are precipitating the AHS. Higher aluminum dosages resulted in improving the DOC removal.

The result at the center point of the factorial design should be analyzed keeping in mind the levels of the parameters. The DOC was 4 mg/L instead of 8 mg/L. Performance at this level could be misleading because variation in AHS concentration could result in variation in percentage removal with the same aluminum dosages (Dempsey, 1984). The high AHS removal suggested that adsorption was the predominant removal mechanism at the center point (pH5.5). Other evidence for adsorption was provided by the high aluminum precipitate measured at pH5.5 (Figure 4.2).

The charge on the AHS used in this study can be calculated

from the work of Weber et al. (1973) who reported a charge of 8.2 meq/g on AHS collected from the same source. The total charge of AHS is 3.28×10^{-5} eq/l, and 6.56 eq/l for DOC concentrations of 4 and 8 mg/L respectively (high level and center point of the factorial design). With the assumption that aluminum species such as $\text{Al}(\text{H}_2\text{O})_6^{3+}$ (Al), $\text{Al}_2(\text{OH})_2(\text{H}_2\text{O})_8^{4+}$ (Al_2), and $\text{Al}_{13}\text{O}_4(\text{OH})_{24}(\text{H}_2\text{O})^{7+}$ (Al_{13}) are present (Akitt et al., 1972), the charges in Table 5.2 were estimated for the dosages used in the coagulation.

As noted in Table 5.2, the solution would be overdosed, in each case, with respect to aluminum except at dosages of 1, 2 and 3 mg/L for Al_{13} . The calculation shows that for charge neutralization conditions, the AHS would be destabilized. The conclusion does not account for the charge involved in the destabilization of the clay particulates. An extension should not be made to estimate the overall charge by summation of the charges on the AHS and the particulate clay. This technique would not be accurate because coating of the particulate bentonite can result in overestimation of the charge.

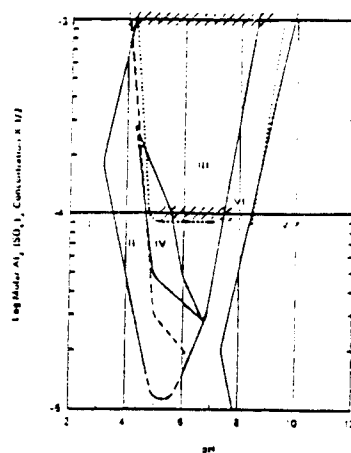
Our results compare favorably with the stability diagrams of Figure 5.5. The stability diagrams are often established to delineate regions of HA or turbidity removal mechanisms. The stability domain for 5 mg/L HA, 24 hr after the addition of alum and settling (Mangravite, 1975) is shown in Figure 5.5 a. The Figure is divided into regions delineated by solid lines. In region I, HA is reported to be stable. In region II, coagulation or precipitation is

achieved by soluble hydrolyzed polynuclear aluminum cations. The boundary between region I and II (below 2×10^{-4} M aluminum) coincides with the hydrolysis of the aluminum ions. Within region III, the AHS is unstable based on the equilibrium constants for $\text{Al}(\text{OH})_3(\text{S})$ and $\text{Al}(\text{OH})_4^-$ formation and the experimental conditions for $\text{Al}(\text{OH})_3(\text{S})$ precipitation in the absence of HA (dotted line). The presence of aluminum hydroxide is expected throughout this region.

Table 5.2: Total charge associated with selected Aluminum species (eq/l).

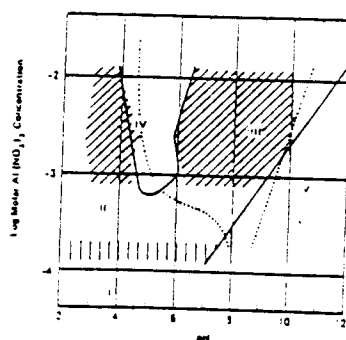
Al species	Al (+3 charge)	Al_2 (+4 charge)	Al_{13} (+7 charge)
Al Dose (mg/L)			
1	11.11×10^{-5}	7.41×10^{-5}	1.99×10^{-5}
2	22.22×10^{-5}	14.81×10^{-5}	3.99×10^{-5}
3	33.33×10^{-5}	22.22×10^{-5}	5.98×10^{-5}
4	44.44×10^{-5}	29.63×10^{-5}	7.98×10^{-5}

The extent of HA removal at the optimum conditions within region II and III is essentially the same. Aluminum hydroxide precipitate is not the only condition necessary for HA removal. Within region II removal was greatest for $2 \times 4 \times 10^{-5}$ M aluminum between pH5 and 6.



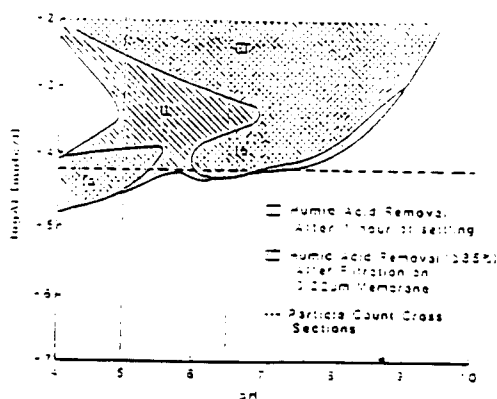
a) Aluminum Sulfate-pH Stability Domain for the Humic Acid Sol (5.0 mg/l) 24 hr After Mixing the Reacting Components

Regions: I, stable sols; II, sols coagulated by soluble aluminum species; III, sols destabilized, aluminum hydroxide present; IV, sols coagulated but stable; V and VI, stable sols. Dotted lines outline the region within which aluminum hydroxide precipitates in the absence of humic acid. Dashed line gives the pH of humic acid- $\text{Al}_2(\text{SO}_4)_3$ systems before pH adjustment. Systems with pH values greater than the dashed line had their pH adjusted with NaOH . Systems at pH values lower than the dashed line had H_2SO_4 added. Hatching gives pH range where 50 per cent or greater humic acid removal occurred after 5 min of microfloation at 10^{-3} and 10^{-4} M aluminum $[\text{Al}_2(\text{SO}_4)_3]$.



b) Aluminum Nitrate-pH Stability Domain for the Humic Acid Sol (50 mg/l) 24 hr After Mixing the Reacting Components

Regions: I, stable sols; II, sols coagulated by soluble aluminum species; III, sols heterocoagulated with precipitated aluminum hydroxide; IV, sols restabilized, and their charge reversed; V, stable sols. Dotted lines outline the region where the precipitation of aluminum hydroxide occurs in the absence of humic acid. Hatched lines with positive slopes give conditions for 50 per cent or greater removal of humic acid after 5 min of microfloation. Hatched vertical lines locate the boundary between regions I and II. NaOH or HNO_3 used for pH adjustment.



c) log Aluminum concentration vs pH stability diagram for humic acid removal (TOC= 10 mg/l).

Figure 5.5: Aluminum coagulation stability diagrams.

a) Aluminum sulfate (Mangravite, 1975)

b) Aluminum nitrate (Mangravite, 1975)

c) Polyaluminum chloride (Weisner et al., 1986)

Chritman (1967) has also recognized pH5 to pH6 as the optimum pH range for color removal. In region IV, HA are aggregated but stable. A solution stability study in the presence of AlCl_3 suggested that stability in region IV is accompanied by charge reversal (Weisner et al, 1986). The region's lowest boundary is the result of insufficient aluminum dosage to stabilize the particles, whereas the upper boundary is believed to be the result of coagulation of the positive charged particles. In region VI, the AHS solution is stable but exhibit turbidities higher than the uncoagulated HA. Turbidity of the stable color particles in region V are similar to those of the uncoagulated solution. The formation of aluminate anions ($\text{Al}(\text{OH})_4^-$) is expected in these two regions, especially in region V. The addition of 3×10^{-4} M Ca^{2+} and 2.5×10^{-4} M SO_4^{2-} eliminated region IV and broadened the pH range of unstable systems toward higher pH values. An increase in Ca^{2+} to 3×10^{-3} M and SO_4^{2-} to 3×10^{-3} M also eliminated region V and caused the pH range of unstable zone to narrow and shift towards slightly higher pH values.

The stability diagram of Figure 5.5 b was obtained by Mangravite with a system containing 50 mg/L HA treated with $\text{Al}(\text{NO}_3)_3$. In region I, the solution remains stable because of insufficient coagulant. In region II, slow coagulation of HA occurs. In region III complete destabilization takes place due to $\text{Al}(\text{OH})_3(\text{S})$. At the higher coagulant dose between pH4 and 6, charge reversal as a result of highly charged complex aluminum species is expected. Also at higher pH values, there is only one stability range (region V).

The third stability diagram in Figure 5.5 c (Weisner and al., 1986) was obtained on 10 mg/L HA treated with polyaluminum chloride as coagulant. Removal by settling was divided into two overlapping zones represented as zone Ia and Ib. In these zones (zone I), the zeta potential approaches zero. Flocs are assumed to consist of aggregate aluminum-humate particles. In this zone a stoichiometric dose of aluminum is required to neutralize and precipitate HA. An increase in initial HA requires an increase in aluminum dose in order to destabilize HA. In zone III HA removal occurs by adsorption on $\text{Al}(\text{OH})_3(\text{S})$. In zone II, the system is overdosed in aluminum species. The aluminum-humate develops a positive charge which produces repulsive double layer forces between particle and prevents their aggregation.

In this study, the aluminum dosage ranged from $10^{-4.43}$ M to $10^{-3.83}$ M. At pH4, the removal region was located in zone II Figure 5.5 a, and zone Ia for Weisner's study. The stability diagrams were evidence that coagulation was achieved by soluble hydrolyzed polynuclear aluminum cations. Our aluminum precipitation and DOC data suggested AHS was removed by CNP at low pH values.

The removal at pH7 occurred through adsorption in zone III or VI. Our data agreed with this conclusion. The center point in our study was located in zone 4 (Figure 5.5 a), zone II (Figure 5.5 b), and zone II (Figure 5.5 c). The region for the center point corresponds to the region of optimum removal as reported by Christman (1967).

At pH7, with the conclusion of section 4.2 where sulfate

was shown to increase the aluminum precipitate formation, an increase in HA removal could be due to supplemental adsorption on the additional precipitate resulted from the addition of sulfate. Hundt (1985) reported similar findings. The addition of sulfate to AlCl_3 ($10^{-3.75}\text{M}$) solution to give a molar ratio of 1.5:1 (same ratio as in alum) improves fulvic acid removal. The filtered fulvic acid stability diagram closely resembled that of alum rather than AlCl_3 . The increased removal corresponded to the rapid increase of $\text{Al}(\text{OH})_3(\text{S})$ formation as was the case in this study. It is also interesting to note that the addition of sulfate to an aluminum chloride solution resulted in titration curves identical to the aluminum sulfate titration curve (Figure 4.2). This similar hydrolysis explains the identical DOC removal noted by Hundt (1985) when using aluminum sulfate coagulant and aluminum chloride to which sulfate was added.

The DOC results are similar to the findings of Dempsey et al. (1984), and Hundt (1985). However, The DOC data in our experiment should be treated with caution because of the large size filter used. Dempsey et al. (1984) found that the removal of fulvic acid by AlCl_3 mimicked the enhanced precipitation of $\text{Al}(\text{OH})_3(\text{S})$ which occurred with added sulfate. Hundt found that the treatment of fulvic acid solution (3.5 mg/L as TOC) with AlCl_3 ($10^{-3.75}\text{M}$) was improved by the addition of sulfate ($1.5 \times 10^{-3.75}\text{M}$). The operation and stability diagram for the filtered fulvic acid was closed to the removal diagram of alum. Similar to Dempsey's findings, increased

sulfate addition resulted in the extension of the zone of fulvic acid removal towards lower pH values.

Charge neutralization/precipitation mechanisms for AHS removal have been reported by several investigators. The region proposed for the CNP mechanisms by Hundt (1985) corresponded to region II in Figure 5.5 a. Dempsey et al. (1984) noted that at pH 4.5 to 5, alum and AlCl_3 precipitation of $\text{Al}(\text{OH})_3(\text{S})$ and formation of large polymers are uncertain in region II. Charge neutralization/precipitation was concluded to be the predominant mechanism for AHS removal. Using Alum at pH 5, Semmers et al. (1980) found no improvement in the removal of humic substances if half the final dosage was applied in each of two successive tests. The samples were filtered between dosages rather than after all the coagulant had been applied in one step. They interpreted from their conclusion that CNP, not adsorption on $\text{Al}(\text{OH})_3(\text{S})$, was responsible for the removal of humic substances. Mangravite et al. (1975) have proposed the removal of humic substances by soluble polymers at low Al between pH 4 and 6.

The removal of AHS by adsorption on $\text{Al}(\text{OH})_3(\text{S})$ or CNP could be explained by the variation of pH. As the pH increase above 5, aluminum continues to hydrolyze until $\text{Al}(\text{OH})_3(\text{S})$ is formed, whereas, as pH decreases, aluminum species formation results in an increase in the positive charges on the soluble polymer species. As a result, a more favorable condition for the adsorption at higher pH occurred as opposed to CNP at lower pH values. Less aluminum may

even be required for AHS removal at lower pH values because of the reduction of the charge on AHS due to protonation of carboxyl groups. This may be one reason for the better performance seen in our experiment at pH4. The other reason could be the size of the filter. A large size filter would allow more aluminum precipitate, to which AHS was adsorbed, to be in the filtrate. This could have resulted in the high DOC concentration at pH7.

Particle restabilization, noted when AHS was added to water, has been reported by other workers. Mangravite (1975) noted that, in region VI, the HA solutions were stable and exhibited turbidity higher than the uncoagulated HA solution. Morris and Knocke (1984) observed similar behavior when treating turbidity with ferric chloride and alum in both laboratory jar test experiments and full scale water treatment plants. The formation of aluminate anions ($\text{Al}(\text{OH})_4^-$) is expected in region VI. Little interaction between the negative aluminate ions and AHS is expected. Insufficient aluminum and the presence of $\text{Al}(\text{OH})_4^-$ (zone II as described earlier) may have caused the increase in turbidity and particle count measurements.

Amirtharajah and Mill (1982) found that good turbidity removal occurred during aluminum coagulation. O'Melia (1972) showed that alum and ferric hydroxide precipitates are all good coagulants for turbidity removal due to sweep floc and subsequent enmeshment of colloids. Weisner et al. (1986) reported particle formation variation with pH in an HA solution coagulated with

$10^{-4.2}$ M aluminum. Particle number decreased from pH4 to pH5.5 and increased with increasing pH to pH7. Less particles were observed at pH7 than at pH4.

Electrostatic attraction which occurs when surfaces are oppositely charged can destabilize particles. The zero point of charge (zpc) of the bentonite particulates used in this study ranges from 2.5 to 4.6 (Montgomery, 1985). At pH values of 4 and 7 the particulates will be negatively charged and the aluminum precipitate positively charged with a zpc of 7.5 to 8.5 (Stumm and Morgan, 1985). Electrostatic attraction could have been involved in the destabilization of the particulates. Packham (1965) showed that the zeta potential of kaolinite decreases with pH from -5 mv at pH4 to -38 mv at pH7.

The potential at pH7 combined with the coagulant demand of HA may have resulted in the stabilization noted for the experiments where no turbidity removal occurred. Interparticle bridging and sweep floc, also shown to contribute to particulate removal from solution (Stumm and O'Melia, 1968), may have been involved in the removal of the particles, particularly, at higher pH values where high aluminum precipitate formation was observed.

The uniformity of the data does not necessarily mean that sulfate and AHS addition had no impact on the particle formation. The conclusion may have been the result of the particle count procedure. The particle count was not performed immediately after sampling. The measurements were taken 1 to 5 hours after sampling.

The time lapse between sampling and analysis may have skewed the results.

The evidence for particle growth was provided by the increase in particle number during coagulation (Table 4.9). The particle counts before and after filtration were always lower than the particle count during coagulation. The higher number of particles formed during coagulation were successfully aggregated to heavier particles. The heavy particles were removed by settling.

Evaluation of the data to determine the sulfate removal mechanisms in coagulation was not possible because no clear trend emerges in Figure 4.12. However, removal can be accomplished through adsorption and/or precipitation. Evidence of sulfate adsorption mechanisms have been supported by De Hek (1978), Snogross (1984) Hundt (1985), and Turner (1956). Removal through precipitation is also possible at pH4 (Rubin, 1976). Precipitation results in the formation of soluble and insoluble polynuclear sulfatohydroxo-aluminum species (Rubin, 1976). The present experimental procedure provided only for the determination of sulfate adsorption onto the positive aluminum precipitate. The adsorption mechanism was provided by the data in Section 4.32 to 4.34.

5.2.1 Summary

The amount of hydroxide required to maintain the pH constant during the jar tests was greater at the higher pH7 and 5.5 values. The corresponding formation ($r = [\text{OH}^-]_b/[\text{Al}]_t$) ranged from 0.17 to 3.57. The range compared well with the values obtained on the aluminum titration curves. At pH4, the addition of AHS resulted in an increase in OH^- demand to compensate for the coagulation demand of AHS. No effect of sulfate addition was noticed at this lower pH value. The OH^- demand was significantly greater at pH7. The demand increased with the addition of AHS regardless of the sulfate concentration. The effect of AHS addition was more pronounced at the higher aluminum dosages. Sulfate had an inconsistent effect on the OH^- demand when AHS was in solution. The results at pH5.5 were closer to the condition of pH7.

AHS removals ranging from 12 to 26% (pH7), 11 to 47% (pH4), and 10 to 70% (pH5.5) was observed. The removal at pH7 corresponded to the region where aluminum precipitate was predominant.

Sulfate increased the aluminum precipitate at pH7 whether or not AHS was present. Adsorption of AHS was concluded to be the main removal mechanism at the higher pH values.

The AHS removal was significantly better at pH4 than at pH7. Charge neutralization was the likely AHS removal mechanism at the lower pH of 4 because of the higher dissolved aluminum

concentration. The high dissolved aluminum suggested the predominance of hydrolysis aluminum hydrolysis products.

The maximum AHS removal was achieved at pH5.5. The relatively high precipitate formation at this pH suggested that the AHS removal occurred through adsorption.

Higher residual aluminum existed at pH5.5 and 7. The high aluminum concentrations suggested that the precipitate particulate size was small enough to pass through the Whatman filter. This effect was more pronounced at pH7.

The turbidity and particle results indicated over 80% of the turbidity was removed in all but the experiments where AHS was added at pH7. Particle growth and stabilization resulted due to insufficient coagulant and/or restabilization.

Sulfate removal did not follow a consistent trend, but removal was observed at all pH values. A systematic study was required to determine the removal of sulfate. The following experiments were designed to do such an investigation.

5.3 AQUATIC HUMIC SUBSTANCES AND SULFATE ADSORPTION ON ALUMINUM PRECIPITATE

The data of Figure 4.14 and 4.16 were obtained to establish the equilibration time and the adsorption capacity for the adsorption of AHS and sulfate on the aluminum precipitate only. No comparison can be made between the different aluminum types and pH values

because the initial adsorbate concentration (C_i) was not the same for all the conditions. For example, C_i values for the aluminum sulfate (pH7) and the aluminum sulfate (pH5.5) conditions were 60.06 mg/L and 35.39 mg/L respectively. The equilibration times of 1 hr for AHS and 30 min for sulfate were used in the procedure for the isotherms.

The AHS data fitted the Freundlich (Figure 4.19) isotherms best. The better fit to the Freundlich isotherm reflects the conclusion of the initial experiments (Figure 4.14) in which the surface sites on the aluminum precipitate adsorbents were not saturated even after the 4th sequence of adsorption.

Some workers have shown, however, that AHS data fit the Langmuir isotherm best using other adsorbent (Hingston et al., 1968; Davis, 1981; Tipping, 1981; Tipping and Cooke, 1982; Parfitt et al. 1977). Tipping (1981) and Tipping and Cooke (1982) quantified the adsorption of a model iron oxide particle, goethite (α -FeOOH). A good fit to the Langmuir isotherm was found with the surface concentration at saturation ranging from 5.3 to 33.4 mg/g and K , the affinity constant of the oxide surface for the humics, from 0.15 to 1.28. The variation of surface concentration at saturation and K depends on the type of iron oxide (α -FeOOH, α -Fe₂O₃, amorphous Fe-gel). Fe-gel was shown with n and K varying from 146 and 0.5 (fresh gel) to 224 and 0.45 (aged gel) respectively. The surface concentration at saturation and the K values are much higher than the results of this study.

The Langmuir fit for AHS adsorption on the adsorbents used by these workers is somewhat surprising in view of the heterogeneity of the humic substances. The only explanation could be that the heterogeneity of AHS is simply in the size of the molecules, rather than, for example, their complements of ionizable groups, so that on the basis of mass adsorbed they could be relatively homogeneous.

Tipping (1981) found that humic substances adsorption to hydrous inorganic oxides decreased with pH. The results were in agreement with the work of Parfitt and Russell (1977), and Parfitt et al. (1977). A similar pH dependency was reported earlier by Evans and Russell (1959) for the adsorption of soil fulvic and humic acids by clay and later by Davis and Gloor (1981) for the adsorption of dissolved organic carbon on aluminum oxide. The humic adsorption varied with pH. The removal reaches a maximum in the pH region of 5 to 6. Because of this maximum, identical % adsorption was obtained at pH 5.5 and 7. These results may explain the small difference in the adsorption efficiencies obtained at pH 5.5 and 7 in our study.

The wide application of the Freundlich and Langmuir isotherms have overshadowed one of the problems with both equations. The logarithm or the inverse of the residual adsorbate concentration C_e is plotted against the logarithm or the inverse surface concentration X/M which is partially obtained from C_e . There is therefore a dependence between C_e and X/M which may affect the final plot. A good discussion of this problem is provided by Harter

and Lehmann (1983).

The greater amount of AHS adsorbed on the aluminum sulfate adsorbent noted in Figure 4.18 is another indication that the aluminum sulfate precipitate formed a different product than did the aluminum chloride precipitate. The presence of sulfate may have resulted in the formation of a more amorphous precipitate with higher surface charge. The difference in the two aluminum precipitates was also evident in the hydrolysis/precipitation (Figure 4.1).

Several processes may be responsible for the adsorption of AHS on the hydroxide surfaces. Ligand exchange involving the surface hydroxyl groups (Al-OH_2^+ , Al-OH , H_2O , and OH^-) of the aluminum hydroxide and some of the ionizable groups of the AHS is possible. The protonation and deprotonation of AHS may result in varying carboxylic and phenolic functional groups on the AHS molecule. Adsorption through ligand exchange could be influenced by the type and nature of these functional groups.

The AHS adsorption can be analogous to the adsorption of AHS on iron oxides described by Tipping (1981). The first of a number of adsorbing molecules must initially decrease the proportion of surface AHS-OH_2^+ and AHS-OH among the groups not involved in the adsorption, but if the pH is held constant, these remaining groups will take up protons to re-establish the proportions of AHS-OH_2^+ , AHS-OH , and Fe-O^- of the original surface, in terms of the type of adsorption sites. The next molecule

to be adsorbed, therefore encounters the same hydroxide surface, in terms of the type of adsorption site. This mechanism will normally give rise to the Langmuir isotherm for simple molecules because there are less sites. However, if the adsorbing molecules are large polyanions such as Humic substances, not all their anionic groups can be involved in the ligand exchange interactions and the excess negative charges would be expected to repel each other. The repulsion would increase as more adsorption takes place, the affinity of the surface for the adsorbate would decrease progressively, and a non Langmuir isotherm, such as the Freundlich isotherm would results.

Proton consumption could also occur. However, protonation of the humic ionizable groups which do not take a direct part in adsorptive interaction with hydroxide surfaces is probably of greater quantitative importance. The protonation of these groups overcomes electrostatic repulsion between adjacent adsorbed humic molecules. Accumulation of protons in the diffuse double layer, and the lower dielectric strength of the interface region relative to the bulk solution are other factors that could promote protonation.

The Langmuir isotherm model fitted to the sulfate data (Figure 4.23) describes the equilibrium between the solution and the adsorption surface as a reversible chemical equilibrium between species. The model considers the adsorbent to be of fixed individual sites. In this case, each site binds only one molecule of adsorbate leading to a monolayer coverage of the sites. No more sulfate

molecule can be adsorbed when the maximum X/M of 0.5 mg/mg (pH5.5) and 0.3 mg/mg (pH7) are reached.

The sulfate adsorption results showed that no sulfate was adsorbed to the aluminum sulfate precipitate. Apparently, the sulfate initially present in the aluminum sulfate solution had already filled any available adsorption sites created during the aluminum precipitate formation. Comparison of sulfate adsorption on aluminum chloride precipitate to that of sulfate adsorbed during aluminum precipitate formation shows why no additional sulfate adsorption was observed on the aluminum sulfate precipitate. The calculations refer to Figure 4.23 (Sulfate adsorption on aluminum chloride precipitant). The X/M ratios for a Ce of 200 mg/l, for example, are about 0.15 mg/mg and 0.45 mg/mg at pH7 and 5.5 respectively. The amount of sulfate adsorbed for a 50 mg aluminum chloride precipitate would be 7.5 mg at pH7 and 22.5 mg at pH5.5. The ratio of SO₄/Al in aluminum sulfate is 1.5 mg/mg. This ratio is much higher than 0.15 mg/mg and 0.45 mg/mg.

The adsorption results revealed that sulfate can be removed via adsorption on the aluminum precipitate as noted by Heck et al. (1978). The work of other researchers showed that sulfate was adsorbed on adsorbents such as soils (Christophensen and Hans, 1982), goethite (Hingston et al., 1977; and Parfitt et al., 1977). Infrared spectra of binuclear bridging complexes of sulfate adsorbed on goethite have indicated the presence of a surface complex Fe-OSO₂O-Fe (Parfitt et al., 1977). Sulfate was shown to be

adsorbed by ligand exchange with two A-type OH groups to give a bridging binuclear complex $\text{FeOS}(\text{O}_2)\text{Fe}$. Sulfate is bonded through two oxygen atoms in the structure. Sulfate ion bonding occurs through two charged oxygen atoms, resulting in an uncharged species. Weak hydrogen bonds to the oxygen atoms are then formed.

The observations of the adsorption study suggests that there may be a change in the characteristics of the sulfate adsorbate and, to a some extent, the nature of the aluminum precipitate at various pH values. There may be two reasons for the variation in the amount of sulfate adsorption with pH. The zero point of charge of the aluminum precipitate has been reported to be between 7.5 and 8.5 (Montgomery, 1985). The precipitate will have more surface charge at pH 5.5 than 7. pH 5.5 is also closer to the dissociation of both the sulfate and its conjugate acid from solution. The acid could dissociate to form coordinate complexes at the hydroxide surface. The higher surface charge of the conjugate acid would result in higher adsorption at pH 5.5. Similar pH dependence has been reported for the adsorption of fluoride on goethite (Hingston et al., 1967).

The difference in the characteristics of the aluminum chloride or aluminum sulfate precipitates at various pH could not be quantified, but the aluminum sulfate precipitate seemed to be more amorphous. As a result, more adsorption was possible. The results also demonstrated that the addition of AHS to the aluminum solutions to form the aluminum precipitates decreased the amount

of sulfate adsorbed.

The AHS adsorption during the precipitate formation process may have resulted in the coverage of a portion of the surface sites by AHS. The AHS adsorption may have changed the charge of the surface sites and provoked a departure from the assumption for Langmuir isotherm.

The absence of sulfate adsorption on the aluminum and AHS precipitate at pH7 showed that AHS would outcompete SO_4^{2-} for the adsorption sites. With sufficient sites created, and/or the change in the nature of the aluminum precipitate and the sulfate adsorbate at pH5.5, both sulfate and AHS adsorption would occur. The competitive adsorption between sulfate and AHS on aluminum precipitates is further detailed with the data of Table 4.18 and Figure 4.28. The amount of sulfate adsorbed in the competitive adsorption was reduced while the amount of AHS was increased in comparison to the adsorption of AHS and sulfate on aluminum chloride precipitate. Similar results were reported by Inskeep (1989) in adsorption studies of sulfate by iron oxide in the presence of organic ligands (humic acid, fulvic acid, tannic acid, oxalic acid, citric acid, and gallic acid). The presence of sulfate in water would, thus, increase the removal of AHS since coagulation is achieved in the sweep floc zone. However, this will be to the detriment of sulfate removal.

5.3.1 Summary

Aluminum hydroxide was the predominant species formed at pH 5.5 and 7 with $\text{AlCl}_3 \cdot 6\text{H}_2\text{O}$ and $\text{Al}_2(\text{SO}_4)_3 \cdot 18\text{H}_2\text{O}$ concentration ranging from 100 to 900 mg/L. The predominance of the precipitate form of aluminum was consistent with the predicted aluminum species of the Al -pH solubility diagram (Figure 2.10). No difference existed between the amount of aluminum chloride and aluminum sulfate precipitate formed at pH 5.5 and 7.

AHS adsorption on the aluminum chloride and aluminum sulfate precipitates was rapid. Little additional adsorption was observed after 1 hr equilibration time and the equilibrium adsorption isotherms fitted the Freundlich equation best.

The aluminum sulfate adsorbent had a greater AHS adsorption capacity than the aluminum precipitated from aluminum chloride. The increase adsorption capacity of the aluminum sulfate adsorbent was observed for both pH 5.5 and 7, and was probably due to the more amorphous precipitate formed due to the presence of sulfate. The pH change from 5.5 to 7 did not impact the AHS adsorption capacity of either the aluminum chloride or the aluminum sulfate precipitate. This was probably due to an adsorption envelope described by other workers in which the adsorption capacities at pH 5.5 and 7 are equal.

The formation of the aluminum chloride or the aluminum sulfate precipitate with AHS did not significantly alter the isotherm

of AHS adsorption on the aluminum precipitates. The decrease of the Al:C ratio from 45:1 to 5.6:1 AHS had no effect. AHS adsorption took place during the Al-AHS precipitate formation.

Sulfate adsorption on the aluminum chloride was quicker. No additional adsorption was observed after 30 min equilibration. No sulfate adsorption took place on the aluminum sulfate precipitate. The adsorption sites were filled by the sulfate initially present in the aluminum sulfate solution used to prepare the aluminum precipitate.

The Langmuir equilibrium isotherm described sulfate adsorption best. Surface charge of the aluminum adsorbent, pH, as well as the constituents of the adsorbate influenced sulfate adsorption. More sulfate was adsorbed at the lower pH 5.5. The higher adsorption at the lower pH was probably due to dissociation of both the anion and its conjugate acid from solution.

The pH variation on the competitive adsorption between AHS and sulfate was only noted with the Al-AHS precipitate. The surface concentration decreased with decreasing pH values

AHS surface concentration in the competitive adsorption of sulfate and AHS on aluminum chloride precipitate was increased and that of sulfate decreased.

CHAPTER 6

CONCLUSIONS AND RECOMMENDATIONS FOR FUTURE RESEARCH

6.1 CONCLUSIONS

The conclusions and results achieved for this endeavor are the following:

The titration curves (mole of hydroxide bound per mole of aluminum, r , against pH) showed that the hydrolysis/precipitation of aluminum chloride and aluminum nitrate was similar. A sequential aluminum speciation occurred with the variation in r values.

Monomers and dimers were the predicted predominant aluminum species formed at the lower r ratios. A plateau developed in the lower r regions. The plateau was the result of further polymerization of aluminum. The added OH^- ions were consumed in the polymerization step. The pH increased sharply in conjunction with the predominance of the $\text{Al}(\text{OH})_4^-$ species, when the polymerization was presumably completed. An amorphous $\text{Al}(\text{OH})_3(\text{S})$ precipitated at an r ratio of 3. The aluminum precipitate dissolved at an r ratio above 3.1.

The aluminum sulfate titration curve ran parallel to and always below the aluminum chloride and aluminum nitrate titration

curves. The curve exhibited a few differences. The dissociation of HSO_4^- at an r ratio of 0.1 caused a small drop for the sulfate curve. A theoretical equilibrium model predicted Jurbanite (Al-SO_4 precipitate) to precipitate at the same r ratio of 0.3 as in the aluminum sulfate precipitation. The incorporation of sulfate in the aluminum precipitate caused the development of a second plateau at the r ratio of 4.5.

A titration curve identical to the aluminum sulfate titration curve developed with the addition of sulfate to aluminum chloride and aluminum nitrate solutions. The curve remained unchanged when the molar Al:SO_4 ratio was varied from 1:1.5 to 1:3. The curves were not altered by hydrochloric, nitric acid and sulfuric acid acidification of the aluminum solutions prior to titration.

The pH values had a significant influence on the coagulation of a well buffered water containing sulfate, AHS and bentonite clay. The hydroxide demand, the formation function r , the AHS concentration, and the aluminum precipitate were significantly higher at pH7 compared to pH4.

The AHS removal varied as a function of pH, the AHS concentration, and aluminum dosage. The AHS exerted a significant hydroxide demand at both pH5.5 and 7 regardless of the sulfate concentration. Sulfate addition improved the AHS removal. The improvement was the result of higher aluminum precipitate formation due to the sulfate addition. The removal at pH7 was predominantly through adsorption compared to charge

neutralization/precipitation at pH4. The maximum removal was achieved at pH5.5. However, this may not be the optimum condition because the AHS concentration and the pH were half the concentration at pH4 and 7 respectively.

Particulate removal was not affected by the variation in sulfate concentrations. The removal was dependent upon the aluminum dosage, the AHS concentration, and pH. The AHS influence was more pronounced at pH7. Particle restabilization occurred when the aluminum dosage was insufficient and the AHS high. The restabilization condition showed the competitive coagulant demand between AHS and particulate.

Sulfate was removed at both pH5.5 and 7. However, little difference was observed with the addition of AHS and pH variations.

Aluminum hydroxide was the predominant aluminum species at pH5.5 and 7. No difference existed between the aluminum chloride and aluminum sulfate precipitants.

AHS adsorption on aluminum chloride and aluminum sulfate precipitants was rapid. Little additional adsorption took place after 1 hr equilibration time.

The adsorption capacity of the aluminum precipitants increased with successive replenishment of the AHS adsorbate for the same adsorbent. The multilayer type of adsorption from the increased adsorption capacity was confirmed by the adsorption isotherms which fit the Freundlich isotherm best.

The addition of AHS in the aluminum chloride or aluminum sulfate solution prior to the aluminum precipitate formation decreased the adsorption capacity of both adsorbents. The isotherms were not greatly impacted.

pH variation from 5.5 to 7 did not have any impact on the adsorption of AHS on both aluminum precipitants.

Sulfate adsorption on the aluminum chloride precipitate was quicker. The adsorption maxima was reached after only 30 min equilibration time for both pH5.5 and 7. The adsorption sites were all occupied by the sulfate initially present in the aluminum sulfate solution. As a results, no sulfate was adsorbed on the aluminum sulfate precipitate.

The adsorption capacity of the aluminum chloride precipitate was exceeded after only one sequence of sulfate adsorption. The adsorption isotherm fit of the data confirmed that sulfate adsorption was best described by the Langmuir isotherm.

Sulfate adsorption on the aluminum chloride precipitate was increased with decreasing pH values from 7 to 5.5. The greater adsorption at pH5.5 was probably due to the dissociation of the anion and its conjugate acid at the lower pH.

The presence of sulfate increased the AHS adsorption in the competitive adsorption of sulfate and AHS on the aluminum chloride precipitate. AHS exchanged for sulfate occurred on the aluminum chloride precipitate at pH7.

6.2 RECOMMENDATIONS FOR FUTURE RESEARCH

This study provided some indications of the impact of sulfate on the Al(III) hydrolysis/precipitation process, the coagulation chemistry of aquatic humic substances and particulate bentonite. The adsorption isotherms of AHS and sulfate were developed and a fluorogenic aluminum method was evaluated. Further studies could be directed toward the following:

- 1) Expansion of the the titration experiments by adding varying concentrations of AHS to the Al(III) solutions before titration. An identical experiment can be conducted with bentonite clay solution. The comparison among the titration curves would provide an indication of several zones of AHS and particle removal as a function of the formation function and/or the aluminum species hypothesized at the r values.
- 2) Repetition of the titration experiments with AHS. Samples should be collected at given r ratios. The DOC concentration measurements would provide the AHS removal as a function of r .
- 3) Back titration of the Al(III) solutions with acid to the initial pH. The reverse titration curves could determine whether the aluminum speciation vary as a function of the initial pH condition. The back titration experiments should

include the aluminum solutions containing AHS, and bentonite. The pH for the conditions with AHS should not be above 10 to avoid denaturation of the AHS molecules.

- 4) Characterization of all the aluminum precipitants by X ray diffraction and other methods which may describe the structure of the precipitants. The knowledge of the structural composition would be most helpful for the precipitants formed with AHS. The results would clarify the AHS incorporation into the aluminum precipitate. The identification would help quantify the AHS removal by either precipitation or adsorption in coagulation at any given formation function r or pH value.
- 5) Systematic coagulation of AHS with varying sulfate concentrations. The experiment can be conducted in two ways. First, the optimum pH and aluminum coagulant dosage should be determined. The impact of varying sulfate concentrations at the optimum coagulation condition can be evaluated. The other experiment would consist of varying the sulfate concentration in the AHS solution to study the effect of sulfate addition on the aluminum dosage required to achieve maximum AHS removal.
- 6) Repeat the experiments of step 5) with particle bentonite instead of AHS.
- 7) Study further the aluminum species formed during coagulation. The addition should include species such as

organically bound aluminum species.

- 8) Quantification of the particle charge with electrophoresis measurements. The charge before and after coagulation would provide the stability of the particles as well as the destabilization effect of the various coagulants.
- 9) An investigation of particle growth during coagulation. The data collected in this research did not provide a conclusive pattern of particle growth. The particles were usually counted 2 to 3 hours after sample collection. The procedure could be improved upon by measuring the particle immediately after collection.
- 10) Further study of the adsorption of AHS and sulfate on Al(III) precipitants. The study should be extended to a wider pH range.
- 11) Additional experiments on the competitive adsorption of AHS and sulfate. The data collected will complete the limited number of experiments conducted in this research. The other combination may involve variation of the sulfate and AHS concentrations, the pH values, and the selection of other aluminum adsorbents.
- 12) Improvement of the the fiber optic aluminum technique. Several problems were encountered during the course of this research. Among the problems were the immobilization technique, the transfer of the immobilized morin to the fiber optic bundle, and the instrumentation apparatus. The

next phase of the study should concentrate on the characterization of the immobilized morin and the development of a consistent technique for the procedure. The cellulose technique can be improved upon by finding a better support to entrap the morin-cellulose matrix. Extensive study of the PVOH immobilization technique is required before the evaluation of the experimental procedure. The interest should be extended to other matrices and complexing agents.

REFERENCES

Aiken, G.R., D.M. McKnight, R.L. Wershaw, and P. McCarthy, (eds.).1985. Humic Substances in Soils, Sediment, and Water. Geochemistry, Isolation and Characterization. A Wiley Interscience Publication, New York, 692pp.

Aiken, G.R., E. M. Thurman, and R. L. Malcom. 1979. Comparison of XAD Macroporous Resins for the Concentration of Fulvic Acid from Aqueous Solution. Anal. Chem. Vol. 51, No. 11, September 1979, pp 1799-1803.

Aiken, G.R., E.M. Thurman, and R.L. Malcom. 1978. Prediction of Capacity Factors for Aqueous Organic Solutes Adsorbed on a Porous Acrylic Resin. Anal. Chem. Vol. 50. Number 6, May 1978, pp 775-779.

Akitt, J. W., N. N. Greenwood, B. L. Khandelwal, G. D. Lester. 1972. Aluminum Nuclear Magnetic Resonance Studies of the Hydrolysis and Polymerization of the Hexa-Aquo-Aluminum III Cation. Part 1, J. Chem. Soc. Dalton, pp 604-610.

Akitt, J. W., N. N. Greenwood, B. L. Khandelwal, G. D. Lester. 1981. Aluminum Nuclear Magnetic Resonance Studies of the Hydrolysis and Polymerization of the Hexa-Aquo-Aluminum III Cation. Part 2. Gel Permeation, J. Chem. Soc. Dalton, pp 1606-1608.

Akitt, J. W., N. N. Greenwood, B. L. Khandelwal, G. D. Lester. 1981. Aluminum Nuclear Magnetic Resonance Studies of the Hydrolysis and Polymerization of the Hexa-Aquo-Aluminum III Cation. Part 3. Stopped Flow Kinetics Studies, J. Chem. Soc. Dalton, pp 1609-1614.

Akitt, J. W., N. N. Greenwood, B. L. Khandelwal, G. D. Lester. 1981. Aluminum Nuclear Magnetic Resonance Studies of the Hydrolysis and Polymerization of the Hexa-Aquo-Aluminum III Cation. Part 5, J. Chem. Soc. Dalton, pp 1624-1628.

Akitt, J. W., N. N. Greenwood, and G. D. Lester. 1969. Aluminum-27 Nuclear Magnetic Resonance Studies of Acidic Solutions of Aluminum Salts. J. Chem. Soc. A, 803.

Amirtharajah, A., K. M. Mills. 1982. Rapid Mix Design Mechanisms of Alum Coagulation. JAWWA, Vol.74, No. 4, pp210-216.

Amy, G.L., M.R. Collins, J. Kuo, and P.H. King. 1985. A Comparison of Gel Permeation Chromatography and Ultrafiltration for Molecular Weight Characterization of Aquatic Organic Matter and Humic Substances. Proc. The National AWWA Conf. June 1985, 14pp.

Angel, S.M. 1987. Optically Selective Fiber Optic Sensors. Spectroscopy, 2 (4), 38pp.

Baes, C.F. Jr., R.E. Mesmer. 1976. Hydrolysis of Cations, Wiley Interscience, New York, NY.

Baker, R. A. 1970. Trace Organic Contaminant Concentration by Freezing. IV Ionic Effects. Water Res., 4, 559-573.

Baker, R. A. 1967. Trace Organic Contaminant Concentration by Freezing. I Low Inorganic Aqueous Solution. Water Res., 1, 61-67.

Barnes, R. B. 1975. Determination of Specific Forms of Aluminum in Natural Water. Chem. Geol., 15, 177-191.

Barnett, P. R., M. W. Skorrstard, and K. J. Miller. 1969. Chemical Characterization of a Public Water Supply. JAWWA, 61:2:60. Feb 1969

Batchelor, B., J. B. McEween, P. Roberta 1986. Kinetics of Aluminum Hydrolysis: Measurement and Characterization of Reaction Products. Env. Sci. and Technol., Vol. 20, Number 9, pp891-894.

Beck, K. C., Reuter J. H., and Perdue E.M. 1974. Organic and Inorganic Geochemistry of Some Coastal Plain Rivers of the Southeastern United States. Geochim. Cosmochim. Acta. 38, 341-364.

Behr, B., and H. Z. Went. 1962. Electrochem. 66, 223.

Black, A.P., and C.L. Chen. 1967. Electrokinetics Behavior of Aluminum Species in Diluted Dispersed Kaolinite System. JAWWA, Vol. 59, pp1173-1183.

Black, A. P. and R.F. Christman. 1963a. Chemical Characteristics of Colored Surface Waters. JAWWA. 55, 753-770.

Black, A. P. and R.F. Christman. 1963b Chemical Characteristics of Fulvic Acid. JAWWA. 55 (7), 897-912.

Bersillon, J. L., Pa Ho Hsu, and F. Fiessinger. 1980. Characterization of Hydroxy-Aluminum Solutions. Soil Sci. Soc. Am. J. 44:630-634.

Bersillon, J. C, J.L. Pa Ho Hsu. 1978. Studies of Hydroxy-Aluminum Complexes in Aqueous Solution. J. Res. US Geol. Surv. 6 (3) : 325-337.

Buffle, J., Deladoey P., and Haerri W. 1978. The Use of Ultrafiltration for the Separation and Fractionation of Organic Ligands in Fresh Waters. Anal. Chem. Acta 101:339-357.

Buffle, J., F.L. Greter, and W. Haerdi. 1977. Measurement of Complexation Properties of Humic and Fulvic Acids in Natural Waters with Lead and Copper Ions Selective electrodes. Anal. Chem. 49, 216-222.

Buffle, J., N. Parthasarathy, W. Haerdi. 1985. Importance of Speciation Methods in Analytical Control of Water Treatment Processes with Application to Fluoride Removal from Waste Waters. Water Res., 19, pp7-23.

Camp, T.R., and P.C. Stein. 1943. J. Boston Soc. Civ. Eng., Vol. 37, pp219.

Campbell, P.G. 1986. Aluminum Speciation in Running Waters on the Canadian Precambrian Shield: Kinetic Aspects, Water, Air, and Soil Pollution, 30, 1023-1032.

Campbell, P.G. et al. 1983. Speciation of Aluminum in Acidic Freshwaters. *Anal. Chem.*, 55, 2246-2252.

Cheng, K. L. 1977. Separation of Humic Acid with XAD Resins. *MicroChim. Acta* 1977-II, 389-396.

Chritophensen, N. and M.S. Hans. 1982. A Model for Streamwater Chemistry at Birkenes, Norway. *Water Res. Res.*, Vol. 18, No. 4, pp977-996.

Chung, Y.S. 1978. The Distribution of Atmospheric Sulfates in Canada and Its Relationship to Long Range Transport of Air Pollutants. *Atmospheric Env.* Vol. 12, pp1471-1480.

Christman, R.F. 1968. Chemical Structure of Color Water Producing Organic Substances in Water. In: *Symposium on Organic Matter in Natural Water*. Hood, D.W. Edit., University of Alaska, College, pp181-198.

Christman, R.F., M. Ghassemi. 1966. Chemical Nature of Organic Color in Water, *JAWWA*, 58 (6), pp 723-741.

Collins, M.R. 1985. Ph.D. Dissertation. University of Arizona. Tucson. AZ.

Collins, M.R., G.L. Amy, C.J. Kuo, Z.K. Chowdhury, and R.C. Bales. 1987. The Effects of Humic Substances on Particle Formation, Growth and Removal during Coagulation Using Aluminum Sulfate. *Div. Env. Chem. Am. Chem. Soc.* 6pp.

Cosby, B.J., G.M. Hornberger, and J.N. Galloway. 1985. Modeling the Effect of Acid Deposition: Assessment of a Lumped Parameter Model of Soil Water and Streamwater Chemistry. *Water Res. Res.*, 21, pp 51-63.

Costello, J.J. 1984. Post Precipitation in Distribution Systems. *JAWWA*, Vol. 76, No. 11, pp 46-49.

Davis, J.A. 1982. Adsorption of Natural Dissolved Organic Matter at the Oxide/Water Interface. *Geochim. Cosmochim. Acta*, Vol. 46, pp2381-2393.

Davis, J.A. 1980. Adsorption of Natural Organic Matter from Freshwater Environment by Aluminum Oxides. In *Contaminants and Sediments*. Vol. 2, R.A. Baker Editor, Ann Arbor Sci. Publ. Inc., Michigan, pp 279-303.

Davis, M.L., and D.A. Cornell. 1985. *Introduction to Environmental Engineering*. PWS Engineering Publishers, Boston, MA, 591pp.

Davis, J.A., and R. Gloor. 1981. Adsorption of Dissolved Organics in Lake Water by Aluminum Oxide. Effect of Molecular Weight. *Amer. Chem. Soc. Vol. 15*, 10, October pp 1223-1229.

Day, R.A., A.L. Underwood. 1985. *Quantitative Analysis*. 4th Edition. Prentice Hall Inc. Englewoods Cliffs, NJ, 660pp.

deGrosbois, E., P.J. Dillons, H.M Seip. and R. Seip. 1986. Modeling Hydrology and Sulfate Concentration in Small Catchments in Central Ontario. *Water, Air, and Soil Pollution*. 31: 45-57.

De Heck, H., R. J. Stol, P.L. De Bruyn. 1978. Hydrolysis Precipitation Studies of Aluminum (III) solutions 3: Role of Sulfate. *J. Colloid Interface Sci.*, 64, 72-89.

Deinzer, M., Melton, R., and Mitchell D. 1975. Trace Organic Contaminants in Drinking Water; Their Concentration by Reverse Osmosis. *Water Res.* 9, 799-805.

Dempsey, B.A. 1987. The Chemistry of Coagulants. Proceedings, AWWA Seminar on Influence of Coagulation on the Selection, Operation, and Performance of Water Treatment Facilities. Kansas City, MO, June 14, 1987, pp31-47.

Dempsey, B.A. 1987. The Reaction Between Fulvic Acid and Aluminum. Effects on the Coagulation Process. Presented before Div.

Env. Eng. ACS, Denver, CO, April 5-10, 1987, 20pp.

Dempsey, B.A., R. Ganho, C. O'Meila. 1984. The Coagulation of Organic Substances by Means of Aluminum Salts. JAWWA, 76 (4), 141-150.

Dillons, P.J., R.A. Reid, and R. Girand. 1986. Changes in The Chemistry of Lakes Near Subury, Ontario Following Reduction of Sulfur Emissions. Water, Air, and Soil Pollution. 31:59-65.

Driscoll, C.T. 1984. A Procedure for the Fractionation of Aqueous aluminum in Drinking Water. Intern. J. Env. Anal. Chem., Vol. 16, pp267-283.

Driscoll, C.T., L. Raymond. 1988. Chemistry and Fate of Al(III) in Treated Drinking Water. Journ. Environ. Eng. Vol. 114, Number 1, Feb., 37pp.

Driscoll, C.T., J.P. Baker, J.J. Bisogni, C.L. Schofield. 1980. Effect of Aluminum Speciation on Fish in Dilute Acidified Waters. Nature, Vol. 284, pp 161-164.

Edwards, G.A. and Amirtharajah. 1985. Removing Color Caused By Humic Acids. J. AWWA Research and Technology. March. pp50-57.

Edzwald, J.K. 1986. Conventional Water Treatment and Direct Filtration. Treatment and Removal of Total Organic Carbon and Trihalomethane Precursors. Org. Carcinogens in Drinking Water. Detection , Treatment and Risk Assessment. N.M. Rem. Christman Edition. Wiley, N.Y. pp199-235.

Edzwald, J.K., B. Joseph, C. O'Melia. 1974. Coagulation in Estuaries. Env. Sci. and Techn., Vol. 8, No. 1, Jan. pp58-63.

Edzwald, J.K., J. McIntyre, R.L. Sanks, M.J. Semmens, and J.S. Taylor. 1979. Organic Removal by Coagulation: A Review and Research Needs, JAWWA, Vol. 71, pp588-603.

Edzwald, J.K., W. Becker, and K. Wattier. 1985. Surrogate Parameters for Monitoring Organic Matter and Trihalomethane Precursors in Water Treatment. JAWWA, Vol. 77, No. 4, pp122-132.

Evan, L.T., E.W. Russell. 1959. The Adsorption of Humic and Fulvic Acids by Clays. J. Soil Sci., 10, 119-132.

Gjessing, E. T. 1976. Physical and Chemical Characteristics of Aquatic Humus. Ann Arbor Science Publisher inc. Ann Arbor Michigan, 120pp.

Gjessing, E. T. 1970. Ultrafiltration of Aquatic Humus. Environ. Sci. Technol., 4:5:437-438

Greeland, D. 1971 Interactions Between Humic and Fulvic Acids and Clays. Soil Science, Vol. 3, No. 1, pp30-34.

Grunwald, E. and W.F. Dodd . 1969. Acidity and Association of Aluminum Ion in Dilute Aqueous Acid. J. Phys. Chem. 650.

Harter, D.R., R.G. Lehmann. 1983. Use of Kinetics for the Study of Exchange Reactions in Soils. Soil Sci. Soc. Am. J. Vol. 47, No.4, pp666-669.

Hayden, P.C. A.J. Rubin. 1976. Systematic Investigation of The Hydrolysis and Precipitation of Aluminum (III). In Aqueous-Environmental Chemistry of Metals. (Chapter 9. J. Rubin (ed.), Ann Arbor Science, Ann Arbor, Michigan.

Hem, J. D. and C. Robertson. 1967. Form and Stability of Aluminum Hydroxide Complexes in Dilute Solution. US Geol. Surv. Paper 1867-A. GPO Washington, D.C.

Hingston, F.J., R.J. Atkinson, A.M. Postner, and J.P. Quirk. 1968. Specific Adsorption of Anions on Goethite. Trans. 9th Int. Congr. Soil Sci. Adelaide, 669-678.

Hingston, F.J., R.J. Atkinson, A.M. Postner, and J.P. Quirk. 1972. Anion Adsorption by Goethite and Gibbsite. The Role of Proton in Determining Adsorption Envelopes. *J. Soil Sci.*, Vol. 23, pp177-192.

Hirschfeld, T. 1986. Remote and in-situ Analysis. *Fres. Z. Anal. Chem.* 324 (618).

Holmes, L.P., D.L. Cole, and E.M. Eyring. 1968. Kinetics of Aluminum Ion Hydrolysis in Dilute Solutions, *J. Phys. Chem.* 72 (1): 301-304.

Hsu, P.H. 1977. Aluminum Oxides and Oxyhydroxides. In Dixon, J.B. and Weed (eds.) *Minerals in Soil Environments*. Soil Sci. Soc. Amer. Madison, WI.

Hsu, P.H., T. Bates. 1964. Formation of X-Ray Amorphous and Crystalline Aluminum Hydroxide. *Mineral Magazine*, 33, 749-768.

Hubel, R. and David Letterman. 1987 Removing Trihalomethane Precursors By Coagulation. *AWWA Journal Research and Technology*. July pp98-106.

Hundt, T. 1985 Aluminum Fulvic Acid Interaction. Mechanisms and Application. PH. D. Dissertation. Submitted to The John Hopkins University 232pp.

Hunter, K.A. 1983. On the Estuarine Mixing of Dissolved Substances in Relation to Colloid Stability and Surface Properties. *Geochim. Cosmochim. Acta*, Vol. 47, pp467-473.

Hunter, K.A. 1982. Organic Matter and the Surface Charge on Suspended Particles in Estuarine and Coastal Waters. *Limnol. Oceanogr.*, 27, (2), 322-335.

Hunter, K.A. 1980. Microelectrophoretic Properties of Natural Surface-Active Organic Matter in Coastal Seawater. *Limnol. Oceanogr.* Vol. 25, (5), 807-822.

Hunter, K.A., and P.S. Liss. 1979. The Surface Charge of Suspended Particles in Estuarine and Coastal Waters. *Nature*, Vol. 282, 823-825.

Inskeep, W.P. 1989. Adsorption of Sulfate by Kaolinite and Amorphous Iron Oxide in the Presence of Organic Ligands. *J. Environ. Qual.* 18:379-385.

Jekel, M.R. 1986 The Stabilization of Dispersed Mineral Particles by Adsorption of Humic Substances. *Water Res.* Vol. 20 No. 12 pp1543-1554.

Johnson, P.N., and A. Amirtharajah. 1982. Ferric Chloride and Alum as Single and Dual Coagulants. *JAWWA* 74 (4):210.

Katyal, M. 1968. Flavones as Analytical Reagents- A Review, *Talanta*, Vol. 15, pp 95-106.

Katyal, M., S. Prakash, 1977. Analytical Reactions of Hydroxyflavones. *Talanta*, 24, 367-375.

Katz, S. Pitt, W. W. Scott, C.D., and Rosen, A.A. 1972. The Determination of Stable Organic Compounds in Waste Effluents at the Microgram Per Liter Levels by Automatic High Resolution Ion Exchange Chromatography. *Water Res.* 6, 1029-1037.

Kerekes, J.J., R.T. Beachamp. 1986. Source of Sulfate Acidity in Nova Scotia. *Water, Air, and Soil Pollution.* 31:207-214.

Khan, S.U. 1972. The Retention of Hydrophobic Compounds by Humic Acids. *Geochemica et Cosmochimica Acta*, 36, 745-754.

Konova, M.M. 1966. *Soil Organic Matter*. Pergamon, Elmsford, N.Y., 544pp.

Koottatep, S. and Odegaard H. 1982. Removal of Humic Substances from Natural Waters by Reverse Osmosis. *Water Res.* 16, 613-620.

Leenheer, J.A. 1981. Comprehensive Approach to the Preparative Isolation and Fractionation of Dissolved Organic Carbon from Natural Waters and Wastewaters. *Env. Sci. and Technol.*, Vol. 15, No. 5, May, pp578-587.

Letterman, R.D., and C.T. Driscoll Jr. 1987. Survey of Residual Aluminum in Filtered Water. AWWA Research Foundation Funded Research Project Summary Report, 26pp.

Letterman, R.D., S.G. Vanderbrook. 1983. Effect of Solution Chemistry on the Coagulation with Hydrolyzed Al(III). Significance of Sulfate and pH. *Water Resources*, Vol. 17, 195pp.

Liao ,W., R.F. Christman, J.D. Johnson, and D.S Millington. 1982. Structural Characterization of Aquatic Humic Material. *Env. Sci. and Technol.*, 16, 403-410.

Lindsay, W.L. 1979. Chemical Equilibria in Soils. Chapter 3: Aluminum. A Wiley Interscience Publication. New York, pp35-49.

Loder, T.C. and P.S. Liss. 1985. Control by Organic Coatings of the Surface Charge of Estuarine Suspended Particles. *Limnol. Oceanogr.*, 30, (2), 418-421.

Malcom, R.L., E.W. Thurman, E.M. Wershaw, D.J. Pinckney. 1982. Molecular size of Aquatic Humic Substances. *Org. Geochem.*, 4, 27-35.

Mangravite, F., T Buzzell, E. Alan, E Matijevic, G. Saxton. 1975. Removal of Humic Acid and Microflotation. *JAWWA*, Vol. 67, pp88-94.

Mantoura, R. F., and J. P. Riley. 1975. The Analytical Concentration of Humic Substances from Natural Waters. *Anal. Chim. Acta*, 76, 97-106.

Marion, S.P., and A. W. Thomas. 1946. Effect of Diverse Ions on the pH of Maximum Precipitation of Aluminum Hydroxide. *J. Colloid Sci.*,

1:221.

May, H.M., Helmke, P.A., and Jackson, M.L. 1979. Gibbsite Solubility and Thermodynamic Properties of Hydroxyl-Aluminum Ions in Aqueous Solution at 25°C. *Geochim. Cosmochim. Acta* 43:861-868.

McCarthy, P. and S. O'Conneide. 1974. Fulvic Acid: Partial Fractionation. *J. Soil Sci.* 25, 420-428.

McSwain, R.M., J.E. Douglas, R.J. Watrous. 1974. Improved Methyl Thymol Blue Blue Procedure for Automated Sulfate Determination. *Anal. Chem.* Vol. 46, No. 9, August. pp1329-1331.

Methods of Soil Analysis. Part 1. Physical and Mineralogical Properties, Including Statistics of Measurement and Sampling. 1965. Black, C.A. Editor-in-Chief. American Society of Agronomy, Inc. Publishers, Madison, WI. pp 545-558.

Midwood, R. B., and G. T. Felbeck Jr. 1965. Analysis of Yellow Organic Matter from Fresh Water. *JAWWA*. 60: 357

Miller, J., and J. Miller. 1984. Statistics for Analytical Chemistry. Wiley and Sons, New York, N.Y.

Miller, L.B. 1925. A Study of the Effect of Anions Upon the Properties of Aluminum. *Public Health Reports*, 40:351.

Moed , J. R. 1970. Aluminum Oxide as Adsorbent for Natural Water-Soluble Yellow Material *Limnol. Oceanogr.* 15, 140-142.

Montgomery, J.M. Consulting Engineers, Inc. 1985. Water Treatment. Principles and Design. A Wiley-Interscience Publication, New York, 696pp.

Morris, J.K., and W.R. Knocke. 1984. Temperature Effects on the Use of Metal-Ion Coagulants for Water Treatment. *JAWWA*, Research and Technology, March, pp74-79.

Neihof, R.A., and G.I. Loeb. 1974. Dissolved Organic Matter in Seawater and the Electrical Charge of Immersed Surfaces. *J. Marine Res.* Vol. 32, pp5-12.

Neihof, R.A., and G.I. Loeb. 1972. The Surface Charge of Particulate Matter in Seawater. *Limnol. Oceanogr.* 17:7-16.

Nichols, D.S., R. E. McRoberts. 1986. Relation Between Lake Acidification and Sulfate Deposition in Northern Minnesota, Wisconsin, and Michigan. *Water, Air, and Soil Pollution.* 31:197-206.

Norberg, G.F., R.A. Goyer, and T.W. Clarkson. 1985. Impact of Effect of Acid Precipitation on Toxicity of Metals. *Env. Health. Perspect.* Vol. 63, pp 169-180.

Nordstrom, D.K. 1982. The Effect of Sulfate on Aluminum Coagulation in Natural Waters: Some Stability Relations in The System Al_2O_3 , SO_3 , H_2 . *Geochimica Cosmochimica Acta*, 46, 681.

Oliver, B. G., and S. A. Visser. 1980. Chloroform Production from the Chlorination of Aquatic Humic Material: The Effect of Molecular Weight, Environment, and Season. *Water Research*, 14:1137-1141.

Packham, R.F. 1965. Some Studies of the Coagulation of Dispersed Clay with Hydrolyzing Salts. *J. Colloid Sci.*, Vol. 20, pp81-92.

Parfitt, R.L., A.R. Fraser and V.C. Farmer. 1977. Adsorption on Hydrous Oxides. III. Fulvic Acid on Goethite, Gibbsite and Imogolite. *J. Soil Sci.*, 28, 289-296.

Parfitt, R.L., R.D. Russell. 1977. Adsorption on Hydrous Oxides. Iv. Mechanisms of Adsorption of Various Ions on Goethite. *J. Soil Sci.*, 28, 297-305.

Parfitt, R.L., R. ST. C. Smart. 1977. Infrared Spectra from Binuclear Bridging Complexes of Sulfate Adsorbed on Goethite. *J. Phys. Chem. Faraday I*, Vol. 5, pp796-802.

Parks, G.A., P.L. DeBruyn. 1962. The Zero Point of Charge of Oxides. J. Phys. Chem. 66:967-972

Parthasarathy, N., J. Buffle. 1985. Study of Polymeric Aluminum (III) Hydroxide Solution for Application in Waste Water Treatment. Properties of the Polymer and Optimal Conditions of Preparation. J. Water Res., 19, pp 25-36.

Perl, D.P. 1985. Relationship of Aluminum to Alzheimer's Disease. Env. Health Perspect., Vol. 63, pp149-153.

Plechanov, N., B. Josefsson, D. Dyrssen, k. Lundquist. 1983. Investigations of Humic Substances in Natural Water. In Aquatic and Terrestrial Humic Materials. Christman, R.F. and Gjessing, E. (eds). Ann Arbor Science, Ann Arbor, Mi.

Randtke, S. 1987. The Influence of Coagulation on Organic Contaminant Removal and Activated Carbon Adsorption. Presented at the AWWA Preconference Seminar " Influence of Coagulation on Selection, Operation, and Performance of Water Treatment Facilities," June 14, 1987, Kansas City, MO., 51pp.

Reuter, J.H. and E.M. Perdue. 1977. Importance of Heavy metal Organic Interaction in Natural Waters. Geochim, Cosmochim. Acta. 41, pp325-334

Rezania, S. 1985. The Occurrence and Control of Aluminum in Drinking Water. Ph. D. dissertation. University of New Hampshire, 122pp.

Robert, G. M., Frederick C.K., Keith K, Judy A.S., and Nancy S. 1984. Occurrence of Aluminum in Drinking Water. JAWWA Research and Technology, Jan. 1984, pp 84-91.

Saar, R.A. 1980. Cadmium(II), Lead(II), and Copper(II) Complexation by Fulvic Acid Derived from Soil and Water: Ion Selective Electrode and Spectrofluorometric Studies. Ph.D. Dissertation, University of New Hampshire, 174pp.

Saari, L. A. 1983. Sensors Based on Immobilized Fluorogenic Reagents, Ph.D. Dissertation, University of New Hampshire, 144pp.

Saari, L.A., and W.R. Seitz. 1983. Immobilized Morin as Fluorescence Sensor for Determination of Al(III), *Anal. Chem.*, 55, 667-670.

Saffman, P.G., and J.S. Turner. 1956. On the Collision of Drops in Turbulent Clouds. *J. Fluid Mech.* 1, 16-30.

Schecher, W.D., and C. T. Driscoll. 1987. An Evaluation of Uncertainty Associated with Aluminum Equilibrium Calculations. *Water Res. Res.*, Vol. 23, No. 4, pp 525-534.

Schecher, W.D., and C. T. Driscoll. 1988. An Evaluation of Uncertainty in Equilibrium Calculations Within Acidification Models: The Effect of Uncertainty in Measured Chemical Components. *Water Res. Res.*, Vol. 24, No. 4, pp 533-540.

Schendel, D. and David Letterman. Polyaluminum Sulfate Vs Alum for the Removal of Humic Substances from a Low Alkaline Surface Water. *JAWWA*, Vol. 76, No. 4, pp141.

Schnitzer, M., and S. Khan. 1972. Humic Substances in the Environment. Marcel Decker, New York, 327pp.

Schnitzer, M., and S. Khan. 1972. The Retention of Hydrophobic Organic Compounds by Humic Acid. *Geochem Cosmochim. Acta*, Vol. 36, pp745.

Seitz, W.R. Chemical Sensors based on Fiber Optics. 1984. *Anal. Chem.*, 56, 16A.

Seitz, W.R., Z. Zhang, Z. Yunke, W. Ma, R. Russell, Z.M. Shakhsher, S. Shack, and C.L. Grant, 1989. Polyvinyl Alcohol as a Substitute for Indicator Immobilization for Fiber Optic Chemical Sensors, *Anal. Chem.*, 61, 202-205.

Serna, C. J., J. L. White, and S.L. Hem. 1977. Anion-Aluminum Hydroxide Gel Interactions. *Soil Sci. Soc. Am. J.*, 41:1009-1013.

Sieburth, J., and Jensen A. 1968. Studies on Algal Substances in the Sea. Humic Acid Material in Terrestrial and Marine Waters. *J. Exp. Mar. Biol. Ecol.* 2, 174-189.

Sigel, H. 1988. Metal Ions in Biological Systems. Volume 24. Aluminum and Its Role in Biology. Marcel Dekker, Inc. New York and Basel, pp58-122.

Singh, B.R. D. Johnson. 1986. Sulfate Content and Adsorption in Soils of Two Forest Watersheds in Southern Norway. *Water Air and Soil Pollution*, Vol. 31, No. 1, pp847-856.

Sinsabaugh III, R.L., R.C. Hoehn, W.R. Knocke, and A.E. Linkins III. 1986. Removal of Dissolved Organic Carbon by Coagulation with Iron Sulfate. *Journal AWWA Research and Technology*, May, pp74-82.

Smith, R.W. and J.D. Hem. 1972. Effect of Aging on Aluminum Hydrolysis Complexes in Dilute Aqueous Solutions. USGS Water Supply Paper 1827-D, GPO, Washington, D.C.

Snodgrass, W.J., M.M. Clark, and C.R. O'Melia. 1984. Particle Formation and Growth in Dilute Aluminum (III) Solutions: Characterization of Particle Size Distributions at pH5.5. *Water Res.*, Vol. 18, No. 4, pp479-488.

Sricharoenchaitit, P. and R.D. Letterman. 1987. Effect of Aluminum (III) and Sulfate Ion on Flocculation Kinetics. Paper Presented to *J. Env. Eng.* Vol. 113, No. 5, October 1987, ASCE, pp1121-1138.

Standard Method for The Examination of Water and Wastewater. 1980. 15th Edition, APHA-AWWA-WPCF, 1134pp.

Stevenson, J.F. 1982. Humus Chemistry. Genesis, Composition, Reaction. John Wiley and Son Publisher, New York. 443pp.

Stol, R. J., V. H. Helden, P.L. De Bruyn. 1976. Hydrolysis Precipitation Studies of Aluminum (III) solutions 2: A Kinetics Study Model. *J. Colloid Interface Sci.*, 57, pp 115-131.

Strycker, L.J., and E. Matijevic. 1969. Conterion Complexing and Sol Stability. II. Coagulation Effects of Aluminum Sulfate in Acidic Solution. *J. Phys. Chem.*, 73, 1484-1487.

Stumm, W., and C.R. O'Melia. 1968. The Stoichiometry of Coagulation, *JAWWA*, Vol. 60, pp 514-526.

Stumm, W., and J.J. Morgan. 1981. *Aquatic Chemistry*, 2nd Edition. Wiley-Interscience, New York.

Stumm, W. and J.J. Morgan. 1962. Chemical Aspects of Coagulation. *JAWWA*, 54:971.

Sullivan, J. H. and J. E. Singley. 1968. Reactions of Metal Ions in Dilute Aqueous Solution: Hydrolysis of Aluminum. *JAWWA*, 60, 1280.

Sung, W. and S. Rezania. 1984. The Effect of pH and Fluoride on the Soluble Fraction of Aluminum. *Env. Techn. Letters*, Vol. 6, pp11-20.

Tang, A.J.S., D.H.S., Chung, and M.A. Lusi. 1986. Spatial and Temporal Pattern of Sulfate and Nitrate Wet Deposition in Ontario. *Water, Air, and Soil Pollution*. 30: 263-273.

Thurman, E.M. 1985. *Organic Geochemistry of Natural Waters*. Martimus Nighoff/Dr W. Junk Publishers. Boston, MA, 497pp.

Thurman, E.M. and R.L. Malcom. 1983. Structural Study of Humic Substances. New Approaches and Methods. In *Aquatic and Terrestrial Humic Materials*. R. F. Christman and E.T. Gjessing Edits. Ann Arbor Science, Ann Arbor, MI, pp1-23.

Thurman, E. M., and R.L. Malcom. 1981. Preparative Isolation of Aquatic Humic Substances. *Env. Sci. and Technol.*, Vol. 15, No. 4, April, 463-466

Thurman, E. M. and R. L. Malcom. 1979 Comparison of XAD Macroporous Resins for the Concentration of Fulvic Acid from Aqueous Solution. *Amer. Chem. Soc. Vol. 51, No. 11*, pp 1799-1803.

Tipping, E. 1986. Some Aspect of the Interaction between Particulate Oxides and Aquatic Humic Substances. *Marine Chemistry*. 18, pp161-169.

Tipping, E. 1981. The Adsorption of Aquatic Humic Substances by Iron Oxides. *Geochim. Cosmochim. Acta*, Vol. 45, pp191-199.

Tipping, E., C. Woof, C.A. Backes, and M. Ohnstad. 1988. Aluminum Speciation in Acidic Natural Waters: Testing of a Model for Aluminum-Humic Complexation. *Water Res.*, Vol. 22, No. 3, pp 321-326.

Tipping, E., C. Woof, D. Cooke. 1981. Iron Oxide from a Seasonally Anoxic Lake. *Geochim. Cosmochim. Acta*, Vol. 45, pp1411-1419.

Tipping, E., D. Cooke. 1982. The Effects of Adsorbed Humic Substances on the Surface Charge of Goethite (α -FeOOH) in Fresh waters. *Geochim. Cosmochim. Acta*, Vol. 46, pp75-80.

Tipping, E., M. Ohnstad. 1984. Colloid Stability of Iron Oxides Particles from a Fresh Water Lake. *Nature*, Vol. 308, pp266-268.

Turner, R.C. 1976. Effect of Aging on Properties of Polynuclear Hydroxyaluminum Cations. *Can. J. Chem.* 54, 1528-1534.

Turner, R.C. 1969. Three Forms of Aluminum in Aqueous Systems by 8-Quinolinolate Extraction. *Can. J. Chem.* 47, 2521-2527

USEPA. 1985. Federal Register, Vol. 50, No. 219, November 13. National Primary Drinking Water Regulations.

Van Benschoten, J. E., J. K. Edzwald. 1988. Aluminum Fractionation Procedure for Water Treatment. Methodology and Application. Paper

submitted to the AWWA, Nov. 15. 15pp.

Van Benschoten, J. and J.K. Edzwald. 1987. Fate and Speciation of Al in Drinking Water Treatment. 25th Annual Conf. Ass. Quebecoise Des Techniques De L'eau. Montreal Canada March 4-7. 11pp.

Vermeulen, A.C., R. J. Stol, J.W. Geus, and P.L. De Bruyn. 1975. Hydrolysis Precipitation Studies of Aluminum (III) solutions I: Titration of Acidified Aluminum Nitrate Solution. J. Colloid Interface Sci., 51, No. 3, pp449-458.

Walpole, G.S. 1914. J. Chem. Soc., Vol. 105, 2501.

Waters, D.N., M.S. Henty. 1977. Raman Spectra of Aqueous Solutions of Hydrolyzed Aluminum (III) Salts. Chem. Soc. J. Dalton Trans., pp 243-245.

Weber, J.H. 1973. Metal Complexes of Components of Yellow Organic Acid in Water. Water Resource Research Center Report. University of New Hampshire. Report No. 21, 33pp.

Weber, J.H., and R.A. Saar. 1982. Fulvic Acid Modifier of Metal-Ion Chemistry. Env. Sci. and Technol. Vol. 16, No. 9, 510A.

Weber, J.H., and R.E. Truitt. 1979. Fate of Metal Ions during Domestic Treatment of Water Containing Organics. Water Resources Research Center Report. University of New Hampshire. W.S. 73 016, 22pp.

Weber, J. H., and S. A. Wilson. 1975. The Isolation and Characterization of Fulvic and Humic Acid from River Water. Water Research, Vol. 9, pp 1079-1084.

Wershaw et al. 1967. Sodium Humate Solution Studied with Small Angle X-Ray Scattering, Science, 157, 1429.

Wiesner, M.R., V. Lahoussine, and F. Fiessinger. 1986. Organic Removal and Particle Formation using a Partially Neutralized $AlCl_3$. Paper to be presented at the AWWA annual conference, Denver CO,

June 22-26.

Wilander, A. 1972. A Study on the Fractionation of Organic Matter in Natural Water by Ultrafiltration Techniques. Schweiz. Z. Hydrol., 34:2:190-200.

Williams, P. M., and A. Zirino. 1964. Scavenging of Dissolved Organic Matter from Seawater with Hydrated Metal Oxide. Nature 204, 462-464.

Wills, M.R. and Savory, J. 1985. Water Content of Aluminum, Dialysis dementia and osteomalacia. Env. Health Perspect. Vol. 63, pp 141-147.

APPENDICES

A1: Sensor for Al(III) Based on Immobilized Morin

The objective of this investigation was the qualitative evaluation of the performance of the sensor. Detailed information on the analytical approach can be found in (Russell, 1989). Two series of analyses were conducted. The first included the measurement of the aluminum solutions with cellulose sensors. The change in fluorescence intensity with time was recorded to determine the response time. The fluorescence intensity of each sample was subsequently recorded after a given time interval. The same procedure was repeated in the second analysis with the polyvinyl alcohol (PVOH) sensor.

The fluorescence intensity variation with the response time for the cellulose sensors are shown in Figures A1 a, b, and c. The fluorescence intensity increased to reach maxima after 90 min for Figure A1 a and 60 min for Figure A1 b. The response time curve was linear for analysis times shorter than 60 min as shown in Figure A1 c.

The response time was not successfully reduced. The fluorescence intensity measurements were taken after 15 and 20 min of elapsed time. The results are presented in Figure A1 d. The intensity decreased with the analysis time. The decrease was greater at the higher aluminum concentrations.

The data of Figure A1 d also shows the variation of the fluorescence intensity measurements between successive analyses with two sensors. The analysis with sensor#4 was done after sensor#6. The lower intensity measurements indicated that a smaller amount of the immobilized morin was transferred to the fiber optic bundle.

In the Polyvinyl alcohol (PVOH) immobilization, the morin was initially preimmobilized, then, crosslinked. The results of Figure A1 e showed that the fluorescence intensity decreased exponentially with time. The procedure was altered by crosslinking then immobilizing the morin in PVOH. The intensity then increased with time as shown in Figure A1 f.

The use of the PVOH did not improve the response time as shown in Figure A1 g. The intensity maxima was not reached in less than 60 min. The variation in the aluminum concentration did not

affect the intensity measurements.

The data of Figure A1 h was obtained from measuring the fluorescence intensity of several 1.85×10^{-5} to 5.3 M aluminum solutions. The pH of the solution was varied from 4.4 to 6.5. The fluorescence intensity decreased with increasing pH.

The fluorescence intensity measurement for both the cellulose and the polyvinyl alcohol (PVOH) matrices were inconsistent. The study focus was changed several times because, in neither case the response time was brought to less than 1 hr. The objectives were shifted toward a trouble shooting procedure.

A series of several unsuccessful experiments were conducted to improve the extremely slow response time. The procedures consisted of preparing new immobilized morin with different cellulose to morin molar ratios. None of the changes provided a consistent response. The response time variation was not improve below 60 min.

The slow response time of over 1 hr was not desired for sample measurements because the advantage sought to record the aluminum concentration was lost. Two alternatives were pursued. The fluorescence intensity measurements were first taken after 15 and 20 min analysis time. The intensity decreased with the analysis time. The decrease was greater at the higher aluminum concentrations.

The lower intensity measurements for sensor#6 in Figure A1 d indicated that a smaller amount of the immobilized morin was transferred to the fiber optic bundle. The dependence of the fluorescence intensity on the amount of morin transferred to the fiber optic bundle was one of the major draw backs of the technique. All the sample in a set of experiments had to be analyzed with one preparation. No appropriate way was at hand or successfully developed to transfer an exact amount of morin for a set of experiments. The attempts made to do such transfer resulted in a wide variation of the fluorescence intensity measurements. The procedure was abandoned.

The alternative, experimented, was to use the same sensor for all the measurements. The only meaningful analyses were conducted starting from the lower to the higher aluminum concentrations. A random measurement technique did not give

consistent results.

The quality control/quality assurance procedure attempted abandoned because of the inconsistencies in the measurements. The only successful data were obtained with measurements taken in solution with increasing aluminum concentrations. The binding sites on the morin were frequently saturated. The equilibrium was then distorted and measurements in more dilute solutions was not possible because the intensity remained at the maxima.

The failure of the cellulose sensor was in part due to limited diffusion when morin was immobilized on the cellulose. The theoretical equilibrium condition assuming a 1:1 immobilized morin to aluminum complex was not observed.

The introduction of the polyvinyl alcohol (PVOH) immobilization did not solve these problems. Crosslinking before immobilization was the corrected procedure that was followed.

The trouble shooting procedure undertaken for the cellulose method was repeated to improve the response time. The measurements were as inconclusive. The equilibrium condition for aluminum binding to immobilized morin was not as theoretically predicted because the reaction was not reversible. The intensity did not drop once the maxima was reached.

The unsuccessful attempts to qualitatively test the Al(III) sensing procedure suggested that the research be directed towards finding an immobilization procedure which would allow a shorter response time. The applications will be of limited value in water treatment if the final procedure does not accomplish two goals. 1) the measurements of aluminum concentration within one minute time. The corrected method could then be compared with other techniques and theoretical aluminum speciation calculations. The comparisons would provide the answer to the exact species measured by the sensing method. Finding an other complex agent may be the route to take in the future.

Summary

The two immobilization procedure attempted did not provide consistent measurements. The protocole initially set up to check the performance of the probe was abandoned. The procedure consisted

mainly of trouble shooting get the pocedure to a start.

Fluorescence intensity measurements gave slow response times of over 1 hr. for both sensors and measurements were not repeatable. The determination of aluminum species mesurements was not feasible because of these problems. Future research should be directed toward finding an other complexing agent.

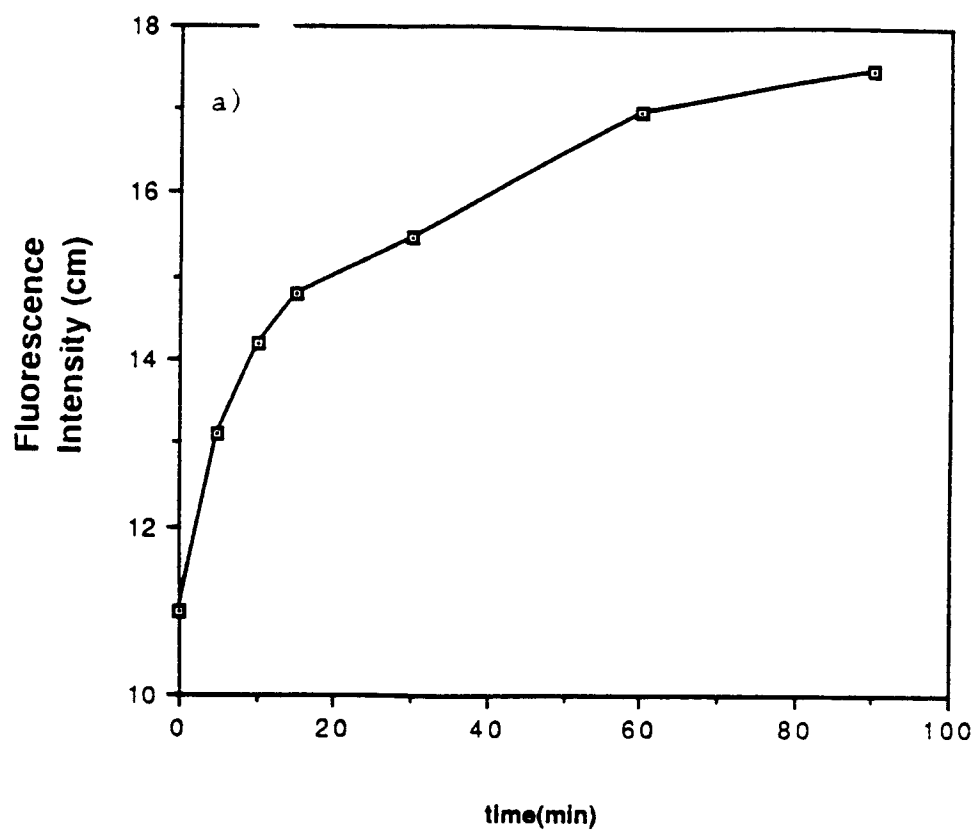


Figure A1 a): Fluorescence intensity measurement for a cellulose sensor#1 ($A_{III} = 1 \times 10^{-4.7} M$)

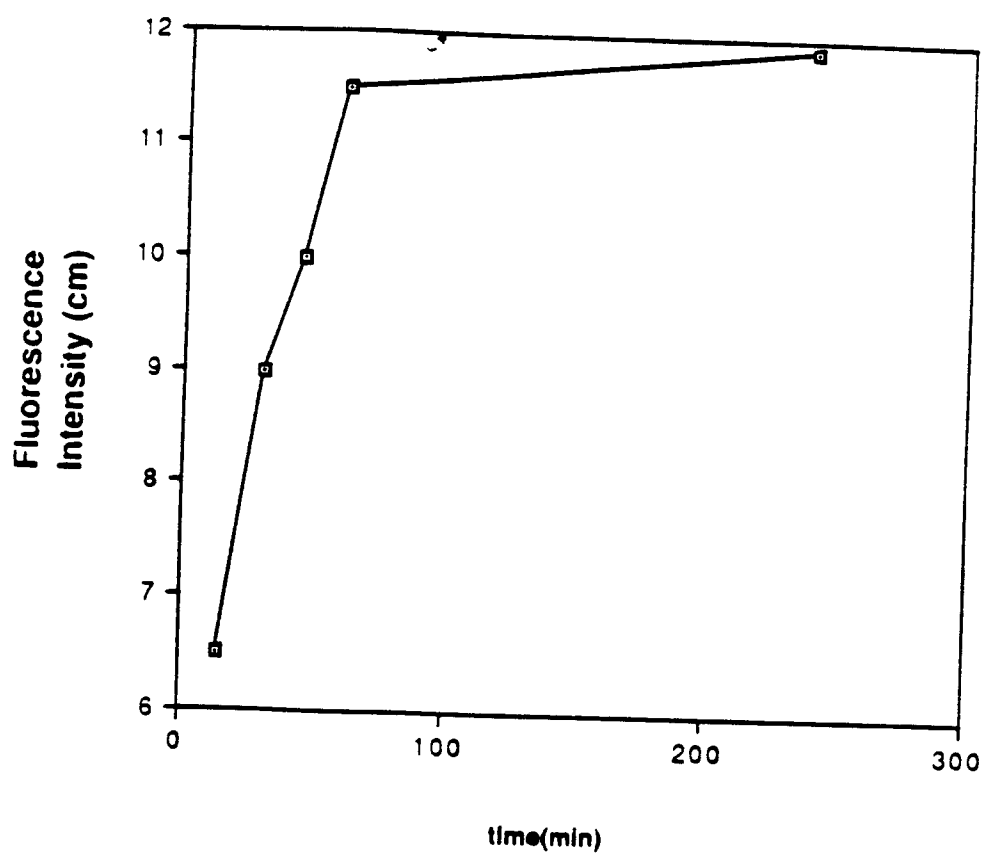


Figure A1 b): Fluorescence intensity measurement for cellulose sensor#2 ($Al(III) = 1 \times 10^{-4.7} M$)

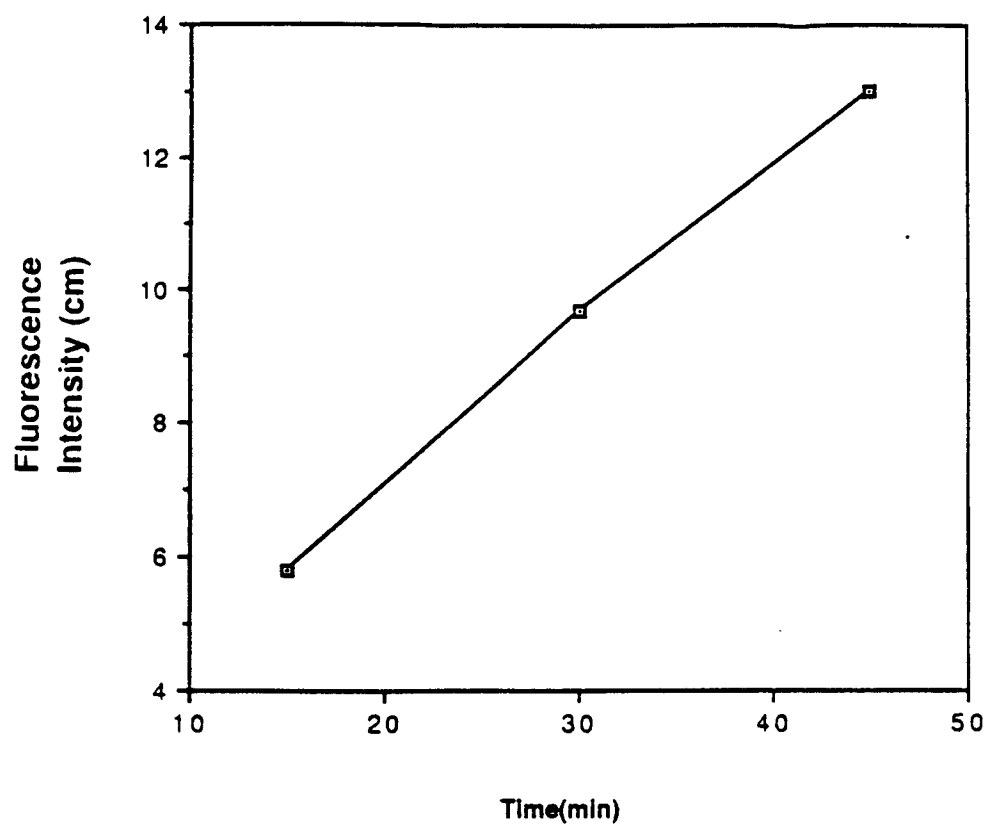


Figure A1 c): Fluorescence intensity measurement for cellulose sensor#3 ($Al(III) = 1 \times 10^{-4.7} M$)

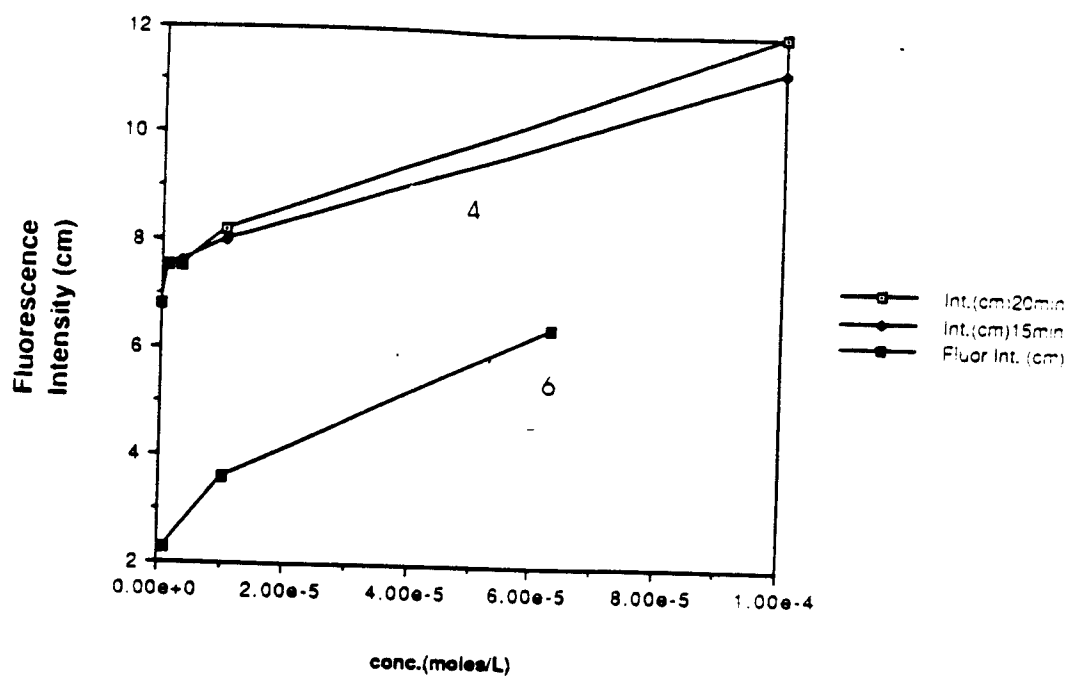


Figure A1 d): Fluorescence intensity measurement variation with analysis time for two cellulose sensors; #4 and #6

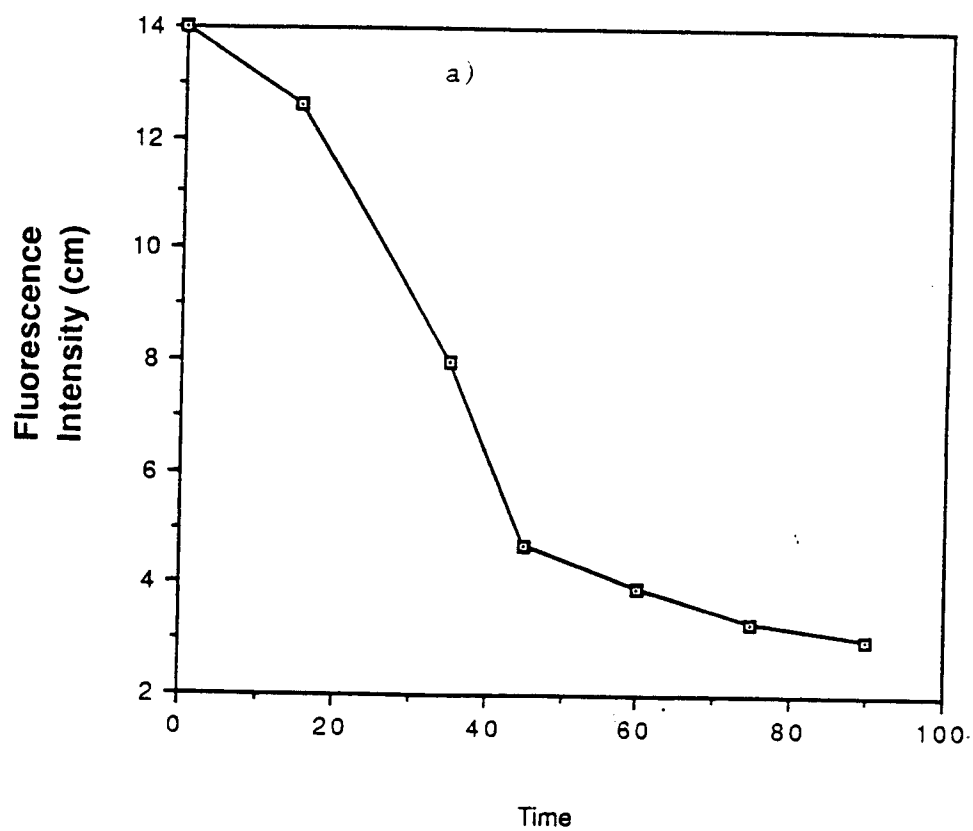


Figure A1 e): Fluorescence intensity measurement for a preimmobilized, then crosslinked PVOH sensor

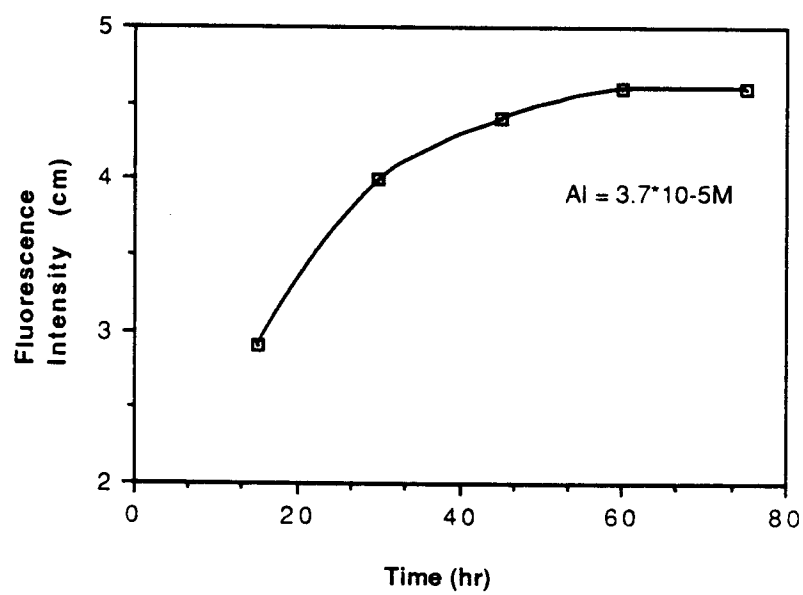


Figure A1 f: Fluorescence intensity measurements for a crosslinked then PVOH-immobilized morin

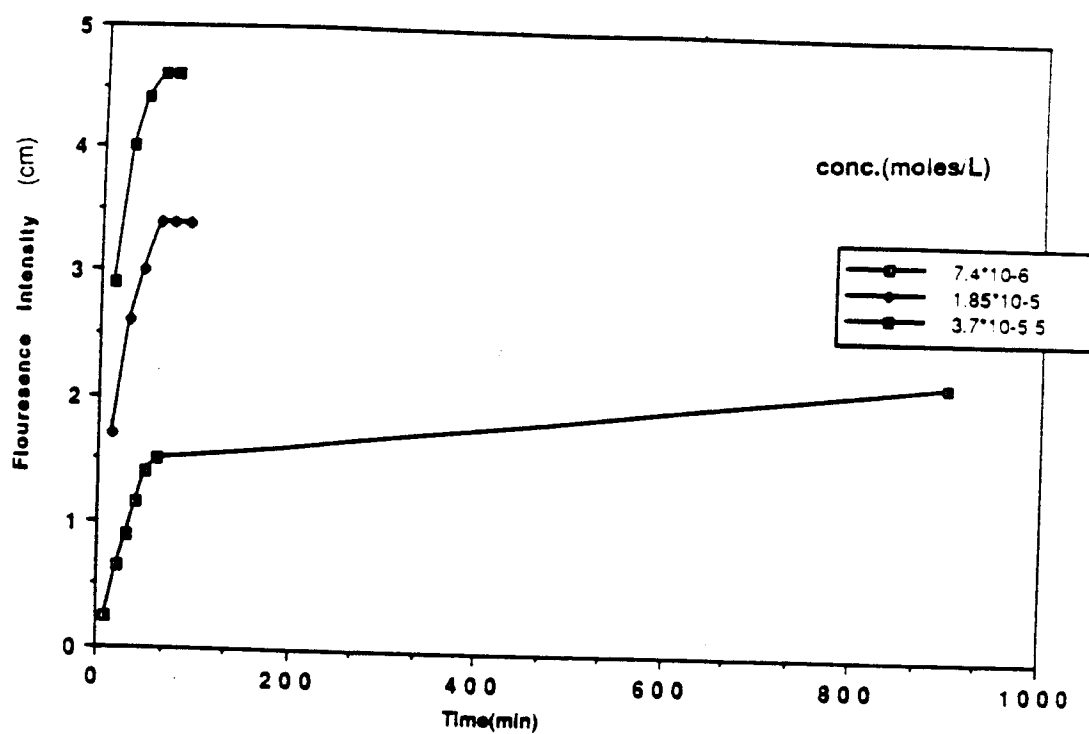


Figure A1 g): Fluorescence intensity measurement for a Al(III) solutions with PVOH sensor

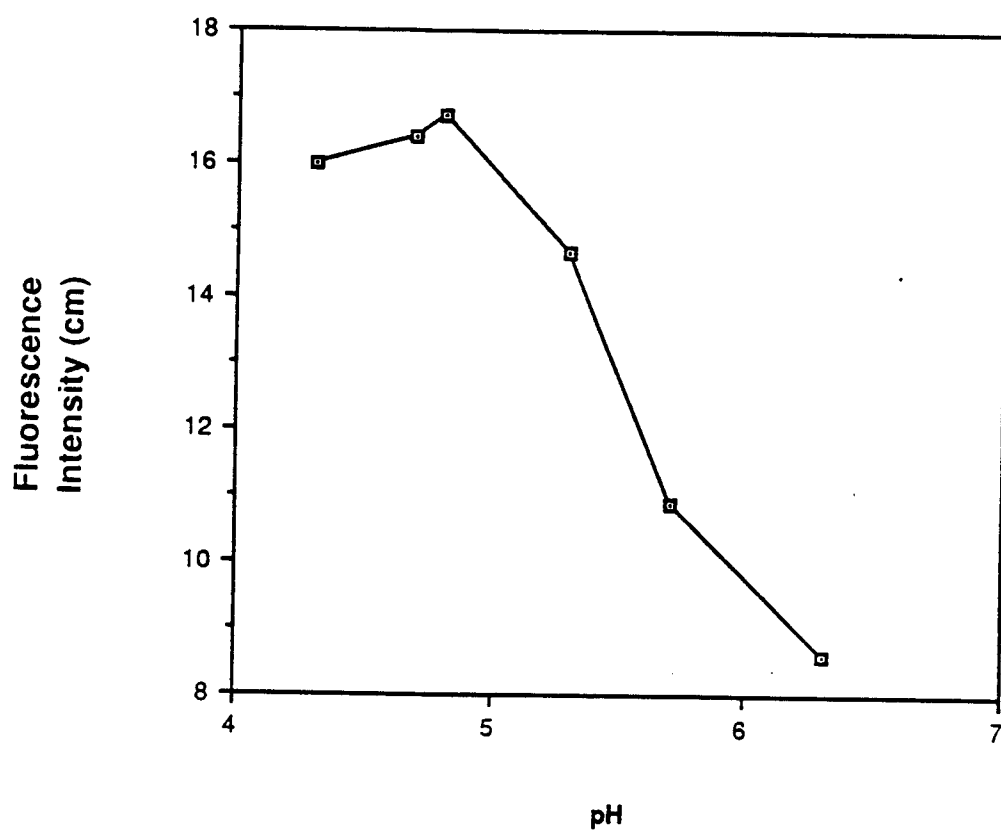


Figure A1 h): Influence of pH variation on PVOH sensor

A2: Determination of Theoretical Settling Time for Bentonite Sedimentation

Small spherical particles of density p_s and diameter X are known to settle through a liquid of density p_l and viscosity μ at a rate of

$$V = X^2 g (p_s - p_l) / 18 \mu \quad (A1)$$

This relationship between the size of a spherical particle and its settling velocity (also known as Stoke's law) furnishes an arbitrary measure of the size of non spherical particles. Thus the separation of clay fraction by sedimentation can be accomplished by homogenizing a soil suspension and decanting all of that which remains above the plane

$$z = -h \quad (A2)$$

after time

$$t = 18 \mu L / g (p_s - p_l) X^2 \quad (A3)$$

Quantitative separation by decantation requires that the residue be resuspended and decanted repeatedly to salvage those particles that had not previously been at the top of the suspension at the start of the sedimentation period. It should be noted that μ is temperature dependent and will affect t . Table A1 was obtained using equation A3.

Table A2: Sedimentation times* for particles of 2 , 5 and 20 μm diameter settling through water for a depth of 10 cm.

Temperature $^{\circ}\text{C}$	settling time with indicated particle diameter					
	2 μm		5 μm		20 μm	
	hr	min	hr	min	hr	min
20	8	0	1	17	4	48
21	7	49	1	15	4	41
22	7	38	1	13	4	35
23	7	27	1	11	4	28
24	7	17	1	10	4	22
25	7	7	1	8	4	16
26	6	57	1	7	4	10
27	6	48	1	5	4	4
28	6	39	1	4	4	0
29	6	31	1	3	3	55
30	6	22	1	1	3	49
31	6	14	1	0	3	44

A3: Determination of the Root Mean Square Velocity Gradient, G

The total energy input into a fluid is related to the root means square velocity gradient, G by (Camp et al., 1943):

$$G = (E/v)^{1/2} \quad (A4)$$

where

E = total energy dissipated per unit time and fluid mass (J/sec lb)

v = kinematic viscosity (ft²/sec)

G can be evaluated by expressing equation A4 in the following form (Edzwald et al., 1974):

$$G = (\partial w/\mu V)^{1/2} \quad (A5)$$

where

∂ = net torque (dyne ft)

w = angular velocity of the rotating paddle (radian/sec)

μ = fluid viscosity (lb/ft sec)

V = fluid volume (ft³)

$$P = \partial w, \quad (A6)$$

$$G = (P/V \mu)^{1/2} \quad (A7)$$

$$= (F_d v/V \mu)^{1/2} \quad (A8)$$

$$= (C_d \rho A v^{3/2} V \mu)^{1/2} \quad (A9)$$

where

P = power utilized (ft lb/sec)

μ = absolute viscosity (lb sec/ft²)

F_d = drag force of paddle, dimensionless

A = area of paddle (ft²)

ρ = fluid density (lb sec²/ft⁴)

v = relative velocity of fluid with respect to paddle (ft/sec)

V = fluid volume (ft³)

$$\text{For } v = k v_p \quad (A10)$$

where

v_p = paddle velocity (ft/sec)

k = ratio of fluid to paddle velocity

and

$$v_p = 2 \pi r N/60 = \pi r N/30 \quad (A11)$$

where

r = paddle radius (ft)

N = revolution per min (rpm)

therefore,

$$G = (C_d \rho A k^3 \pi^3 r^3 N^{3/5.4} 10^4 V \mu)^{1/2} \quad (\text{A12})$$

For the jar test

$k = 0.70$

$C_d = 1.8$

$A = 1 \text{ in} \times 2.0 \text{ in}$

$V = 1 \text{ l}$

$r = 70^\circ\text{F} (21.1^\circ\text{C})$

$\rho = 1.936 \text{ lb sec}^2/\text{ft}^4$

$\mu = 2.050 \cdot 10^{-5} \text{ lb/sec ft}^2$

$$G = 0.08729 N^{3/2} \quad (\text{A13})$$

The variations of G with N are shown in Figure A3.

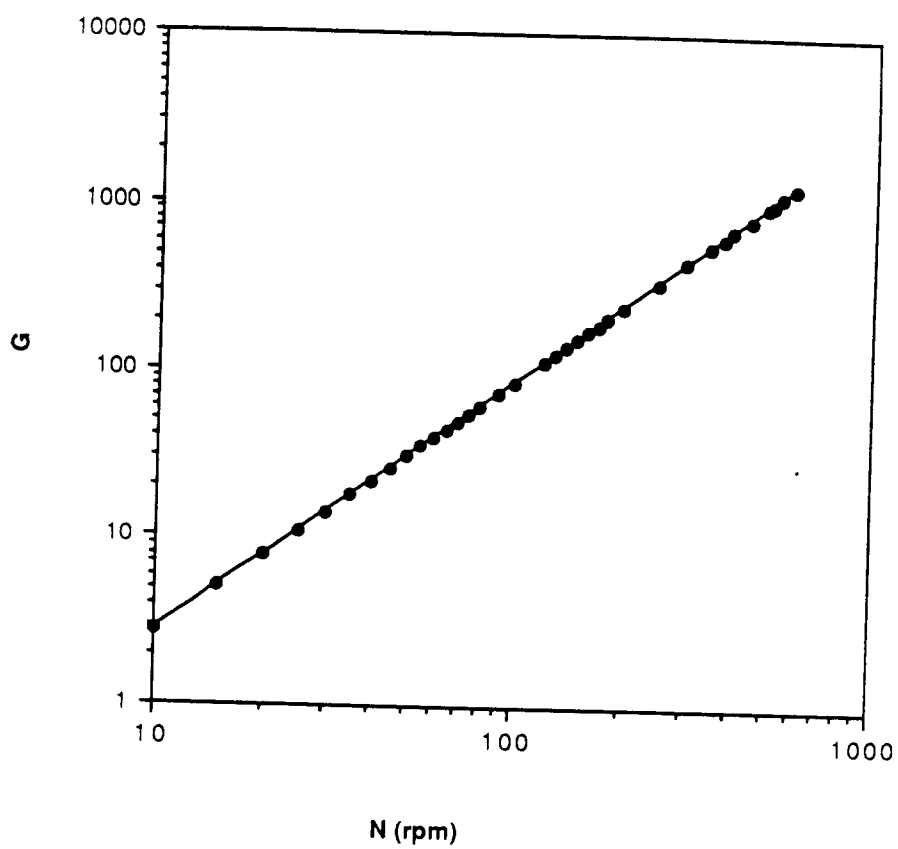


Figure A3: Relation between paddle revolution and root-mean square velocity gradient

A4: Sample Calibration Curves for Analyses

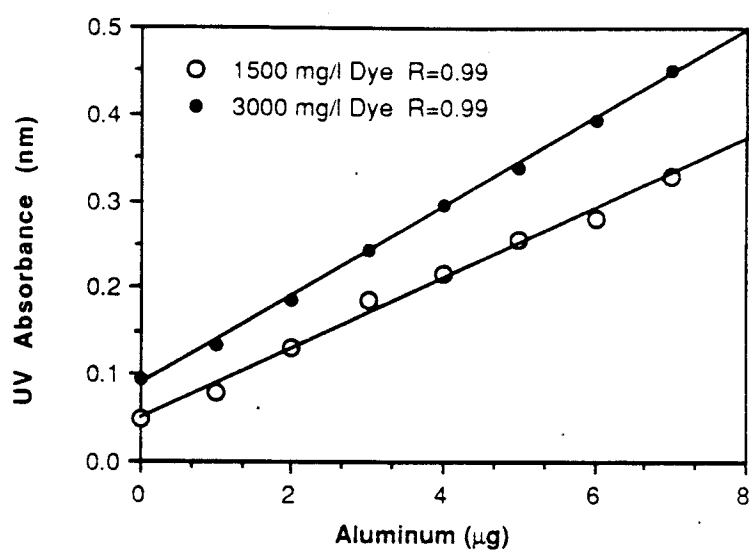


Figure A4 a: Aluminum standard curve for the Eriochrome Cyanine R Method (1cm cell path)

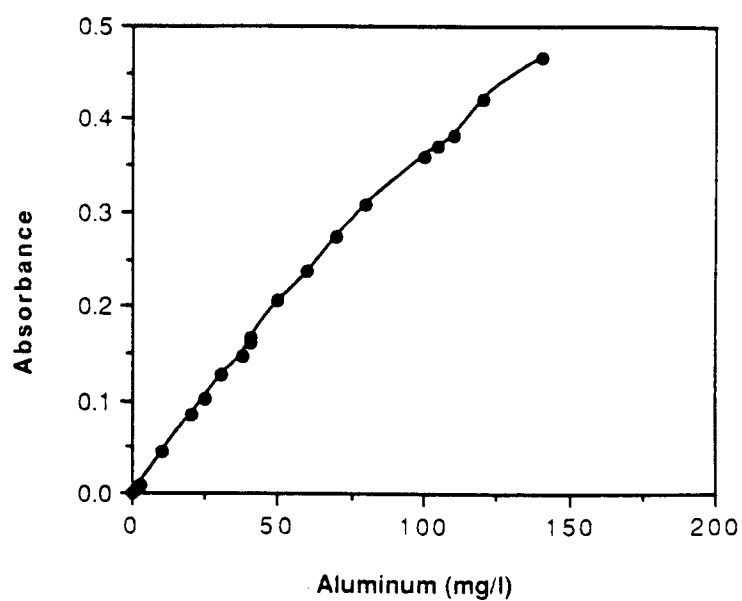


Figure A4 b: Aluminum standard curve for flame analyses

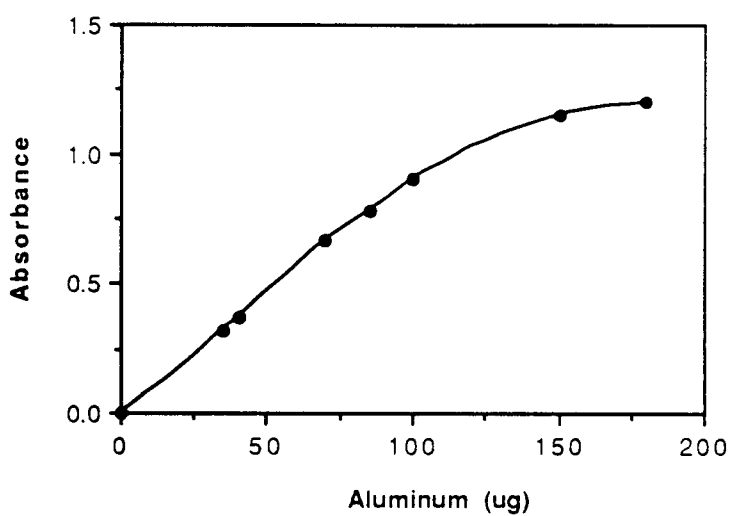


Figure A4 c: Aluminum standard curve for graphite furnace analyses

HGA Program	Step	1	2	3	4	5
	T (C)	90	130	1700	2500	2650
	Ramp	2	20	5	0	1
	Hold	20	20	20	5	3

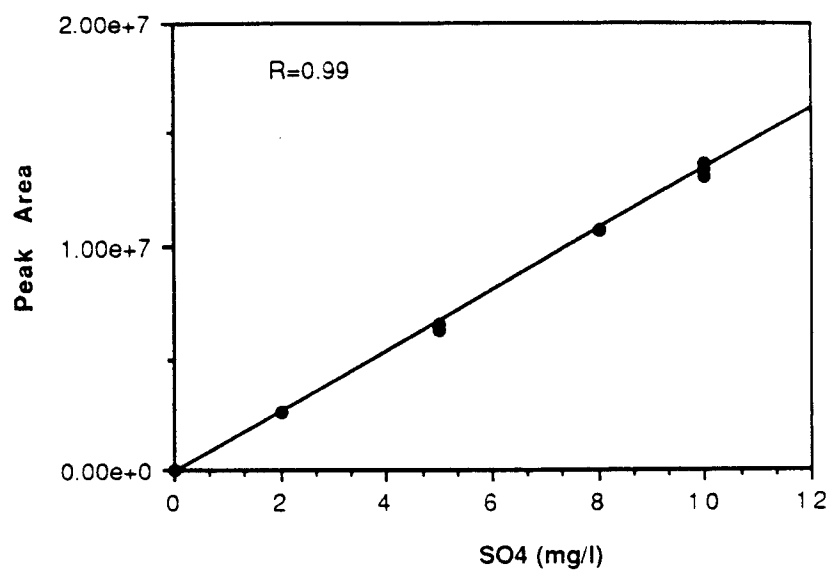


Figure A4 d: Calibration curve for sulfate (IC)

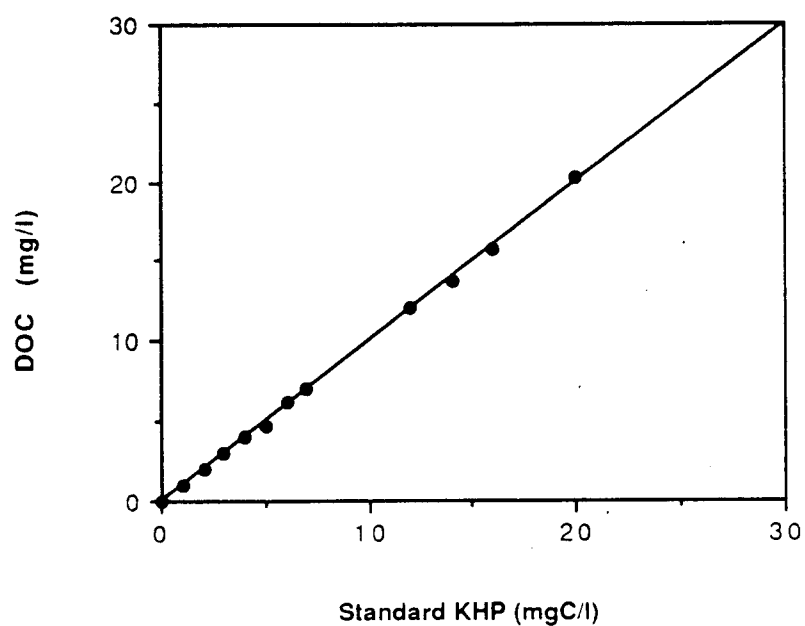


Figure A4 d: Read back calibration curve for DOC analyses

A5: Raw Data

The following are the contents of the table containing the raw data

- a) Al(III) titration
pH, volume 2N NaOH, and the r ratio are presented for
AlCl₃, Alum, AlNO₃, Al/SO₄ = 1/3 , Al/SO₄ = 1/1.5
respectively
- b) Aluminum precipitates formed with Alum and AlCl₃ at pH5.5 and 7
- c) AHS adsorption on AlCl₃, and Alum at pH5.5 and 7
- d) AHS adsorption on aluminum+AHS precipitates
and SO₄ exchange for AHS
- e) SO₄ adsorption (aluminum precipitates
- f) SO₄ adsorption: aluminum + AHS precipitates
- g) Equilibration for the adsorption of AHS and sulfate on aluminum
precipitate
 - a-AHS
 - b-sulfate
- h) Adsorption capacity for the adsorption of AHS and sulfate on
aluminum precipitates
 - a-AHS
 - b-sulfate

a)

Titration data for set 6															
pH	NaCl	Vol. 2N NaOH	[OH] ⁻ /M	Vol. 2N NaOH	pH	NaOH	[OH] ⁻ /M	Vol. 2N NaOH	pH	[OH] ⁻ /M	Vol. NaOH	pH	NaCl/NaOH	[OH] ⁻ /M	Vol. NaOH
1	2.100	0.000	0.000	0.000	2.015	0.000	0.000	0.000	2.330	0.000	0.000	2.020	0.000	0.000	0.000
2		2.500	0.048	2.500	2.025	0.048	2.500			0.048	2.500	2.070	0.048	2.500	0.048
3	2.530	5.000	0.096	5.000	2.062	0.096	5.000	2.300	0.096	5.000	2.120	0.096	5.000	2.110	0.096
4		7.500	0.145	7.500	2.107	0.145	7.500			0.145	7.500	2.180	0.145	7.500	0.145
5	3.370	10.000	0.193	10.000	2.158	0.193	10.000	3.030	0.193	10.000	2.250	0.193	10.000	2.150	0.193
6		12.500	0.241	12.500	2.218	0.241	12.500			0.241	12.500	2.330	0.241	12.500	0.241
7	3.570	15.000	0.289	15.000	2.282	0.289	15.000	3.540	0.289	15.000	2.430	0.289	15.000	2.280	0.289
8		17.500	0.338	17.500	2.368	0.338	17.500			0.338	17.500	2.570	0.338	17.500	0.338
9	3.660	20.000	0.386	20.000	2.457	0.386	20.000	3.680	0.386	20.000	2.740	0.386	20.000	2.400	0.386
10		22.500	0.434	22.500	2.563	0.434	22.500			0.434	22.500	2.900	0.434	22.500	0.434
11		25.000	0.482	25.000	2.706	0.482	25.000	3.720	0.482	25.000	3.250	0.482	25.000	2.730	0.482
12		27.500	0.530	27.500	2.896	0.530	27.500			0.530	27.500	3.380	0.530	27.500	0.530
13		30.000	0.578	30.000	3.132	0.578	30.000	3.760	0.578	30.000	3.490	0.578	30.000	3.140	0.578
14		32.500	0.627	32.500	3.308	0.627	32.500			0.627	32.500	3.550	0.627	32.500	0.627
15		35.000	0.675	35.000	3.417	0.675	35.000	3.780	0.675	35.000	3.590	0.675	35.000	3.440	0.675
16		37.500	0.723	37.500	3.503	0.723	37.500			0.723	37.500	3.640	0.723	37.500	0.723
17	3.750	40.000	0.771	40.000	3.568	0.771	40.000	3.800	0.771	40.000	3.670	0.771	40.000	3.520	0.771
18		42.500	0.820	42.500	3.614	0.820	42.500			0.820	42.500	3.690	0.820	42.500	0.820
19		45.000	0.868	45.000	3.644	0.868	45.000	3.810	0.868	45.000	3.700	0.868	45.000	3.680	0.868
20		47.500	0.916	47.500	3.671	0.916	47.500			0.916	47.500	3.720	0.916	47.500	0.916
21	3.790	50.000	0.964	50.000	3.715	0.964	50.000			0.964	50.000	3.730	0.964	50.000	0.964
22		52.500	1.013	52.500	3.735	1.013	52.500	3.840	1.013	52.500	3.740	1.013	52.500	3.710	1.013
23		55.000	1.061	55.000	3.735	1.061	55.000			1.061	55.000	3.750	1.061	55.000	1.061
24		57.500	1.109	57.500	3.784	1.109	57.500			1.109	57.500	3.770	1.109	57.500	1.109
25	3.800	60.000	1.157	60.000	3.784	1.157	60.000			1.157	60.000	3.780	1.157	60.000	1.157
26		62.500	1.205	62.500	3.777	1.205	62.500			1.205	62.500	3.780	1.205	62.500	1.205
27		65.000	1.254	65.000	3.790	1.254	65.000	3.870	1.254	65.000	3.790	1.254	65.000	3.800	1.254
28		67.500	1.302	67.500	3.814	1.302	67.500			1.302	67.500	3.810	1.302	67.500	1.302
29	3.840	70.000	1.350	70.000	3.836	1.350	70.000			1.350	70.000	3.820	1.350	70.000	1.350
30		72.500	1.400	72.500	3.836	1.400	72.500	3.900	1.400	72.500	3.830	1.400	72.500	3.840	1.400
31		75.000	1.448	75.000	3.858	1.448	75.000			1.448	75.000	3.830	1.448	75.000	1.448
32		77.500	1.495	77.500	3.858	1.495	77.500			1.495	77.500	3.830	1.495	77.500	1.495
33	3.880	80.000	1.543	80.000	3.880	1.543	80.000			1.543	80.000	3.850	1.543	80.000	1.543
34		82.500	1.591	82.500	3.897	1.591	82.500			1.591	82.500	3.850	1.591	82.500	1.591
35		85.000	1.639	85.000	3.897	1.639	85.000	3.940	1.639	85.000	3.880	1.639	85.000	3.900	1.639
36		87.500	1.688	87.500	3.897	1.688	87.500			1.688	87.500	3.880	1.688	87.500	1.688
37	3.920	90.000	1.736	90.000	3.897	1.736	90.000			1.736	90.000	3.900	1.736	90.000	1.736
38		92.500	1.784	92.500	3.897	1.784	92.500			1.784	92.500	3.900	1.784	92.500	1.784
39		95.000	1.832	95.000	3.897	1.832	95.000			1.832	95.000	3.900	1.832	95.000	1.832
40		97.500	1.880	97.500	3.897	1.880	97.500			1.880	97.500	3.910	1.880	97.500	1.880
41	3.950	100.000	1.928	100.000	3.897	1.928	100.000			1.928	100.000	3.910	1.928	100.000	1.928
42		102.500	1.977	102.500	3.897	1.977	102.500			1.977	102.500	3.910	1.977	102.500	1.977

b)

Titration data for set											
pH	ACLS	Vol. ZnNaOH	[OH] ⁻ /M	Vol. ZnNaOH	pH	Alum	[OH] ⁻ /M	Vol. ZnNaOH	pH	[OH] ⁻ /M	Vol. NaOH
43		105 000	2 025	105 000	3 957	2 075	105 000	3 940			105 000
44		107 500	2 073	107 500	2 071	2 073	107 500	2 025			107 500
45		110 000	2 122	110 000	3 974	2 122	110 000	3 960			110 000
46	4 010	112 500	2 170	112 500		2 170	112 500				112 500
47		115 000	2 218	115 000		2 218	115 000	4 000			115 000
48		117 500	2 266	117 500		2 266	117 500				117 500
49	4 070	120 000	2 314	120 000	4 022	2 314	120 000	4 030			120 000
50		122 500	2 363	122 500		2 363	122 500				122 500
51	4 110	125 000	2 411	125 000		2 411	125 000	4 070			125 000
52	4 140	127 500	2 459	127 500		2 459	127 500				127 500
53	4 150	130 000	2 507	130 000	4 078	2 507	130 000	4 120			130 000
54	4 180	132 500	2 555	132 500		2 555	132 500				132 500
55	4 210	135 000	2 604	135 000	4 120	2 604	135 000	4 170			135 000
56	4 270	137 500	2 652	137 500		2 652	137 500				137 500
57	4 310	140 000	2 700	140 000	4 146	2 700	140 000	4 250			140 000
58	4 380	142 500	2 748	142 500		2 748	142 500				142 500
59	4 480	145 000	2 797	145 000	4 206	2 797	145 000	4 360			145 000
60	4 600	147 500	2 845	147 500		2 845	147 500				147 500
61	4 840	150 000	2 893	150 000	4 260	2 893	150 000	4 710			150 000
62	5 240	152 500	2 941	152 500		2 941	152 500				152 500
63	5 460	155 000	2 989	155 000	4 299	2 989	155 000	5 600			155 000
64	5 590	157 500	3 038	157 500	4 341	3 038	157 500	5 970			157 500
65	5 690	160 000	3 086	160 000	4 374	3 086	160 000	6 330			160 000
66		162 500	3 134	162 500	4 390	3 134	162 500	6 720			162 500
67	6 900	165 000	3 182	165 000	4 868	3 182	165 000	7 120			165 000
68		167 500	3 229	167 500	5 160	3 229	167 500	7 550			167 500
69	7 360	170 000	3 279	170 000	5 420	3 279	170 000				170 000
70		172 500	3 325	172 500	5 764	3 325	172 500	8 450			172 500
71	9 060	175 000	3 375	175 000	6 073	3 375	175 000	8 800			175 000
72		177 500	3 420	177 500	6 440	3 420	177 500	9 210			177 500
73	9 750	180 000	3 470	180 000	6 707	3 470	180 000	9 640			180 000
74		182 500	3 565	182 500	7 027	3 565	182 500	10 080			182 500
75	10 100	185 000	3 659	185 000	7 388	3 659	185 000	10 530			185 000
76		187 500	3 750	187 500	7 775	3 750	187 500	11 000			187 500
77	10 390	190 000	3 844	190 000	8 180	3 844	190 000	11 480			190 000
78		192 500	3 939	192 500	8 605	3 939	192 500	12 020			192 500
79	10 690	195 000	4 046	195 000	9 051	4 046	195 000	12 580			195 000
80		197 500	4 154	197 500	9 517	4 154	197 500	13 160			197 500
81	11 480	200 000	4 266	200 000	9 994	4 266	200 000	13 760			200 000
82		202 500	4 380	202 500	10 494	4 380	202 500	14 380			202 500
83		205 000	4 496	205 000	11 019	4 496	205 000	15 020			205 000
84		210 000	4 623	210 000	11 579	4 623	210 000	15 680			210 000

Titration data for set											
pH	ACLS	Vol. ZnNaOH	[OH] ⁻ /M	Vol. ZnNaOH	pH	Alum	[OH] ⁻ /M	Vol. ZnNaOH	pH	[OH] ⁻ /M	Vol. NaOH
85		220 000	4 760	220 000	10 116	4 760	220 000	16 360			220 000
86		225 000	4 882	225 000	10 307	4 882	225 000	17 080			225 000
87		230 000	5 009	230 000	10 507	5 009	230 000	17 820			230 000
88		235 000	5 140	235 000	10 719	5 140	235 000	18 580			235 000
89		240 000	5 275	240 000	10 944	5 275	240 000	19 360			240 000
90		245 000	5 414	245 000	11 184	5 414	245 000	20 160			245 000
91		250 000	5 558	250 000	11 439	5 558	250 000	20 980			250 000
92		260 000	5 709	260 000	11 710	5 709	260 000	21 820			260 000
93		270 000	5 867	270 000	12 000	5 867	270 000	22 680			270 000
94		280 000	6 032	280 000	12 310	6 032	280 000	23 560			280 000

Thu Nov 2 1989 11:41 PM

Al vs Al(OH)3S final

Column 1	Al(OH)3S Alum	Al Std Alum	Al Std AlCl3	Al(OH)3S	Al Std AlCl3	Al(OH)3S AlCl3	Al Std Alum	Al(OH)3S Alum
1	Aluminum in 0.000	0.000	0.000	0.000	0.000	0.000	1	124.500
2	standard 120.300	119.380	86.800	70.500	113.700	109.600	2	124.500
3	vs 117.800	119.380	82.100	78.400	116.840	100.110	3	120.120
4	Aluminum in 88.760	87.800	110.100	106.000	115.330	105.830	4	120.120
5	precipitate 88.830	87.800	26.100	28.080	142.560	130.740	5	120.660
6	55.440	57.950	26.100	25.700	142.560	132.730	6	120.660
7	59.500	57.950	29.200	27.400	55.380	52.220	7	121.760
8	30.100	29.700	29.200	29.500	82.380	69.570	8	121.760
9	30.800	29.700	59.500	53.000	26.970	25.560	9	19.590
10	120.360	123.030	58.500	58.500	26.970	24.550	10	19.590
11	122.350	123.030	108.810	114.400	51.830	49.930	11	19.590
12	59.700	60.690			77.110	76.240	12	19.590
13	58.610	60.690			108.330	104.160	13	19.650
14	42.050	43.670			108.330	99.970	14	19.650
15	40.570	43.170			113.690		15	19.650
16	120.120	122.300			113.690		16	19.650
17	120.840	122.300			116.840		17	19.650
18					115.300		18	19.650
19					142.560		19	19.650
20							20	19.650

c)

C. ads Al precip only Lorr

Column 1	Ce (mg/l)	X/M AlCl3	X/M AlCl3	Ce (mg/l)	X/M Alum	X/M Alum	Alum. AHS precipitate
1	C. Adsorption						Ce (mg/l) X/M
2	Al precipitant						
3	1.990	0.010	33.010	0.126	0.014	4.010	0.016
4	3.180	0.013	13.230	0.125	0.014	7.700	0.116
5	1.870	0.019	18.760	0.090	0.012	10.140	0.163
6	1.910	0.010	14.460	0.076	0.012	14.710	0.208
7	10.290	0.052	16.430	0.080	0.021	3.270	0.075
8	13.010	0.053	11.280	0.036	0.019	9.420	0.081
9	27.180	0.131	16.970	0.070	0.033	4.760	0.084
10	20.680	0.121	16.970	0.150	0.033	3.510	0.071
11	8.460	0.015	1.800	0.020	0.041		
12	20.710	0.127	3.680	0.020	0.035		
13			3.900	0.020	0.120		
14			1.860	0.020	0.157		
15			1.850	0.018	0.147		
16			2.950	0.018	0.109		
			2.080	0.021			

d)

AHS adsorption on Al-AHS precipitates and Ca exchanged for Na

Column 1	Al-18 mg	AlCl3	SOM	C. released Al-AHS in	Al-AHS in
1	AHS 0.4 mg.				
2					
3	Ce (mg/l)	X (mg)	X (mg)	Filtrate (mg) release (mg)	
4	1.14	1.179	1.263	3.2	1
5	1.07	0.585	1.02	1.21	0.39
6	2.57	0.99	2.6	1.02	0.5
7	1.762	1.054	3.12	2.6	0.92
8	0.87	0.892	3.73	3.12	1.82
9	6.11	1.958	2.81	1.24	
10	5.92	1.234	0.218	1.85	
11	2.25	1.984	0.129	2.25	
12	3.03	0.982	2.228	3.14	1.72
13	1.23	1.247	2.457	4.14	1.49

Al vs Al(OH)3S final

Column 1	Al(OH)3S Alum	Al Std Alum	Al Std AlCl3	Al(OH)3S	Al Std AlCl3	Al(OH)3S AlCl3	Al Std Alum	Al(OH)3S Alum
1	Aluminum in 0.000	0.000	0.000	0.000	0.000	0.000		
2	standard 120.300	119.390	96.800	70.500	113.700	109.660	24.500	116.980
3	vs 117.800	119.390	82.100	58.400	116.840	100.110	24.500	118.560
4	Aluminum in 68.760	87.600	110.100	106.000	115.330	105.330	20.120	115.960
5	precipitate 68.830	87.600	26.100	28.000	142.560	130.740	20.120	111.730
6	55.440	57.950	26.100	25.700	142.560	132.730	20.660	121.980
7	59.500	57.950	29.200	27.400	55.380	52.220	20.660	120.120
8	30.100	29.700	29.200	29.500	82.380	69.570	21.760	112.970
9	30.800	29.700	58.500	53.000	26.970	25.560	19.590	19.930
10	120.380	123.030	58.500	58.600	26.970	24.550	19.590	20.170
11	122.350	123.030	108.810	114.400	51.930	49.930	19.590	20.560
12	59.700	60.690			77.110	75.240	19.590	19.550
13	58.610	60.690			108.330	124.160	19.550	19.470
14	42.050	43.670			108.330	99.970	19.650	19.370
15	40.570	43.670			113.690			
16	120.120	122.300			113.690			
17	120.640	122.300			116.840			
18					115.300			
19					142.560			
20								

SO4 ads final data

Column 1	Ce (mg/l)	X/M AlCl3 pH7	Ce pH5.5	X/M pH5.5
1	AlCl3	0.000	0.000	pH5.5
2		383.270	0.265	71.680
3		482.400	0.207	357.410
4		535.800	0.235	188.980
5		300.900	0.235	19.780
6		338.600	0.257	16.680
7		283.600	0.193	7.280
8		751.330	0.194	35.470
9		340.400	0.254	
10		515.700	0.202	260.000
11		543.800	0.229	250.000
12		200.000	0.143	110.000
13				
14		300.900	0.210	
15		750.000	0.275	
16				
17		100.000	0.110	

SO4 ads Al +C pH7 data final

Column 8	Ce (mg/l) Al+C	X/M (Al+C)	1/Ce (Al+C)	1/X/M (Al+C)
1	SO4 ads	0.000	0.000	
2	AlCl3 +C	81.600	0.198	5.051
3	18 mg Al	170.800	0.152	6.579
4	+ 0.4mg C	168.900	0.328	3.049
5	pH7	151.600	0.213	4.695
6		221.300	0.250	4.000
7				

g)

Time (hr)	AlCl ₃ ·6H ₂ O Precipitant		Alum Precipitant	
	(19.4 mg as Al)	(17.6 mg as Al)	(21.2 mg as Al)	(18.1 mg as Al)
	pH 7	pH 5.5	pH 7	pH 5.5
0.5	1.79	1.25	1.97	1.25
1	1.99	1.44	2.41	1.53
1.5		1.5	2.56	1.55
2	2.03	1.52	2.65	1.56
2.5	2.09	1.6	2.71	
3	2.08	1.59	2.69	1.59
3.5	2.06		2.69	
4		1.64	2.71	1.6

Equilibration Time for Sulfate Adsorption on aluminum precipitate

Time (hr)	AlCl ₃ ·6H ₂ O Precipitant		Alum Precipitant	
	(48.8 mg as A)	(48.9 mg as A)	(48.9 mg as A)	(48.8 mg as A)
	pH 7	pH 5.5	pH 7	pH 5.5
0.5	30.14	40.44	3.73	0.41
1	29.83	40.09	3.93	0.47
1.5	29.67	40.23	4.45	0.45
2	30.27	40.01	3.71	0.8
2.5	30.59	40.49	4.17	0.62
3	30.75	40.26	4.45	0.48
3.5	30.78	41.25	4.93	
4	30.5	40.87	5.98	1.49

h)
-a

AlCl3.6H2O Precipitant				Alum Precipitant			
(19.0 mg as Al)		(17.6 mg as Al)		(19.0 mg as Al)		(20.3 mg as Al)	
pH 7		pH 5.5		pH 7		pH 5.5	
Cumulative C Added (mg)	Cumulative C Adsorbed (mg)	Cumulative C Added (mg)	Cumulative C Adsorbed (mg)	Cumulative C Added (mg)	Cumulative C Adsorbed (mg)	Cumulative C Added (mg)	Cumulative C Adsorbed (mg)
0.97	0.58	1.2	0.63	0.97	0.58	1.25	1.07
1.94	0.69	2.39	1.3	1.94	0.69	2.5	1.8
2.91	0.87	3.59	1.47	2.91	0.87	3.74	2.02
3.88	0.98	4.78	1.69	3.88	0.98	5	2.14

Aluminum Precipitate Adsorbent Capacity with Sulfate as Adsorbate

-b

AlCl ₃ ·6H ₂ O Precipitant				Alum Precipitant			
15.7 mg as A		14.8 mg as A		15.3 mg as A		14.8 mg as A	
pH 7		pH 5.5		pH 7		pH 5.5	
Cumulative SO ₄ Added mg	Cumulative SO ₄ Adsorbed mg	Cumulative SO ₄ Added mg	Cumulative SO ₄ Adsorbed mg	Cumulative SO ₄ Added mg	Cumulative SO ₄ Adsorbed mg	Cumulative SO ₄ Added mg	Cumulative SO ₄ Adsorbed mg
41.7	27.3	76.8	39.5	39.4	2.9	76.8	1.44
125.3	29	151.2	40.7	158.9	3	154.6	2.8
244.1	28.9	227.3	42	237.5	2	233.7	7.2
307.1	30.1	304.8	43.5	317.4	3.2	312.3	10.6